

## Noble, Philip W. (2011) Characterisation of anti-glycan monoclonal antibodies. PhD thesis, University of Nottingham.

### Access from the University of Nottingham repository:

[http://eprints.nottingham.ac.uk/12071/1/Final\\_Thesis\\_for\\_Submission\\_16.6.11.pdf](http://eprints.nottingham.ac.uk/12071/1/Final_Thesis_for_Submission_16.6.11.pdf)

### Copyright and reuse:

The Nottingham ePrints service makes this work by researchers of the University of Nottingham available open access under the following conditions.

- Copyright and all moral rights to the version of the paper presented here belong to the individual author(s) and/or other copyright owners.
- To the extent reasonable and practicable the material made available in Nottingham ePrints has been checked for eligibility before being made available.
- Copies of full items can be used for personal research or study, educational, or not-for-profit purposes without prior permission or charge provided that the authors, title and full bibliographic details are credited, a hyperlink and/or URL is given for the original metadata page and the content is not changed in any way.
- Quotations or similar reproductions must be sufficiently acknowledged.

Please see our full end user licence at:

[http://eprints.nottingham.ac.uk/end\\_user\\_agreement.pdf](http://eprints.nottingham.ac.uk/end_user_agreement.pdf)

### A note on versions:

The version presented here may differ from the published version or from the version of record. If you wish to cite this item you are advised to consult the publisher's version. Please see the repository url above for details on accessing the published version and note that access may require a subscription.

For more information, please contact [eprints@nottingham.ac.uk](mailto:eprints@nottingham.ac.uk)



The University of  
**Nottingham**

Characterisation of anti-glycan  
monoclonal antibodies

Philip .W. Noble B.Sc (Hons)

Thesis submitted to the University of Nottingham  
for the degree of Doctor of Philosophy, April 2011



I dedicate thesis in memory of my Nan, Janet Ellis

## Table of Contents

Table of Contents.....	i
Abstract.....	vi
Abbreviations.....	viii
Acknowledgements.....	xiii
Chapter 1 Introduction .....	1
1.1 Cancer .....	1
1.1.1 Treatment of colorectal and ovarian cancer.....	1
1.2 Immunity.....	2
1.2.1 The B cell.....	2
1.2.2 B cell Maturation .....	4
1.2.3 Humoral immune response.....	8
1.2.4 Antibody Structure.....	11
1.2.5 Antibody Glycosylation.....	13
1.2.6 Effector mechanisms of antibodies.....	15
1.2.7 Complement.....	16
1.2.8 Complement cascade .....	16
1.2.9 Antibody dependent cellular cytotoxicity .....	20
1.2.10 Antibody dependent cellular phagocytosis.....	22
1.2.11 Monoclonal antibodies .....	22
1.2.12 Monoclonal antibody production .....	22
1.2.13 Monoclonal antibodies for therapeutic use .....	23
1.2.14 Approved monoclonal antibodies.....	28
1.3 Glycolipids.....	37
1.3.1 Synthesis and structure of GSL.....	39
1.3.2 Function of GSLs.....	41
1.3.3 Mechanisms of altered expression of glycans.....	45
1.3.4 Aberrant expression of glycosyl epitopes in cancer.....	46
1.3.5 Glycolipids as targets for monoclonal antibodies.....	50
1.4 Cell death .....	53
1.4.1 Oncosis.....	61
1.4.2 Autophagy.....	61
1.4.3 Pyroptosis.....	62
1.4.4 Apoptotic Pathways .....	55
1.4.2 Intrinsic Pathway.....	56
1.4.3 Extrinsic pathway .....	58
Aim of thesis .....	63

Chapter 2 Materials and Methods.....	65
2.1 mAbs and Human cancer cell line culture .....	65
2.1.1 Commercial mAbs .....	65
2.1.2 In house production of mAbs.....	65
2.1.3 Biotin and FITC labelling of mAbs .....	66
2.2 Cell culture .....	67
2.2.1 Cell lines and hybridomas .....	67
2.2.2 Maintenance of cell lines and hybridomas .....	68
2.3 Immunohistochemical analysis.....	69
2.3.1 Tissue preparation .....	69
2.3.2 Antigen retrieval .....	71
2.3.3 Prevention of non-specific binding .....	71
2.3.4 Application of primary antibody .....	72
2.3.5 Washing.....	72
2.3.6 ABC method .....	73
2.3.7 Visualisation of the primary antibody.....	74
2.3.8 IHC protocol .....	75
2.3.10 Evaluation of staining.....	76
2.3.11 Data processing.....	76
2.4 Immunohistochemical staining of colorectal TMA for cleaved capsase-3 and MHC-II expression .....	77
2.4.1 Patient study and design.....	77
2.4.2 Clinicopathological variables for the patient cohort (n = 462) .....	78
2.4.3 Monoclonal antibody binding to ovarian cancer and normal tissue TMA.....	80
2.5 Screening of mAbs on The Consortium for Functional Glycomics array.....	82
2.5.1 Screening on glycan array .....	82
2.6 <i>In vitro</i> functional studies of mAbs, murine serum and hybridoma supernatants.....	82
2.6.1 Analysis of antibody binding to cancer cells .....	83
2.6.3 Analysis of binding to cancer cell glycolipid extraction .....	86
2.6.4 Analysis of antibody mediated direct cell death.....	89
2.6.5 Antibody dependent cellular cytotoxicity and complement dependent cytotoxicity assays .....	92
2.7 Immunisations.....	93
2.7.1 Preparation of whole cancer cells.....	93
2.7.2 Preparation of glycolipid .....	93
2.7.3 Preparation of liposomes.....	94
2.7.4 Adjuvants .....	94
2.7.5 Immunisation protocol.....	95

2.7.6 Analysis of antibody response to immunisations .....	95
2.7.7 Isolation of splenocytes .....	95
2.7.8 Collection of large quantities of sera from immunised mice.....	96
2.7.9 Fusion of Mice splenocytes with NS0 myeloma cells .....	96
2.8 Statistical analysis of data .....	97
2.8.1 Immunohistochemical analysis.....	97
2.8.2 Other analysis .....	97
Chapter 3 Cleaved caspase-3 expression in colorectal cancer .....	98
3.1 Background .....	98
3.2 Results.....	101
3.2.1 Clinical and pathological data .....	101
3.2.2 CC3 expression .....	103
3.2.3 Markers of apoptosis and inflammation: Bcl2, p53, CD3, CD68, CD16 and MHC-II expression .....	105
3.2.4 Relationship between CC3 expression and standard clinicopathological variables .....	105
3.2.5 Relationship between MHC-II expression and standard clinicopathological variables .....	106
3.2.6 Relationship between CC3 expression and markers of immune activation and apoptosis .....	107
3.2.7 Relationship between MHC-II expression and markers of immune activation and apoptosis .....	107
3.2.8 Relationship between CC3 expression and survival .....	108
3.2.9 Relationship between MHC-II expression and survival .....	110
3.2.10 Multivariate analysis of CC3 expression and standard clinicopathological variables.....	110
3.3 Discussion.....	112
Chapter 4 Characterisation of Lewis y/b mAb specificity and <i>in vitro</i> functionality.....	116
4.1 Introduction .....	116
4.2 Results.....	118
4.2.1 Defining the epitopes recognised by the Lewis y/b antibodies using the Consortium for Functional Glycomics glycan array.....	118
4.2.2 Binding characteristics of anti-Lewis y/b mAbs on a range of antigen positive cell lines .	124
4.2.3 Determining self-binding (homophilic binding) of the Lewis antibodies.....	126
4.2.4 Induction of ADCC and CDC in cancer cells by 692/29, BR96 and 2-25 LE.....	131
4.2.5 Induction of cell death in colorectal cancer cells by 692/29, BR96 and not 2-25 LE .....	133
4.2.6 Cross-linking the IgG <sub>1</sub> mAb 2-25 LE does not induce direct cell death.....	136
4.2.7 692/29 and BR96 induce cell death via an alternative mechanism to apoptosis death ...	137
4.3 Discussion.....	141
Chapter 5 Lewis a mAbs.....	146
5.1 Introduction .....	146
5.2 Results.....	147

5.2.1 Analysis of 505/4 therapeutic value by normal and colorectal cancer distribution.....	147
5.2.2 Characterisation of 505/4 antigen .....	152
5.2.3 Analysis of 505/4, CA19.9 and 7LE binding to the Consortium for Functional Glycomics array .....	153
5.2.4 Analysis of 505/4, CA19.9 and 7LE colorectal cell line binding.....	157
5.2.5 Direct killing ability of 505/4, 7LE and CA19.9 mAbs .....	159
5.2.6 Mechanism of killing of colorectal cancer cells by 505/4, 7LE and CA19.9mAbs .....	162
5.3 Discussion.....	165
Chapter 6 The production of monoclonal antibodies targeted against ovarian cancer glycolipid.....	170
6.1 Background .....	170
6.2 Results .....	171
6.2.1 Glycolipid extracted from C170 cells binds both 692/29 and 505/4 mAbs .....	171
6.2.2 Immunisation of BALB/c mice with ovarian cancer cells .....	172
6.2.2 Fusion (F012) of OVCA 433 immunised mouse splenocytes yields anti-ovarian cancer glycolipid hybridomas .....	173
6.2.3 Immunisation with the mAb TIB 207 depletes mouse T cells <i>in vivo</i> .....	175
6.2.4 Depletion of CD4 cells is ineffective at increasing the anti-ovarian cancer glycolipid response.....	176
6.2.5 Fusion (F013) of TIB-207/OVCA 433 immunised mouse splenocytes yields anti-ovarian cancer cell but not anti-glycolipid hybridomas.....	177
6.2.7 Immunisation of BALB/c mice with an NK cell adjuvant.....	178
6.2.9 Immunisation of colorectal cancer glycolipid extract does not give an anti-glycolipid response.....	179
6.2.10 Ovarian cancer cell glycolipid immunisation .....	181
6.2.11 Preparation of ovarian cancer glycolipid-containing liposomes for immunisation.....	183
6.2.12 Immunisation with OVCA glycolipid-containing glycolipid with $\alpha$ GalCer .....	184
6.2.13 Fusion of splenocytes from mice 2-1R and 2-1L .....	185
6.2.14 Immunisation with 2.5% OVCA glycolipid and $\alpha$ GalCer containing liposomes boosted with OVCAR-4 cells.....	187
6.2.15 Fusion of splenocytes from 2-1L and initial screening.....	189
6.2.16 Further characterisation and cloning of F019/1A7 and F019/1D3.....	190
6.2.17 Screening of F019/1A7 against ovarian cancer tissue array .....	192
6.2.18 Staining of normal tissue array with F019/1A7 .....	195
6.2.19 Evaluation of direct killing with F019/1A7.....	200
6.2.20 F019/1A7 cytotoxicity at different temperatures and with cross-linking.....	202
6.2.21 Ability of F019/1A7 to induce ADCC in target cells with cross-linking.....	203
6.3 Discussion.....	204
Chapter 7 Final Discussion .....	210
What is the therapeutic potential of mAbs? .....	210



Why target glycolipids?.....	210
What are the ideal antigens?.....	211
Functionality of the anti-tumour mAb.....	212
Human mAbs.....	215
Serum half-life.....	216
Other potential targets .....	217
Bibliography .....	223

## Abstract

The aims of this thesis are to establish the therapeutic value of two anti-glycan mAbs produced in-house, to develop an immunisation protocol with the aim of improving the immunogenicity tumour-associated glycolipids with the intention of producing therapeutically valuable mAbs and to determine the implication of a mAb with the ability to induce apoptosis in colorectal cancer.

The anti-glycan mAbs 692/29 and 505/4 have previously been produced in-house and this study aimed to determine their fine specificity using a glycan array. 692/29 displayed binding predominantly to Lewis b as well as Lewis y-containing glycans. 505/4 was discovered to bind to sialyl Lewis a as well as sialyl di-Lewis a, with no cross-reactivity with other blood group antigens. This was compared to other anti-Lewis mAbs, with differences in specificity being observed. Characterisation of 505/4 mAb distribution showed binding to 80% of colorectal tumours and low levels of binding to normal tissues by IHC, suggesting it may be therapeutically useful.

This thesis aimed to assess the ability of 505/4 and 692/29 to mediate immune mediated and non-immune mediated cell death as well as to determine whether non-immune-mediated cell death would be a desirable therapeutic property. Resistance to apoptosis is one of the hallmarks of cancer cells and mAbs stimulating apoptosis may not be very effective. To investigate the significance of apoptosis in cancer a large tissue microarray of colorectal tumours was assessed for apoptosis and its relationship to patient prognosis. Cleaved caspase-3 is a good marker of apoptosis as it is the executioner caspase for both the extrinsic and intrinsic pathways. Immunohistochemical analysis of colorectal tumour samples revealed that a high expression of cleaved caspase-3 in tumour was associated with good prognosis in colorectal cancer. This suggested that some tumours were still susceptible to apoptotic death but some are resistant and an alternative mechanism of cell death may be an advantage in these tumours. High expression of cleaved caspase-3 in the tumour-associated stroma was also an independent marker of good prognosis in colorectal cancer. This may be because apoptosis of the tumour-associated stroma reduces the level of pro-tumour signals

originating from tumour-associated immune cells and stromal cells. As the tumour microenvironment can act in an immunosuppressive and pro-tumour manner, the ability of a mAb to induce direct cell death without the need for effector cells or complement would be an advantage. Lewis y and Lewis b are blood group antigens commonly overexpressed on the surface of a range of cancers. Characterisation of effector functions of 505/4 and 692/29 demonstrated that both mAbs have the ability to mediate apoptosis by antibody dependent cellular cytotoxicity, complement dependent cytotoxicity and cause direct cell death in an oncosis-like manner. Comparison with other anti-Lewis mAbs demonstrated that a number of anti-Lewis mAbs can induce direct cell death independently of apoptosis. Thus, they could effectively target apoptotic sensitive and resistant colorectal cancers.

Tumours aberrantly express glycolipids and these molecules may be involved in a number of cellular pathways. In addition a large proportion of anti-glycan mAbs, including 505/4 and 692/29 in this thesis, have displayed the ability to induce direct cell death. Therefore this thesis aimed to develop an immunisation protocol capable of increasing the immunogenicity of tumour-associated glycolipid for the production of anti-tumour glycolipid mAbs directed against ovarian cancer. This study suggests that the incorporation of tumour glycolipid into liposomes and their immunisation along with the iNKT cell adjuvant  $\alpha$ -galactosylceramide, elicits an anti-tumour glycolipid immune response, which can yield IgG mAbs capable of binding a high proportion of ovarian cancers.

In summary, this thesis confirmed specificity of 692/29 to Lewis y and Lewis b and 505/4 to sialyl Lewis a and sialyl di-Lewis a. Furthermore, this thesis demonstrated a promising tissue distribution of 505/4 *in vitro*. Characterisation of mAb effector functions suggest that both Lewis y and sialyl Lewis a directed mAbs have the ability to cause direct cell death, independently of apoptosis in antigen positive cells, as well as the ability to cause immune-mediated cell death. This may be an important factor in the immune-suppressive tumour microenvironment. Furthermore, this thesis provides the basis for the production of new anti-glycolipid antibodies that may also be able to induce direct cell death.

## Abbreviations

$\alpha$ GalCer	$\alpha$ -galactosylceramide
ABTS	2,2'-Azinobis [3-ethylbenzothiazoline-6-sulfonic acid]-diammonium salt
ADCC	Antibody dependent cell-mediated cytotoxicity
AID	Activation-induced deaminase
AML	Acute myeloid leukaemia
APC	Antigen presenting cell
ATCC	American Type Culture Collection
ATL	Adult T cell lymphoma
BcR	B cell receptor
BRCA1	Breast cancer susceptibility gene 1
BRCA2	Breast cancer susceptibility gene 2
BSA	Bovine serum albumin
Ca <sup>2+</sup>	Calcium ion
CAF	Carcinoma-associated fibroblast
CARD	Caspase recruitment domain
CC3	Cleaved caspase-3
CD	Cluster of differentiation
CDC	Complement dependent cytotoxicity
CLL	Chronic lymphocytic leukaemia
CR	Complement receptor
CSR	Class switch recombination
CTLA-4	Cytotoxic T lymphocyte antigen-4
DAB	3, 3'-diaminobenzidine
DAF	Decay accelerating factor

DC	Dendritic cell
DCP	Dicetylphosphate
DD	Death domain
DED	Death effector domain
DISC	Death receptor-induced signalling complex
DMSO	Dimethyl sulfoxide
<i>d</i> H <sub>2</sub> O	Distilled H <sub>2</sub> O
DSS	Disease-specific survival
DPX	Distyrene, plasticiser and xylene
DR	Death receptor
ECM	Extracellular matrix
EGF	Epidermal growth factor
ELISA	Enzyme-linked immunosorbent assay
EpCAM	Endothelial cell adhesion molecule
FACS	Fluorescence activated cell sorter
FADD	Fas-associated death domain
FAP	Fibroblast activation protein
Fc	Constant region
FCS	Foetal calf serum
FDA	U.S. Food and Drug Administration
FFPE	Formalin fixed paraffin embedded
FIGO	International Federation of Obstetrics and Gynaecology
FITC	Fluorescein isothiocyanate
FL	Follicular lymphoma
FLIP	FLICE-like inhibitory protein

<i>FUT</i>	Fucosyltransferase
Fv	Variable fragment
GAG	Glycosaminoglycan
Gal	Galactose
GC	Germinal centre
Glc	Glucose
GlcCer	Glucosylceramide
GPI	Glycosylphosphatidylinositol
GSL	Glycosphingolipid
HAHA	Human anti-human antibody
HAMA	Human anti-mouse antibody
HAT	Hypoxanthine, aminopterin, thymidine
HCC	Hepatocarcinomas
HER2	Human epidermal growth factor receptor-2
HGPRT	Hypoxanthine guanine phosphoribosyl transferase
HLA	Human leukocyte antigen
HMT	Hypoxanthine, methotrexate, thymidine
HRP	Horseradish peroxidase
HSA	Human serum albumin
HSPG	Heparin sulphate proteoglycans
HUVEC	Human umbilical vein endothelial cell
IFN- $\gamma$	Interferon-gamma
Ig	Immunoglobulin
Ig-H	Immunoglobulin heavy chain
Ig-L	Immunoglobulin light chain

IGF-IR	Insulin-like growth factor-I receptor
IHC	Immunohistochemistry
IL-	Interleukin
ITAM	Immunoreceptor tyrosine-based activation motif
ITIM	Immunoreceptor tyrosine-based inhibitory motif
ITR	Integrin receptor
ITTC	Intra-tumoural T cells
LacCer	Lactosylceramide
mAb	Monoclonal antibody
MAC	Membrane attack complex
MBC	Mannose-binding lectin
MCP	Membrane cofactor protein
MHC	Major histocompatibility complex
MR	Mannose receptor
MUC1	Mucin-1
Na <sup>+</sup>	Sodium ion
NBCS	Newborn calf serum
NHL	Non-Hodgkin's Lymphoma
NHS	N-hydroxysuccinimide
NK Cell	Natural killer cell
NSS	Normal swine serum
OS	Overall survival
PBMC	Peripheral blood mononuclear cell
PBS	Phosphate buffered saline
PC	Phosphocholine

PI	Propidium iodide
PSGL-1	P-selectin glycoprotein ligand 1
PTPC	Mitochondrial permeability transition pore complexes
RT	Room temperature
Siglec	Sialic acid-binding immunoglobulin like
SHM	Somatic hypermutation
SMase	Sphingomyelinase
TAM	Tumour associated macrophages
TCC	Terminal complement complex
TGF	Transforming growth factor
TI	T cell independent antigen
TMA	Tumour microarray
TGF	Transforming growth Factor
TNF	Tumour necrosis factor
TNM	Tumour, node, metastasis
TRADD	TNF-R-associated death domain protein
TRAIL-R	TNF-related apoptosis-inducing ligand receptor
VEGF	Vascular endothelial growth factor
z-VAD-fmk	Carbobenzoxy-valyl-alanyl-aspartyl-[O-methyl]-fluoromethylketone (pan caspase inhibitor)



## Acknowledgements

I would like to express my upmost gratitude to my supervisor Professor Lindy Durrant who has helped me throughout my PhD with constant support and guidance, without which I would not be the scientist I am today. I would also like to thank Dr Ian Spendlove for his supervision and help throughout my project, his questioning has helped a great deal.

It is important I thank Dr Martin Garnett for who generously donated his time and knowledge of liposomes and the Consortium for Functional Glycomics whose glycan array technology I have used.

I would also like to thank all members of The Academic Department of Clinical Oncology, both past and present who have all helped a great deal. Particular thanks must go to Amy Popple, for her friendship since day 1. I would also like to thank Rob Moss for his continued help throughout my PhD, who has not only provided scientific help, but a lot of laughter too!

Finally, I would like to thank my family and friends for all of their support. In particular Helen, without whom, I would not have completed this chapter of my life.

## Chapter 1 Introduction

### 1.1 Cancer

Cancer is defined by the uncontrolled growth of cells, the invasion of the surrounding tissue and metastasis. Cancer is one of the leading causes of death in the modern world, with 298,000 new cases of cancer diagnosed each year in the UK, and more than 1 in 3 people developing some form of cancer through their life (CRUK, 2010). This relates to 1 in 4 deaths in the UK. Colorectal cancer is the second most common of cancer death, after lung cancer, with ovarian cancer being the fourth most common form of cancer in women, accounting for 6% of death in women (CRUK, 2010; NICE, 2003b).

#### 1.1.1 Treatment of colorectal and ovarian cancer

The current recommendation for treatment of colorectal cancer is surgery, with 80% of patients undergoing surgery. Of these patients about 40% remain disease free. Surgery is not possible in the remaining 20% as the disease is too far progressed for any curative treatment (NICE, 2004). Following surgery, patients receive a six month course of oxaliplatin in combination with infusional 5-fluorouracil (FU) plus folinic acid (FOLFOX) or irinotecan in combination with infusional 5-FU plus folinic acid (FOLFIRI) as first line treatment of colorectal cancer. Both FOLFOX and irinotecan alone are recommended as subsequent therapy options (NICE, 2008). Oral analogues of 5-FU capecitabine and tegafur in combination with uracil and folinic acid are also recommended for first line treatment of colorectal cancer (NICE, 2003a). Monoclonal antibodies (mAbs) directed at vascular endothelial growth factor (VEGF; bevacizumab) and the epidermal growth factor receptor (EGFR; cetuximab) have been approved for the treatment of metastatic colorectal cancer and will be discussed further in a later section (section 1.2.14).

The early stages of ovarian cancer are asymptomatic resulting in patients presenting at more advanced stages. Surgery is usually the first form of treatment in ovarian cancer; however, removal of the whole tumour is not possible in most cases, due to the advanced stage. Platinum-based therapy alone or in combination with paclitaxel is used as first and second line chemotherapy (NICE, 2003b). Despite advances in the treatment of other cancers, ovarian cancer treatment has not changed over the past decade, advocating further study into alternative treatments. More recently, alternative treatments, including small molecule inhibitors and mAbs, have shown promise against ovarian cancer. The presence of breast cancer susceptibility gene 1 (BRCA1) and breast cancer susceptibility gene 2 (BRCA2) deficient ovarian cancers has led to the study of small molecule poly (ADP-ribose) polymerase (PARP-1) inhibitors. PARP-1 is a DNA repair protein involved in base excision repair that repairs single strand DNA breaks (Shrivastav et al., 2008). In tumours deficient in BRCA1/BRCA2 mediated repair, the inhibition of PARP-1 leads to the accumulation double-stranded DNA breaks during replication, resulting in apoptosis of the tumour cell. A range of PARP-1 inhibitors have shown stabilisation or regression of ovarian cancers with BRCA1 or BRCA2 mutations, including olaparib (AZD2281) which has shown anti-tumour activity in a number of phase I clinical trials (Fong et al., 2010; Khan et al., 2011).

More recently the immune system in general and mAbs in particular are emerging as leading players in the fight against cancer.

## 1.2 Immunity

### 1.2.1 The B cell

B cells, also known as B lymphocytes produce antibodies when stimulated. They are produced and mature in the bone marrow. A key component of B cells is their B cell receptor (BcR) which binds specific antigens. The BcR is a multiprotein cross-membrane complex; that contains membrane bound immunoglobulin (mIg) consisting of Ig heavy (Ig-H) and light (Ig-L) chains and the associated

Ig- $\alpha$  and Ig- $\beta$  heterodimer (Reth & Wienands, 1997). It is expressed once a small pre-B cell becomes an immature B cell (Fig 1.1). The Ig-H and Ig-L chains are required for the recognition of antigens, which results in signal transduction inside the cell mediated by the Ig- $\alpha$  and Ig- $\beta$  chains, which contain immunoreceptor tyrosine-based activation motifs (ITAM) in their cytoplasmic domains (Reth & Wienands, 1997). Cross-linking of a number of BcRs on the cell surface by antigen leads to the translocation of the BcR and co-stimulatory molecules to lipid rafts, where protein-tyrosine kinases (PTK), such as LYN reside (Reth & Wienands, 1997). However, a recent model has been proposed where BcRs can exist as either active monomers, providing a survival signal for the B cell or as 'closed' oligomers, that auto inhibit their activation. In the presence of antigen, the equilibrium is shifted towards more active monomers, allowing signalling. Only a polyvalent antigen can keep the BcR monomers apart, therefore allowing their activation (Yang & Reth, 2010). Whether oligomeric BcR are activated or monomeric BcR are cross-linked by antigen, LYN and other tyrosine kinases then phosphorylate the ITAM of Ig- $\alpha$  and Ig- $\beta$  (Kurosaki, 2002). This provides a binding site for SCR-homology 2 (SH2) binding proteins such as PI3K and VAV. Activation of PI3K and VAV leads to downstream signalling.

The activation of the BcR can either be promoted or inhibited by a number of co-receptors present on the surface of the B cell. The CD19-CD21 complex is a tetrameric complex consisting of CD19, CD21, CD81 and leu13 that is co-ligated to the BcR via binding C3d-tagged antigens and enhances BcR signalling (Tedder et al., 1997). This occurs by CD21 binding the C3d-tagged antigen (Cherukuri et al., 2001a). The coupling CD19/CD21 to the BcR reduces the B cell activation threshold due to the phosphorylation of the ITAM on CD19 by tyrosine kinases, as well as increasing translocation of the BcR to lipid rafts and prolonging the activation signal (Cherukuri et al., 2001a; Cherukuri et al., 2001b). An example of an inhibitory co-receptor expressed on B cells is CD22 (Nitschke, 2009). CD22 is a membrane protein that is a member of the sialic acid-binding immunoglobulin-like (Siglec) family which specifically recognise sialic acids attached to the terminal regions of cell-surface glycoconjugates (Crocker et al., 2007). CD22 contains three cytoplasmic immunoreceptor tyrosine-

based inhibitory motifs (ITIM) which are phosphorylated by LYN upon activation of the BcR (Smith et al., 1998). Phosphorylation of the ITIMs leads to the recruitment of SHP-1, a protein tyrosine phosphatase. SHP-1 inhibits BcR activation by interfering with tyrosine kinase activity (Nitschke & Tsubata, 2004). CD22 can also recruit positive signalling molecules such as PI3K (Crocker et al., 2007).

### **1.2.2 B cell maturation**

Maturation of a B cell serves to create a large population of immunoglobulin-diverse cells that can recognise a large number of antigens. In order to protect an individual against all potential antigens in its environment it must be capable of producing at least  $10^7$  different antibody specificities. To achieve this amount of diversity a large proportion of an individual's DNA would be needed. This diversity is therefore created by genetic rearrangement. Diversity arises at four molecular levels; joining and rearrangement of variable region gene segments, somatic hypermutation (SHM) of the rearranged variable regions, class switch recombination (CSR) of heavy chain constant genes and gene conversion of variable genes (Maul & Gearhart, 2010). The rearrangement of variable region genes occurs during B cell maturation and the genetic rearrangement and expression of immunoglobulin genes mark the distinct stages of B cell maturation from stem cell to immature B cell (Fig 1.1). The stem cell has no rearrangement of its light and heavy chain immunoglobulin genes. The assembly of the heavy chain variable region requires two rearrangements involving three different types of gene segments, V, D and J (Early et al., 1980). The  $D_H$  and  $J_H$  segments are fused first, marking the progression of the stem cell to early pro-B cell (Fig 1.2). The rearrangement of the  $V_H$  segment marks the progression to the late pro-B cell. There are nine alternative C region sequences (each with multiple exons) with only the  $C_\mu$  and  $C_\delta$  sequences initially transcribed. The primary transcript can then be spliced one of two ways to generate mRNAs that encode  $\mu$  or  $\delta$  H chains with identical V domains. Additional diversity is created by imprecise joining/junctional

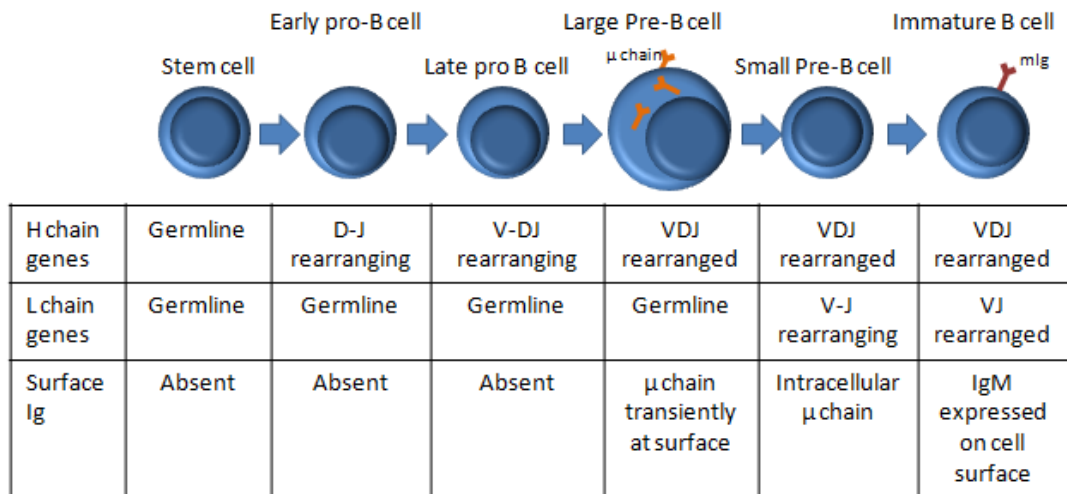


**Figure 1.1 Maturation of B cells.** Germline unrearranged immunoglobulin heavy chain D and J regions are rearranged forming the early pro-B cell, followed by v region rearrangement, marking the transition to late pro-B cells. Transient expression of the  $\mu$  chain at the surface marks the transition to large pre-B cell before V-J region rearranging denotes the small pre-B cell. Expressions of mIg at the surface after both the heavy and light chain have been rearranged results in the immature B cell.

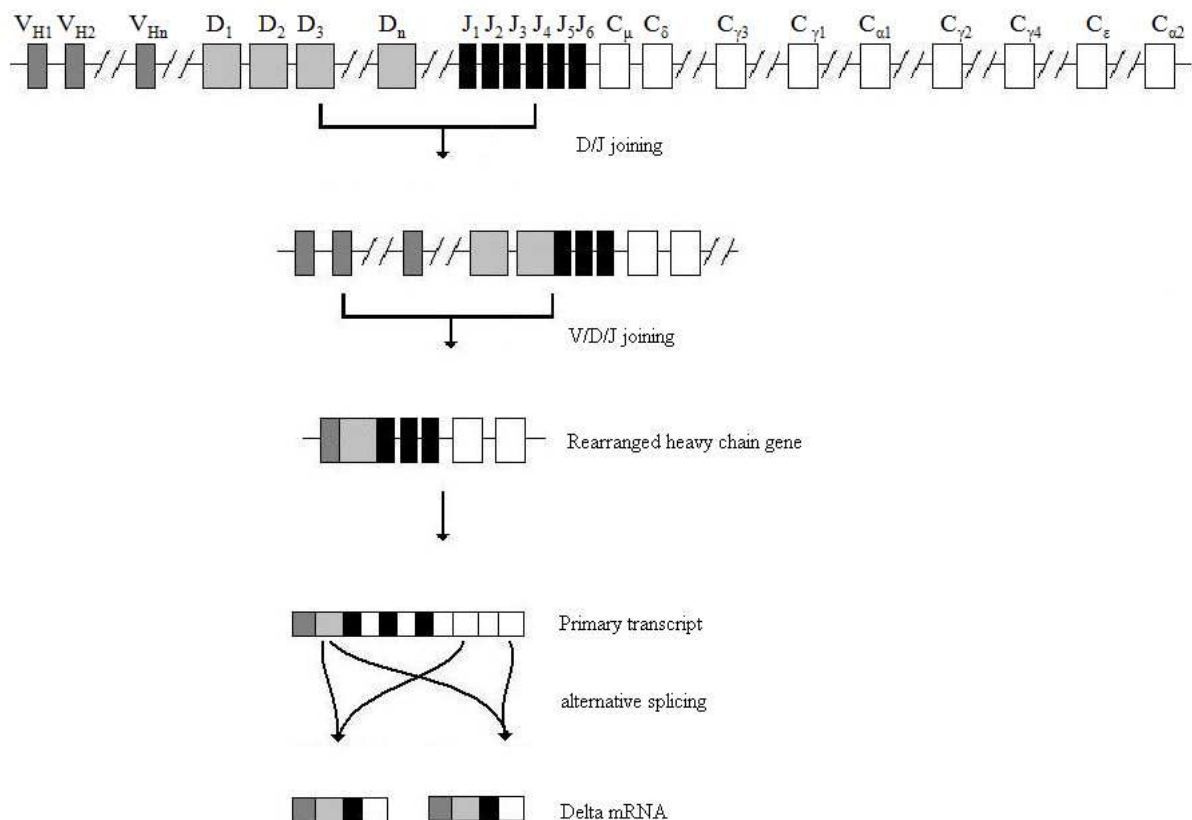


**Figure 1.2 Rearrangement and expression of the H chain locus.** D and J regions are fused marking the progression of stem cell to early pro-B cell. Rearrangement of the V region is then followed by the transcription of either C <sub>$\mu$</sub>  or C <sub>$\delta$</sub> . The primary transcript can then be spliced in two ways yielding an H chain with either a C <sub>$\mu$</sub>  or C <sub>$\delta$</sub>  domain, with an identical variable region.

diversity. This involves a loss of nucleotides at the joining between segments (Sakano et al., 1979). In the heavy chain additional nucleotides may be added which is referred to as N region insertion. Rearrangement is controlled by the presence of conserved heptamer and nonamer DNA sequences adjacent to the gene segments (recombination signal sequences; RSS). They are separated by 12 or 23 bp. The RSS are recognised by a complex of lymphocyte-specific recombination proteins RAG1 and RAG2. These cleave the DNA between the coding sequence and RSS. The coding strands are then rejoined (which can lead to junctional diversity or N region insertion) to give a rearranged gene segment. The recombination machinery can only join sequences separated by 12 or 23 bp, (12/23 rule) therefore only allowing the correct segments to be joined (Cooper, 2000). In the absence of RAG proteins, B cells cannot mature (Mombaerts et al., 1992). Transient expression of the  $\mu$  chain at the cell surface marks the progression of the late pro B cell to a large pre-B cell. Up to this point the light chain remains un-rearranged. The  $\kappa$  light chain locus consists of numerous V segment regions, numerous J segment regions and a unique  $C_\kappa$  exon. A DNA rearrangement event (either looping out and deletion or inversion) fuses one V segment to one J segment forming a single exon (Fig 1.3), marking the transition of large pre-B cell to a small pre-B cell. The V/J exon is then transcribed together with the J exons downstream of the V/J exon and the  $C_\kappa$  exon. The transcript is then transcribed and spliced to form mRNA. In this step, the un-rearranged J segments that were downstream of the V/J exon are removed as part of the intron during RNA splicing. At the  $\lambda$  L chain locus, there are 6-9 alternative  $C_\lambda$  exons, each with a nearby  $J_\lambda$  segment. DNA rearrangement fuses a V segment with a J segment and its associated C segment (Fig 1.4), marking the last step rearrangement, forming the immature B cell with rearranged light and heavy chains and mIg expressed on the cell surface.

As mentioned above, the production of rearranged variable regions during B cell maturation is only one way in which diversity of Ig is produced. Upon antigen recognition, somatic hypermutation (SHM) and class switch recombination (CSR) occur, further increasing the diversity of B cell Ig response. SHM produces point mutations throughout the rearranged V region and selection in

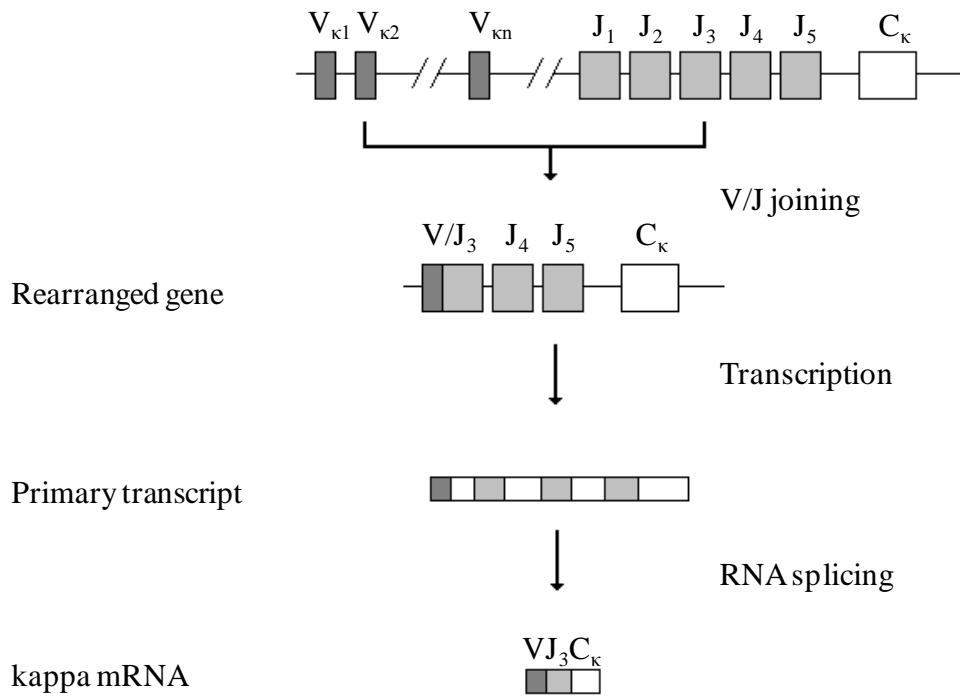


**Figure 1.3 The assembly and expression of the  $\kappa$  L chain locus.** Looping out or inversion results in fusion of V segments to J segments and a unique  $C_{\kappa}$  exon, marking the transition of large pre-B cell to small pre-B cell. RNA splicing results in the removal of downstream J regions, leaving one V, J and C region.

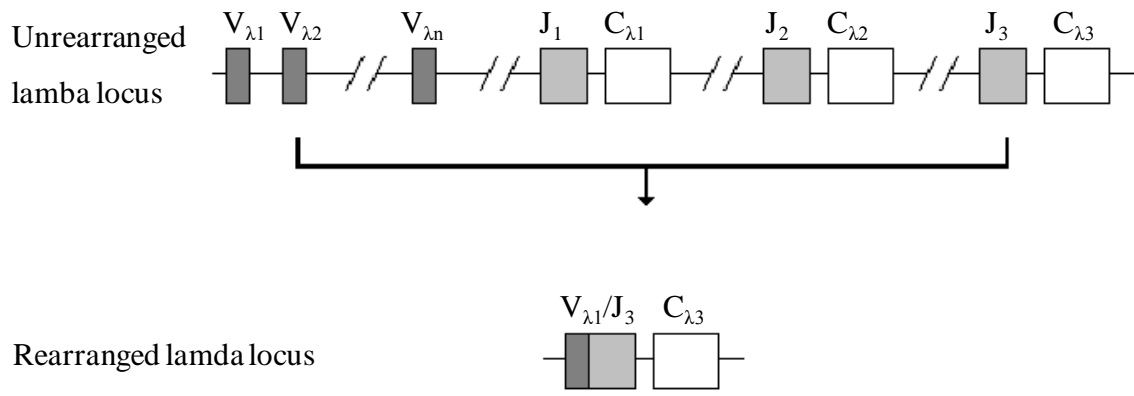


**Figure 1.3 The assembly of the  $\lambda$  L chain locus.** At the  $\lambda$  locus, there are 6-9 C segments each with a nearby J segment. DNA rearrangement fused a V segment with a J segment and its associated C segment, marking the last rearrangement, forming the immature B cell.

germinal centres occurs for high-affinity antibody-producing cells against a certain antigen. Therefore, the implication of mutation in the V gene is to generate antibodies with high affinity to antigens. CSR is region-specific recombination that replaces the heavy chain C region gene from  $C_{\mu}$  to other downstream  $C_H$  genes. This results in the B cell expressing IgG, IgE, or IgA isotypes, without



affecting affinity for the antigen. Both SHM and CSR occur after antigen stimulation of the B cell and are controlled by the B cell specific enzyme activation-induced deaminase (AID; (Maul & Gearhart, 2010; Muramatsu et al., 2000)). AID deaminates cytosine to uracil in single stranded DNA (Dickerson et al., 2003). Depending on how the uracil is processed in the DNA, mutations can occur. Mutations at C:G by AID-dependent insertion of uracil can occur by being left in, resulting in a C to T transition, the uracil could be removed by uracil glycosylase, leading to an abasic site, which can be filled with low fidelity DNA polymerase, resulting in mutation (Petersen-Mahrt et al., 2002). AID also induces staggered nick cleavage in the switch region, which is 5' to constant region coding regions and rich in tandem repeats, allowing looping out deletion of coding regions (Rush et al., 2004). Both functions require different domains of the AID protein (Shinkura et al., 2004).

The production of auto-antibodies (antibodies directed at self-antigens) is avoided through the termination of B cells recognising self-antigens, termed clonal deletion. This is initiated in the bone marrow by the binding of self-antigens to the mlg on the immature B cells. Continuous binding of a self-antigen to the mlg causes arrested development, blocking the acquirement of additional surface molecules, such as IgD, the L-selectin lymph node homing receptor and complement receptors 1 and 2 which are required for the B cell to enter the blood stream and migrate to the spleen and lymph nodes to become mature B cells. This subsequently results in cell death (Hartley et al., 1993).

### **1.2.3 Humoral immune response**

During B cell maturation, the B cells have developed independently of antigens. Once in the spleen and lymph nodes, mature B cells can encounter antigens, triggering a humoral response.

#### **MHC-mediated response**

Mature B cells continually move through secondary lymphoid organs, searching for antigen. Once antigen has been encountered, the B cell acts as an antigen presenting cell (APC) by binding protein antigen via the BcR. Binding of the BcR with antigen and its subsequent activation (as described above) leads to the BcR and antigen being endocytosed. This is followed by the antigen being

processed in the cell, forming small antigenic peptides. B cells then move to the boundary between B and T cell follicles and present antigen to helper T cells in the groove of the major histocompatibility complex (MHC). Specifically, proteolytic peptides from extracellular pathogens are presented by MHC-II to CD4<sup>+</sup> T cells, with peptides from intracellular pathogens being presented by MHC-I to CD8<sup>+</sup> T cells. Polysaccharides are processed into low molecular weight carbohydrates and presented by MHC-II to CD4<sup>+</sup> T cells (Cobb et al., 2004). As well as the co-receptors described earlier, B cells also express CD40, which binds to the CD40 ligand (CD40L) on T cells during antigen presentation. Binding of CD40 to CD40L leads to B cell antibody production directed at the antigen and is essential for the development of B cell memory (Foy et al., 1994; Wu et al., 1995). The importance of CD40-CD40L interaction is observed in the x-linked hyper-IgM syndrome (HIM), which is the result of a mutation in CD40L, resulting in reduced B cell proliferation and low or absent levels of IgG, IgD and IgA (Aruffo et al., 1993).

### **CD1-mediated response**

B cells can also recognise and present lipid antigens in a similar way to peptides, but without the need for T cell help (thymus independent). Lipid antigens are internalised in the same way, but are presented by the MHC-I-like cell surface molecules, cluster of differentiation-1 (CD1). In humans, there are five subsets of CD1 molecules; CD1a, CD1b, CD1c, CD1d and CD1e. Each subset is specialised to bind a specific type of lipid antigen, based on differences in the antigen binding groove (Barral & Brenner, 2007). All mammals tested so far have CD1 molecules, although mice only have CD1d (Barral & Brenner, 2007). CD1 molecules share sequence homology and overall structure with MHC class I molecules comprising of a heavy chain with three extracellular domains that are non-covalently associated with  $\beta_2$ -microglobulin ( $\beta_2m$ ). The overall molecule consists of up to 4 pockets (A', C', F' and T') and antigen portals (C' and F'; (Moody et al., 2005)). The CD1 molecules can be categorised into three groups based on sequence analysis; group 1 consists of CD1a, CD1b and CD1c, group 2 consists of CD1d and CD1e makes up group 3, although CD1e does not have a known function in antigen presentation (Angenieux et al., 2000). Both dendritic cells (DCs; (van den Elzen et

al., 2005)) and B cells can use the low-density lipoprotein receptor (LDL-R) to endocytose apolipoprotein E (ApoE)-bound lipid antigens, with B cells also being able to take up lipid antigens via the BcR (Allan et al., 2009). The lipid antigens are then processed in the cell and loaded onto CD1 molecules in the ER with the help of microsomal triglyceride transfer protein (MTP or MTTP; (Zeissig et al., 2010)). The importance of MTP can be seen in the autosomal recessive disorder abetalipoproteinemia, where mutation in the MTP gene leads to the inability of APCs to present lipid antigens via any of the CD1 molecules (Zeissig et al., 2010). The CD1-lipid complex is then displayed at the cell surface for presentation to T cells. Group 1 CD1 molecules display lipid antigens to CD1-restricted T cells specific for microbial lipid antigens, and have highly diverse  $\alpha$  and  $\beta$  TCR chains. Group 2 (CD1d) molecules are specifically recognised by semi invariant NKT (iNKT) cells. iNKT cells express a semi-invariant  $\alpha/\beta$  TCR with the  $\alpha$  chain being variable (Cohen et al., 2009b). iNKT cells exist in a resting state where they are partially activated, leading to a faster, innate-like response when recognising lipid antigen. Once activated iNKT cells produce IL-4 and IFN- $\gamma$  which leads to activation of DCs (Fujii et al., 2003), which in turn release IL-12, further activating the iNKT cells (Tomura et al., 1999). As well as the fast response and activation of innate immune cells, iNKT cells have also been shown to provide help for B cells, increasing B cell proliferation and Ig production, through the ligation of CD40 and release of IFN- $\gamma$  (Galli et al., 2003; Leadbetter et al., 2008).

### **Differentiation of B cells**

Once activated by antigen and receiving a second signal from helper T cells, B cells can either differentiate into plasma cells, or memory B cells. The level of certain chemokine receptors (CXCR5, CCR7 and CXCR4) expressed on the B cell and the level of their ligands expressed in different areas of the secondary lymphoid organs determine whether the B cells migrate along the germinal centre (GC) pathway or plasmablast pathway. In the GC follicle, B cells differentiate into memory B cells, with the help of follicular helper T cells. The follicular helper T cells provide signals for B cell survival and Ig production (Breitfeld et al., 2000). These B cells are long lived and have high affinity for their antigen and enable the triggering of second immune response. If faced with the same antigen they

are able to divide rapidly into antibody producing cells, generating a faster, longer-lasting and more effective response to the infection. B cells that migrate along the plasmablast pathway to extrafollicular foci differentiate to form plasma B cells (MacLennan et al., 2003). These plasma cells have undergone class switching, but have low levels of hypermutation (Gatto & Brink, 2010).

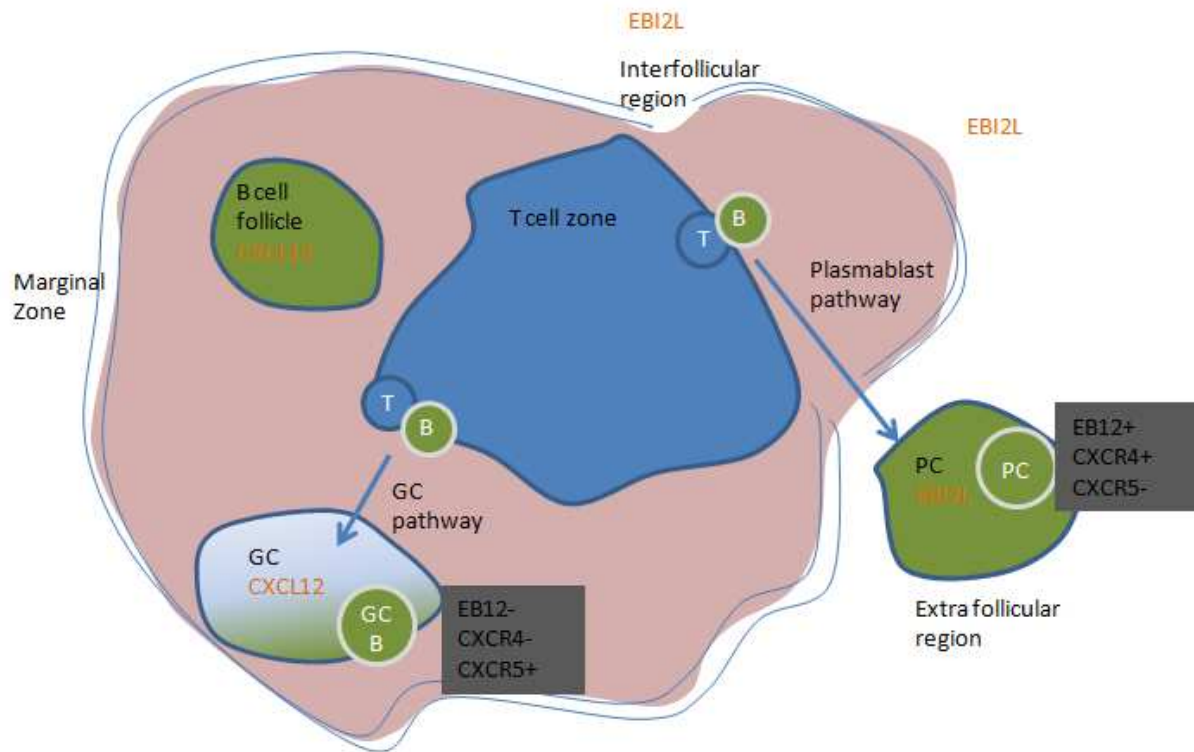


**Figure 1.4 Schematic representation of secondary lymphoid organ in relation to B cell differentiation.** B cells encounter antigen and receive help from helper T cells (Blue) at the B and T cell zone margin. B cells expressing the CXCL12 receptor, CXCR5 and have lost expression of the EB12L receptor, EB12 (Grey box) migrate along the GC pathway to the GC, which is where they undergo somatic hypermutation and class switching, yielding GC memory B cells. B cells without the CXCR5 receptor and positive for the EB12 receptor migrate to extrafollicular regions high in EB12L and differentiate into plasma B cells.

### 1.2.4 Antibody Structure

Antibodies (immunoglobulins) are soluble glycoproteins found in serum and tissue fluids and are produced in response to contact with immunogenic foreign molecules (antigens) as part of adaptive immunity (Schroeder & Cavacini, 2010). Antibodies can be divided into two parts according to their function. The variable fragment (Fv) binds specifically to the antigen epitope and the constant region (Fc) gives effector functions, such as complement activation or binding to Fc receptors on effector cells (Fig 1.5). Each antibody contains 2 Ig-L and 2 Ig-H. The Ig-L is made up of one variable and one

constant region, and the Ig-H is made up of one variable, and 3-4 constant regions. There are 5 classes of human antibody, IgG, IgM, IgA, IgD and IgE (Table 1.1). Each has the same basic four-polypeptide chain structure (Fig. 1.5).

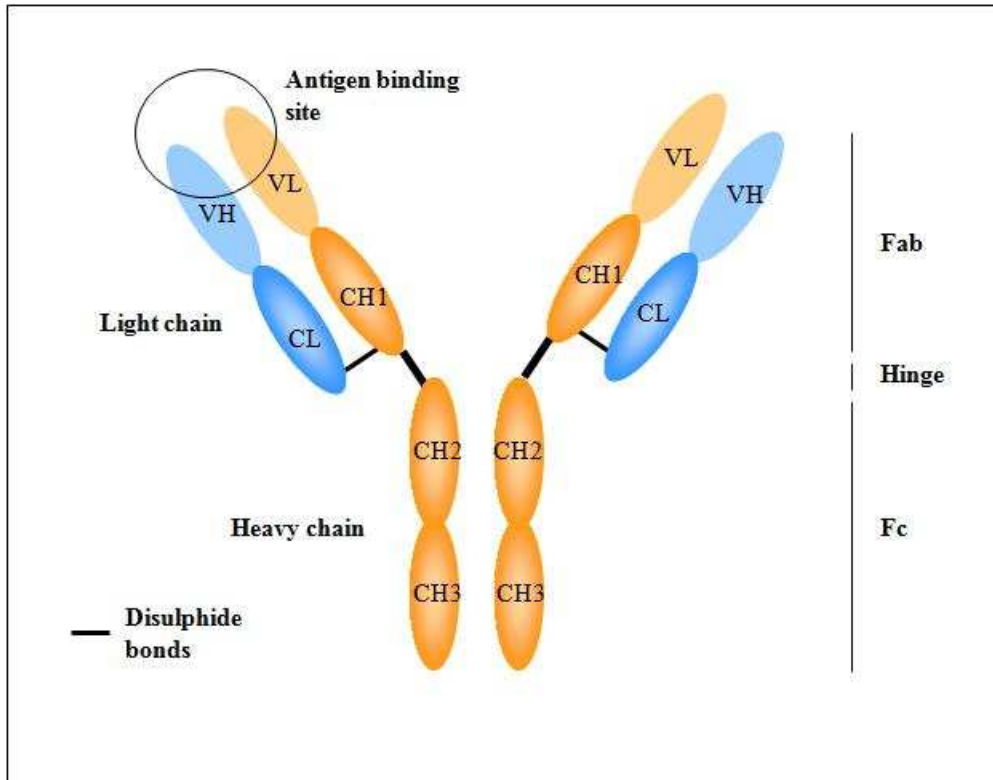


**Figure 1.5 A schematic representation of an antibody.** The antibody is made up of 4 polypeptide chains, 2 light chains (blue) and 2 heavy chains (orange) linked by disulphide bonds. Antigen binding sites (semi-transparent) are located at the amino (N) terminal ends of the chains in the Fab region. The Fc region is responsible for binding C1q and Fc receptors on effector cells.

**Table 1.1 Summary of antibody types.**

Name	Types	Description	Number of monomers
IgA	2	Mucosal areas preventing colonisation of pathogens. Also in saliva, tears and breast milk	1, 2 or 3
IgD	1	Antigen receptor on mature B cells	1
IgE	14	Binds to allergens triggering histamine release.	1
IgG	4	Provides majority of antibody-based immunity against invading pathogens. Only antibody capable of crossing the placenta to foetus	1
IgM	1	Expressed as receptor on B cell. Also secreted in early stages of humoral immunity	5

The principle differences between the classes of antibodies are the amino acid sequence of the heavy chain constant regions and the number of Ig 'monomers' or 'units' that form the antibody structure. The IgM class makes up 10% of total Ig in normal serum and one IgM is a pentamer made

up of five Ig units. This gives it 10 identical antigen-binding sites. It is the predominant antibody in the early primary response in humans and in mice. It can also be found on the surface of B cells (BcR). IgG consists of 4 subclasses (IgG1, IgG2, IgG3 and IgG4) and makes up 75% of total Ig in normal serum (IgG1, IgG2, IgG3, IgG4 are 70%, 20%, 8% and 2% of normal serum IgG). Mouse IgG also consists of 4 subclasses, named IgG1, IgG2a, IgG2b and IgG3. IgG is the predominant antibody in the secondary response in humans. IgGs bind to Fc receptors on lymphocytes and monocytes and act as opsonins. IgA is made up of two subclasses IgA1 and IgA2 and makes up 10% of normal serum total Ig. IgA exists mainly as a monomer in serum but is present as either a dimer or trimer in secretions. It is specialised for transport to areas in which antibody producing B cells are normally absent (e.g. the gut and mucous membranes). IgD is present in the serum at low levels and is present as a monomer. IgD is found on the surface of B cells and is often co-expressed with IgM. It allows specific antigen binding by the B cell leading to proliferation. IgE is also present at low levels in the serum and exists as a monomer. IgE has roles in response to some parasites, hypersensitivity and allergy. Contact of IgE to antigen leads to the release of inflammatory agents, such as histamine. One characteristic of the immune response is that antibodies have the ability to bind specifically to their respective antigen and this is fundamental to an immune response. Each antigen has a set of antigenic determinants, epitopes, which are bound by the antibody. Each antigen may have repeated epitopes (e.g. polysaccharides) or consist of a range of different epitopes (e.g. most proteins). A hapten is a compound of a low molecular weight that is itself not immunogenic, but becomes immunogenic when conjugated to a carrier. The second main characteristic of the immune response is its large diversity.

### **1.2.5 Antibody Glycosylation**

Immunoglobulins are glycoproteins with the number and location of glycosylation varying between antibody isotype (Fig 1.6). Glycosylation of antibodies play an important role in the structure and function of the antibody (Arnold et al., 2007). Glycosylation of antibodies can be N-linked, O-linked

or oligomannose glycans. The most heavily glycosylated isotypes are IgM, IgD and IgE, with Ig-H glycosylation making up 12-14% of total antibody weight. IgG are the most lightly glycosylated with Ig-H glycosylation making up 2-3% of the total weight. The Ig-L is not glycosylated in any of the antibody isotypes (Rudd & Dwek, 1997).

For IgG antibodies, there is a conserved N-linked glycosylation site at asparagine (Asn)-297 on each of the 2 C<sub>H</sub>2 domains. The core of this glycan is conserved throughout the isotype and is made up of a bi-antennary heptasaccharide consisting of N-acetylglucosamine and mannose. Each Asn-297 site displays one of a family of 32 glycans that can be assigned to 3 subsets, giving IgG-G0, IgG-G1 and IgG-G2. IgG-G2 glycans have both arms terminating in galactose residues, IgG-G1 have a galactose missing from one of the arms, exposing a glucosylamine residue and in IgG-G0, neither arm terminates with a galactose, exposing a glucosylamine residue on both arms. IgG-G0, IgG-G1 and IgG-G2 make up 86% of the total IgG serum levels, with the remaining 14% being made up of IgG-G1 and IgG-G2 antibodies with sialylated glycans. Furthermore, the glycan present on Asn-297 can differ within the same molecule. The glycan at Asn-297 has been found to be crucial in maintaining an open conformation of the Ig-Hs allowing interaction of the IgG with C1 in complement activation and Fc-FcγR interactions (Anthony & Ravetch, 2010). The addition of sialic acid to the Asn-297 glycan, present in about 10% of IgG (Arnold et al., 2007) has been shown to act in an anti-inflammatory manner through interaction with the inhibitory FcR, FcRγRIIB. Through the study of a panel of IgG-Fc with truncated glycoforms, Mimura et al., were able to show that glycosylation was key to the thermodynamic stability, quaternary structure and functional activity of IgG (both C1 and FcR (Mimura et al., 2000).

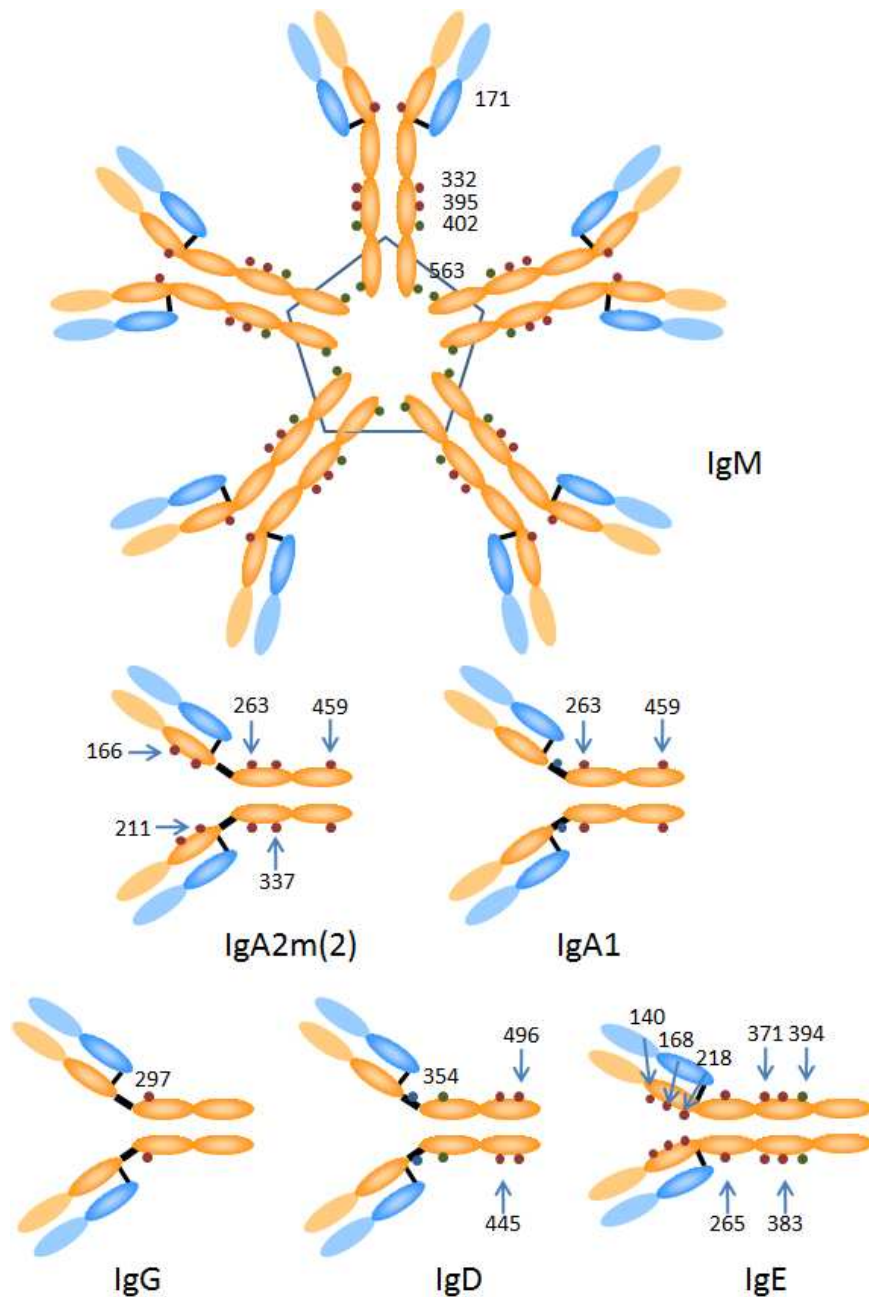


**Figure 1.6 Structure and glycosylation properties of immunoglobulins.** Ig-Ls (blue) and Ig-Hs (orange) interact via disulphide bridges (black). Sites of N-glycosylation (red), oligomannose glycans (green) and clusters of O-glycosylation (blue). Numbers relate to amino acid residues. Figure adapted from (Arnold et al., 2007).

### 1.2.6 Effector mechanisms of antibodies

The first mechanism of antibodies is the recognition of antigen and subsequent internalisation by the BcR, as described above. Once the B cell has been activated and antibody secreted, the antibody can then block the adherence of bacteria to host cells, neutralise toxins and viruses, activate the



complement cascade via the classical pathway (CDC) and activate antibody dependent cell-mediated cytotoxicity (ADCC).

### **1.2.7 Complement**

The complement cascade is a major effector function of the humoral branch of immunity (Reviewed (Lambris et al., 2008; Walport, 2001a; Walport, 2001b)). The cascade consists of more than thirty soluble glycoproteins synthesised mainly by liver hepatocytes, tissue macrophages and epithelial cells of the gastrointestinal (GI) and genitourinary tracts. The components of the cascade interact, activation each other in a regulated enzymatic manner. The complement cascade can be activated via three pathways, the classical, alternative (Kinoshita, 1991) and the lectin route, with all ending with the formation of the membrane attack complex (MAC or terminal complement complex; TCC). The MAC is able to induce lysis of many types of cells, including bacteria and viruses.

### **1.2.8 Complement cascade**

The classical pathway (Fig 1.8a) is initiated by the binding of antibody to its antigen on a whole cell. Binding of the antibody to its antigen results in a conformational change within the Fc region of the IgG or IgM. This exposes a complement binding site, where the complement component C1 can bind. C1 is made up of six identical units of C1q, made up of a globular head with a long collagen-like tail, C1r and C1s (Fig 1.8b). Upon C1 binding to the antibody-antigen complex, C1q followed by C1r undergo conformational changes, activating C1r protease which cleaves C1s. The cleavage of C1s forms an active enzyme which cleaves C4 and C2, leading to the formation of C4a and C4b. These form a complex with C2, C4abC2a. C4abC2a is the C3/C5 convertase of the classical pathway. It is able to cleave multiple C3 and C5 molecules, which magnifies the initial signal.

The alternative pathway activates the complement cascade independently of antibody (Fig 1.8a). It is initiated by various cell surface constituents that are foreign to the host. The alternative pathway is

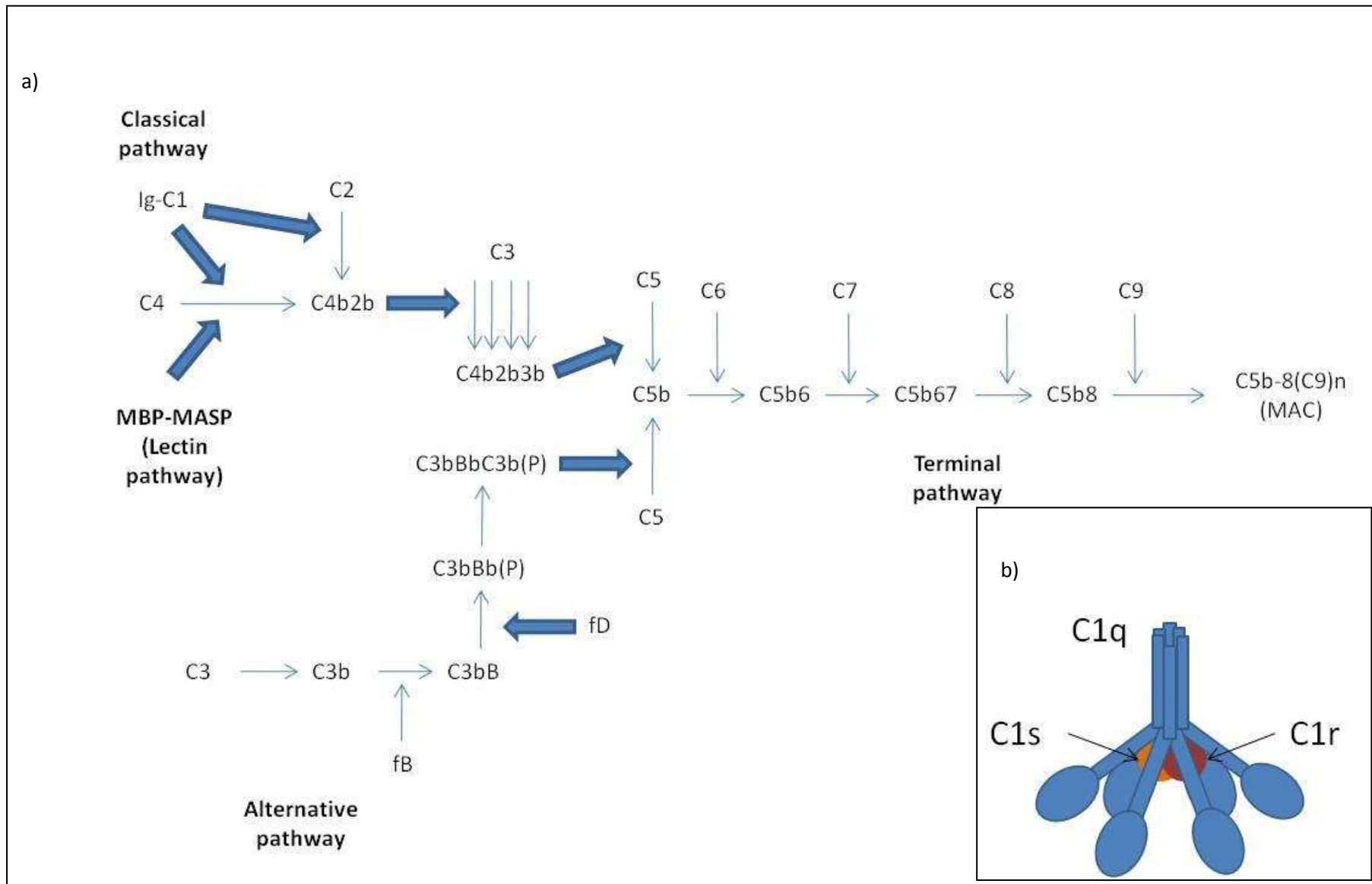


**Figure 1.8 Complement cascade.** The complement cascade (a) is activated by the binding of C1 (b) to the antibody-antigen complex.

continually activated at low levels in the plasma. C3 is present at high levels in the plasma and C3b is produced by spontaneous cleavage of C3. This is possible through the hydrolysis of the thioester bond in C3. C3b is then able to bind to the plasma protein 'factor B'. Factor B is then cleaved by a protease 'factor D', leading to the formation of Ba and Bb. Bb remains associated with the C3Bb complex, resulting in a C3 convertase capable of converting C3 to C3a and C3b. Most of the C3b formed is quashed by hydrolysis, but some attaches covalently to host cells or pathogens. Bound C3b is then able to bind factor B, allowing its cleavage by factor D, giving Ba and Bb. This results in the formation of the alternative pathway C3 convertase C3bBb.

The lectin pathway uses a protein similar to C1q to trigger the complement cascade, the mannose binding lectin (MBL; Fig 1.8a). MBL binds specifically to mannose residues or other sugars arranged in a uniform pattern on pathogens. As host cells do not display mannose-containing molecules in a uniform manner, MBL does not bind to host cells. MBL is a six-headed molecule similar to C1q that associates with mannose-associated serine proteases-1 and -2, which are homologous to C1r and C1s. This complex binds to the pathogen cell surface and activates C4 and C2 in a similar fashion to C1 in the classical pathway, resulting in the same C3 convertase formed from C2b and C4a and b. The formation of C3 convertase is the convergence of all three pathways. In the classical and lectin pathways C5 convertase is formed by the binding of C3b to C4b2b (classical and lectin pathways) or to C3bBb (alternative pathway). C5 then binds to the C3b subunit of the C5 convertase, allowing it to be cleaved by C2b (classical or lectin pathway) or Bb (alternative pathway), forming C5a and C5b. The production of C5b initiates the assembly of the terminal complement components. C5b binds to C6 which is in turn recognised by C7. The C5bC7 complex binds to the membrane of the pathogen as well as to C8 and C9. Polymerisation of C9 enables penetration of the cell membrane, MAC development and the subsequent lysis of the cell.

## Regulation of the complement cascade

Activation of the complement cascade is very rapid, due to the magnification of signal with each step. The natural state of the alternative pathway is to 'tick over' on the surface of all cells. Due to these factors, unregulated activation of the pathway would result in uncontrolled activation of the cascade, causing harm to host cells and the exhaustion of complement proteins. Due to these reasons, the complement cascade is tightly regulated along the cascade. There are three types of complement inhibitory proteins; fluid phase regulators, membrane-bound regulators and membrane-bound complement receptors. Due to the non-specific way that C3b is able to bind to host cells or pathogens, complement-regulatory proteins are present on the surface of host cells, preventing the progression of the complement cascade. Membrane bound complement inhibitory proteins include CD35 (complement receptor 1; CR1), CD21 (complement receptor 2), CD46 (membrane cofactor protein; MCP), CD55 (decay activation receptor; DAF) and CD59. These receptors act to attenuate the activation of the complement cascade.

For example, the glycoprotein CD46 can exist as four isoforms due to alternative splicing and is expressed on all cells. CD46 acts as a cofactor (cofactor activity; CA) for factor 1, cleaving C3b and C4b into enzymatically inactive forms (iC3B and C4c respectively; (Liszewski et al., 1991)). CD55 is also a glycoprotein membrane receptor and can act as a cofactor for CD46, as well as causing decay accelerating activity of convertases (Brodbeck et al., 2000). CD55 can bind to C4bC2b leading to the dissociation of C2a from C4b.

Complement receptors are commonly upregulated on cancer cells, providing a mechanism for tumours to avoid complement mediated cell death (Thorsteinsson et al., 1998; Watson et al., 2006a).

### 1.2.9 Antibody dependent cellular cytotoxicity

ADCC is an important effector function of antibodies that recruit effector cells to kill target cells (Janeway, 2001). When an antibody binds to its antigen on a target cell via the Fab region, it can also bind to an FcR on innate immune effector cells such as basophils, neutrophils, monocytes and macrophages via the Fc region of the antibody. Binding of the antibody to the effector cell causes activation of the cell to release cytokines and cytotoxic granules (Fig 1.9). There are three classes of FcR; Fc $\alpha$ , Fc $\epsilon$  and Fc $\gamma$ . There is only one type of Fc $\alpha$ , Fc $\alpha$ RI, also known as CD89. It is a member of the

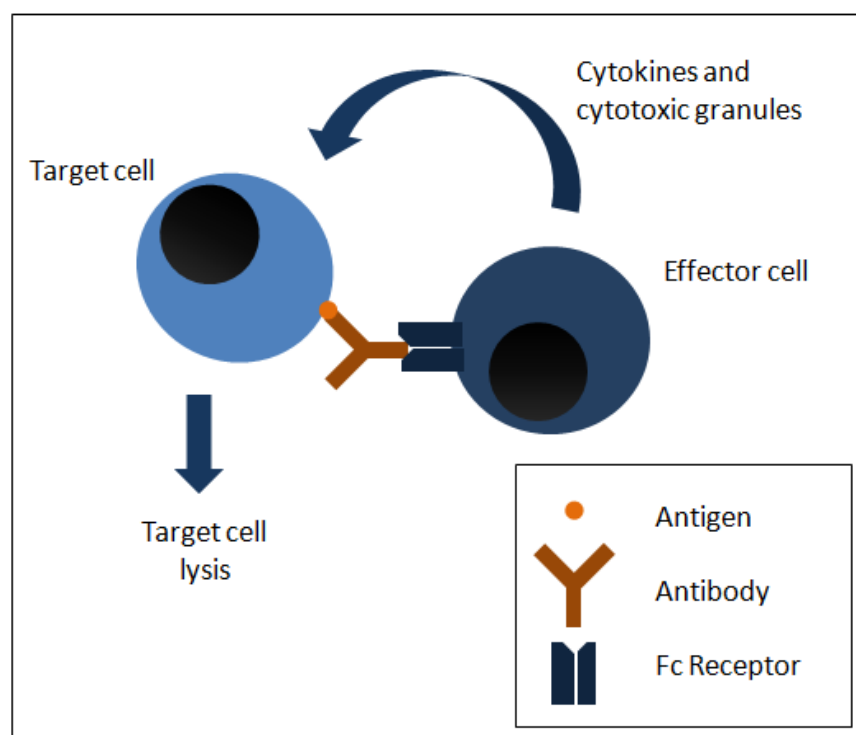


**Figure 1.9 Antibody dependent cellular cytotoxicity.** Upon antibody binding to the antigen on the target cell, an effector cell can be recruited via Fc-Fc receptor binding, leading to the release of cytokines including IFN $\gamma$  and cytotoxic granules containing perforin and granzymes. This results in target cell lysis.

immunoglobulin family and is expressed on neutrophils, eosinophils, monocytes and some macrophages. It binds IgA antibody and signals when coupled to two Fc $\gamma$ R. There are two FcRs belonging to the Fc $\epsilon$  class, one high affinity (Fc $\epsilon$ RI) and one low affinity (Fc $\epsilon$ RII) receptor. The  $\epsilon$  class of receptors are involved in the allergic response and bind IgE. There are six types of Fc receptors for IgG (Fc $\gamma$ R); Fc $\gamma$ RI, Fc $\gamma$ RIIA, Fc $\gamma$ IIB, Fc $\gamma$ RIIC, Fc $\gamma$ RIIIA and Fc $\gamma$ IIIB. Of the six, five are activating

receptors, with FcγRIIB the only known inhibitory receptor (Nimmerjahn & Ravetch, 2008). Each of the receptors are predominantly found on specific cell types, summarised in Table 1.2. There are two types of FcR which can be split based upon their function; activating and inhibiting receptors. FcγRIA, FcγRIIA and FcγRIIIA are activating receptors and function via the ITAM in the intracellular domain of the receptor recruiting activating signalling pathways, whereas the FcγRIIB recruits inhibitory signalling pathways through an ITIM in its cytosolic domain.

**Table 1.2 Summary of human FcR classes.**

Receptor	Antibody Ligand	Affinity	Cell Distribution	Effect of antibody binding
FcαRI	IgA	High	Monocytes Macrophages Neutrophils Eosinophils	Phagocytosis Cell activation Activation of respiratory burst Induction of microbe killing
FcεRI	IgE	High	Mast cells Eosinophils Basophils Langerhan's cells	Release of inflammatory mediators
FcεRII	IgE	Low	B cells Eosinophils Langerhan's cells	Cleavage of receptor forming soluble fragments
FcγRI	IgG	High	Macrophages Neutrophils Eosinophils Dendritic cells	ADCC Endocytosis
FcγRIIA	IgG	Low	Macrophages Neutrophils Eosinophils Platelets Langerhan's cells	Uptake Granule release
FcγRIIB	IgG	Low	B cells Mast cells Macrophages Neutrophils Eosinophils	No uptake Inhibition of stimulation
FcγRIIIA	IgG	Low	NK cells Macrophages	Induction of killing
FcγRIIIB	IgG	Low	Eosinophils Macrophages Neutrophils Mast cells Follicular dendritic cells	Induction of killing

### **1.2.10 Antibody dependent cellular phagocytosis**

Antibody dependent cellular phagocytosis is a mechanism by which either murine IgG3 or human IgG1 can mediate, through low affinity FcγR (FcγRII and FcγRIII), phagocytosis of target cells by monocyte-derived macrophages (Munn et al., 1991).

### **1.2.11 Monoclonal antibodies**

Due to the two main characteristics of antibodies, their high degree of specificity and ability to cause target cell death, research has been targeted at creating antibodies to be used as therapeutics.

### **1.2.12 Monoclonal antibody production**

Monoclonal antibodies can be produced in two ways. The first and most common is a method based upon work carried out in the 1970's by Kohler and Milstein who stated 'Such cultures could be valuable for medical and industrial use' (Kohler & Milstein, 1975). The method involves immunising an animal with antigen, leading to an immune response. The splenocytes from a responsive animal are then fused with myeloma cells using polyethylene glycol (PEG) producing a hybridoma. Splenocytes are unable to survive in culture, leaving the unfused myeloma cells and hybridomas (Kohler & Milstein, 1975). The hybridomas are selected for in hypoxanthine, methotrexate, thymidine (HMT) or hypoxanthine, aminopterin, thymidine (HAT)-supplemented media. Myeloma cells are unable to synthesise the enzyme hypoxanthine guanine phosphoribosyl transferase (HGPRT). HAT and HMT contain aminopterin or methotrexate respectively that block the *de novo* synthesis of DNA. This makes the cells rely on the salvage pathway to synthesise DNA. The salvage pathway requires HGPRT to allow complete synthesis of DNA. Since the unfused myeloma cells do not have the HGPRT enzyme, they are unable to replicate and therefore die, leaving the hybridomas only. The hybridomas maintain the immortal properties of the myeloma cell and secrete antibody. The resulting hybridomas are then grown at low density in multi-well plate format and screened for

binding to antigen. Positive wells are then isolated and re-grown at low density, with the aim of producing a clone of cells from the same hybridoma cell, to produce one mAb. Once a clone has been isolated, the hybridoma is transferred to serum-free media and grown in large quantities to increase antibody production (Glassy et al., 1988).

The second method of antibody production is using the phage-display library method. Gene segments encoding the variable region of antibodies are fused to the genes responsible for the synthesis of the coat protein of bacteriophage. The bacteriophage is then used to infect bacteria, resulting in antigen-binding sites being coated on the outside of the bacteria. A library of different phage each having the ability to display a different antigen-binding site are available. The antigen target is then added, with the bacteriophage that binds to the complementary antigen being selected. The phage can then be used to infect fresh bacteria, to increase phage numbers. The variable genes can then be recovered and joined to genes encoding the rest of the antibody molecule. The gene sequence can then be transfected into cells that secrete the antibody in a similar fashion to hybridomas (Winter & Milstein, 1991).

### **1.2.13 Monoclonal antibodies for therapeutic use**

The first monoclonal antibody used for treatment was described in 1982 (Miller et al., 1982). An anti-idiotypic mAb was used to treat patients with B cell lymphoma with one patient showing a complete remission for a period of 17 years. This finding set off a field of research focussed on the use of antibodies for the treatment of many diseases. Early animal and human trials of mAbs failed to reproduce the results observed in 1982. Despite a large proportion of homology between murine and human Ig, murine mAbs were recognised by the host (e.g. patient) immune system, leading to the development of human anti-mouse antibodies (HAMA), inactivating and removing murine mAbs (Tjandra et al., 1990). Due to the host immune response to murine mAbs, subsequent doses of the mAb could be cleared more quickly. However, adverse effects or symptoms, for example allergic response, upon repeated doses were rare and usually easily reversed (Khazaeli et al., 1994). One



exception to the problems associated with murine mAbs was the transplant rejection mAb, Muromonab-CD3 (Orthoclone OKT-3™) approved in 1986. Muromonab has the ability to reverse the rejection of transplantation when administered intravenously (Fung et al., 1987). Muromonab-CD3 works by binding to CD3 on the surface of mature T cells and due to the association of CD3 with the TCR, muromonab-CD3 blocks the binding of the TCR to antigen, thereby modulating the antigen response to the transplant by blocking antigen recognition and function of cytotoxic T cells (Norman, 1995).

### **Chimerisation of murine mAbs**

Due to the immunogenicity, fast clearance *in vivo* and the weaker ability to induce effector functions, murine mAbs were engineered producing chimeric mAbs (Presta, 2006). Chimeric mAbs are produced by mouse variable regions being cloned into a mammalian expression vector that contains human heavy and light chain constant regions, resulting in a human mAb with mouse variable regions (Birch & Racher, 2006). The production of chimeric mAbs reduced the HAMA response seen with fully murine mAbs, with the first chimeric mAb, abciximab (ReoPro) being approved by the U.S. Food and Drug Administration (FDA) in 1994 (Kohmura et al., 1993). Abciximab is used to inhibit platelet aggregation during percutaneous coronary intervention (also known as coronary angioplasty) by binding the glycoprotein GPIIb/IIIb. Despite fears that the murine variable regions of the chimeric mAb may still be able to produce a HAMA response *in vivo*, chimeric antibodies have been very successful in the clinic with a further four being approved by the FDA for use in the clinic and chimeric mAbs still being entered into clinical trials (Figure 1.10; (Rossi et al., 2010)).

### **Humanisation of murine mAbs**

Despite the success of chimeric mAbs, immunogenicity can be a problem with some mAbs, leading to the production of mAbs with a reduced proportion of murine sequence (Liu et al., 2008). To achieve this, the CDR regions from the murine variable region were spliced into a human antibody,

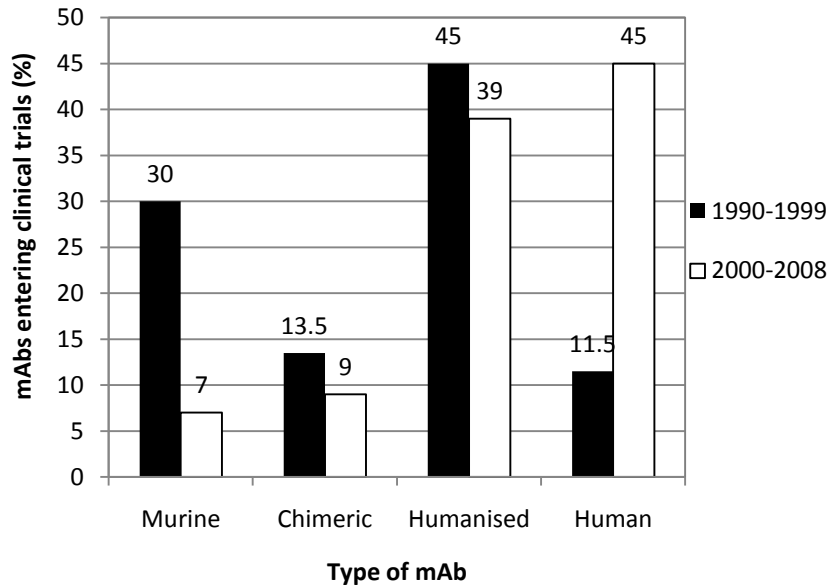


**Figure 1.10 Trends in mAb trials.** Data showing the number of murine, chimeric, humanised and fully human mAbs to enter clinical trials between 1990 and 2008. The figure is adapted from (Nelson et al., 2010).

resulting in mAbs with a greater proportion of human sequence (Jones et al., 1986). Most approved therapeutic antibodies are either chimeric or humanised, with most of new mAbs entering clinical entering clinical trials worldwide being fully human (Figure 1.10; (Reichert, 2008)). Despite the high percentage of human antibody region, humanised antibodies can still be immunogenic, eliciting a human-anti-humanized (HAHA) response *in vivo* (Hwang & Foote, 2005). A study comparing the immunogenicity of murine, chimeric and humanised mAbs revealed that all three types displayed levels of immunogenicity, ranging from 'negligible' to 'marked'. The study also showed that the main impact of humanising on immunogenicity is reduction of the 'marked' category of immunogenicity, with comparable levels of tolerable and negligible immunogenicity with chimerised mAbs (Hwang & Foote, 2005). However, a reduction in immunogenicity after humanising a mAb should not be assumed as one study has shown that despite humanising the anti-glycoprotein murine mAb A33, the humanised mAb (huA33) still showed high levels of HAHA response *in vivo* (Ritter et al., 2001). Further engineering of humanised antibodies has also been employed to reduce HAHA responses, such as removal of T cell epitopes. This is achieved by immunogenic epitopes of the mouse region being replaced with non-T cell reactive sequences reducing the HAHA response. These are known as

deimmunised antibodies (Peng et al., 2005). Fully human mAbs have also been developed by creating transgenic mice. By introducing almost the entire set of human immunoglobulin genes into mice with an inactivated murine antibody system, fully human antibodies can be produced in mice (e.g. HuMab mouse™; (Fishwild et al., 1996)). An example of this is the FDA approved anti-CD20 mAb ofatumumab (Teeling et al., 2004).

Interestingly, a study into the immunogenicity of murine, chimeric and humanised mAbs showed that the most effective reduction in immunogenicity of mAbs was the move from murine to chimeric mAbs, due to most *in vivo* responses targeted at the Fc region (Hwang & Foote, 2005).

### **Engineering of mAbs**

As well as efforts to reduce the immunogenicity of mAbs for therapy by increasing human portion of the mAb, research has focussed on engineering the mAb to increase the *in vivo* effect of mAbs (Kubota et al., 2009). Research is centred on increasing *in vivo* efficacy, by increasing the ability to induce ADCC and CDC and the *in vivo* half-life of the mAb. The first step in the induction of potent ADCC is having the correct isotype. Simply, the choice between IgG1 and IgG2 is made depending on whether effector function is desired (IgG1) or not (IgG2; (Salfeld, 2007)). This is because the IgG1 isotype Fc region has the ability to bind FcγRs on immune effector cells, leading to ADCC as well as binding C1q, initiating CDC. If the use of effector functions is desired, steps can be taken to increase its *in vivo* potency (Strohl, 2009). One mechanism of increasing *in vivo* function centres around the premise that higher levels of therapeutic mAb are required to produce optimal levels of ADCC *in vivo* due to the presence of an excess of endogenous IgG (Preithner et al., 2006). One way in which this can be combated is through the defucosylation of the N-glycosylation in the Fc region at Asn-297 of IgG1 (Okazaki et al., 2004). The N-glycosylation at Asn-297 is a biantennary structure containing a mannosyl-chito-biose core to which GlcNac, fucose, galactose, mannose and/or sialic acid are attached (Yamane-Ohnuki & Satoh, 2009). Removal of the fucose residue at Asn-297 leads to a subtle conformational change, that leads to a increased affinity for the FcγRs, with no effect on antigen affinity or ability to induce CDC (Niwa et al., 2005). This increased affinity for FcγR relates to

an increase in ADCC. The effect of defucosylation on ADCC potency can be over 100-fold, as seen with a defucosylated anti-CD20 mAb produced in a *FUT8* knockout Chinese hamster ovary cell line (Yamane-Ohnuki et al., 2004) or the defucosylated anti-CD20 mAb GA101. GA101 is produced in cells overexpressing the recombinant b1,4-N-acetylglucosaminyltransferase III (GnT-III), which shows greater B cell depletion than rituximab in *ex vivo* CLL samples (Patz et al., 2011). Another example is the anti-CC-chemokine receptor-4 (CCR4) defucosylated mAb KW-0761, which showed highly enhanced ADCC *in vitro* as well as complete and partial responses in patients with relapsed CCR4 positive adult T-cell leukaemia-lymphoma (ATL) or peripheral T-cell lymphoma (PTCL) at 10-20 times lower doses than other mAbs (Yamamoto et al., 2010). As well as the defucosylation of Asn-297, studies have also shown that computational and high throughput screening techniques to produce amino acid-substituted Fc regions with an increased capacity to induce ADCC (Shields et al., 2001). Examples of this include the anti-CD20 mAbs ocrelizumab and AME-133, which have mutated Fc regions and induce enhanced ADCC compared to Rituximab (Weiner et al., 2010).

As well as the ability to induce effector mechanisms, the half-life of a mAb is important in a therapeutic setting. The FcRn plays an important role of IgG homeostasis in mammals and the interaction between IgG Fc region and FcRn is pH-dependent; IgG bind to the FcRn with high affinity at pH 6, but as the pH is raised to 7.4, the binding affinity decreases. If a mAb can bind FcRn at pH 6 with a high affinity, in the acidic endosome, then the mAb would be recycled to the membrane and released, whereas, if the mAb bound with a higher affinity at pH 7.4, it would bind less effectively to the FcRn in the endosome, resulting in the mAb being degraded. Therefore, the ability to bind FcRn at pH 6 results in the prolonged serum half-life of a mAb (Yeung et al., 2009). An example of this is the humanized anti-respiratory syncytial virus (RSV) mAb, MEDI-524-YTE, which has been engineered with a triple amino acid mutation ('YTE') in the Fc region. This lead to a 4-fold increase in serum half-life in cynomolgus monkeys, compared with the unmutated mAb (Dall'Acqua et al., 2006).

Another mechanism of antibody engineering is the production of bispecific mAbs. Bispecific mAbs are engineered to bind to two antigens with one monomer, with each antibody arm specific for a

different epitope. This allows a mAb to inhibit or activate two separate targets. An example is the EU-approved mAb catumaxomab, which is used in the treatment of malignant ascites when other treatment has failed. Catumaxomab binds the adhesion molecule, epithelial cell adhesion molecule (EpCAM) with one arm and the T cell antigen CD3 with the other. This enables the mAb to target tumours by binding EpCAM, which is upregulated on various carcinomas, while simultaneously binding and CD3, stimulating T cells with the other arm. This allows T cell-mediated killing of EpCAM positive tumour cells, as well as Fc region mediated activation of ADCC (Seimetz et al., 2010). However, it relies on the close proximity of tumour and T cells, which may not be achievable in other settings.

#### **1.2.14 Approved monoclonal antibodies**

As of May 2011, there are 23 therapeutic mAbs approved by the FDA, with ten of these targeting cancers (Table 1.3).

##### **CD20**

CD20 antigen is expressed on the surface of all B cells, but not on stem cells, making it an ideal mAb target for lymphoma treatment. Rituximab (Rituxan) was the first mAb to be approved for the treatment of cancer (FDA, 1997; James & Dubs, 1997). Rituximab is a chimeric antibody with human IgG1<sub>κ</sub> constant region and mouse variable regions. The mAb has been shown to induce lysis of CD20+ B cells and is approved for the treatment of CD20+ B cell, non-Hodgkin's lymphoma and for moderately to severe rheumatoid arthritis (FDA, 2002). Studies have shown that rituximab is a very potent inducer of CDC (Cragg et al., 2003) and is also able to induce *in vivo* cell death by ADCC as well as directly inducing cell arrest and death (Cragg et al., 2003; Janas et al., 2005; Pedersen et al., 2002; Shan et al., 1998; van Meerten et al., 2006). Rituximab has been shown to cause direct cell death by cross-linking CD20 and translocation of CD20 to lipid rafts. This creates close-proximity with src-family kinases and induces a number of signalling events including protein tyrosine

**Table 1.3 List of currently FDA approved mAbs. MABs targeting cancers are in bold.**

Year approved by FDA	Product (Trade Name)	Target	Source	Indication
1986	Muromanab-CD3 (Orthoclone®)	CD3	Murine	Transplant rejection
1994	Abciximab (ReoPro™)	GPIIb/IIIb	Chimeric	Percutaneous transluminal coronary angioplasty
<b>1997</b>	<b>Rituximab (Rituxan™)</b>	<b>CD20</b>	<b>Chimeric</b>	<b>B cell lymphoma</b>
1997	Dacliximab (Zenapax®)	IL-2r	Humanised	Transplant rejection
1998	Basiliximab (Simulect®)	IL-2r	Chimeric	Transplant rejection
1998	Infliximab (REMICADE®)	TNF	Chimeric	Crohn's disease, Rheumatoid arthritis
1998	Palivizumab (Synagis™)	Respiratory Syncytial Virus (RSV)	Humanised	RSV in infants
<b>1998</b>	<b>Trastuzumab (Herceptin®)</b>	<b>HER2</b>	<b>Humanised</b>	<b>Breast cancer, prostate cancer lymphomas,</b>
<b>2000</b>	<b>Gemtuzumab ozogamicin (Mylotarg™)</b>	<b>CD33</b>	<b>Humanised</b>	<b>Acute Myelogenous Leukaemia</b>
<b>2001</b>	<b>Alemtuzumab (Campath®)</b>	<b>CD52</b>	<b>Humanised</b>	<b>B cell chronic lymphocytic leukaemia</b>
<b>2002</b>	<b>Irbitumomab tituxetanytiium (Zevalin®)</b>	<b>CD20</b>	<b>Murine with yttrium<sub>90</sub> or indium<sub>111</sub></b>	<b>Non-Hodgkin's lymphoma</b>
2002	Adalimumab (HUMIRA™)	TNF	Human	Moderate to severe rheumatoid arthritis
<b>2003</b>	<b>Tositumomab &amp; Tositumomab I<sup>131</sup> (Bexxar®)</b>	<b>CD20</b>	<b>Murine with Iodine<sub>131</sub></b>	<b>Low grade Non-Hodgkin's Lymphoma</b>
2003	Omalizumab (Xolair®)	IgE	Humanised	Severe (allergic) asthma
<b>2004</b>	<b>Cetuximab (Erbix™)</b>	<b>EGFR</b>	<b>Chimeric</b>	<b>Colorectal cancer, head and neck cancer</b>
<b>2004</b>	<b>Bevacizumab (Avastin™)</b>	<b>VEGF</b>	<b>Humanised</b>	<b>Metastatic colorectal cancer, non-small cell lung cancer, metastatic breast cancer</b>
2004	Natalizumab (TYSABRI®)	α4 subunit of α4β1	Humanised	Multiple sclerosis, Crohn's disease

<b>2006</b>	<b>Panitumumab (Vectibix™)</b>	<b>EGFR</b>	<b>Human</b>	<b>Metastatic colorectal cancer</b>
2006	Ranibizumab (LUCENTIS™)	VEGF-A	Humanised Fab	Wet Macular Degeneration
2007	Eculizumab (Soliris®)	CD59	Humanised	Paroxysmal nocturnal hemoglobinuria
2008	Certolizumab pegol (CIMZIA®)	TNF-α	Humanised Fab	Morbus Crohn, rheumatoid arthritis
2009	Golimumab (Simponi™)	TNF-α	Human	Rheumatoid & psoriatic arthritis, active ankylosing spondylitis
2009	Ustekinumab (Stelara™)	IL12/IL23	Human	Moderate to severe psoriasis
2009	Canakinumab (Ilaris®)	IL-1β	Human	Cryopyrin-associated periodic syndrome
2009	Denosumab (Prolia™)	RANKL	Human	Postmenopausal women with risk of osteoporosis
<b>2009</b>	<b>Ofatumumab (Arzerra®)</b>	<b>CD20</b>	<b>Human</b>	<b>Chronic lymphocytic leukaemia</b>
2010	Belimumab (Benlysta®)	BlyS	Human	Systemic lupus erythematosus
<b>2011</b>	<b>Ipilimumab (Yervoy)</b>	<b>CTLA-4</b>	<b>Human</b>	<b>Malignant melanoma</b>

phosphorylation, activation of protein kinase C and upregulation of Myc (Shan et al., 1998). This lipid raft recruitment has been shown to lead to calcium ion (Ca<sup>2+</sup>) influx and cell death in target cells (Janas et al., 2005).

As CD20 had been shown to be a good target for the mAb therapy, the murine parent molecule of rituximab has been used in radioimmunotherapy. The rituximab murine mAb was linked to tiuxetan, a chelating agent that provides a high affinity binding site for radionuclides. To this site, <sup>90</sup>yttrium (<sup>90</sup>Y) has been conjugated, forming the mAb <sup>90</sup>Y-irbritumomab (Zevalin) that was approved by the FDA in 2002 for cancer therapy (Stern & Herrmann, 2005). The murine parent of rituximab was chosen as its higher immunogenicity promotes a more rapid clearance of the antibody from the circulation. <sup>90</sup>Y-irbritumomab is used to treat low grade non-Hodgkin's lymphoma (NHL). It can cause

tumour cell death induced by  $\beta$ -particles from  $^{90}\text{Y}$  or by the induction of apoptosis in a similar fashion to rituximab.

$^{131}\text{I}$ -tositumomab (Bexxar™) is a murine IgG2a, anti-CD20 mAb that is used for the treatment of NHL (Cheung et al., 2009). Patients receive a dose of unconjugated tositumomab, before receiving further doses of the radiolabelled  $^{131}\text{I}$ -tositumomab. The  $^{131}\text{I}$  isotope enables tositumomab to deliver gamma photons and beta particles directly to the tumour and surrounding area, as well as inducing ADCC and CDC (Davis et al., 2004; Stern & Herrmann, 2005). Tositumomab has also been shown to induce direct cell death in CD20+ cell lines (Cardarelli et al., 2002).

Fundamental differences between rituximab and tositumomab allow them to be split into two groups; type I (rituximab) and type II (tositumomab; (Cragg & Glennie, 2004). Type-I anti-CD20 mAbs have the ability to translocate CD20 into lipid rafts, whereas, type II mAbs do not. Differences in their effector functions has also been noted (Cardarelli et al., 2002; Cragg et al., 2003), leading to debate as to which type of antibody would be better therapeutically. Tositumomab shows a higher level of direct cell death than rituximab (Cardarelli et al., 2002), whereas, rituximab is a more potent inducer of CDC *in vitro* than tositumomab, due to its ability to redistribute to lipid rafts, creating a high concentration of mAb (Cragg et al., 2003). However, it has been suggested that the potent induction of CDC by rituximab *in vivo* may lead to the reduction of CD20 molecules on the B cell as a result of C3b deposition after type-I mAb binding, due to the shaving reaction (Li et al., 2007). Furthermore, deposited C3b may inhibit interaction between the Fc region of rituximab and the CD16 receptor on natural killer (NK) cells, reducing the activation of NK cells (Wang et al., 2008). Therefore, the efficiency of CDC mediated by rituximab may reduce the level of CD20 on the surface of B cells and also block ADCC, thereby reducing the efficacy of Rituximab *in vivo*. However, type-II anti-CD20 mAbs do not induce CDC. More recently, rituximab and tositumomab were compared for *in vivo* efficacy by engineering type-I and type-II mAbs with the same mouse isotype. In this study, the level of B cell depletion was measured and the type-II mAb provided a longer depletion of B cells from the



blood and secondary lymphoid organs than the type-I mAb, suggesting that type-II anti-CD20 mAbs may be better in the treatment of B cell diseases (Beers et al., 2008).

Differences in the mechanism of cell death induced by rituximab and tositumomab have also been observed. Studies have shown that rituximab induces direct cell death in a caspase-independent manner, with the influx of  $\text{Ca}^{2+}$  being noted as an important factor (Daniels et al., 2008; Stanglmaier et al., 2004). Whereas tositumomab-mediated cell death has been shown to occur in a more classical-apoptotic manner, when the mAb is cross-linked on the cell surface (Shan et al., 1998).

More recently, ofatumumab (Arzerra or HuMax-CD20, previously 2F2), a fully human IgG1 mAb, produced in transgenic mice and was approved for the treatment of two groups of patients with chronic lymphocytic leukaemia; those refractory to fludarabine and alemtuzumab and patients not considered for alemtuzumab treatment by the FDA under the accelerated approval process (FDA, 2009). Ofatumumab binds to the small loop epitope of CD20 (differently to rituximab and tositumomab). Ofatumumab has been characterised as a type I anti-CD20 mAb due to its ability to recruit CD20 to lipid rafts (Teeling et al., 2004). As expected of a type I anti-CD20 mAb, ofatumumab induces CDC, however, ofatumumab is a more potent inducer of CDC than rituximab *in vivo* due to its slower rate of dissociation from the antigen (Teeling et al., 2004; Teeling et al., 2006). A recent abstract at the American Society of Hematology showed that ofatumumab can also induce ADCC at lower antibody concentrations than rituximab *in vitro* when human peripheral blood mononuclear cells (PBMCs) were incubated with ARH-77 lymphoma cells and mAb (Craig, 2009). A number of clinical studies have been undertaken using ofatumumab in chronic lymphocytic leukaemia (CLL) and follicular lymphoma (FL) with response rates ranging from 11 to 58% (Lin, 2010). Despite being a fully human mAb, some adverse effects have been observed upon mAb administration. Most commonly; neutropenia, pneumonia, pyrexia, cough, diarrhoea, anaemia, fatigue, dyspnoea, rash, nausea, bronchitis, and upper respiratory tract infections (FDA, 2009). Larger clinical trials will provide a better understanding on the efficacy of ofatumumab in a clinical setting.

## HER2

Trastuzumab (Herceptin) is a humanised IgG1<sub>k</sub> derived from a murine mAb (Stancovski et al., 1991) and produced in Chinese hamster ovary cells (Goldenberg, 1999). Trastuzumab targets the tyrosine kinase receptor, human epidermal growth factor receptor 2 (HER2) which is overexpressed on 25-30% of breast cancers due to gene amplification (Slamon et al., 1987). Trastuzumab was approved for the treatment of metastatic breast cancer patients whose tumours overexpress the HER2 protein in 1998 (FDA, 1998) and is now approved for adjuvant treatment of HER-2-overexpressing node positive or node negative breast cancer as well as in combination with chemotherapy for HER2-overexpressing metastatic gastric cancer patients (FDA, 2010). HER2 cannot dimerise itself and has no ligand binding site. It can however dimerise with other members of the HER family and has an intracellular signalling domain. The most common heterodimer is HER1/2 and the most potent is HER2/3 (Olayioye et al., 2000). Trastuzumab acts by blocking HER2, thereby inhibiting dimerisation and activation of the receptor by epidermal growth factor (EGF), transforming growth factor  $\alpha$  (TGF $\alpha$ ) and other growth factors (Valabrega et al., 2007). This inhibits intracellular signalling via PI3K and AKT, reducing cell proliferation and can increase apoptosis (Delord et al., 2005). Trastuzumab has also been shown to inhibit angiogenesis (Klos et al., 2003). Trastuzumab is also thought to inhibit HER2 cleavage and subsequent release into the serum (Molina et al., 2001). Although research has mainly focussed on the mechanism by which trastuzumab blocks the HER2 receptor and the impact that has on cell proliferation and death, trastuzumab is also an IgG1 and therefore has the ability to induce ADCC. Studies have shown that trastuzumab can induce ADCC *in vitro* and *in vivo* (Gennari et al., 2004; Gianni, 2008). As previously described, engagement of effector cells with the mAb-tumour cell complex is mediated via FcR on the effector cells via the antibody Fc region. A study showed a decreased level of trastuzumab activity in Fc $\gamma$ R knockout mice compared to wild-type, suggesting that the induction of ADCC has an important role *in vivo* (Clynes et al., 2000). Furthermore, a recent study showed that polymorphisms in Fc $\gamma$ R11a had a significant effect on clinical outcome of patients treated with trastuzumab, with patients homozygous for Valine/Valine at amino acid 158 having the

best clinical outcome, due to a higher affinity between antibody and the Valine-containing FcR on effector cells (Musolino et al., 2008).

More recently, the humanised IgG1 anti-HER/2 mAb, pertuzumab (2C4, Omnitarg) has been shown to inhibit dimerisation of HER2 *in vivo*, by binding at a different site on HER/2 to trastuzumab, thereby blocking intracellular signalling (Adams et al., 2006). Recent trials of pertuzumab administered in combination with trastuzumab in patients who progressed after trastuzumab treatment have shown promising results, with an objective response rate of 24.2% in 66 patients (Baselga et al., 2010).

### **CD33**

Gemtuzumab ozogamicin (Mylotarg) is a humanised IgG4 antibody conjugated to the anti-tumour drug calicheamicin  $\gamma^1$ . Gemtuzumab binds to CD33, a myeloid-specific, transmembrane receptor that binds sialic acids and is involved in cell adhesion. More significantly, it is expressed on leukemic blast, but not haematopoietic stem cells in most (~90%) acute myeloid leukaemia (AML) patients (Dinndorf et al., 1986). In order to increase the potency of mAb treatment, calicheamicin  $\gamma^1$  was conjugated to gemtuzumab (Sievers et al., 1999). Calicheamicin  $\gamma^1$  belongs to the enediyne class of antibiotics isolated from the bacteria *Micromonospora echinospora* (Zein et al., 1988). Calicheamicin contains an enediyne moiety that binds and cleaves double stranded DNA in a site specific manner, resulting in apoptosis of the cell (Walker et al., 1992). Gemtuzumab ozogamicin was approved for the treatment of acute myelogenous leukaemia in 2000. Unfortunately, a post-approval trial failed to show any clinical benefit of the gemtuzumab ozogamicin compared with chemotherapy alone with several deaths occurring in the groups of patients receiving gemtuzumab. As a result of this trial, the mAb was withdrawn from therapy in the US and UK in June 2010 (FDA, 2010).

### **CD52**

Alemtuzumab (Campath), a humanised rat IgG1 $\kappa$  binds to CD52, a glycosylphosphatidylinositol (GPI)-anchored protein expressed on mature lymphocytes, but not on stem cells (Hale et al., 1988; Hernandez-Campo et al., 2007). It has a good therapeutic value due to CD52 expression on all low

grade B cell lymphomas and most high grade B cell NHLs (Salisbury et al., 1994). Alemtuzumab is used in the treatment of B cell chronic lymphocytic leukaemia, the most common adult leukaemia in the western hemisphere and is undergoing clinical trials for the treatment of multiple sclerosis (Barten et al., 2010; Ries et al., 2000). Alemtuzumab has been shown to cross-link CD52 on the cell surface, leading to growth inhibition and subsequent cell death (Rowan et al., 1998), although research suggests that direct cell death is not the prominent mechanism of action *in vivo* (Zent et al., 2008). More significantly *in vivo* is alemtuzumab's ability to induce CDC and ADCC (Golay et al., 2004; Hu et al., 2009; Zent et al., 2008).

## **EGFR**

Cetuximab (Erbix) was the first monoclonal antibody approved for the treatment of advanced colorectal cancer (2004; (FDA, 2004)). Since its approval for colorectal cancer it has also been approved for the treatment of head and neck cancers (FDA, 2006). Cetuximab is a chimeric IgG1 that blocks EGFR (Goldstein et al., 1995). The mechanism of action centres around its ability to bind to the EGFR with a higher affinity than EGF (Goldstein et al., 1995). This blocks the phosphorylation of the EGFR and inhibition of the RAS/RAF/MAPK, STAT, and PI3K/AKT signalling pathways (El-Rayes & LoRusso, 2004). This effects cell cycle progression, reduces angiogenesis, promotes apoptosis and decreases proliferation (Baselga, 2001; Mukohara et al., 2005; Peng et al., 1996). As well as inhibition of EGFR signalling, cetuximab has also been shown to induce ADCC, but not CDC *in vitro* (Kawaguchi et al., 2007; Kimura et al., 2007).

Panitumumab (Vectibix; formally ABX-EGF) is a fully human IgG2 monoclonal antibody and was developed using XenoMouse technology (Yang et al., 2001). It was approved for use in the treatment of advanced colorectal cancer in 2007. Panitumumab binds to the EGFR with a very high affinity, therefore, the inability of the IgG2 mAb to induce potent ADCC and CDC responses should reduce toxicity to normal cells. Upon binding, panitumumab blocks the binding of EGFs and causes internalisation of the receptor, preventing downstream signalling (Yang et al., 2001). This leads to

inhibition of cell cycle progression, reduces angiogenesis, promotion of apoptosis and decreases proliferation. As a fully human mAb, the frequency of infusion reactions has been lower than observed in comparison to cetuximab (Cohenuram & Saif, 2007).

## **VEGF**

Bevacizumab (Avastin) is a humanised IgG1 mAb that reacts with and neutralises vascular endothelial growth factor (VEGF). It was approved for the treatment of metastatic colorectal cancer in 2004 (Hurwitz et al., 2004) and for the treatment of nonsquamous, non-small cell lung cancer (NSCLC) in 2006 (Cohen et al., 2007) and for the treatment of glioblastoma multiforme (GBM; (Cohen et al., 2009a)). VEGF is upregulated in many tumours and bevacizumab is thought to have anti-vascular effects *in vivo* (Willett et al., 2004). Specifically by decreasing vascular volume and microvascular density, and alteration of blood flow, restoring normality (Willett et al., 2004). More recently, bevacizumab has been trialled in ovarian cancer with promising results, which may prompt Roche to apply for FDA approval of bevacizumab for the treatment of ovarian cancer (Roche, 2011).

## **CTLA-4**

Ipilimumab is a fully human mAb approved by the FDA for the treatment of malignant melanoma in March 2011 (Ledford, 2011). Ipilimumab's target is the inhibitory receptor cytotoxic T lymphocyte antigen-4 (CTLA-4) present on T cells (Krummel & Allison, 1995). The mAb does not induce ADCC or CDC, but by blocking CTLA-4, T cell activation is increased, allowing a tumour targeted T cell response via APC presented melanoma antigens (Tarhini et al., 2010). Unsurprisingly, the non-specific upregulation of T cell activation can lead to severe side effects, which need to be carefully monitored. However, despite adverse effects, studies have shown an increased survival in stage III and IV melanoma patients when compared to gp100 alone (a melanoma antigen). Patients received either ipilimumab, gp100 or both, with both ipilimumab groups showing a significantly greater survival compared to the gp100 group (21.6%, 23.5% and 13.7% at 24 months (Hodi et al., 2010))

All currently approved mAbs recognise protein antigens; however, mAbs recognising glycolipids are becoming increasingly interesting.

### 1.3 Glycolipids

The term lipid describes a molecule that is insoluble in water, but is soluble in organic solvents. Lipids can be roughly separated into three groups; simple or neutral lipids, complex lipids and proteolipids. Simple lipids can be segregated into the groups, fatty acids, waxes, triglycerides and sterols. Complex lipids have polar properties and can be divided into; phospholipids, arsonolipids, glycolipids and lipoamino acids. The third group of lipids are proteolipids, which are fatty acylated proteins.

The human cell membrane is made up predominantly of phospholipids, which form a bilayer due to their hydrophilic, phosphate-containing head and hydrophobic fatty-acid tails. Lipids make up ~50% of an animal cell membrane which relates to about  $10^9$  lipid molecules per cell (Alberts, 2002). Glycolipids consist of a lipid tail with a carbohydrate head (Fig 1.11) and constitute about 5% of lipid molecules in the outer monolayer (Alberts, 2002).

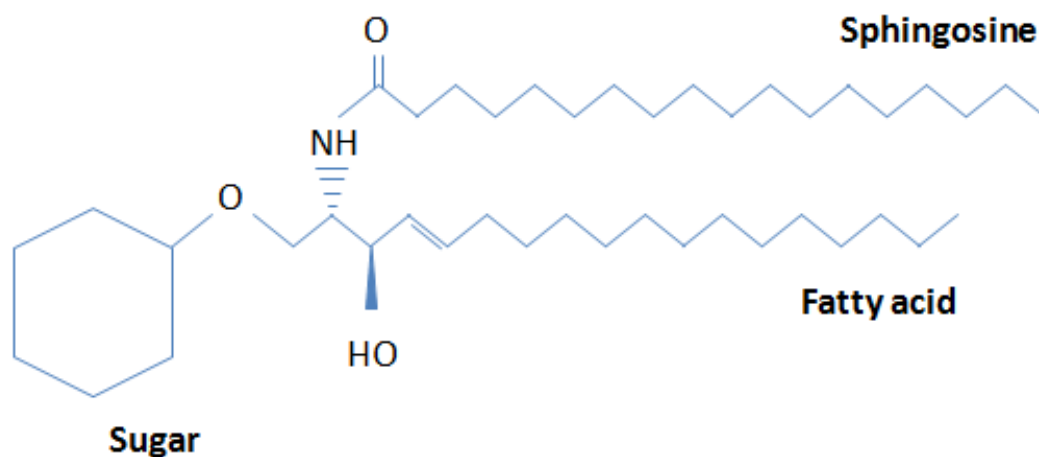


**Figure 1.11 A glycolipid.** Glycolipids consist of two lipid tails (fatty acids or fatty acid and sphingosine) and a polar glycosylated head (sugar).

**Table 1.4 Types of glycolipid and their function.**

Type of glycolipid	Lipid base	Sub-classes	Location	Function
<b>Glycoglycerolipid</b>	Glycerol	Neutral glyco- glycerolipids Glycophospholipids Sulfoglyco- glycerolipids	Chloroplast of plants and algae, mucosal lining of stomach	Mechanical and chemical protection
<b>Glycosylphosphatidylinositols (GPI)</b>	Dilichols (poly prenyls)	Variations on glycan side chains Lipid anchor variation; diacylglycerol, alkylacylglycerol or ceramide	Outer leaflet of membrane (Associate with lipid rafts)	Anchors proteins to membrane via phosphoethanolamine linker
<b>Glycosphingolipids (GSL)</b>	Ceramide	Lacto Series Globo Ganglioside Galactosylceramide	Outer leaflet of membrane (associate with glycosynapses)	Associate with functional proteins Role in cell adhesion, motility, growth

Glycolipids can be divided into three main groups, glycoglycerolipids, glycosylphosphatidylinositols (GPI) and glycosphingolipids (GSL) based on the type of lipid component (Table 1.4). Glycoglycerolipids are lipids consisting of either mono or oligosaccharides linked to the hydroxyl group of glycerol, these are mainly found in plants, algae and bacteria where they are involved in photosynthetic membranes, but can also be found in animals, although expression is limited (Holzl & Dormann, 2007). In humans, they are normally found in the testes and nervous system and stomach wall at low levels, however, they have been observed in the colorectal carcinoma cell line HT29 (Pahlsson et al., 2001). They are important membrane components, sulphated glycoglycerolipids are an important factor in the mucosal lining of the stomach wall, protecting it from mechanical and chemical damage (Urich, 1994). GPIs contain a carbohydrate or glycosyl groups linked to phosphatidylinositols. They are widespread in nature and are a post-translational modification of many proteins, positioned at the C-terminus of the protein, allowing anchoring of the protein to the outer leaflet of the cell membrane (GPI-anchored proteins; (Paulick & Bertozzi, 2008)). They are known to partition to lipid rafts, and be involved in signal transduction. For example GPI-anchored proteins play an important role in TCR signalling (Horejsi, 2003). They have been shown to be

involved in prion diseases and are important for the amplification and spread of prion activity from cell to cell (Bate et al., 2010; Priola & McNally, 2009). GSLs are a major component of the human plasma membrane and are normally found in the outer membrane of cells. Approximately 300 different GSL have been identified and they, along with glycoproteins form a layer of carbohydrates over the cell membrane, protecting the cell from chemical and mechanical damage (Chester, 1998; Varki, 1993). As well as the protection of cells, research has shown that GSLs perform a range of functional roles on the cell surface and subsequent signalling (Hakomori Si, 2002). They have also been implicated in a number of diseases, including cancer and GSL-lysosomal storage diseases (Ginzburg et al., 2004; Hakomori & Zhang, 1997).

### **1.3.1 Synthesis and structure of GSL**

GSL biosynthesis begins with ceramide (a sphingosine and a fatty acid). Ceramide is synthesised through one of three pathways (Fig 1.12). The first involves the hydrolysis of sphingomyelin and is catalysed by a group of enzymes named sphingomyelinases (SMases). SMases are distinguished by different pH optima and therefore referred to as acid, neutral or alkaline SMases (Levade & Jaffrezou, 1999). SMases are rapidly activated by diverse stress signals (Ballou et al., 1996). In turn, SMase hydrolyses the phosphodiester bond of sphingomyelin forming ceramide and phosphocholine (Levade & Jaffrezou, 1999). The *de novo* pathway of ceramide involves the condensation of pantoic-CoA and serine by serine pantoic transferase to form 3-keto-dihydrosphingosine. In turn, 3-keto-dihydrosphingosine is reduced to dihydrosphingosine. This is then acylated to produce dihydroceramide. Finally, formation of ceramide is completed by dihydroceramide desaturase which removes the two hydrogen atoms (Merrill et al., 1997). The third pathway involves the degradation of sphingolipids and glycosphingolipids in endosomes and lysosomes. Fragments of the plasma membrane containing GSLs to be degraded are endocytosed and traffic to lysosomes (Sandhoff & Kolter, 1996). In the lysosomes, GSLs are de-glycosylated by exohydases, which cause the stepwise release of monosaccharides from the sphingolipid. The sphingomyelin is then converted to ceramide



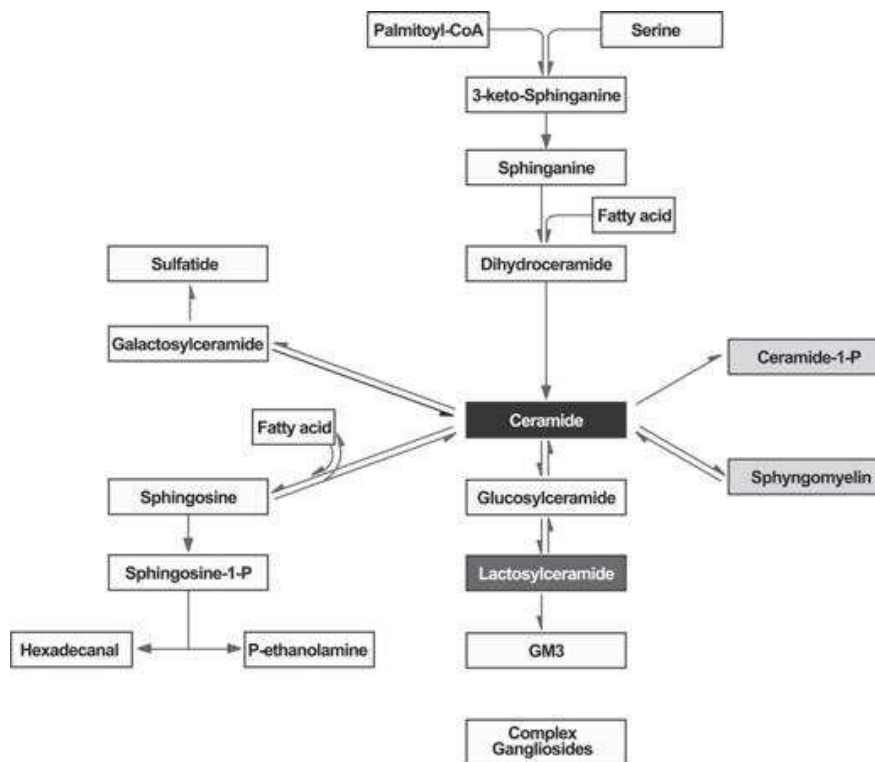


**Figure 1.12 Schematic diagram of ceramide synthesis through various pathways.** De novo synthesis involves the condensation of palmitoyl-CoA and ceramide. Ceramide can also be scavenged through the hydrolysis of sphingomyelin or through the condensation shingolipids or Synthesis of ceramide. Figure taken from (Won et al., 2007).

by SMase, as in the sphingomyelin hydrolysis pathway (Kitatani et al., 2008). Once ceramide has been synthesised through the various pathways, it has an important role as a second messenger in a variety of cellular pathways, including apoptosis, senescence, differentiation, proliferation and cell cycle arrest (Mathias et al., 1998). As well as its role in cell physiology, ceramide acts as the base of GSLs. Most commonly, a glucose (Glc) is added to the ceramide by the Type I transmembrane protein glucosylceramide (GlcCer) synthase, forming GlcCer (Ichikawa & Hirabayashi, 1998; Sprong et al., 1998). Galactose (Gal) is then added to GlcCer by  $\beta$ -1,4-galactosyltransferases forming lactosylceramide (LacCer) in the lumen of the Golgi apparatus (Fig 1.13; (Lannert et al., 1994; Won et al., 2007)). LacCer is the acceptor for various transferases that generate three major classes of GSLs; Lacto(neo), globo series and gangliosides (Fig 1.14; (Hettmer et al., 2004)). Alternatively, Gal can be added to the ceramide forming GalCer which in turn leads to the synthesis of less common structures, including GM4 and sulfatide (Fig 1.14; (Won et al., 2007)).

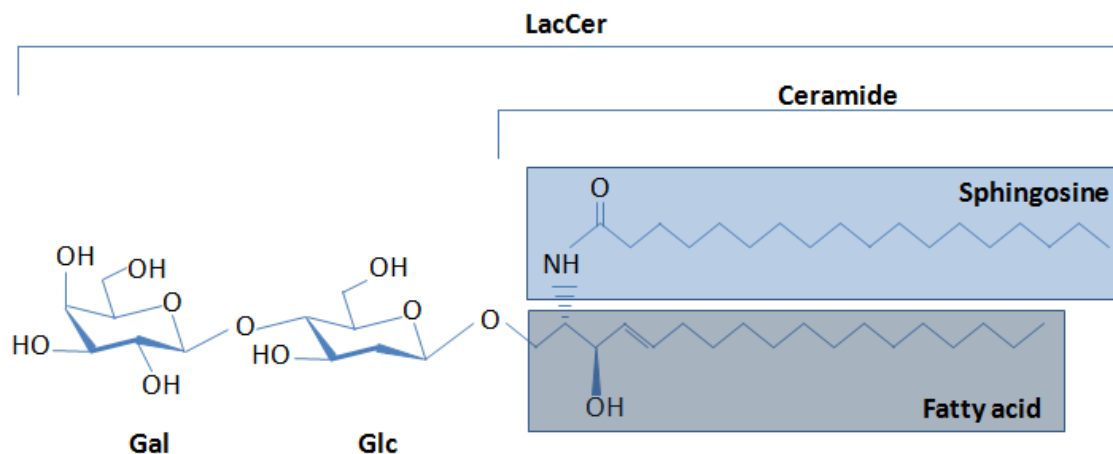


**Figure 1.13 The structure of LacCer.** The core complex for most GSLs. Ceramide is produced through the sphingomyelin hydrolysis, *de novo* or salvage pathways and is made up of sphingosine and a fatty acid. To the ceramide Glc is added followed by Gal, producing LacCer. The addition of more monosaccharides can produce hundreds of different GSLs. Alternatively Gal can be added before Glc to the ceramide producing GalCer.

### 1.3.2 Function of GSLs

As established above, GSLs perform many functions on the surface of cells. One main characteristic of GSLs that allows them to perform such versatile roles is their ability to form clusters. These clusters are able to interact with functional molecules on the cell surface. These clusters are termed 'glycosynapses' and have been characterised using a range of cancer cell lines *in vitro*, (Fig 1.15;(Hakomori, 2002)). Significantly, they have contrasting properties with lipid rafts (Table 1.5), another form of cluster present on the cell surface involved in signal transduction, studied using living cells *in vitro*, for example, B and T cells and a number of cancer cell lines (Lingwood & Simons, 2010). Glycosynapses rely on the ability of GSLs to bind via cis-carbohydrate to carbohydrate interactions, forming clusters in membrane and interact with functional proteins. Currently 3 types of glycosynapses have been described. "Glycosynapse 1" represents a GSL-GSL or GSL-binding protein interactions between cells, mediated by the glycosyl epitope of the GSL. The GSL are associated with signal transducers and are also stabilised by proteolipid protein. "Glycosynapse 2" is the term used for cell to cell adhesion based on O-linked mucin-type glycoproteins that are recognised by carbohydrate binding proteins. The O-linked glycans and the recognising proteins are associated with signal transducers. "Glycosynapse 3" refers to the adhesion of a cell to the

extracellular membrane (ECM), which is mediated by N-glycosylated adhesion receptors complexed with tetraspanin and GSL (Mitsuzuka et al., 2005).

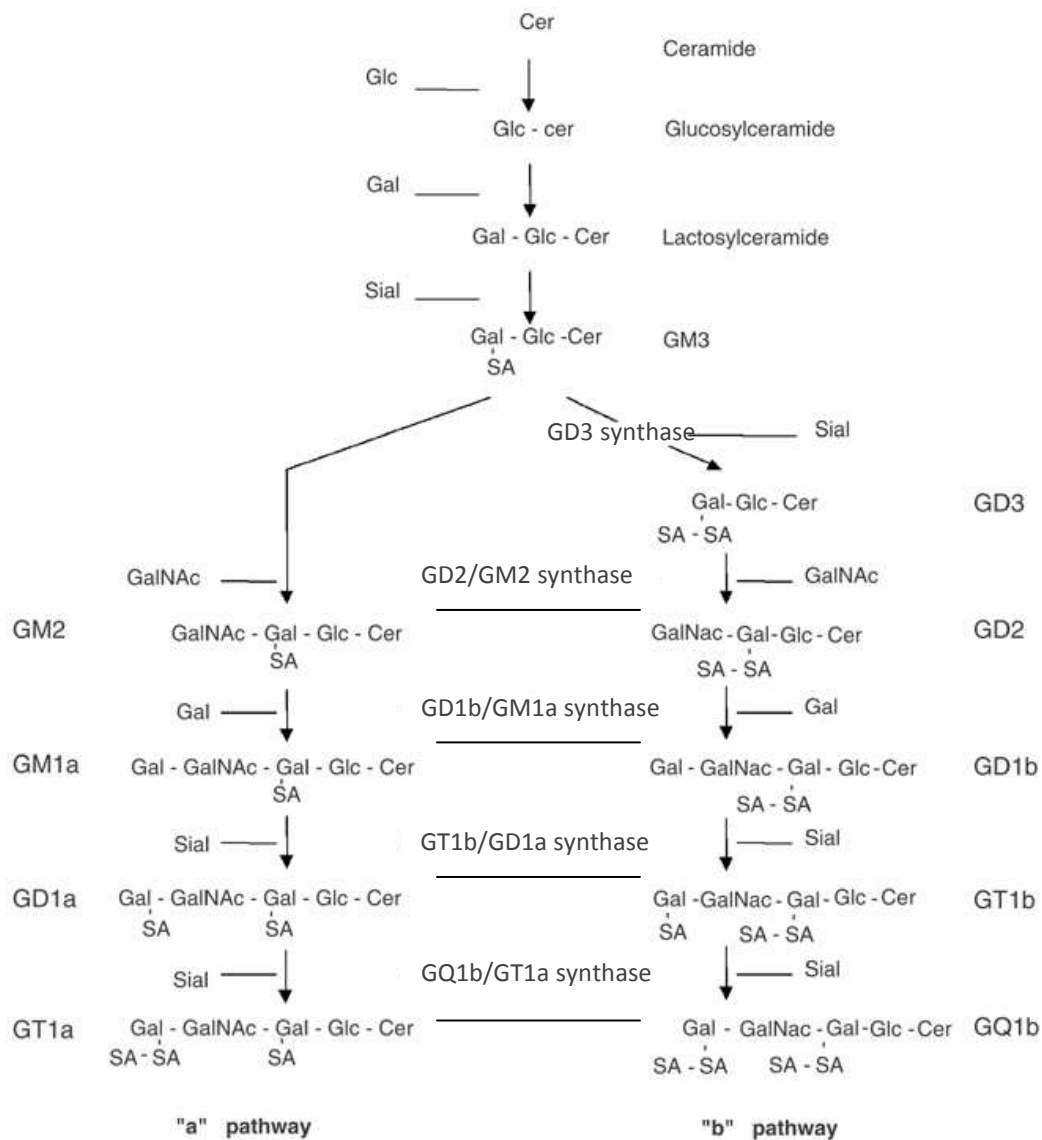


**Figure 1.14 Schematic representation of the major pathways of ganglioside biosynthesis.** The monosialoganglioside GM3, derived from lactosylceramide, is the common precursor for both 'a' and 'b' pathway gangliosides. Each ganglioside species consists of a ceramide backbone (CER), and a carbohydrate chain (Glc=glucose, Gal=galactose, GalNAc=N-acetylgalactosamine) containing one or more sialic acid (SA) residues. 'a' and 'b' pathway gangliosides downstream of GD1b/GM1a synthase were designated complex 'a' (CaG) and complex 'b' (CbG) gangliosides, respectively. Parallel steps in both pathways are catalysed by the same glycosyltransferases of the Golgi apparatus (Li and Ladisch, 1997): GD3 synthase ( $\alpha$ -2,8-sialyltransferase), GM2/GD2 synthase ( $\beta$ -1,4-N-acetylgalactosaminyltransferase); GD1b/GM1a synthase ( $\beta$ -1,3-galactosyltransferase); GT1b/GD1a synthase ( $\beta$ -2,3-sialyltransferase); GQ1b/GT1a synthase ( $\alpha$ -2,8-sialyltransferase). Adapted from (Hettmer et al., 2004).

**Table 1.5 Contrasting properties of lipid raft and glycosynapses.** Adapted from Hakomori, 2008.

Lipid Raft	Glycosynapse
1% Triton X-100 insoluble	1% Triton X 100 soluble 0.5% Brij95 insoluble
Cholesterol-dependent (disrupted by cholesterol-binding reagent)	Cholesterol-independent (resistant to cholesterol-binding reagent)
Tetraspanin-independent	Tetraspanin dependent
Diameter 10nm to <100nm	Diameter >100nm, usually 500-1000nm
Highly mobile	Less mobile – non-mobile
Not involved in cell adhesion	Involved in cell adhesion with concurrent signalling

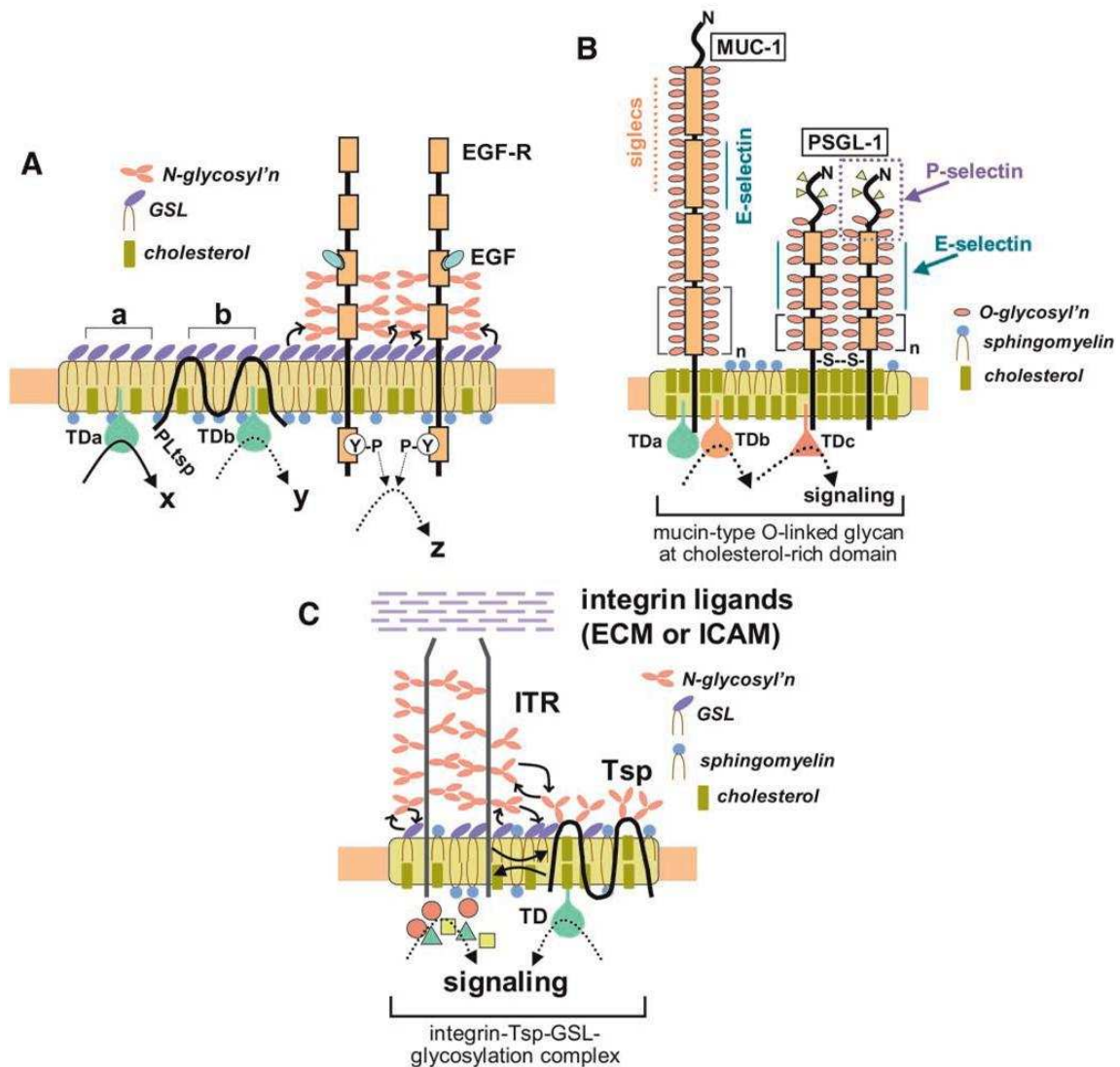


**Figure 1.15 Schematic representations of glycosynapses.** (A) Type 1 glycosynapse with GSL clusters, proteolipid tetraspanin (PLtsp), and growth factor receptor. Clusters of GSLs are organized with signal transducer molecules (TDa, TDb). Stimulation of GSL region “a” causes strong signaling “x” through TDa, whereas stimulation of region “b” causes weaker signaling “y” through TDb because of the presence of the blocking factor PLtsp. The growth factor EGF-R can be located in a GSL-rich domain. Signalling by tyrosine phosphorylation can be blocked by association of EGF-R with GSL. Binding of GSL to EGF-R may result from interaction of GSL with carbohydrates N-linked to EGF-R. (B) Type 2 glycosynapse with mucin-type transmembrane glycoprotein at cholesterol-rich membrane domain. Examples are shown for MUC1 and

PSGL1. The tandem repeat units of MUC1 and PSGL, have multiple O-linked structure with glycosyl adhesion epitope and are organized with various signal transducers (TDa, TDb, TDc). In human and mouse T-cell lines, cSrc, Ick56, Lyn, Fyn, and CD45 are detected. Both MUC1 and PSGL1 are associated with a membrane domain rich in cholesterol (indicated by yellow rods). Cells expressing type 2 glycosynapse are capable of binding to cells expressing P-selectin, E-selectin, or siglecs. (C) Type III glycosynapses contain N-glycosylated transmembrane adhesion receptors (usually integrin; ITR) complexed with tetraspanins (Tsp) and GSLs. Type 3 glycosynapse with integrin receptor (ITR) having  $\alpha$ - and  $\beta$ -subunits and tetraspanin (Tsp.). N-glycosylation (pink oval chains) of ITR is essential for connection and stabilization of  $\alpha$ 5- and  $\beta$ 1-subunits and also for interaction of ITR with tetraspanin CD82. Figure taken from (Hakomori, 2002).

### **Glycosynapse-1**

GSLs can form clusters and are organised with cytoplasmic signal transducers and proteolipid tetraspanin (Fig 1.15; (Iwabuchi et al., 1998)). These synapses can also contain growth factors. The main GSL in these synapses mediates cell adhesion that in turn leads to activation of cytoplasmic signal transducers (e.g. TDa, TDb, TDc). This activation leads to downstream signalling and changes in transcription factor expression. This can lead to increased cell adhesion, spreading and enhanced cell motility (Iwabuchi et al., 1998; Kojima & Hakomori, 1991). The impact of GSL activation can be reduced by the presence of an inhibitor in the synapse (e.g. Pltsp; (Hakomori Si, 2002)). If a growth factor is associated with a type I synapse (e.g. EGFR) its activation would be inhibited by phosphorylation via linkage of the GSL to carbohydrates associated with EGFR (Zhou et al., 1994).

### **Glycosynapse-2**

Type II glycosynapses involve transmembrane mucin-type glycoproteins (e.g. mucin-1 [MUC1] or P-selectin glycoprotein ligand-1 [PSGL-1]) in cholesterol-rich regions of the membrane, but not GSLs (Fig 1.15). They associate with cytoplasmic signal transducers (Tda, Tdb, Tdc). Activation of the mucin-type glycoproteins by P-selectin, E-selectin and others ligands lead to signal transduction and changes in transcription factors, as in type I synapses (Suzuki & Kojima, 2007).

### **Glycosynapse-3**

The third type of glycosynapse contains transmembrane adhesion receptors (such as integrin receptor [ITR]) complexed with tetraspanin and GSLs (Fig 1.15). Both GD2, GD3 and GM3

gangliosides have been shown to be associated with the tetraspanin CD51 in glycosynapses (Thorne et al., 2007). Their presence in the glycosynapse is essential for the receptors to be N-glycosylated to allow connection to, and stabilisation of the  $\alpha 5$  and  $\beta 1$  subunits of the ITR and for interaction with tetraspanin (Zheng et al., 1994). Alteration of this glycosylation effects interaction of integrin with tetraspanin, leading to significant inhibition or promotion of cell motility (Ono et al., 2000). The activation of transmembrane receptors in type III glycosynapses also leads to intracellular signalling and changes in transcription factor expression (Zheng et al., 1993).

### **1.3.3 Mechanisms of altered expression of glycans**

Hakomori and colleagues formulated the concept that the alteration of glycolipids on cancer cells occurs due to incomplete and neosynthesis of glycans. Studies since then have shown that not only are glycolipids altered on cancer cells, but a wide variety of carbohydrate determinants are altered on cancer cells (Dabelsteen, 1996; Reis et al., 2010).

#### **Incomplete synthesis**

Originally, the overexpression of some glycans on the surface of cancer cells was thought to be due to the increased transcription of glycosyltransferases involved in their synthesis. However, studies have shown that the level of glycosyltransferase transcription was not increased compared to normal cells. Further studies have shown that cancer cells lack the transferases to complete synthesis of some carbohydrate determinants due to silencing of the genes responsible. This is due to DNA methylation of genes encoding transferases involved in glycan production and histone deacetylation (Kawamura et al., 2008).

One example is sialyl Lewis x, which is used as a serum marker in a number of epithelial-derived tumours, for example breast (Wei et al., 2010). Increased expression of this glycan on tumour cells is caused by the DNA hypermutation and histone deacetylation and therefore silencing of genes involved in the sulphation of sialyl Lewis x. The inability of cancer cells to form sialyl 6-sulpho Lewis

x, a glycan on normal cells that acts as a ligand for Siglec-7, means the increase of the non-sulphated sialyl Lewis x, which is a ligand for E-selectin, endothelial cell leukocyte adhesion molecule-1 (ELAM-1). This leads to increased tumour cell adhesion and motility, resulting in increased metastasis (St Hill et al., 2011; Wei et al., 2010).

### **Neo-synthesis**

As well as the incomplete synthesis of glycans on tumour cells, glycans can be further expressed through a neo-synthesis mechanism (Kannagi et al., 2008). Neo-synthesis is mediated by hypoxic regions of solid tumours, resulting in the enhanced transcription of glycosyltransferases and sugar transporters, including fucosyltransferase VII (*FUT7*), ST3Gal-I (*ST3O*), UDP-galactose transporter-1 (*UGT1*) and glucose-transporter-type-I (*GLUT1*; (Koike et al., 2004; Ogawa et al., 1997)). These factors are increased in cancer, leading to the increased expression of glycans including E-selectin ligands sialyl Lewis x and a (Koike et al., 2004).

### **1.3.4 Aberrant expression of glycosyl epitopes in cancer**

Glycosylation of proteins as well as lipids, as described above, is important for their function. For example, glycosylation of immunoglobulins are important in maintaining the structure as well function of Ig. It has long been established that both glycolipids and glycoproteins are aberrantly expressed on the surface of cancer cells (Dennis et al., 1999; Hakomori, 1985; Hakomori & Murakami, 1968), giving the cancer enhanced mobility, adhesion and proliferation. Cancers can gain significant advantages from alterations in glycosylation of glycoproteins, glycolipids and proteoglycans.

### **Fucosylation**

Fucosylation is a common modification of O- and N-linked glycosylation on both glycolipids and glycoproteins. Upregulation of enzymes involved in the addition of fucose residues to glycans can

lead to an increase in fucosylation in cancer. For example,  $\alpha$ -fetoprotein (AFP) is increased in chronic hepatitis and liver diseases, but fucosylated AFP is overexpressed only in hepatocarcinomas (HCC). For this reason, it was approved as a tumour marker for HCC by the FDA in 2005 (Moriwaki & Miyoshi, 2010). Upregulation of fucosylated AFP in HCC is due to an increase in fucosylation enzymes such as fucosyltransferases, guanosine 5'-diphosphate (GDP)-fucose synthetic enzymes and GDP-fucose transporter (Miyoshi et al., 2008). Interestingly, a decrease in fucosylation can lead to escape from NK cell-mediated tumour surveillance, leading to reduced TRAIL-mediated death of cancer cells (Moriwaki & Miyoshi, 2010).

### **Glycoproteins**

Approximately half of eukaryotic proteins are glycosylated with either N- or O-linked glycans. Both N- and O-glycans can be affected during cancer progression. N-glycosylation consists of an oligosaccharide chain N-linked to asparagine within the sequence Asn-X-Ser/Thr, where X is any amino acid except proline (Varki, 2009). N-glycans are produced as a precursor which is transferred onto the protein in the ER. Further processing of the glycan then occurs in the ER, with glucose removal and addition which helps in protein folding. Once in the Golgi apparatus, the glycan is completed. O-glycosylation consists of a glycan linked to a serine or threonine residue. The first step in O-glycosylation involves the addition of GalNAc to the serine or threonine, forming the Tn antigen, the core 1 structure. This is then synthesised by Gal-transferase, adding a Gal to the GalNAc, forming the T antigen (Core 1; (Peter-Katalinic, 2005)). Either the T or Tn antigen can be sialylated forming sialyl-Tn, sialyl-T or disialyl-Tn or disialyl-T antigens. The enzyme core 2  $\beta$ 1,6-N-acetylglucosaminyltransferase (C2GnT1) adds a GlcNAc to GalNAc, initiating the core 2 extension. C2GnT1 is the key branching enzyme in core 2 O-glycan biosynthesis. Further glycosyltransferases then add more residues to the glycan, with the addition of sialic acid terminating the glycan. Examples of core 2 O-glycans are the Lewis and ABO-glycan based blood group antigens that can be present on glycoproteins as well as glycolipids (Marionneau et al., 2001). Both N- and O-linked



glycans on membrane bound and secreted proteins can be altered on cancers (Feizi, 1985). Mucins are highly O-glycosylated due to their high density of serine/threonine residues. Mucins have altered glycosylation on cancer cells, due to either termination of normal glycans, or the addition of unusual terminal structures, most commonly the sialylation of the terminal saccharide. An example of altered glycosylation of glycoproteins is the increased level of N-linked glycan acceptor sequence motifs in the variable region of surface Ig in follicular lymphoma (Zhu et al., 2002). The extra sites for N-linked glycosylation are introduced through somatic mutation and are tumour specific. Furthermore, the glycans commonly terminated with mannose residues, unlike most glycoproteins, which usually exist as precursors in the ER, before being further modified in the Golgi (Rudd & Dwek, 1997). Recently, it has been shown that the increased level of mannosylated glycans on the surface Ig of follicular lymphoma cells increases binding to C-type lectins, such as mannose receptor (MR) and DC-specific intracellular adhesion molecule-3-grabbing nonintegrin (DC-SIGN) expressed on innate immune cells, including DCs and macrophages, providing the FL with survival signals (Coelho et al., 2010).

## **GSLs**

There have been a range of human tumour-associated GSL antigens found. The Lewis antigen blood groups expressed on GSLs can be altered and overexpressed on a range of cancers. Many of these glycosylated epitopes can be defined as tumour-associated antigens (e.g.  $\beta$ 6GlcNAc branching in N-linked structure, sialyl Lewis a, sialyl Lewis x in O-linked glycans and Lewis y in either O- or N-linked glycan structure (Hakomori Si, 2002) .Tumour cells can gain significant advantages from alterations in the glycocalyx. A range of gangliosides (GD2, GD3, GM2) have been shown to be overexpressed on the cell membrane of neuroblastomas and melanomas. Studies have shown that some gangliosides can be shed into the tumour microenvironment (Chang et al., 1997). For example, GM2, GM3 and GD1a gangliosides have been shown to be shed by medulloblastoma cell lines (Chang et al., 1997). One possible mechanism by which tumour-promoting is the internalisation of gangliosides by

activated T cells, triggering their apoptosis via the intrinsic pathway (Sa et al., 2009), providing a mechanism for cancers to evade the immune system. The glycolipid isoglobotetraosylceramide (IsoGb4) has been shown to be a marker of metastasis and overexpressed on tumours, with limited expression on normal tissue (Brodin et al., 1986). Furthermore, a mAb directed against IsoGb4 has been shown to induce apoptosis in target cells (Zhong et al., 2001).

### **Proteoglycans**

Proteoglycans are composed of a core protein with covalently attached glycosaminoglycan (GAG) side chains. The GAG side chains are linear polysaccharides consisting of a disaccharide repeat made up of an unronic acid and acetylated amino sugar. The chain can be sulphated at various sites, leading to areas of high sulphation that provide a docking site for a variety of protein ligands including cytokines, growth factors, enzymes and ECM. Heparin sulphate proteoglycans (HSPGs) have N-acetylglucosamine and glucuronic/iduronic acid disaccharide named heparin sulphate and are expressed on all cells. The existence of a range of classes of core proteins as well as variation in disaccharide chains means that HSPGs are a large heterogeneous family. The heterogenic nature of HSGPs means that a cell can respond to its microenvironment in different ways. Due to the ability of HSGPs to interact with a range of ligands, they have a range of functions including cell adhesion to the ECM by binding laminin and fibronectin, ECM degradation through interaction with heparanase and growth factor sequestering by binding fibroblast growth factor or hepatocyte growth factor (Sasisekharan et al., 2002). Studies have shown that HSPGs are aberrantly expressed on a range of cancers, which 'hijacks' the functions that HSGPs perform, contributing to progression of cancers through angiogenesis, promoting tumour growth and metastasis (Blackhall et al., 2001; Sasisekharan et al., 2002).

### **1.3.5 Glycolipids as targets for monoclonal antibodies**

The alteration of glycan structures, on glycolipids, glycoproteins and proteoglycans suggests that they may be good targets for mAb therapy. Targeting tumour-restricted glycans on glycolipids that may be involved in the optimal functioning of membrane proteins involved in a variety of cell signalling pathways with mAbs could inhibit the pro-tumour activity of the altered molecules, leading to tumour cell death, as well as utilising the effector mechanisms of mAbs; ADCC, CDC and direct cell death. MAbs that target tumour-specific glycolipid and glycan antigens have been reported.

#### **GD2**

GD2 is a disialylganglioside antigen expressed on the surface of tumours of neuroectodermal origin, including neuroblastoma and melanoma (Mujoo et al., 1987). In addition GD2 is also expressed on glioma and non-small cell lung cancer (Mujoo et al., 1987). It is abundantly expressed on 100% of neuroblastoma tumours, regardless of stage (Wu et al., 1986). Normal tissue expression is limited to neurons, skin melanocytes, and peripheral fibres. Furthermore, GD2 has been shown to be involved in cell growth and differentiation and apoptosis (Yoshida et al., 2002).

A number of anti-GD2 mAbs have been produced, including 14.G2a, ch14.18 (Barker et al., 1991; Frost et al., 1997), ch.60C3 (Alvarez-Rueda et al., 2007), 3F8 (Kramer et al., 2007), and KM8138 (Nakamura et al., 2001) to target neuroblastoma, melanoma, and non-small cell lung cancers. Currently, the use of antiGD2 mAbs in clinical trials in conjunction with chemotherapy is the mainstay of neuroblastoma therapy (Modak & Cheung, 2007). The benefit of targeting GD2 on the surface of cells is that unlike other gangliosides studied, GD2 is not shed by the cells into the microenvironment (Kramer et al., 1998). The first anti-GD2 mAb tested was the murine mAb 3F8, which was produced by immunising BALB/c mice with a range of neuroblastoma cell lines (Cheung et al., 1985). 3F8 has shown significant anti-tumour effect against neuroblastoma alone (Cheung et al.,

1998) as well as when administered with granulocyte-macrophage colony-stimulating factor (GMCSF; (Kushner et al., 2001)), or radiolabelled with  $I^{131}$  (Kramer et al., 2000). Despite promising clinical studies, 3F8 showed HAMA responses *in vivo*, limiting the therapeutic value. 14.18 is an IgG3 murine mAb targeted to GD2 and 14.G2a is a class-switch variant developed to enhance the ADCC effect of the mAb. When administered with IL-2, 14.G2a showed minimal effectiveness and suffered similar HAMA responses to 3F8 (Frost et al., 1997).

To overcome the HAMA responses seen with the murine mAbs, chimeric mAbs ch14.18 and c.60C3 were produced. ch14.18 was shown to be more effective than its murine counterpart, with overall survival greater than with maintenance therapy (Frost et al., 1997). Recently, a phase I study with ch14.18 administered with GMCSF and IL-2 was undertaken to ascertain the dose-limiting toxicity of the therapy (Gilman et al., 2009). The chimeric mAb c.60C3 was cloned from the murine anti-GD2 mAb 60C3 and has been shown to induce ADCC and CDC *in vitro* and suppress tumour growth *in vivo* (Alvarez-Rueda et al., 2007). The humanised mAb Hu18K322A was created from ch14.18 in order to increase the half-life of the mAb *in vivo*. As well as being humanised, Hu18K22A was engineered with an amino acid change in the Fc region at position 322 and produced in the YB2/0 cell line rather than CHO lines, which lacks fucosylation in the Fc region, with the purpose of increasing the efficacy of CDC and ADCC *in vivo* (Yang & Sondel, 2010).

### **GD3**

The ganglioside GD3 has been described as a melanoma marker due to its overexpression (Tsuchida et al., 1989) and as a valid target for mAb therapy due to anti-GD3 mAb-mediated melanoma cell lysis being observed with the mAb MB3.6 (Cheresh et al., 1985). During apoptosis, GD3 is rapidly synthesized from ceramide by a sialyltransferase resident in the Golgi apparatus. It then relocates to the mitochondria where it contributes to the opening of the mitochondrial permeability transition pore complex, followed by the release of cytochrome c and other pro-apoptotic factors (Malisan & Testi, 2002). R24 is a mouse mAb that recognises GD3 and has undergone numerous clinical trials

(Chapman et al., 1990). It has been used to treat melanoma patients and in one trial showed a complete response in one patient that lasted 2 years and a partial response in one patient that lasted 2 months (Kirkwood et al., 2000). It also displayed a human anti-mouse antibody response in patients, but the low level of response meant that the antibody was not humanised (Kaminski et al., 1999).

## **GM2**

GM2 is expressed at low levels in most normal tissues, but is highly expressed in certain cancers including melanoma (Portoukalian et al., 1979). It is a strongly immunogenic ganglioside as reflected by the fact that anti-GM2 IgM antibodies have been detected in some patients with dysimmune neuropathies (Cavanna et al., 2001). GM2 has also been shown to associate with lipid rafts (Tomioka et al., 2009). DMF10.167.4 is a hamster mAb raised against a murine T cell lymphoma cell line and has been shown to induce apoptosis of that cell line *in vitro* (Fernandes et al., 1999). Subsequently it was found to bind to GM2 and could bind to both melanoma and small cell lung cancer cell lines, but showed minimal binding to normal tissues (Retter et al., 2005). Its ability to induce apoptosis in a range of cell lines *in vitro* also transferred to *in vivo* studies, where it was shown to inhibit the formation of tumours in murine models (Retter et al., 2005).

## **Other glycan-targeting mAbs**

RAV12 is a chimeric mAb that has been shown to bind a minimal epitope of Gal $\beta$ 1-3GlcNAc $\beta$ 1-3Gal on the N-linked carbohydrate antigen RAAG12, which has been observed on 90% of intra-abdominal tumours, but also on mucosal and glandular/ductal epithelium (Coberly et al., 2009; Loo et al., 2007). RAV12 has been shown to directly kill the colorectal cancer cell Colo 205 *in vitro* independently of apoptosis by oncosis (Loo et al., 2007). A study has shown that RAAG12 is present on insulin-like growth factor-I receptor (IGF-IR) and binding of RAV12 leads to increased phosphorylation of IGF-IR in RAAG12 positive cell lines, leading to accelerated desensitisation of the Akt/PKB pathway (Li & Li, 2007). A recent phase I study in 33 recurrent adenocarcinoma patients

showed some anti-tumour activity of RAV12, although toxicity of the mAb precluded the delivery of maximal doses (Burriss et al., 2010).

Interestingly, F77, a mAb targeted at an as of yet unidentified glycolipid target, is also able to induce direct cell death by oncosis. The mAb has been shown to bind to a large proportion of both primary and metastatic prostate cancer specimens by immunohistochemistry (Zhang et al., 2010a). F77 is proposed to induce oncosis by recruiting antigen to lipid rafts and through the production of large membrane pores (Zhang et al., 2010a).

## 1.4 Cell death

Cell death is a term that covers a range of pathways and mechanisms by which a cell may die. The most studied is apoptosis. Apoptosis involves tightly regulated, energy requiring intracellular mechanisms. It has a key role in both the development and homeostasis of all multi-cellular organisms. For example, apoptosis contributes to the normal development of foetal and pre-natal lungs (Schittny et al., 1998) and is involved with the removal of damaged cells that could become a danger to the organism and the removal of a cell with DNA damage (Green & Martin, 1995) or virally infected cells (Shibata et al., 1994). Apoptosis is sometimes referred to as programmed cell death, although this is a misuse of the term programmed cell death as this term can be used to describe other forms of non-accidental cell death, such as pyroptosis (Majno & Joris, 1995). All forms of cell death have distinct morphologies that distinguish themselves from each other (Fig 1.16).

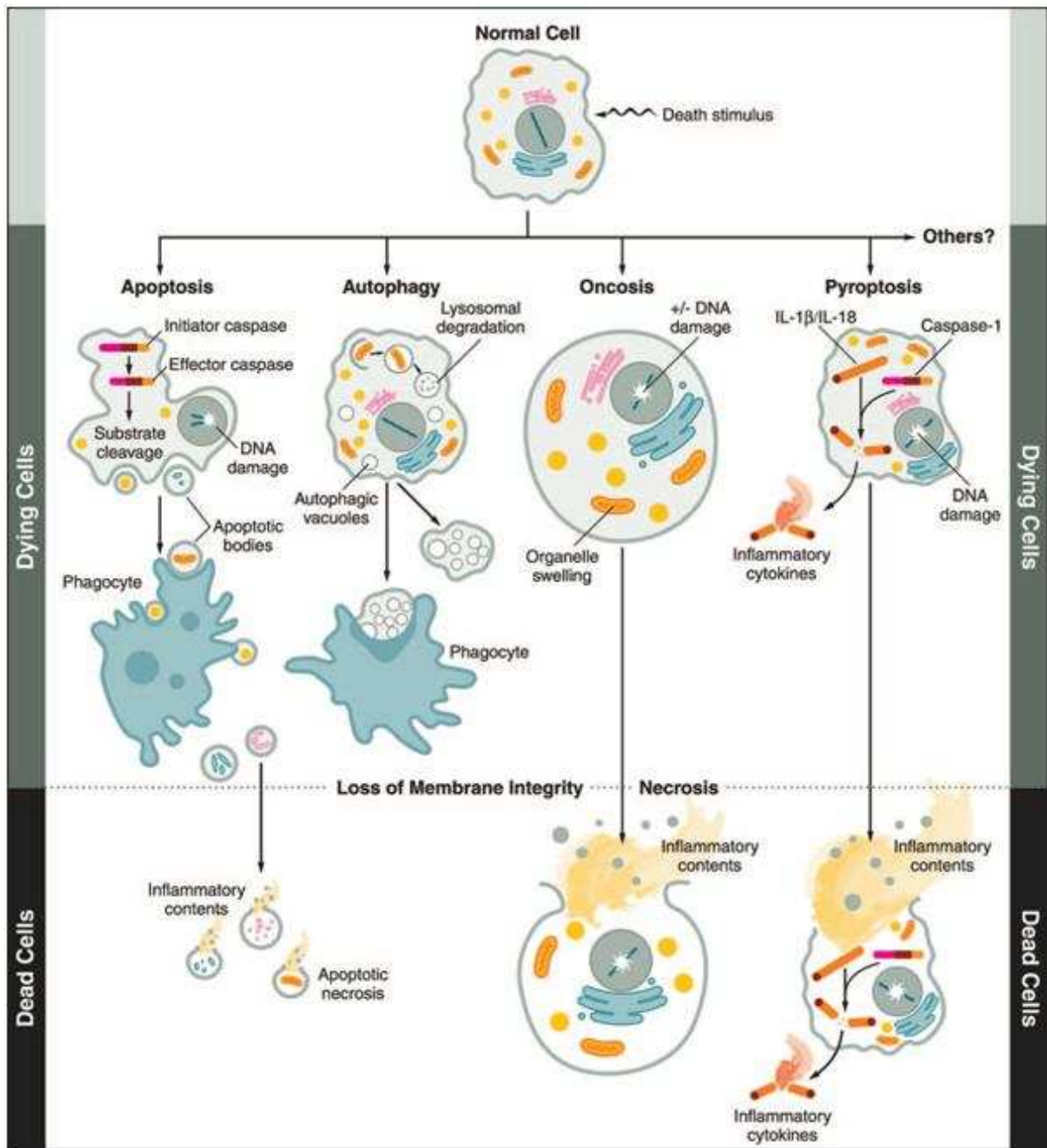


**Figure 1.16 Cell death pathways.** Different forms of cell death exist, each with distinct characteristics. Upon stimuli, a cell can die by apoptosis which is a result of the initiation of the caspase-cascade, followed by the cleavage of DNA. It is characterised by initial cytoplasmic and nuclear shrinkage followed by blebbing of the cell surface, leading to the formation of apoptotic bodies which are phagocytosed. Cell membrane integrity is maintained throughout. Alternatively, apoptotic bodies can undergo necrosis, causing a low level of inflammation. Autophagy involves the formation of autophagosomes inside the dying cell, which contain a large amount of cytoplasmic contents, and are degraded by the lysosome. Autophagic cells can also be phagocytosed. Oncosis describes cellular and organelle swelling, with increased cell membrane permeability before the release of inflammatory cellular contents. Pyroptosis involves the activation of caspase-1 after bacterial infection leading to cell lysis and the release of pro-inflammatory cytokines and bacteria. Necrosis describes the end point of inflammatory cell death, characterised by loss of cell membrane integrity and the uncontrolled release of intracellular, inflammatory contents. Figure taken from (Fink & Cookson, 2005).

### 1.4.4 Apoptotic Pathways

Apoptosis occurs in a variety of physiological conditions. Initially, cell membrane integrity is maintained and nuclear fragmentation occurs by the cleavage of DNA by activation of endogenous endonucleases. The cell fragments into apoptotic bodies that are phagocytosed by neighbouring cells and degraded (Fig 1.16). Alternatively, apoptotic bodies can reach necrosis, releasing their inflammatory contents. Apoptosis is mediated by a family of cysteine aspartyl-specific proteases, caspases. This family of 14 proteases are expressed as inactive precursors or zymogens (pro-caspases), of which 7 mediate apoptosis (Table 1.6).

**Table 1.6 Properties of the members of the caspase family.** Adapted from (Vermeulen et al., 2005).

Name of caspase	Other names	Tetrapeptide preference	Function
<b>Caspases important for execution and signalling events of apoptosis</b>			
Caspase - 2	ICH-1/mNedd2	DEHD/VDVAD	Initiator
Caspase - 8	MACH/FLICE/Mch5	LETD/IETD	Initiator
Caspase - 9	ICE-LAP6/Mch6	LEHD	Initiator
Caspase - 10	Mch4, FLICE2	IEAD/DMQD	Initiator
Caspase - 3	CPP32/Apopain/Yama	DEVD	Effector
Caspase - 6	Mch2	VEID/VEHD	Effector
Caspase - 7	Mch3/ICE-LAP3/CMH-1	DEVD	Effector
<b>Caspases involved in control of inflammation</b>			
Caspase - 1	ICE	WEHD/YEVD	Pryoptosis
Caspase - 4	TX/ICH-2/ICErel-II	LEVD/(W/L)EHD	
Caspase - 5	TY/ICErel-III	(W/L)EHD	
mCaspase - 11	ICH-3		
mCaspase - 12			
Caspase - 13	ERICE		
mCaspase - 14	MICE		



These caspases are activated by proteolysis following apoptotic stimuli (Los et al., 1999; Manimala et al., 2007). Apoptotic stimuli can be from either intracellular or extracellular sources. For example, irreparable DNA damage, telomere shortening, withdrawal of growth factors, hypoxia, oncogene induction or immune response. These stimuli lead to the intrinsic or extrinsic pathways of apoptosis.

#### **1.4.2 Intrinsic Pathway**

The intrinsic (mitochondrial-dependent) pathway (Fig 1.17) is initiated by intracellular apoptotic stimuli as described above. The main step in the intrinsic pathway is the release of cytochrome c from the mitochondria. The mechanism by which this occurs is not entirely clear. According to some authors, (Scarlett & Murphy, 1997; Vander Heiden & Thompson, 1999) cytochrome c release is preceded by mitochondrial swelling, leading to a disruption of the membrane. However, more recent research has shown that the formation of pores at the contact sites of the outer and inner membranes of the mitochondria (Vermeulen et al., 2005) cause the release of cytochrome c. These pores, termed mitochondrial permeability transition pore complexes (PTPC; Fig 1.18), are comprised of the adenine translocator (ANT) at the inner membrane and the voltage-dependent anion channel (VDAC) at the outer membrane, (also known as porin) as well as other proteins; hexokinase II (HKII), mitochondrial creatine kinase (mtCK), cyclophilin D (Cyp-D) and peripheral benzodiazepine receptor (PRB). Intrinsic pathway activation and consequently the formation of pores, is caused by cell stress, free radical damage or growth factor deprivation. These factors lead to the dephosphorylation of the intracellular protein complex 14-3-3/Bad. This releases Bad from 14-3-3, allowing it to disrupt Bcl-2 homodimers (an anti-apoptotic protein; Table 1.8) on the outer membrane of the mitochondrion. The pro-apoptotic protein Bax also disrupts Bcl-2:Bcl-XL heterodimers on the mitochondria membrane. Bax and Bad also form homodimers on the outer membrane of the mitochondria. This break-up and formation of dimers disrupts the balance of anti- and pro-apoptotic proteins on membrane. This is thought to cause high levels of matrix  $\text{Ca}^{2+}$  and  $\text{Mg}^{2+}$  concentration and high levels of ADP/ATP leading to pore opening and cytochrome c release (Schinzel et al., 2005). Along with

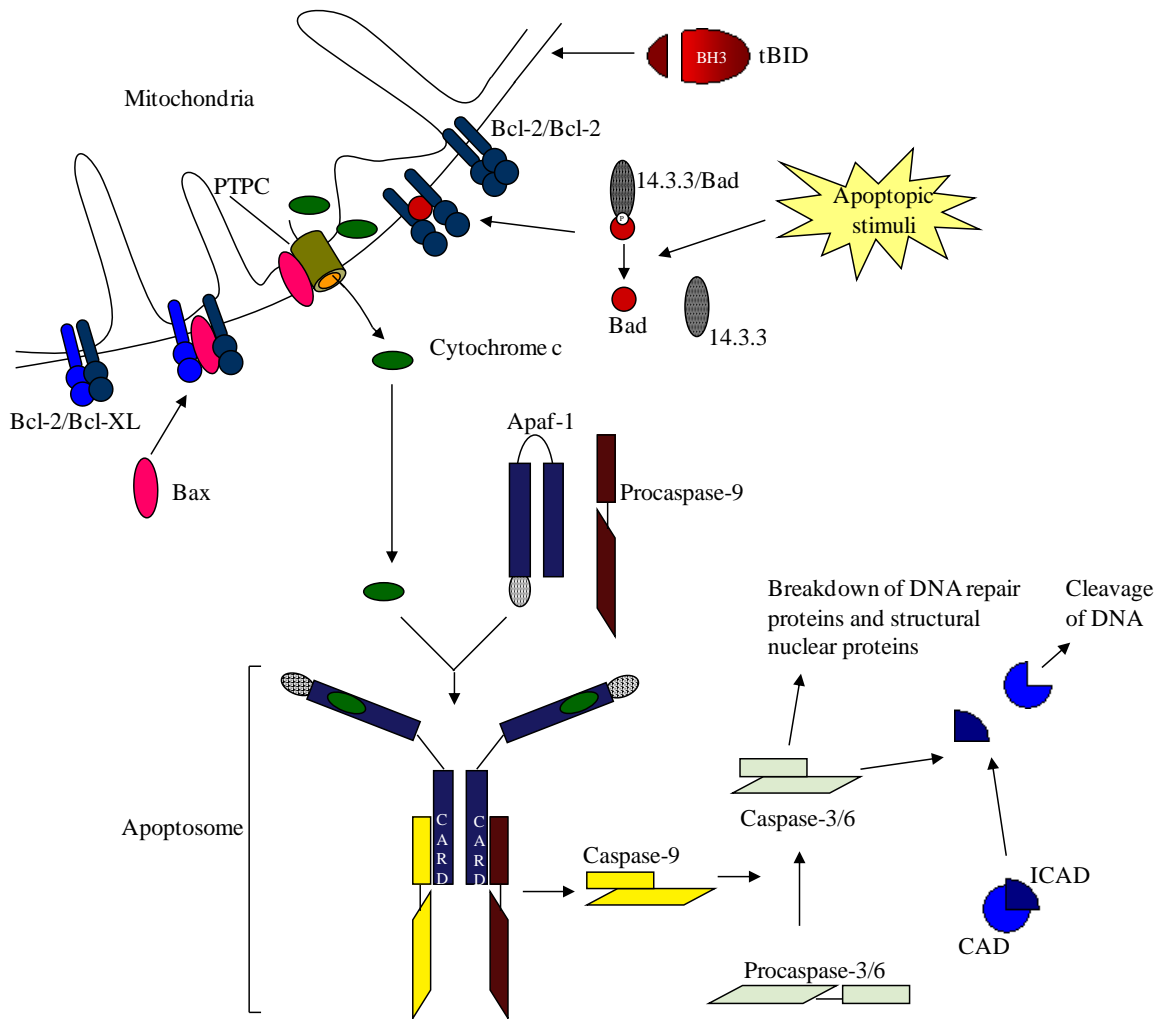


**Figure 1.17 Simplified schematic diagram of the intrinsic pathway.** Apoptotic stimuli cause the dephosphorylation of 14.3.3/Bad allowing Bad to disrupt anti-apoptotic protein dimers (e.g. Bcl-2/Bcl-2) on the mitochondria outer membrane. The pro-apoptotic protein Bax disrupts other anti-apoptotic dimers. This causes an imbalance in apoptotic signals, leading to PTPC formation in the mitochondria membrane. Bax complexes with the PTPC allowing the release of cytochrome c. Cytochrome c binds to Apaf-1 causing oligomerisation in the presence of ATP. Procaspase-9 is recruited (forming the apoptosome) and activated forming caspase-9. This then allows the activation of effector caspases, such as caspase-3. Effector caspases then cleave nuclear structural proteins and DNA repair proteins (such as laminins and PARP respectively). Caspase-3 cleaves ICAD allowing CAD to cleave DNA.

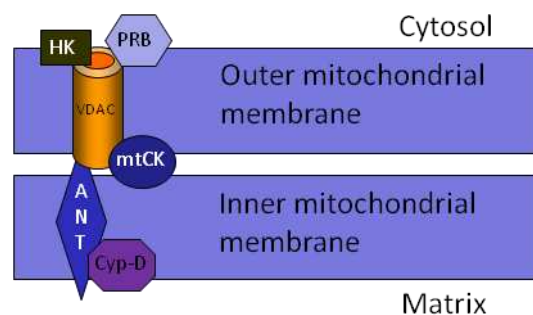


**Figure 1.18 A schematic representation of the PTPC.** Comprised of the VADC (also known as porin), ANT and other proteins which include; HK, PRB, mtCK and Cyp-D.

**Table 1.8 Members of the Bcl-2 family**

<b>Anti-apoptotic proteins</b>	<b>Pro-apoptotic proteins</b>
Bcl-2	Bad
Bcl-XL	Bax
	Bid

cytochrome *c* the pro-apoptotic proteins Smac/Diablo (second mitochondria-derived activator of caspases/direct IAP-binding protein with low pI), apoptosis inducing factor (AIF), Omi/HtrA2 and endonuclease G are released (Susin et al., 2000). The PTPC has been shown to physically and functionally interact with Bax (Boya et al., 2001; Szewczyk & Wojtczak, 2002) allowing the normally narrow PTPC to widen allowing release of cytochrome *c* and apoptosis inhibitory protein (AIP). Upon release of cytochrome *c* from the mitochondria, the consensus nucleotide binding domain of Apaf-1 is hydrolysed in the presence of ATP. Cytochrome *c* then binds to Apaf-1 promoting oligomerisation of Apaf-1 forming a large 'apoptosome' complex (700 to 1400 kDa)(Levade & Jaffrezou, 1999; Los, 2002; Luo et al., 1998). The apoptosome then recruits procaspase-9 via its caspase recruitment domain (CARD) and is activated through auto-catalysis. The activated caspase-9 is released from the complex (Levade & Jaffrezou, 1999). Caspase-9 then in turn activates downstream effector caspases such as caspase-3, -6, and -7 (Fig 1.17) (Levade & Jaffrezou, 1999; Li et al., 1997). Effector caspases translocate to the nucleus where they can cause DNA fragmentation by the cleavage of DNA repair proteins and structural nuclear proteins (such as PARP and laminin respectively). Caspase-3 cleaves ICAD allowing CAD to cleave DNA. Alongside caspase activation, AIF and endonuclease G induce nuclear chromatin condensation as well as large scale DNA fragmentation (Susin et al., 2000).

### **1.4.3 Extrinsic pathway**

The extrinsic (receptor-dependent) pathway involves the activation of caspases via receptors belonging to the tumour necrosis factor (TNF)-receptor superfamily at the plasma membrane (Fig 1.19). The family includes Fas (Apo-1/CD95), TNF-receptor-1 (TNF-R1), death receptor-3 (DR3 or TNF-

receptor-related apoptosis-mediating protein [TRAMP] or Apo-3), TNF-related apoptosis-inducing ligand receptor-1 (TRAIL-R1 or DR4), TRAIL-R2 (DR5 or Apo-2) and DR6 (Izban et al., 1999; Vermeulen et al., 2005). The most studied death receptor is Fas, which is activated by the Fas-ligand (FasL). FasL (for example on the surface of a CTL) or agonistic antibodies, such as the anti-Apo-1 mAb, bind to the Fas receptor (Dhein et al., 1992). As FasL is homo-trimeric it causes trimerisation of the Fas receptor. This activation leads to the recruitment of the adaptor molecule Fas-associated death domain (FADD; made up of CAP1 and CAP2) that binds to Fas via the death domain (DD) in its cytoplasmic region. The complex formed is referred to as the death receptor-induced signalling complex (DISC). In addition to a DD, FADD also contains a death effector domain (DED) that recruits the DED-containing procaspase-8 to the DISC (Medema et al., 1997). Procaspase-8 is then proteolytically activated forming caspase-8 which in turn activates effector caspases (e.g. caspase-3 and -7). This mechanism for caspase activation is similar for most death receptors. For example the ligand TNF- $\alpha$  binds to its receptor TNF-R1 causing receptor trimerisation and the recruitment of the TNF-R-associated death domain protein (TRADD; Fig 1.19; (Shen et al., 2002)). The DD of TRADD interacts with the DD of FADD, allowing the recruitment of procaspase-8 (Stennicke et al., 1998). In addition to death receptors, four decoy receptors that belong to the TNFR family have been identified (DcR1/TRID, DcR2/TRUNDD, DcR3 and osteoprotegerin (OPG)). Decoy receptors compete with death receptors for ligand binding, thereby inhibiting ligand-induced apoptosis. Decoy receptors are either devoid of an intracellular DD (DcR1/TRID) or have a partially deleted DD (DcR2/TRUNDD). Therefore, ligand can bind the cell via the decoy receptor and does not provide a pro-apoptotic signal. Alternatively, both DcR3 and OPG are secreted and bind FasL and TRAIL respectively, blocking apoptosis (Sheikh & Fornace, 2000; Van Poznak et al., 2006).

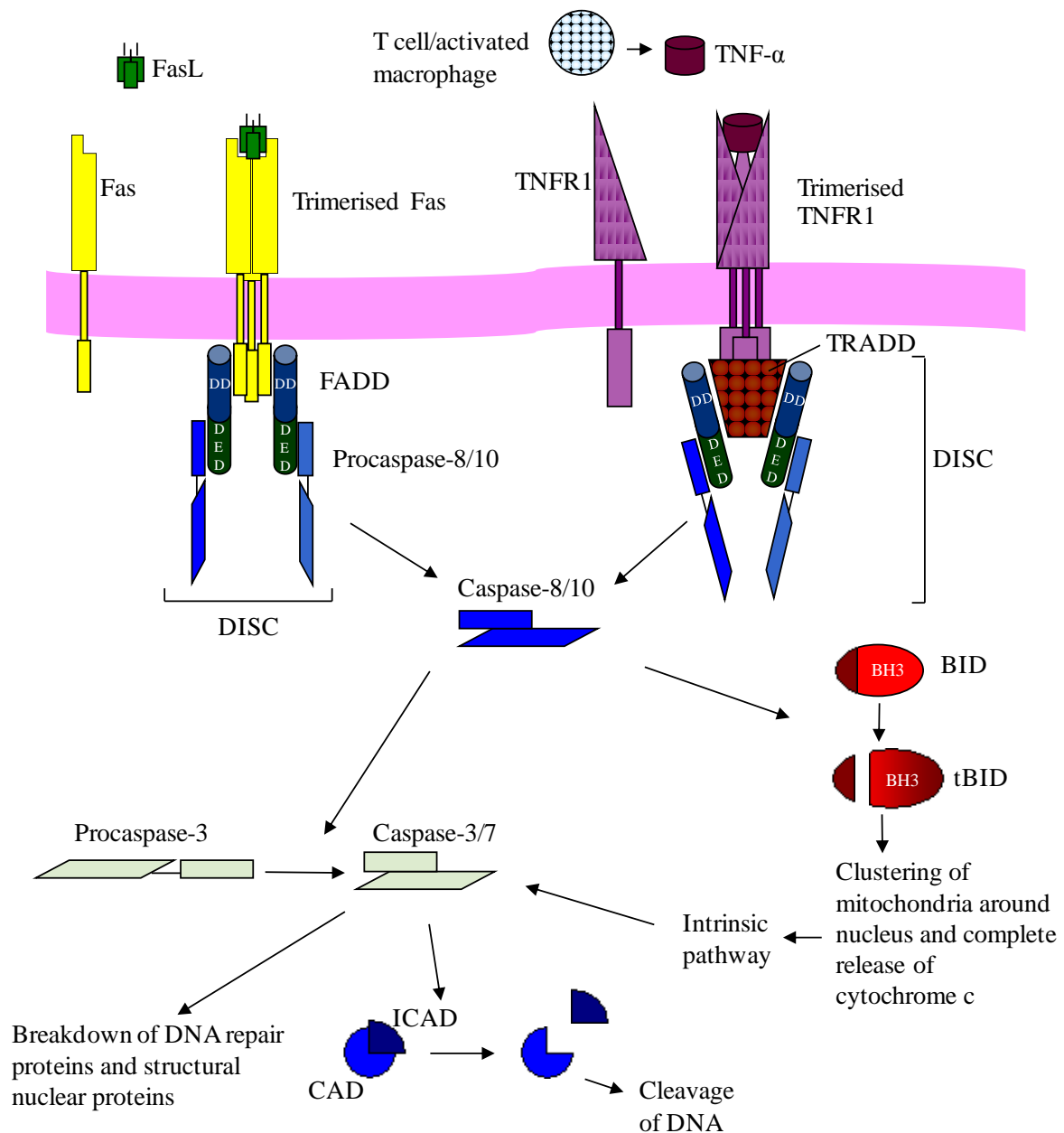


**Figure 1.19 Two examples of death receptors involved in the extrinsic pathway.** FasL binds to the Fas receptor, causing trimerisation. This allows binding of the adaptor molecule FADD to the DD of Fas. Procaspase-8 clusters at the receptor completing the DISC. Binding of procaspase-8 to the DED of FADD causes cleavage of the initiator caspase, allowing the activated caspase-8 to activate downstream caspases, such as caspase-3. Caspase-8 can also cleave BID which, when activated causes release of cytochrome *c* from the mitochondria, initiating the intrinsic pathway. T cells or activated macrophages release TNF- $\alpha$  which trimerises the TNF-R1. TRADD binds to the intracellular DD of TNF-R1. The DD of TRADD recruits FADD, completing the DISC. FADD binds procaspase-8 causing activation by cleavage. Activation of caspase-3 is followed by the cleavage of ICAD, releasing CAD, which cleaves the DNA. Also, DNA repair proteins and structural nuclear proteins, such as PARP and laminins respectively, are inactivated by cleavage.

### 1.4.1 Oncosis

Oncosis is an example of non-apoptotic cell death (Fig 1.16). Oncosis was first proposed in 1910 by von Recklinghausen and is accompanied by cellular and organelle swelling, blebbing, and increased membrane permeability (Majno & Joris, 1995) as well as non-specific DNA damage (Jugdutt & Idikio, 2005). Therefore, oncosis differs from apoptosis with respect to the fact that the cell *swells* then dies (onco, Greek for 'swelling' or mass) and an apoptotic cell initially decreases in cellular volume, followed by budding of the cell membrane before the formation of apoptotic bodies (apoptosis from Greek; *apó* meaning from and *ptósis* meaning a fall). Cellular swelling in oncosis is followed by the breakdown of the cell membrane and the release of intracellular components and inflammation (Fig 1.16). The term oncosis is widely used to describe cell death as a result of ischemia in various diseases, such as acute myocardial infarction and acute renal and liver failure (Chu et al., 2007; Gujral et al., 2003; Jugdutt & Idikio, 2005). The oncotic hallmark of cellular swelling has been shown to be due to ion pump failure due to a lack of ATP (Cao et al., 2010; Majno & Joris, 1995). It has been thought that oncosis is an un-regulated event with a cell swelling beyond its capacity resulting in the cell bursting. However, studies have shown that biochemical mechanisms lead to oncotic cell death. For example, influx of sodium and  $\text{Ca}^{2+}$  leads swelling of the cell (Chen et al., 2002; Trump & Berezsky, 1996). Also the influx of  $\text{Ca}^{2+}$  has been shown to activate calpain, which has been shown to mediate the degradation of several cytoskeletal proteins, resulting in membrane permeability (Cao et al., 2010; Liu et al., 2004). Calpain has also been shown to disrupt the mitochondria via cleavage of Bid, the pro-apoptotic protein, initiating a cell death pathway that is either independent or dependent on caspases (Chen et al., 2002).

### 1.4.2 Autophagy

Autophagy is derived from the Greek meaning *phagy*-to eat and *auto*-oneself and is a mechanism used to degrade proteins and cytosolic organelles. Large amounts of cytoplasmic contents are sequestered in a double membrane vacuole termed autophagosomes, before being delivered to the

lysosome for degradation (Levine & Klionsky, 2004). The formation of autophagosomes is also observed in cell survival in conditions of limited nutrients, through the degradation of a large amount of cytoplasmic materials. An interesting example of this can be seen in apoptosis-deficient tumours where the induction of autophagy results in cell survival, avoiding necrosis and inflammation (Degenhardt et al., 2006). Autophagy consists of two pathways which vary on the way cytoplasmic material is delivered to the lysosome. Microautophagy involves cytoplasm being engulfed directly at the lysosome surface by invagination, whereas macroautophagy involves the creation of double-membrane vacuoles from the cell membrane that engulf a large proportion of the cytoplasmic (Fink & Cookson, 2005). Autophagy has also been observed as a mechanism of cell death, characterised by the degradation of cellular components in autophagic vacuoles of dying cells (Fig 1.16). Autophagic cell death is triggered when elimination of a large number of cells is required. It functions to cause cell death as well as providing a way for the cell to be disposed when phagocytes are unable to cope with the large numbers of cells (Levine & Klionsky, 2004).

### **1.4.3 Pyroptosis**

Pyroptosis, from the Greek meaning *pyro*-fire or fever and *ptosis*-falling off which relates to its proinflammatory nature (Fig 1.16). Pyroptosis results from infection of cells with bacterial pathogens, such as *Salmonella* and *Shigella* species. Bacterial infection triggers the activation of caspase-1, a non-apoptotic member of the caspase family, which processes the proforms of IL-1 $\beta$  and IL-18 into active forms, leading to the death of the host cell along with the release of IL-1 $\beta$  and IL-18 proinflammatory cytokines (Fig 1.16; (Foss et al., 2001)). It is thought that pyroptosis is a form of host defence, sacrificing one cell to produce a proinflammatory signal. An example of pyroptosis can be seen in the invasion of *Salmonella* into the epithelial cells of the gut before non-vacuole bacteria hyper-replicate, causing cell extrusion and pyroptosis, resulting in the release of pro-inflammatory cytokines and release of *Salmonella* which is either cleared by immune cells or re-invades other epithelial cells (Knodler et al., 2010).

## Aim of thesis

The aims of this thesis are to establish the therapeutic value of two anti-glycan mAbs produced in-house, to develop an immunisation protocol with the aim of improving the immunogenicity tumour-associated glycolipids able to produce therapeutically valuable mAbs and to determine the significance of a mAb with the ability to induce apoptosis in colorectal cancer.

MABs have been shown to utilise various mechanisms to yield anti-tumour effects including ADCC, CDC, by blocking cellular pathways and by inducing cell death directly. The latter has been shown to be mediated via classical apoptosis as well as independently of apoptosis. The first aim of this thesis is to establish whether mAbs directed at colorectal cancer would benefit from mediating apoptosis of the tumour directly or by inducing cell death independently of apoptosis, as observed with a number of anti-glycan mAbs. This will be achieved by quantifying the level of cleaved caspase-3 in a large cohort of colorectal cancer patients by immunohistochemistry.

A panel of five IgG mAbs recognising the Lewis y/b hapten were previously produced in house following immunisation with rat anti-idiotypic antiserum to C14, an IgM Lewis y/b hapten mAb. The mouse IgG3 mAb 692/29 was selected for further characterisation in this thesis based on its distribution on a large number of colorectal primary tumours and lack of normal tissue binding by IHC. This mAb has previously been shown to have specificity for both Lewis y and Lewis b glycan antigens by thin layer chromatography and cause direct cell death independently of effector cells or complement. Therefore, the aim was to confirm the fine specificity of the mAb as well as further characterise its functional effector mechanisms, including its ability to cause direct cell death.

The mAb 505/4 is a mouse IgG1 monoclonal antibody produced by immunising with whole colorectal cancer cells. Preliminary experiments have shown that it binds to a range of colorectal cancer cell lines and that its antigen is a sialylated glycan. Therefore, the aim was to further characterise 505/4 and evaluate its suitability for use as a therapeutic mAb. To achieve this, the antigen would be



characterised, binding to tumour and normal tissues would be assessed and its ability to mediate effector functions would be determined.

MABs have been proven to be successful forms of cancer treatment with 7 currently approved for clinical use in cancer (June 2011) with all mAbs approved targeting protein antigens. Glycolipids have been shown to be aberrantly expressed on the surface of cancer cells. Furthermore, glycolipids are thought to be essential membrane components and have been associated with various functional membrane proteins. Glycolipids have been shown to be involved in a range of cell signalling pathways, for example, cell adhesion and growth. Therefore it is likely that glycolipids act on the cell surface as accessory molecules to functional membrane proteins and are required for optimal functional activity of their associated molecules. The aim of this thesis was to develop a protocol designed to produce mAbs directed at tumour-associated glycolipids, for therapeutic use. Specifically, to produce mAbs that showed specificity for tumour glycolipids, with minimal binding and have a functional effect in blocking the activity of the glycolipid. A therapeutically valuable mAb would also be able to induce traditional mAb-mediated anti-tumour effects. MABs have been shown to induce direct cell death of tumour cells both via apoptosis and independently of apoptosis. Interestingly, a striking number of anti-glycan and anti-glycolipid mAbs have been shown to induce direct cell death, independently of apoptosis.

## Chapter 2 Materials and Methods

All procedures were carried out using aseptic technique where appropriate and relevant safety regulations were followed. Standard protocols were either developed or followed for all assays and, where necessary, modifications were incorporated into the protocols for use in specific conditions. All animal work was carried out under a Home Office approved project licence (Licence number 40/2936). All reagents were purchased from Sigma (UK) unless otherwise stated.

### 2.1 mAbs and Human cancer cell line culture

#### 2.1.1 Commercial mAbs

Cleaved caspase-3 (Asp175) mAb was purchased from Cell Signalling Technology, (MA, USA). 7LE, CA19.9 and 2-25 LE were purchased from Abcam (Cambridge, UK). The human activating anti-Fas mAb was purchased from Upstate (now part of Millipore, MA, USA). The anti-MHC-II (HLA DP DQ DR clone WR18 mAb was purchased from AbD Serotec (Oxford, UK) and anti-HLA-ABC (clone W6/32) was purchased from eBioscience (CA, USA). Anti-CD46 was purchased from BD Pharmingen (NJ, USA) and anti-CD59 mAb (clone BRIC 229) was purchased from International Blood Group Reference Laboratory (IBGRL; Bristol, UK).

#### 2.1.2 In house production of mAbs

505/4 was isolated from the 505/4 mouse hybridoma produced by immunising whole colorectal cancer cell lines, 692/29 was isolated from 692/29 mouse hybridoma produced from an anti-idiotypic rat mAb raised against whole colorectal cancer cells, 692/42 was isolated from 692/42 mouse hybridoma produced in the same fusion as 692/29 and BR96 was isolated from HB10036 hybridoma purchased from the ATCC. All hybridomas were maintained in serum-free hybridoma media (Invitrogen Scotland, UK) and spent media collected regularly. Once enough supernatant was collected (~2 litres), it was filtered through Whatman paper before sterilising through a 0.2µm filter.

Supernatant was passed over a Protein G Sepharose column overnight. A standard glycine release protocol was followed to collect the IgG from the column. Table 2.1 shows the reagents used for antibody purification. 20ml of buffer C ran over the protein G Sepharose column at a speed of 1 ml per minute to equilibrate the column (using a vacuum pump). Spent culture supernatant was run then over the column overnight at 4°C. 50ml of buffer C was then passed over the column to remove residual supernatant and balance the pH. 20ml of glycine was slowly added, preventing disruption of Protein G and allowed to run through at 1ml per minute. 1ml fractions were collected in 1.5ml eppendorf tubes containing 500µl of Tris-HCl. 20ml of buffer C was then ran over the column to equilibrate the column. The samples were analysed by spectrophotometry with protein concentration being determined by reading optical density at 280nm, referenced against a sample of 1ml glycine, 500µl Tris-HCl. The samples containing antibody were pooled and either injected into a Slide-a-Lyze cassette (Thermo Scientific, MA, USA) or placed into dialysis tubing, before placing in 500ml of sterile PBS and samples dialysed for 24 hours at 4°C. The purified antibody was then quantified by spectrophotometry and indirect immunofluorescence assay (Section 2.6.2).

**Table 2.1 Reagents for antibody purification fro culture supernatant using Protein G sepharose column.** All components obtained from Sigma and all reagents 0.2µm filter-sterilised.

Reagent	Composition
100mM Glycine-HCl pH 2.7	0.75g of Glycine 100ml of distilled water Adjust pH to 2.7 with 5M HCl
1M Tris-HCl	0.303g of Tris base 25ml distilled water Adjust pH to 9 with 5M HCl
Na <sub>2</sub> HPO <sub>4</sub> (Buffer A)	3.04g Na <sub>2</sub> HPO <sub>4</sub> 100ml of distilled water
NaH <sub>2</sub> PO <sub>4</sub> ( Buffer B)	2.76g of NaH <sub>2</sub> PO <sub>4</sub> 100ml of distilled water
Buffer C	Add Buffer B to Buffer A until pH=7.4

### 2.1.3 Biotin and FITC labelling of mAbs

For fluorescein isothiocyanate (FITC) labelling, 1mg antibody was dialysed into carbonate buffer (pH 9.0) overnight at 4°C in either dialysis tubing or a Slide a Lyze cassette. FITC powder was dissolved at

1mg/ml in acetone and 20-50µg/ml FITC per mg of antibody was dried in a glass bijoux. Once the acetone had evaporated, the antibody was removed from dialysis tubing/cassette and added to the glass bijoux. The bijoux was then shaken for 1 hour at room temperature (RT). To biotinylate antibody, ~1mg of antibody was dialysed into PBS overnight at 4°C. Once dialysed, the antibody was mixed with 150µl 1mg/ml NHS-LC-biotin in dH<sub>2</sub>O while vortexing. The antibody and biotin mixture was incubated at RT for 45min.

After incubation of antibody with FITC or biotin, a PD10 column (GE Healthcare, Buckinghamshire, UK) was washed with 25ml PBS before adding the FITC-antibody or biotin-antibody solution. 20ml PBS was then added and 1ml fractions collected in 1.5ml eppendorf tubes. The samples were analysed by spectrophotometry with protein concentration being determined by reading optical density at 280nm, referenced against a sample of PBS or dH<sub>2</sub>O. The samples containing antibody were pooled and either injected into a Slide a Lyze cassette (Thermo Scientific, MA, USA) or placed into dialysis tubing, before placing in 500ml of sterile PBS and samples dialysed for 24 hours at 4°C. The purified antibody was then quantified by spectrophotometry and indirect immunofluorescence assay (Section 2.6.2).

## 2.2 Cell culture

All cell culture was carried out using aseptic technique in a class II safety cabinet.

### 2.2.1 Cell lines and hybridomas

All Human cancer cell lines were maintained in RPMI 1640 supplemented with 10% heat inactivated (HI) newborn calf serum (NBCS) unless otherwise stated. NS0 cells were maintained in 10% HI foetal calf serum (FCS)-supplemented RPMI 1640. Hybridomas were maintained in 10% HI FCS-supplemented RPMI 1640 and 1x HAT supplement (0.136g hypoxanthine, 0.00176g aminopterin and 0.0388g thymidine per 500ml media). Cell lines are summarised in Table 2.2.

**Table 2.2 Summary of cell lines used.**

Cell Line	Origin	Type
791T	Produced in house	Human osteosarcoma
C170	Produced in house	Human colon adenocarcinoma
Colo 201	ECACC # 87091201	Human Caucasian colon adenocarcinoma from primary tumour
Colo 205	ECACC # 87061208	Human Caucasian colon adenocarcinoma isolated from ascites of same patient as Colo 201
DLD1	ECACC # 90102540	Human colon adenocarcinoma
HT29	ECACC # 91072201	Human Caucasian colon adenocarcinoma from primary tumour
HUVEC	Produced in house	Primary human umbilical vein endothelial cells isolated from umbilical cords, used up to passage 6
Jurkat	ECACC # 88042803	Human leukemic T cell lymphoblast
LoVo	ECACC # 87060101	Human colon adenocarcinoma
SW480	ECACC # 87092801	Human colon adenoma
SW620	ECACC # 87051203	Human colon adenocarcinoma, established from lymph nodes of same patient as SW620
MCF-7	ECACC # 86012803	Human breast adenocarcinoma
MCF10A	ATCC # CRL-10317	Non-tumourigenic epithelial cell line from mammary gland
MDA-MB-231	ECACC # 92020424	Human breast adenocarcinoma
MKN-45	ATCC # CCL-171	Human gastric adenocarcinoma
MRC-5	ECACC # 05090501	Normal human foetal lung
NS0	ECACC #85110503	Mouse (BALB/c) lymphoblastoid myeloma
OAW28	ECACC # 85101601	Human ovarian tumour epithelial from cystadenocarcinoma
OAW42	ECACC # 85073102	Human ovarian tumour epithelial from cystadenocarcinoma
OVCA 433	Gift from Gift from Department of Obstetrics and Gynaecology, Royal Derby Hospital	Human ovarian serous cystadenocarcinoma
OVCAR-3	ATCC # HTB-161	Poorly differentiated papillary human ovarian adenocarcinoma
OVCAR-4		Human ovarian adenocarcinoma
SK-OV3	ECACC # 91091004	Human ovarian adenocarcinoma
T47D	ECACC # 85102201	Human breast ductal carcinoma

### 2.2.2 Maintenance of cell lines and hybridomas

All stock cells were obtained from liquid nitrogen storage. The cells were submerged in a 37°C water bath to ensure complete thawing. Cells were transferred to 25ml universal tubes and 1ml of complete media, cell specific, was added drop-wise to the cells under agitation. A further 5ml of complete media was added slowly to the tubes whilst gentle agitation was supplied. The volume was

then increased with complete media to 25ml and the tubes were centrifuged at 150g for 5min at RT. The supernatant was aspirated from the cell pellets which were resuspended in complete media. All cells were then washed with complete media and finally resuspended in media and transferred to T25 tissue culture flasks (Corning). All cells were cultured at 37°C in 5% CO<sub>2</sub> and were maintained by regular replacement of complete culture media and splitting to maintain log phase growth. If large cell numbers were required, cells were transferred to T175 culture flasks. Cells were cultured until approximately 80% confluency was reached, at which point they were split in order to maintain healthy cultures. Supernatant was aspirated from adherent cell lines and replaced with 10ml 1 x Trypsin/EDTA and incubated for 10min at 37°C. Non-adherent lines were transferred to 50ml tubes and centrifuged at 150g for 5min. Trypsinised cells were transferred to 25ml universal tubes and complete media was added up to 25ml total volume (serum contained in the media inactivates trypsin activity). Tubes were centrifuged at 100g for 5min at RT and all supernatants were aspirated from the pellets. Cells were resuspended in 10ml of complete media and 1ml was transferred to a new flask and the cells were maintained. Cells which were to be used in experimental procedures were counted using a haemocytometer with trypan blue, staining for viability assessment and used as stated. Some cells were frozen in order to maintain stocks and were resuspended at 5x10<sup>6</sup> cells/ml in 5% DMSO (dimethyl sulfoxide)/FCS (v/v) and 1ml was added per cryovial (Nalgene, USA). Vials were frozen by reducing the temperature by 1°C per minute to a temperature of -80°C by placing the vials in isopropanol containers, at which point cells were transferred to liquid nitrogen storage (-170°C).

## 2.3 Immunohistochemical analysis

### 2.3.1 Tissue preparation

Immunohistochemistry (IHC) exploits the specific interaction between an antibody and its antigen to estimate expression of that antigen on a section of tissue. IHC can be performed on freshly frozen

tissue or formalin fixed paraffin embedded (FFPE) tissue which can be kept for many years. This study used both frozen and FFPE tissue, using an ovarian and colorectal tumour microarray (TMA), as well as whole sections and a FFPE normal tissue array, purchased from either Super Bio Chips (Seoul, Korea) or AMS Biotechnology (Abingdon, UK). All tissues require the same technique, with slight alterations depending on type of tissue, antigen and antibody.

The colorectal cancer TMA produced and validated by our group needed to be reproduced before staining with further markers could be carried out. Therefore, a TMA was constructed as described previously (Kononen et al., 1998). For each tumour, 5 $\mu$ m section slides stained with haematoxylin-eosin were first used to locate representative areas of viable tumour tissue. 0.6mm needle core-biopsies from the corresponding areas on the paraffin-embedded tumour blocks were then placed at pre-specified coordinates in recipient paraffin array blocks (Fig 2.1) using a manual tissue-arrayer (Beecher Instruments, Sun Prairie, WI). Array blocks were constructed with between 80–150 cores in each, with analysis of a single core from each case. Fresh 5 $\mu$ m sections were obtained from each TMA block and placed on coated glass slides to allow the immunohistochemical procedures to be performed, preserving maximum tissue antigenicity.

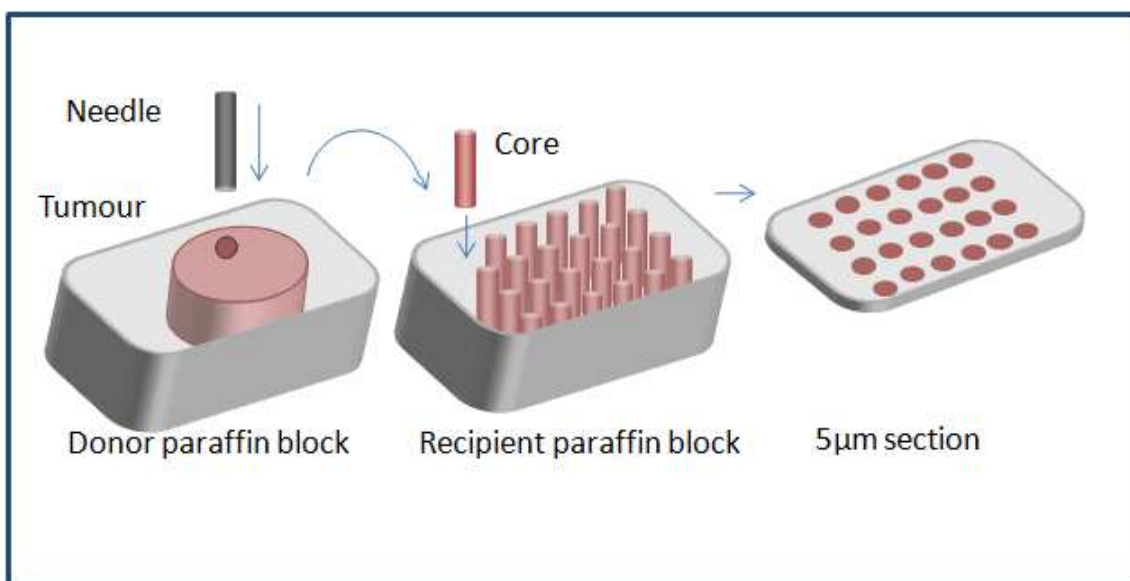


**Figure 2.1 Production of a TMA block.** A core is taken from the donor tumour and inserted into a pre-drilled hole in the recipient block. Once the TMA is completed, sections of the TMA can be cut and mounted on microscope slides ready for staining.

5µm sections of TMA or whole sections were cut as close to the date of staining as possible to minimise any degradation of antigen. Slides were then mounted onto positively charged slides to improve tissue adherence (Superfrost Plus, Surgipath Europe, Peterborough, UK). The control tissues used were of the tissue used in that experiment.

To remove the paraffin-wax from FFPE slides, the slides were heated in a dry oven at the melting point of wax (60°C) for 20min and were immediately placed in a xylene (BDH, Poole, UK) to dissolve the paraffin for 20min. The tissue was then rehydrated through a series of graded alcohols of 100%, 90% and 70% ethanol. All reagent baths were in a fume hood.

### **2.3.2 Antigen retrieval**

Although chemically fixing and heating tissue to 60°C of tissue leads to the denaturation of the antigenic epitopes, treating tissue using antigen retrieval solutions and heat has been shown to help antigens regain immunogenicity (Shi et al., 1991). In this study, antigen retrieval was heat mediated in citrate buffer at pH 6.0 (Table 2.1). The sixth sense setting on a Whirlpool microwave (Whirlpool, UK) was used to keep the solution at boiling point for 20min.

### **2.3.3 Prevention of non-specific binding**

A primary antibody is designed to bind to a specific epitope in order to detect antigen presence. If there is no antigen, then no staining should be seen. However, antibodies can undergo non-specific hydrophobic interactions with tissue in the absence of their specific marker, producing non-specific staining. To prevent this, normal swine serum (NSS; Dako, Ely, UK) was applied to the sections and also used in diluting the primary antibody. NSS contains proteins which interact with and mask non-specific hydrophobic binding sites, blocking antibody interaction with these sites.



### 2.3.4 Application of primary antibody

The optimal working dilution for a primary antibody is defined as the dilution that gives the most intense staining with the least amount of background staining. The level of staining can be affected by many factors including; how the tissue was originally fixed, the concentration, age and method of storage of the antibody, the retrieval method used and length of incubation. For these reasons, antibody activity can vary between laboratories. Therefore, all primary antibodies used were first titrated on a series of whole sections prior to the full experiment. Primary antibodies used are displayed in table 2.3. The optimum concentrations were determined by subjective visual assessment using a light microscope. The negative control used had all the reagents applied apart from the primary antibody, confirming that all staining seen was due to the primary antibody reacting with its antigen.

**Table 2.6 List of primary antibodies used in IHC.**

Antigen	Antibody Name (Clone)	Antibody Type	Company	Dilution
Sialyl di-Lewis a	505/4	Mouse IgG	In house	1:300
Lewis a	7LE	Mouse IgG	Abcam (Cambridge, UK)	1:1000
Sialyl Type I precursor	CA19.9	Mouse IgG	Abcam (Cambridge, UK)	1:200
Large fragment of active caspase-3 (Asp175)	Cleaved Caspase-3, Asp175 (5A1E)	Rabbit IgG	Cell Signalling (MA, USA)	1:00
MHC-II	Anti- HLA DP DQ DR (WR18)	Mouse IgG <sub>2</sub>	AbD Serotec, (Oxford UK)	1:100
Unknown	F019/1A7	Mouse IgG <sub>1</sub>	In-house	1:100

### 2.3.5 Washing

The slides were housed in a humidity chamber for the duration of the experiment. Thorough washing of the sections was performed using PBS (Table 2.4) to avoid drying out of the sections. Washing also removed excess reagent from the previous step.

**Table 2.4 The in-house production of solutions used in IHC. All reagents obtained from Sigma.**

<b>Solution</b>	<b>Materials</b>	<b>Quantity</b>	<b>Method</b>
<b>Citrate buffer X10 concentration</b>	Citric acid H <sub>2</sub> O	21g	Working dilution: Dilute 1:10, adjust pH to 6.0 using 5-10mmol HCl
	NaOH pellets	10g	
	dH <sub>2</sub> O	1000ml	
<b>PBS X10</b>	NaCl	80g	Working dilution: Adjust pH to 7.4 and add additional dH <sub>2</sub> O to 1000ml
	KCl	2g	
	Na <sub>2</sub> HPO <sub>4</sub>	14.4g	
	KH <sub>2</sub> PO <sub>4</sub>	2.4g	
	dH <sub>2</sub> O	800ml	
<b>0.5% copper sulphate solution</b>	CuSO <sub>4</sub>	2.5g	To make 500ml of 0.5% CuSO <sub>4</sub> add 2.5g of CuSO <sub>4</sub> to 500ml dH <sub>2</sub> O and add the 4g NaCl
	NaCl	4.0g	
	dH <sub>2</sub> O	500ml	

### **2.3.6 ABC method**

As well as recognition of an antigen by the antibody, IHC requires an amplification step to allow visualisation of antibody binding (Fig 2.2). The ABC method used a secondary antibody, “C”, labelled with multiple molecules of biotin that recognises the primary antibody. The reagents streptavidin (“A”) and “B” (biotin complexed with HRP) were mixed and allowed to associate for 30min. After associating to form “AB”, the mixture was added to the tissue allowing the complex to bind to each biotin site on the secondary antibody, multiplying the sites available for chromogen binding. The ABC method was carried out using a commercial kit from Dako (StreptABC Complex/HRP, Mouse/Rabbit). “A” = streptavidin in 0.01mol/L PBS, 15mmol NaN<sub>3</sub>; pH 7.2 diluted to 1:100, “B” = biotinylated horseradish peroxidase in 0.01mol/L PBS, 15mmol/ NaN<sub>3</sub>; pH 7.2 diluted to 1:100, “C” = biotinylated goat anti-mouse/rabbit secondary antibody diluted to 1:100. Many tissues (including colorectal) exhibit endogenous avidin binding activity, which can lead to non-specific staining. Therefore, before the primary antibody was added, the tissue was incubated with avidin and then

biotin (Avidin-Biotin blocking kit; Vector Labs, CA, USA). This saturates any avidin binding sites, and also stops any biotin binding by adding excess biotin. This prevents any “AB” from binding non-specifically.

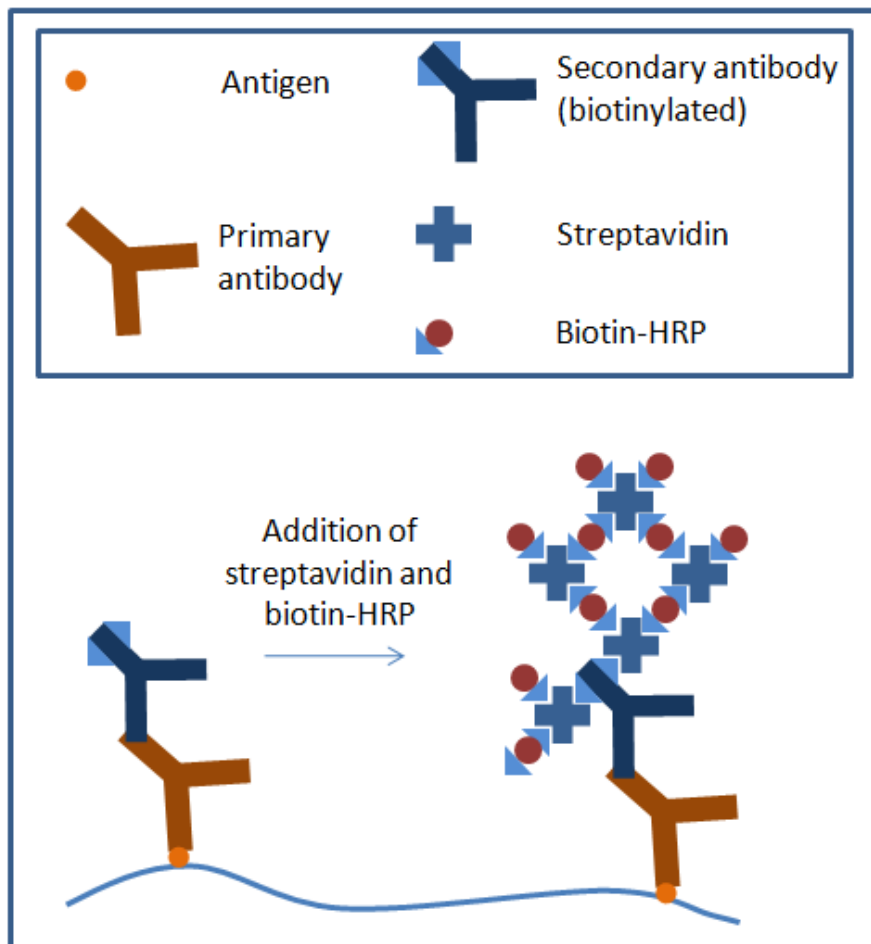


**Figure 2.2 ABC amplification method.** The biotinylated (triangle) secondary antibody (“C”) binds to the primary antibody bound to its antigen. Streptavidin (“A”) and biotin-HRP (“B”) are pre-incubated before adding to the tissue. Due to streptavidin’s ability to bind four molecules of biotin, it can bind more than one molecule of biotin-HRP, amplifying the signal.

### 2.3.7 Visualisation of the primary antibody

In order to visualise the primary antibody-secondary antibody-streptavidin-biotin-HRP complex to determine antigen expression, the chromogen 3, 3'-diaminobenzidine (DAB; Dako) was used. On oxidation by HRP, DAB produces a brown product which can be seen on microscopy.

Endogenous peroxidase in tissues can non-specifically oxidise DAB. In order to prevent this, the endogenous peroxidase activity was blocked before antigen retrieval using 0.3% hydrogen peroxide in methanol.

After application of DAB, the staining was darkened by the addition of 0.5% copper sulphate in 0.8% sodium chloride (Table 2.4) and haematoxylin (Vector Labs) was used to counterstain the background blue.

In order to preserve the slides, they were dehydrated in a series of alcohols (70%, 90% and 100% ethanol) before clearing in xylene. A coverslip was then added on top of the tissue using distyrene, plasticiser and xylene (DPX; BDH). This was performed in a fume hood and the slides were left overnight to allow the DPX to dry and excess xylene to evaporate.

### **2.3.8 IHC protocol**

The techniques described above are condensed into the following protocol.

Tissue array sections were first deparaffinised with xylene, rehydrated through graded alcohol and immersed in methanol containing 0.3% hydrogen peroxide for 20min to block endogenous peroxidase activity. In order to retrieve antigenicity, sections were immersed in 500ml of pH 6.0 citrate buffer and heated for 20min on the 6<sup>th</sup> sense setting of a microwave. Endogenous avidin/biotin binding was blocked using an avidin/biotin blocking kit (Vector Labs). In order to block non-specific binding of the primary antibody, all sections were then treated with 100µl of 1/5 NSS in PBS for 15min.

Test sections were incubated with 100µl of primary antibody diluted in PBS for 1 hour at 22°C or overnight at 4°C. Positive control tissue comprised whole sections of colorectal cancer tissue stained with β2-microglobulin at 1/1000 dilution (in PBS; Dako). The primary antibody was omitted from the negative control, which was left incubating in NSS.

After washing with PBS, all sections were incubated with 100µl of biotinylated goat anti-mouse/rabbit immunoglobulin (Dako) diluted 1:100 in NSS, for 30min. Sections were washed again in PBS and incubated with 100µl of pre-formed streptavidin-biotin/horseradish peroxidase (HRP) complex (Dako) for 60min at RT. Subsequently, visualisation of antigen expression was achieved using DAB. Finally, sections were lightly counterstained with haematoxylin (Dako), dehydrated in alcohol, cleared in xylene (Genta Medica, York, UK) and mounted with distyrene, plasticizer and xylene (DPX; BDH).

### **2.3.10 Evaluation of staining**

In order to allow permanent storage of the slides, they were imaged at x20 using a NanoZoomer 2.0 slide imaging system (Hamamatsu, Higashi-ku, Japan). Expression of markers on the tissue was analysed using the images in the NanoZoomer Digital Pathology Virtual Slide Viewer (Hamamatsu). Screening of marker expression was performed concurrently by two investigators with previous experience of scoring, blinded to the clinical information. For H score, cores were briefly analysed and representative cores of negative, weak, moderate and strong cores were used as guides for the whole TMA. As well as the intensity of the staining, the percentage of positively stained tumour cells was estimated. The two scores were then combined to form the H score, where H= percentage cells stained X intensity (range=0-300). For the active caspase-3 staining, a different approach was used due to the lower levels of staining. Using the NanoZoomer Slide Viewer, the area of both tumour and stroma were measured (Fig 2.3) and number of positive cells in each area counted. A value of positive cells per mm<sup>2</sup> was then calculated.

### **2.3.11 Data processing**

Following scoring, data needed appropriate grouping to facilitate statistical analysis. This was most commonly achieved using a binary cut off of either negative-positive, or high-low, (either side of the median). In the case of active caspase-3 staining where the scores of number of positive cells per

mm<sup>2</sup> ranged from 0 cells/mm<sup>2</sup> to 14000 cells/mm<sup>2</sup> the program X-Tile (Yale University, CT, USA) was used to determine low/high expression groups.

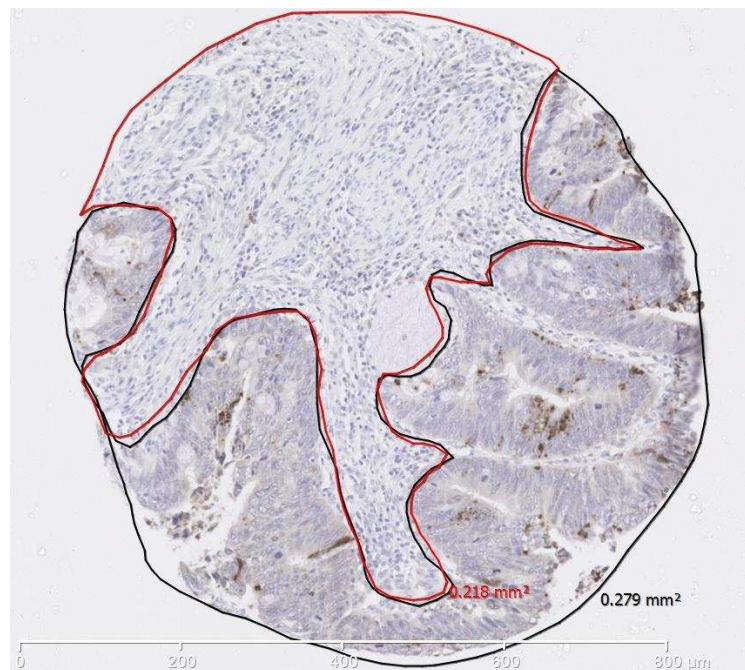


**Figure 2.3 CRC core from TMA.** A CRC core from the TMA stained with anti-cleaved caspase-3. The area of tumour and tumour associated stroma are measured using the freehand area tool in NanoZoomer Slide Viewer. The number of positive cells can then be counted and expressed as number of positive cells per mm<sup>2</sup>. Image is taken at x8 original magnification.

## 2.4 Immunohistochemical staining of colorectal TMA for cleaved caspase-3 and MHC-II expression

### 2.4.1 Patient study and design

The study population comprised a series of 462 consecutive patients undergoing elective surgical resection of a histologically proven sporadic primary colorectal cancer at the University Hospital, Nottingham, UK (Table 2.5; (Duncan et al., 2007; Durrant et al., 2003; McGilvray et al., 2009; Simpson et al., 2010; Ullenhag et al., 2007; Watson et al., 2005; Watson et al., 2006b). These patients were treated between 1st January 1994 and 31st December 2000; this time period allowed meaningful assessment of the prognostic markers studied. All patients treated during this time-

frame were considered eligible for inclusion in the study. Tumours were classified as mucinous carcinoma, when more than 50% of tumour volume consisted of mucin (Kakar et al., 2004).

**Table 2.5 Clinicopathological variables for colorectal TMA patient cohort (n = 462).**

<b>Variable</b>	<b>Categories</b>	<b>Frequency of total cohort (%)</b>
<b>Gender</b>	Male	266 (58)
	Female	199 (42)
<b>Age (years)</b>	Median	72
	Range	58-93
<b>Status</b>	Alive	169(37)
	Dead	293(63)
<b>Tumour Grade</b>	Well differentiated	29 (6)
	Moderately differentiated	353 (77)
	Poorly differentiated	71 (15)
	Unknown	8 (2)
<b>Tumour Site</b>	Colon	238 (52)
	Rectum	181 (39)
	Unknown	43 (9)
<b>TNM Stage</b>	0 (T <sub>is</sub> )	3 (1)
	1	69 (15)
	2	174 (28)
	3	155 (33)
	4	54 (12)
	Unknown	7 (2)
<b>Extramural Vascular Invasion</b>	Negative	224 (48)
	Positive	128 (28)
	Unknown	110 (24)
<b>Histological Type</b>	Adenocarcinoma	392 (85)
	Mucinous carcinoma	51 (11)
	Columnar carcinoma	4 (1)
	Signet ring carcinoma	7 (1)
	Unknown	8 (2)

#### **2.4.2 Clinicopathological variables for the patient cohort (n = 462)**

Only cases where the relevant pathological material was unavailable were excluded from the study. Follow-up was calculated from time of resection of the original tumour with all surviving cases being censored for data analysis at 31st December 2003, this produced a median follow up of 37 months (range 0–116) for all patients and 75 months (range 36–116) for survivors.

A prospectively maintained database was used to record relevant clinicopathological data, with data provided from the UK Office for National Statistics; this was available in more than 99% of cases. The information collected was independently validated through case note review of deceased patients. Disease specific survival was used as the primary end point; however, data was also collected on the various other relevant clinical and histopathological parameters these are summarised in table 2.4. Adjuvant chemotherapy consisting of FOLFOX was reserved for those patients with positive lymph nodes, although, surgical and adjuvant treatment was at the discretion of the supervising physician. Prior ethical review of the study was conducted by the Nottingham Local Research and Ethics Committee, who granted approval for the study.

Construction of the array blocks incorporated a wide spectrum of electively resected colorectal tumours and was found to be broadly representative of the colorectal cancer population in the UK. 266 (58%) patients were male and 196 (42%) female. The median age at the time of surgery was 72 years, consistent with a median age at diagnosis of colorectal cancer of 70–74 years in the UK (Quinn MJ, 2001). 69 (15%) tumours arrayed were tumour, node metastasis (TNM) stage 1, 174 (38%) stage 2, 155 (34%) stage 3 and 54 (11%) stage 4; there were 3 cases of *in-situ* disease. These figures are comparable with national figures for distribution of stage 1–4 at diagnosis of 11, 35, 26 and 29% respectively (NICE, 2004). The majority of tumours (392, 85%) were adenocarcinomas, and were most frequently of a moderate histological grade (353, 77%). 128 (28%) tumours were noted to have histological evidence of extramural vascular invasion, 224 (48%) had no evidence of vascular invasion, and this information was not available in 110 (24%) cases.

At the time of censoring for data analysis 228 (49%) patients had died from their disease, 64 (14%) were deceased from all other causes, and 169 (37%) were alive. The median five-year disease-specific survival for the cohort was 58 months, comparable with the national average of approximately 45% five-year survival for colorectal cancer in the UK (NICE, 2004).



### **2.4.3 Monoclonal antibody binding to ovarian cancer and normal tissue TMA**

New mAbs were screened for normal and tumour binding on an ovarian cancer TMA and a normal tissue TMA (AA9 Human, Normal organs; Super bio Chips, Seoul, Korea).

The ovarian cancer TMA represents a cohort of 362 patients with primary ovarian cancer treated at Nottingham University Hospitals between 2000 and 2007. Staging of the cancers was performed using the International Federation of Obstetrics and Gynaecology (FIGO) criteria. All patients included in this study were treated according to the current standard chemotherapy regimens with either single agent carboplatin in 65 patients (41.4%) or platinum-based combination chemotherapy in 89 patients (56.7%), with 3 patients refusing chemotherapy. Platinum-resistant cases were defined as patients who progressed on first-line platinum chemotherapy during treatment or who relapsed within 6 months after treatment. All patients underwent surgery; over 44% of cases (n=69) were deemed to be suboptimally debulked (tumour remaining <1 cm) after initial surgery. Patients were followed-up by physical examination, computed tomography, and CA-125 levels. Haematoxylin and eosin-stained sections from the tumours of these patients were reviewed by a gynaepathologist blinded to the clinical data and pathological diagnosis. For each tumour, a review of its type and differentiation was also carried out by SD. Clinical data associated with each case was collected and recorded from the patients' notes or via the hospital's electronic records (NotIS). Such information included: patients' age at diagnosis, FIGO stage, extent of surgical cyto-reduction, and the type, duration and response to chemotherapy. Details of adjuvant treatment, disease-specific survival (DSS) and overall survival (OS) were documented for all patients. Survival was calculated from the operation date until 30th of May 2008 when any remaining survivors were censored. Median follow up was 36 months. Ethical approval to collect the samples and relevant data for the study was granted by the Nottinghamshire Local Research Ethics Committee.

The normal tissue TMA contained 59 cores representing 38 normal organs. Each core was categorised according to the origin of the sample; normal tissue from a non-cancer patient, normal

tissue from a cancer patient, but the cancer involves an unrelated organ, normal tissue adjacent to the cancer. The tissue type and category is detailed in Table 2.6.

**Table 2.6 Details of normal tissue TMA and tissue type.**

Core Number	Organ	Associated lesion Tissue type	Tissue type <sup>1</sup>
1	Skin	Breast cancer	B
2	Skin breast cancer	Breast cancer	B
3	Subcutis	Fatty abdomen	A
4	Breast	Breast cancer	C
5	Breast	Breast cancer	C
6	Spleen	Stomach cancer	B
7	Spleen	Stomach cancer	B
8	Lymph node	Stomach cancer	B
9	Lymph node	Stomach cancer	B
10	Skeletal	Muscle angiosarcoma	B
11	Nasal mucosa	Chronic sinusitis	A
12	Lung	Metastatic cancer of lung (from stomach)	B
13	Lung	Lung cancer	C
14	Bronchus	Lung cancer	C
15	Heart	No abnormal finding	A
16	Salivary gland	Oropharyngeal cancer	B
17	Liver	Hepatocellular carcinoma	C
18	Liver	Stomach cancer	B
19	Liver	Hepatocellular carcinoma	C
20	Gallbladder	Rectal cancer	B
21	Pancreas	Stomach cancer	B
22	Pancreas	Pancreas islet cell tumour	C
23	Tonsil	Chronic tonsillitis	A
24	Oesophagus	Oesophageal cancer	C
25	Oesophagus	Oesophageal cancer	C
26	Stomach	Body stomach cancer	C
27	Stomach	Body stomach cancer	C
28	Stomach	Antrum stomach cancer	C
29	Stomach	Smooth muscle stomach cancer	C
30	Duodenum	Ampulla of Vater cancer	C
31	Small bowel	Pseudomyxoma peritonei	B
32	Small bowel	Colonic diverticulosis	A
33	Appendix	Metastatic cancer of ovary (from stomach)	B
34	Colon	Rectal cancer	C
35	Colon	Colon cancer	C
36	Rectum	Rectal cancer	C
37	Kidney	Cortex renal cell carcinoma	C
38	Kidney	Cortex renal cell carcinoma	C
39	Kidney	Medulla renal cell carcinoma	C
40	Urinary bladder	Invasive bladder carcinoma	C
41	Prostate	Bladder cancer	B

<sup>1</sup> Tissue type denotes the following categories; A. Normal tissue from a non-cancer patient; B. Normal tissue from a cancer patient, but the cancer involves unrelated organ; C. Normal tissue adjacent to the cancer.

42	Prostate	Bladder cancer	B
43	Seminal vesicle	Bladder cancer	B
44	Testis	Prostate cancer	B
45	Endometrium	Proliferative benign ovarian neoplasm	A
46	Endometrium,	Secretory ovarian cancer	B
47	Myometrium	Adenomyosis	A
48	Uterine cervix	Leiomyoma	A
49	Salpinx	Cervix cancer	B
50	Ovary	Ovary cancer	C
51	Placenta	Mature placenta	A
52	Placenta	Mid-trimester placenta	A
53	Umbilical cord	Mature placenta	A
54	Adrenal gland	Renal cell carcinoma	B
55	Thyroid	Thyroid cancer	C
56	Thymus	Lymphoid hyperplasia	A
57	Brain	White matter no abnormal finding	A
58	Brain	Gray matter no abnormal finding	A
59	Cerebellum	No abnormal finding	A

## 2.5 Screening of mAbs on The Consortium for Functional Glycomics array

### 2.5.1 Screening on glycan array

505/4, 692/29 and BR96 were FITC labelled and sent to the Consortium for Functional Glycomics where they were screened against between 311 and 460 glycans. Briefly, synthetic and mammalian glycans with amino linkers were printed onto N-hydroxysuccinimide (NHS)-activated glass microscope slides. Printed slides were incubated with 1µg/ml mAb for 1 hour before detecting mAbs with Alexa488-conjugated goat anti-mouse IgG. Slides were then dried before scanning. 2-25 LE screening data was obtained from the Consortium for Functional Glycomics database.

## 2.6 *In vitro* functional studies of mAbs, murine serum and hybridoma supernatants

In order to characterise mAbs, murine serum and hybridoma supernatant, a range of *in vitro* assays were used.

## **2.6.1 Analysis of antibody binding to cancer cells**

### **Indirect immunofluorescence analysed by flow cytometry**

Flow cytometry was used to study the level of binding by antibodies, or hybridoma supernatant to a range of cell lines. Flow cytometry was also used to assess the level of binding of mAbs to normal cells including fresh hepatocytes or primary HUVECs below passage 6. The cell lines described previously (Table 2.2) were harvested and counted by diluting cells 1:1 with trypan blue, to ascertain cell viability, and counting using a haemocytometer. For cell binding assays the cells were plated at  $1 \times 10^5$  per well in a Nunc, round bottomed 96 well plate (Thermo Fisher Scientific, Waltham, MA, USA). The plate was then centrifuged (100g, 5min; ALC Multispeed centrifuge PK121, Jencons, UK) and supernatant flicked out before the addition of 50 $\mu$ l of antibody, serum or hybridoma supernatant diluted in 2% NBCS/PBS. Most commonly, the mAb or hybridoma supernatant was incubated on ice for 1 hour, before the addition of 200 $\mu$ l PBS to wash. The plate was then centrifuged at 100g, 5min before removing the supernatant. A labelled secondary antibody was then added at the relevant concentration (See table 2.7 for list of secondary mAbs and working dilutions) diluted in PBS. Most commonly the secondary antibody was incubated on ice for 1 hour. After incubation with the secondary, 200 $\mu$ l PBS was added to wash, before centrifuging (100g, 5min). The supernatant was flicked from the plate before the cells were resuspended in 200 $\mu$ l PBS. The cells were then transferred to a FACS tube before adding an extra 200 $\mu$ l 1% formaldehyde. The fluorescence of the cells was then analysed on a flow cytometer (Beckman Coulter, FC5000 (Beckman Coulter, CA, USA). After acquisition of the data was analysed using Windows Multiple Document Interface (WinMDI) 2.9 software (Joseph Trotter, Scripps Research Institute, La Jolla, CA, USA).

**Table 2.7 Details of secondary antibodies.**

<b>Antibody name</b>	<b>Company</b>	<b>Dilution</b>
Polyclonal rabbit anti-mouse Ig-FITC	Dako	1:100
Polyclonal rabbit anti-mouse IgM-FITC	Dako	1:100
Polyclonal rabbit-anti mouse IgG-HRP	Dako	1:1000
Polyclonal rabbit anti-mouse Ig-HRP	Dako	1:1000
Polyclonal rabbit anti-mouse IgM-HRP	Dako	1:1000

### **Enzyme-linked immunosorbent assay**

The analysis of the level of binding of antibodies to cell lines was also carried out using enzyme linked immunosorbent assay (ELISA). ELISAs allows a large number of hybridoma supernatants, antibody or serum dilutions to be measured in one assay more easily than by flow cytometry. However, it is limited to cells that adhere to the plastic tissue culture plate.

First, cells were harvested from cell culture and counted as previously described. Cells were plated at  $1 \times 10^5$  cells per well in a Nunc, flat-bottomed 96 well tissue culture plate (Thermo Fisher Scientific, MA, USA). Cells were then incubated in 200 $\mu$ l growth media for 2-3 days in tissue culture conditions (37°C, 5%CO<sub>2</sub>) until the cells were confluent. Once confluent the growth media was removed carefully before the plate was either fixed with 200 $\mu$ l 1% formaldehyde for 1 hour on ice, followed by washing well in PBS and blocking with 200 $\mu$ l 1% bovine serum albumin (BSA; PAA, Pasching, Austria)/PBS for 1 hour on ice, or the cells were blocked without fixing. Subsequent to fixing/blocking or blocking, the cells were incubated with 50 $\mu$ l of hybridoma supernatant or mAbs at various concentrations, diluted in 0.1% BSA/PBS. This was carried out on ice for 1 hour before washing with PBS X3. 50 $\mu$ l secondary antibody labelled with horse radish peroxidase (HRP) was then added at the relevant concentration (Table 2.7) and incubated on ice for 1 hour. The plate was then washed X3 with PBS. The cells were then incubated with 150 $\mu$ l of 0.2ml of 1.5mg/ml 2,2'-Azinobis [3-

ethylbenzothiazoline-6-sulfonic acid]-diammonium salt (ABTS) and 10 $\mu$ l 30% H<sub>2</sub>O<sub>2</sub> solution in 10ml of 0.1M citrate buffer. The plate was then left in the dark to allow any HRP to oxidise the ABTS, yielding a green end product. The plate was then read at 405nm using an absorbance microplate reader (Anthos htII, originally Anthos Labtec, now part of Beckman Coulter).

### **Homophilic binding analysis**

A number of monoclonal antibodies have been shown to bind to antigen and also to a separate and distinct binding domain on V<sub>H</sub> on itself. The ability of an antibody to bind to itself is termed homophilic binding. To test whether a mAb displayed homophilic characteristics, mAb was titrated on a cell line up to a high concentration with saturation not being reached with a homophilic mAb. A second assay used to test a mAbs ability to bind homophilically involved the incubation of cells with a very high concentration of un-labelled mAb and then competing with FITC-labelled mAb. These assays are described below.

Cells were harvested from culture and counted as previously described. 1x10<sup>5</sup> cells were plated per well before centrifugation (100g, 5min, RT). The supernatant was removed before adding 50 $\mu$ l antibody at 0.1-30 $\mu$ g/ml per well or 100 $\mu$ g/ml unlabelled mAb in PBS. The antibody was incubated with the cells for 1 hour on ice before adding 200 $\mu$ l PBS to wash. The plate was centrifuged (100g, 5min, RT) before removing the supernatant. 50 $\mu$ l of anti-Ig-FITC labelled antibody (titration assay; Dako) was added to the cells that received a titration of mAb, whereas FITC-labelled mAb at 1, 3 and 10 $\mu$ g/ml was added to the cells that received 100 $\mu$ g/ml unlabelled mAb (competition assay). The cells were then incubated for a further 1 hour on ice. After incubation with the secondary antibody or FITC-labelled mAb, the cells were washed with 200 $\mu$ l PBS before centrifugation (100g, 5min, RT) and removal of supernatant. The cells were resuspended in 200 $\mu$ l 1% formaldehyde and transferred to FACS tubes. A further 200 $\mu$ l PBS was added to the tubes (total 400 $\mu$ l, 0.5% formaldehyde/PBS) before the cells was analysed by flow cytometry.

In order to determine whether the binding of one antibody resulted in the exposure of other antigenic sites on the cell surface, binding of mAb to fresh and formaldehyde-fixed cells was compared. Cells were harvested and counted as previously described.  $5 \times 10^6$  cells were incubated in 500  $\mu$ l 1% formaldehyde (fixed) while  $5 \times 10^6$  cells were incubated in PBS (fresh). Cells were re-counted before plating  $1 \times 10^5$  per well before centrifugation at 100g, 5min, RT. The supernatant was removed before adding 50  $\mu$ l antibody at 0.1-30  $\mu$ g/ml per well to both fresh and fixed cells. The antibody was incubated with the cells for 1 hour on ice before adding 200  $\mu$ l PBS to wash. The plate was centrifuged (100g, 5min, RT) before removing the supernatant. 50  $\mu$ l of anti-IgG-FITC labelled antibody (Dako) was added to each well before incubating on ice for 1 hour. The cells were washed a final time with 200  $\mu$ l of PBS before being centrifuged at 100g, 5min, RT and the supernatant was removed. The cells were resuspended in 200  $\mu$ l 1% formaldehyde and transferred to FACS tubes. A further 200  $\mu$ l PBS was added to the tubes before the cells was analysed by flow cytometry.

### **2.6.3 Analysis of binding to cancer cell glycolipid extraction**

In order to test whether a mAb, serum or hybridoma supernatant binds to glycolipid, glycolipid was extracted from cancer cells before screening by ELISA.

#### **Glycolipid extraction**

In order to extract glycolipid from cancer cells,  $10^8$  cells were required. Therefore, colorectal and ovarian cancer cell lines were grown in large quantities, harvested and stored at  $-80^\circ\text{C}$  until needed. Cells were harvested either with (adherent) or without (non-adherent) trypsin-EDTA. The cells were washed three times in PBS to remove trypsin and growth media. The cells were centrifuged resuspended in 1ml PBS and transferred to a 1.5ml eppendorf, before centrifuging at 850g, 2min in a bench-top microfuge. The supernatant was removed and eppendorf tubes stored at  $-80^\circ\text{C}$ . For glycolipid extraction  $5-10 \times 10^8$  cells were thawed at RT before the addition of 3ml 100% methanol. After pooling cells from eppendorf tubes in 3ml methanol in a 15ml tube (Falcon) an additional 6ml

100% chloroform was added (final ration 2:1 chloroform: methanol). The tube was then rock and rolled overnight at 4°C. The resulting emulsion was split into 9 eppendorf tubes (1ml each) before centrifugation at 850g, 30min. The result of this centrifugation was two aqueous phases separated by a solid phase two liquids layers a 'lipid' layer (layer 2) and an aqueous layer (layer 3) separated by a solid 'denatured protein' layer (layer 1; Fig 2.4. The aqueous phases were separated.

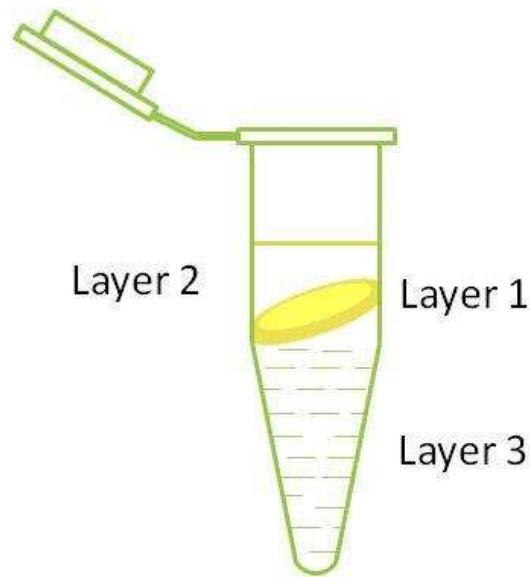


**Figure 2.4 Result of 2:1 chloroform: methanol glycolipid extraction of cancer cell lines.** Centrifugation of the emulsion results in two liquids layers a 'lipid' layer (layer 2) and an aqueous layer (layer 3) separated by a solid 'denatured protein' layer (layer 1).

#### **Analysis of mAb, serum and hybridoma supernatant binding to glycolipid**

In order to characterise the binding of antibodies to glycolipid, the layers resulting from extraction were prepared. Layer 1, made up of denatured proteins was dissolved in DMSO; Layer 2 was dried down under N<sub>2</sub> gas before resuspending in PBS. After preparation of the layers, they were diluted between 1:10 to 1:3000 before adding to a 96 well polystyrene plate. The extracted layers were dried to the plate overnight at 40°C. Before addition of mAb, serum or hybridoma supernatant, the plate was blocked with 200µl 1% BSA/PBS for 1 hour on ice. The BSA was removed before 50µl antibody sample was added to the plate. The plate was then incubated for 1 hour on ice, before washing three times in PBS. Excess PBS was removed by dabbing gently on tissue paper. 50µl



secondary antibody (rabbit anti-mouse IgM/anti-mouse IgG/anti-mouse Ig-HRP) was added and incubated for a further hour on ice. 150µl ABTS solution was added to each well and developed in the dark. The optical density of the plate was determined on an absorbance plate reader at 405nm.

#### **Binding of 692/29 to Lewis y and Lewis b glycans**

The ability of 692/29 to bind to Lewis y and Lewis b glycans (IsoSep, Sweden) was tested by ELISA. 100µl 10µg/ml Lewis y-human serum albumin (HSA) or Lewis b-HSA diluted in 1% BSA/PBS per well was incubated in a 96 well flat-bottomed ELISA plate overnight at 4°C. Supernatant was removed before blocking the plate with 200µl 1% BSA/PBS. The BSA was removed before adding 50µl 1, 3 or 10µg/ml 692/29 or 10µg/ml 505/4 as a negative control. The plate was incubated on ice for 1 hour before washing 3 times in a PBS bath. 50µl 1:1000 anti-IgG-HRP (Dako) was added per well and the plate was incubated on ice for a further 1 hour. The plate was then washed 4 times in a PBS bath before antibody binding was assessed using 150µl ABTS solution (as above) per well. The plate was then allowed to develop in the dark before the optical density of the plate was determined on an absorbance plate reader at 405nm.

#### **Sodium periodate treatment of cells and mAb binding**

Sodium periodate can be used to oxidise carbohydrates on the surface of cells without disturbing protein or lipids. It can therefore be used to determine whether an antibody binds to a carbohydrate determinant on cells, through a lack of binding in a whole cell ELISA format as follows.

Cells were harvested and plated as the whole cell ELISA described previously. On the day of the experiment, 200µl 1% glutaraldehyde/PBS was added to each well and the plate incubated on ice for 1 hour. The plate was then washed three times in PBS before the addition of 100µl 5, 2.5 and 1.25mmol/L sodium periodate (in sodium acetate buffer pH 4.5). The plate was then incubated for 2 hours at 37°C. The plate was then washed three times with PBS before blocking with 200µl 1%

BSA/PBS for 1 hour on ice. 50µl of antibody was then added to the sodium periodate-treated cells and the rest of the ELISA carried as previously described.

#### **2.6.4 Analysis of antibody mediated direct cell death**

The ability of an antibody to cause direct cell death of its target cell may be a useful characteristic for therapy. A range of assays were used to investigate whether mAbs could induce direct cell death of cancer cells and the mechanism of killing observed.

##### **Antibody-mediated propidium iodide uptake**

In order to quantify the percentage of dead cells after antibody treatment, propidium iodide (PI) was used. PI is a 668Da fluorescent molecule that can be taken up by dying and dead cells, but not live cells. Once in the cell, PI intercalates between DNA bases. The fluorescence of cells can then be measured to ascertain a proportion of dead cells. Cells were harvested and counted as described previously. The cells were then plated at  $5 \times 10^4$  cells per well in a Nunc round-bottomed tissue 96 well plate. The plate was then centrifuged (100g, 5min) and supernatant removed. 50µl mAb or hybridoma supernatant in 2.5% NBCS was then added to the cells for a range of incubation periods, from 10min to overnight at either 4°C, RT (22°C) or 37°C. For the last 30min of the incubation, 10µl of 1:10 PI (1mg/ml) in PBS was added. After the 30min incubation, 140µl was added to the cells and they were transferred to FACS tubes. An additional 200µl PBS was added to the tubes before analysing fluorescence by flow cytometry.

In order to determine whether PI uptake observed was the result of cell death, cell viability and number was measured over 5 days of antibody treatment. Cells were harvested and counted as described previously.  $1 \times 10^5$  cells were plated in a 24 well flat-bottomed plate (Nunc) and incubated with 500µl 30µg/ml mAb in 10% NBCS supplemented media. Cells were incubated for 24, 48 or 120 hours at 37°C, 5%CO<sub>2</sub>. After each incubation the supernatants were removed and cells were trypsinised with 100µl trypsin/EDTA. Cells were transferred to 1.5ml eppendorf tubes and washed

with 1ml media before centrifuging at 3200g, 1.5min, RT in a microfuge. Cells were resuspended in 1ml media for cell count and viability check. 10 $\mu$ l cells were added to 10 $\mu$ l trypan blue and counted using a haemocytometer.

In order to establish whether the live cells remaining after antibody treatment were resistant to mAb-mediated cell death, the cells were harvested after 5 days and were subjected to further mAb treatment and compared to untreated cells. The cells were harvested and cell number and viability checked, as above. 5x10<sup>4</sup> mAb treated or fresh, untreated cells were plated in a 96 round bottomed plate (Nunc) before centrifuging (100g, 5min, RT) and removal of supernatant. 50 $\mu$ l of 10 or 30 $\mu$ g/ml mAb in 2.5% NBCS was then added and the cells were incubated at 37<sup>o</sup>C, 5%CO<sub>2</sub> overnight. For the last 30min of the incubation, 10 $\mu$ l of 1:10 PI (1mg/ml) in PBS was added. After the 30min incubation, 140 $\mu$ l was added to the cells and they were transferred to FACS tubes. An additional 200 $\mu$ l PBS was added to the tubes before analysing fluorescence by flow cytometry.

To check whether live cells after 5 days of mAb treatment expressed the same level of antigen as mAb-untreated cells, 1x10<sup>5</sup> mAb treated or fresh, untreated cells were plated in a 96 round bottomed plate (Nunc) before centrifuging (100g, 5min, RT) and removal of supernatant. 50 $\mu$ l of 0.1, 0.3 or 1 $\mu$ g/ml mAb in PBS was then added and the cells were incubated on ice for 1 hour before adding 200 $\mu$ l PBS to wash. The plate was centrifuged (100g, 5min, RT) before removing the supernatant. 50 $\mu$ l of anti-IgG-FITC labelled antibody (Dako) was added to each well before incubating on ice for 1 hour. The cells were washed a final time with 200 $\mu$ l of PBS before being centrifuged at 100g, 5min, RT and the supernatant was removed. The cells were resuspended in 200 $\mu$ l 1% formaldehyde and transferred to FACS tubes. A further 200 $\mu$ l PBS was added to the tubes (total 400 $\mu$ l, 0.5% formaldehyde/PBS) before the cells was analysed by flow cytometry.

### **Detection of mAb-mediated cell death in the presence of cross-linking antibody**

To determine whether mAbs unable to induce direct cell death can with the aid of cross-linking mAbs, rabbit anti-mouse Ig and goat anti-rabbit Ig immunoglobulins were used. Cells were harvested and counted as described previously. The cells were then plated at  $5 \times 10^4$  cells per well in a Nunc round-bottomed tissue 96 well plate. The plate was then centrifuged (100g, 5min) and supernatant removed. 50 $\mu$ l 10 or 30 $\mu$ g/ml mAb with or without 1:50 rabbit anti-mouse Ig and goat anti-rabbit Ig immunoglobulins or hybridoma supernatant in 2.5% NBCS was added to the cells. The plate was then incubated overnight at 37°C, 5% CO<sub>2</sub>. For the last 30min of the incubation, 10 $\mu$ l of 1:10 PI (1mg/ml) in PBS was added. After the 30min incubation, 140 $\mu$ l was added to the cells and they were transferred to FACS tubes. An additional 200 $\mu$ l PBS was added to the tubes before analysing fluorescence by flow cytometry.

### **Inhibition of cell death with pan-caspase inhibitor**

Apoptosis is mediated by a family of proteases named caspases. Their activation results in the death of a cell. In order to establish whether antibody-mediated uptake of PI is either dependent or independent of caspases (i.e. via apoptosis or an alternative pathway) a pan caspase-inhibitor was used. Cells were harvested and  $5 \times 10^4$  cells were added to each well. As well as antibody, 20 $\mu$ M of Z-VAD-FMK (carbobenzoxy-valyl-alanyl-aspartyl-[O-methyl]-fluoromethylketone; Promega, WI, USA) was added to the cells. Z-VAD-FMK is a pan caspase inhibitor that irreversibly binds to the catalytic site of caspase proteases, inhibiting apoptosis. The cells, antibody and inhibitor were incubated overnight at 37°C, 5% CO<sub>2</sub>. 0.1 $\mu$ g PI was then added to the cells 30min prior to the end of the incubation. The plate was then centrifuged and supernatant removed. The plate was then incubated overnight at 37°C, 5% CO<sub>2</sub>. For the last 30min of the incubation, 10 $\mu$ l of 1:10 PI (1mg/ml) in PBS was added. After the 30min incubation, 140 $\mu$ l was added to the cells and they were transferred to FACS tubes. An additional 200 $\mu$ l PBS was added to the tubes before analysing fluorescence by flow cytometry.

### **Analysis of mAb-mediated pore formation on the cell surface**

As well as apoptosis, mAbs can also induce cell death of target cells directly in an apoptosis-independent manner. One mechanism by which this can occur is oncosis. Oncosis is a caspase-independent mechanism of cell death characterised by the swelling of a cell and the formation of large pores on the cell surface. One way by which oncosis can be assessed is through the uptake of larger-sized FITC-labelled dextran beads.

Therefore, cells were harvested and plated at  $1 \times 10^5$  cells/well before adding 50 $\mu$ l 10 or 30 $\mu$ g/ml mAb (for anti-Fas treatment of Jurkat cells, 50 $\mu$ l 250 or 500ng/ml antibody was used). In addition to the antibody, 0.1mg of 3000, 40,000 or 500,000Da dextran-FITC beads were added (Invitrogen). The plate was incubated overnight at 37°C, 5% CO<sub>2</sub>. 30min prior to the end of the incubation, 0.1 $\mu$ g PI was added to the cells. 200 $\mu$ l PBS was added to each well, the plate centrifuged (100g, 5min RT) and supernatant removed twice. The cells were resuspended in 200 $\mu$ l PBS and transferred to FACS tubes. An additional 200 $\mu$ l PBS was added to each tube before analysis the cells by flow cytometry.

### **2.6.5 Antibody dependent cellular cytotoxicity and complement dependent cytotoxicity assays**

In order to establish whether mAbs or hybridoma supernatant could induce ADCC and CDC, chromium-51 (Cr<sup>51</sup>) release assays were carried out.

Target cells were harvested and  $2 \times 10^6$  cells incubated with 50 $\mu$ l Cr<sup>51</sup> in 1ml 10% NBSC-supplemented RPMI for 1 hour at 37°C. For the ADCC assay, peripheral blood mononuclear cells (PBMC) were isolated from a human blood sample taken on the day of the experiment. Whole blood was diluted 1:2 in RPMI before layering on histopaque-1077 in a 50ml centrifuge tube. The blood was then centrifuged at 425g, 20min, with the brake not on. PBMCs were isolated from the 50ml tube and washed twice in 20ml RPMI. For the CDC assay, serum was isolated from whole blood by allowing

the blood to clot at RT for 1-2 hour. The tube was then centrifuged at 425g, 10min. Serum was pipetted off leaving behind the clot. Care was taken not to lyse red blood cells in the clot.

After the 1 hour incubation with Cr<sup>51</sup>, the target cells were washed twice with 20ml RPMI, counted and plated at  $5 \times 10^3$  cells in 50 $\mu$ l per well. To the target cells,  $5 \times 10^5$  PBMCs or isolated serum were added in 100 $\mu$ l along with 50 $\mu$ l X4 concentrated mAb/hybridoma supernatant, giving a total volume of target cells/effectors/antibody of 200 $\mu$ l per well. The plate was then incubated at 37°C, 5% CO<sub>2</sub> for 4 hours. For maximum and spontaneous Cr<sup>51</sup> release, Triton X100 detergent (12%) or irrelevant Ig (respectively) was added to control wells. After the 4 hour incubation 50 $\mu$ l supernatant was taken and transferred to 96 well lumaplate (Packard Bioscience, Groningen, Netherlands) containing solid scintillant and the plate was left air-dry overnight at RT. The plate was then analysed on a Topcount scintillation counter (Canberra Packard, Pangbourne, UK). The relative percentage cell lysis was calculated as a percentage of maximum lysis (Triton X100 – spontaneous).

## 2.7 Immunisations

### 2.7.1 Preparation of whole cancer cells

Cancer cells were harvested from culture on the day of immunisation as previously described. Cells were washed twice in sterile PBS before resuspending in PBS at  $5 \times 10^7$  cells per ml. Cells were stored at 4°C until used.

### 2.7.2 Preparation of glycolipid

Glycolipid was extracted from whole cancer cells as described previously (Section 2.5.2). The eppendorf used to dry down Layer 2 under N<sub>2</sub> gas was weighed before and after drying. The glycolipid was then resuspended in PBS at 10mg/ml. Glycolipid was then stored in the fridge until used.

### 2.7.3 Preparation of liposomes

Cholesterol, dicetylphosphate (DCP) and phosphocholine (PC) were suspended in 2:1 chloroform: methanol at 1mg/ml. Cancer cell line glycolipid extract was dried down in a pre-weighed round-bottomed flask using a rotary evaporator at 60°C. The resulting lipid film was resuspended at 1mg/ml in 2:1 chloroform: methanol. The 1mg/ml solutions were mixed in a round bottomed flask at various ratios (Table 2.8) to a total volume of 10ml and 10 mgs of lipids. The mixture was then dried down using a rotary evaporator at 60°C until all chloroform and methanol had evaporated, leaving a uniform lipid film on the inside of the flask. 1ml dH<sub>2</sub>O was then added to the film and vigorously shaken until all lipids were resuspended in the 1ml dH<sub>2</sub>O. All work with chloroform and methanol was carried out in a fume hood.

**Table 2.8 Liposome constituents.** Tumour glycolipid denoted by TGL and  $\alpha$ -galactosylceramide depicted by  $\alpha$ GalCer.

Liposome	Cholesterol (mg)	DCP (mg)	PC (mg)	TGL extract (mg)	$\alpha$ GalCer (mg)	Total (mg)
90% TGL	0.00	0.00	0.40	9.60	0.00	10.00
90% TGL + $\alpha$ GalCer	0.00	0.00	0.00	9.57	0.43	10.00
10% TGL	3.25	0.46	4.61	1.68	0.00	10.00
10% TGL + $\alpha$ GalCer	3.23	0.46	3.91	1.68	0.72	10.00
2.5% TGL	3.34	0.47	5.76	0.43	0.00	10.00
2.5% TGL + $\alpha$ GalCer	3.32	0.47	5.04	0.43	0.74	10.00

### 2.7.4 Adjuvants

Along with glycolipid, mice received either complete or incomplete Freund's adjuvant subcutaneously and intraperitoneally respectively at a ratio of 1:1 with cancer cell glycolipid-extract. 50 $\mu$ g Poly(I:C) (Invivogen, CA, USA) was immunised with each whole cell immunisation in the same site as the cells. CD4 cell depletion prior to whole cell immunisation was achieved by immunising 200 $\mu$ l TIB-207 (at 1mg/ml; anti-CD4 antibody produced in-house from TIB-207 hybridoma (American Type Culture Collection) intraperitoneally on day 0, 7 and 14 as well as with the whole cell

immunisation.  $\alpha$ -galactosylceramide ( $\alpha$ GalCer; Alexis Biochemicals, Nottingham, UK) was used as an adjuvant for liposome immunisation and was incorporated into the liposomes at a concentration relating to 10 $\mu$ g per 100 $\mu$ l immunisation.

### **2.7.5 Immunisation protocol**

BALB/c mice were used aged between 6 and 8 weeks (Charles River, UK) and cared for by the staff at the Biomedical Services Unit at the University of Nottingham. Prior to any immunisation protocol, sera were collected via a tail bleed extraction. The blood was centrifuged at 8500g, 5min to remove the blood cells and the serum was stored at -20°C to be used a negative control in screening assays. Immunisations were carried out at two weekly intervals in a maximum volume of 200 $\mu$ l (sample diluted in PBS) using a 1ml insulin syringe (BD Bioscience, Spain). In the cases where an adjuvant was used, the immunogen and adjuvant were combined in 1:1 ratio and administered intravenously, subcutaneously or intraperitoneally. Seven days post-immunisation, serum was collected via tail bleed extraction as previously described.

### **2.7.6 Analysis of antibody response to immunisations**

Antibody responses to immunisations were assessed using the whole cell ELISA technique described previously (Section 2.5.1) where the sera from mice were serially diluted at concentrations ranging from 1:100, to 1:100,000. After the addition of HRP-conjugated secondary antibody and ABTS solution, the level of antibody response was compared to the pre-bleed serum control.

### **2.7.7 Isolation of splenocytes**

Mice were sacrificed as per schedule 1 protocol (cervical dislocation) and sprayed with 70% ethanol to sterilise the working area. Using several sets of sterile dissecting instruments, the spleens were removed from the mice. Excess fat and connective tissue was removed and the spleen was transferred to a sterile 100mm Petri dish. 5ml of serum free RPMI 1640 was added to the dish and



the spleen was washed with the media using a syringe and 25-gauge needle. The media was passed through the spleen several times and finally the spleen was homogenised with sterile forceps. The homogenate was passed through sterile gauze into a universal 25ml tube, total volume was increased to 25ml with serum free RPMI, and the tube centrifuged at 100g for 10min. The media was aspirated off, leaving approximately 1ml remaining in the cone of the tube. The cells were resuspended in 5ml serum free media and counted using trypan blue.

### **2.7.8 Collection of large quantities of sera from immunised mice**

Cardiac blood was collected using insulin syringes (Microfine 11-100 insulin 12.7mm syringe, 1ml capacity; Becton Dickinson, France) at the time of splenocyte collection.

### **2.7.9 Fusion of Mice splenocytes with NS0 myeloma cells**

Mice producing the highest sera titres are chosen to generate antibody-producing hybridomas. NS0 cells were harvested, resuspended in serum free RPMI and counted for fusion with splenocytes. Cells were combined in a ratio of 1: 5 (NS0: splenocytes) e.g. ( $2 \times 10^7$ :  $1 \times 10^8$ ) in a universal 25ml tube and centrifuged for 5min at 150g. The supernatant was aspirated and the combined cell pellet was resuspended in 800 $\mu$ l polyethylene glycol (PEG) gradually over 1min. The PEG breaks the lipid membranes and allows fusion of the cell populations. The cells were agitated for 1min prior to the addition of 1ml of serum free RPMI 1640 which was added over 1min while continuing to agitate. A further 5ml of serum free media was added to the cell suspension over a min while continuing to agitate and finally the volume was slowly increased to 25ml with serum free media. The suspension was centrifuged for 5min at 150g and the supernatant was removed. The cells were resuspended in 15ml hybridoma media (RPMI 1640, 10% FCS plus HAT supplement). The cell suspension was spread evenly across a 96 well plate and the cells were incubated at 37°C for approximately 8 days, by which time successful hybridomas had grown. Cells were re-fed approximately every two days with fresh hybridoma media. Following 8 days supernatants were collected and analysed for the presence

of antibodies, using the whole cell ELISA and flow cytometry protocols described previously (Section 2.5.1). Positive wells were harvested, washed in complete media and spread across 96 well plates at 0.3 cells per well to acquire a clone. The plate was then screened for positive wells by whole cell ELISA. Positive wells were grown until a sufficient number of cells was obtained to spread across a 96 well plate at 0.3 cells per well for a second time. If the resulting number of colonies equalled ~30 and all hybridomas were positive, the hybridoma was considered a clone.

## 2.8 Statistical analysis of data

### 2.8.1 Immunohistochemical analysis

Statistical analysis of the study data was performed using the SPSS package (version 16 for Windows, SPSS Inc., IL, USA). Pearson  $\chi^2$  chi-square tests were used to determine the significance of associations between categorical variables. Disease-specific survival calculations included all patients whose death related to colorectal cancer. In contrast, patients whose deaths resulted from non-colorectal cancer related causes were censored at the time of death. Kaplan-Meier curves were used to assess factors which influenced survival. The statistical significance of differences in disease-specific survival between groups with differing caspase expression was estimated using the log-rank test. The Cox proportional-hazards model was used for multivariate analysis in order to determine the relative risk and independent significance of individual factors. In all cases  $p$ -values  $< 0.05$  were considered as statistically significant.

### 2.8.2 Other analysis

The mean and standard deviations of data were calculated in Microsoft Excel. Significant difference between two sets of data was calculated using a two-tailed Students T Test with  $p < 0.05$  accepted as a significant difference.

## Chapter 3 Cleaved caspase-3 expression in colorectal cancer

### 3.1 Background

MAbs have been shown to induce direct cell death of cancer target cells. In order to determine the therapeutic value of a mAb's ability to induce direct cell death independently of apoptosis, this study determined the level of apoptosis in colorectal cancer using a large TMA cohort. One of the hallmarks of cancers is their ability to accumulate mutations that confer increased growth and the ability to metastasize and avoid apoptosis (Hector & Prehn, 2009; Yang et al., 2009). Resistance to apoptosis can occur via the extrinsic or intrinsic pathways. The extrinsic pathway is triggered by ligands such as TRAIL and Fas ligand. Cancer therapies targeting Fas ligand were of limited value due to hepatotoxicity (Klos et al., 2003) and the observation that most colorectal cancers are resistant to Fas-mediated killing (O'Connell et al., 2000). In contrast, early results suggested that cancer was more sensitive to TRAIL-mediated apoptosis (Wiley et al., 1995). However, there has been conflicting evidence that colorectal cancer is resistant to TRAIL mediated lysis (Hale et al., 1988) due to over-expression of decoy receptor 3 (Mild et al., 2002) or over-expression of the inhibitor FLICE-like-inhibitory protein-long (FLIP-L; (Ullenhag et al., 2007)). In line with these observations, clinical trials with the pro-apoptotic ligand Apo2L/TRAIL or TRAIL receptor blocking antibodies have shown mixed responses (Ashkenazi & Herbst, 2008). As well as resistance to extrinsic stimuli, colorectal cancer cells accumulate a range of mutations that give rise to aberrant levels of apoptotic proteins. For example the anti-apoptotic protein, Bcl-2, is progressively increased during colorectal cancer progression (Krajewska et al., 2008) whereas expression of the pro-apoptotic proteins Bax and Bak decreases (Coppola et al., 2008; Duckworth & Pritchard, 2009). Over 50% of colorectal cancer patients express a mutated, inactive form of p53 leading to resistance to apoptosis. Indeed, the p53 negative/Bcl-2 positive phenotype is an independent indicator of good prognosis in colorectal cancer (Watson et al., 2005). Recent studies have shown that both DCC and UNC5C are dependence

receptors that induce apoptosis in the absence of ligand (Mazelin et al., 2004). Both of these receptors are frequently deleted in colorectal cancer increasing resistance to apoptosis.

Apoptosis within the tumour environment may be a consequence of nutrient deprivation due to excessive proliferation without an adequate blood supply or due to immune attack. Tumours express a range of stress related molecules which act like Toll-like receptors (TLRs) and alert the immune system to the danger (Nausch & Cerwenka, 2008; Waldhauer & Steinle, 2008). This process is termed immune surveillance. In a recent addition to this theory it has become clear that the transformed cells can acquire further mutations which make them resistant to the immune response (Dunn et al., 2005). There is then a period of immune equilibrium where the tumour mutates and the immune system adapts to continue to control tumour growth. This can last for many years and T cell infiltration, expression of MHC class I and the IFN- $\gamma$  induced transcription factor STAT-1 continue to be strong independent prognostic factors even in established colorectal tumours (Galon et al., 2006; Simpson et al., 2010). MHC-II expression is induced on epithelial, endothelial and fibroblast cells and is up regulated on T cells and macrophages by IFN- $\gamma$ . MHC-II expression on tumour cells and within stroma may therefore be a good marker of immune surveillance. Ultimately, if the immune system is sculpting the tumour phenotype, a process termed "immune editing", the tumour may become resistant to immune attack. One consequence of immune editing is alteration of the tumour microenvironment which becomes increasingly immunosuppressive. Tumours down-regulate stress molecules and fail to alert the immune response (Jordanova et al., 2008; McGilvray et al., 2009; Watson et al., 2006c). They also secrete immunosuppressive cytokines such as IL-10, TGF- $\beta$  and VEGF (Fukumura et al., 1998), which condition the tumour-associated macrophages (TAM) within the tumour to the M2 phenotype (Sica et al., 2008) and induce the trans-differentiation of fibroblasts into activated smooth-muscle fibroblasts, termed myofibroblasts (or carcinoma-associated fibroblasts [CAFs]). M2 macrophages and CAFs induce tissue repair, remodelling, angiogenesis, promoting tumour growth and metastasis, through the secretion of matrix-degrading enzymes and immunosuppressive cytokines (Mantovani et al., 2007).

The complexity of the roles that each component of the tumour microenvironment plays poses the question as to whether cell death of the tumour or tumour-associated stroma leads to a better or worse prognosis in cancer. Apoptosis mediated by either the intrinsic or extrinsic pathways results in cleavage of caspase-3. Caspase-3 is also rarely mutated in colorectal cancer (Soung et al., 2004) and is therefore an ideal marker for measuring apoptosis in these tumours. The CC3 mAb used in this study has previously been shown to bind specifically to the cleaved fragment of capase-3 in archival paraffin-embedded IHC (Gown & Willingham, 2002) as well as only to the large cleaved fragment of caspase-3 by western blot (Cheong et al., 2003; Garnier et al., 2003). This study therefore aims to measure the level of apoptosis both within the stroma and in tumour cells using the validated CC3 mAb and to correlate this with MHC-II expression as a marker of immune surveillance in a large cohort of colorectal cancers utilising high-throughput tissue microarray technology.

## 3.2 Results

### 3.2.1 Clinical and pathological data

The clinicopathological features of the 462 cases included in the present study are shown in Table 3.1. Patients had a median follow-up of 37 months (range 0 to 116) and there were slightly more male than female patients (58% and 42% respectively). 52% of tumours were of colonic origin and 39% of rectal origin, and in 9% of cases the site was not recorded. Well-differentiated tumours comprised 6% of the series, while 77% showed moderate differentiation and 15% were poorly differentiated. Examination of the standard clinicopathological features identified the expected associations between DSS and TNM stage (log-rank=211.37,  $p<0.0001$ ), DSS correlated with extramural vascular invasion (log-rank=44.30,  $p<0.0001$ ) but not with differentiation (log-rank=5.75,  $p=0.12$ ).

**Table 3.1** Clinicopathological variables for the patient cohort (n = 462) and cores stained for both tumour and tumour-associated stroma with CC3 (n=334).

<b>Variable</b>	<b>Categories</b>	<b>Frequency of total cohort (%)</b>	<b>Frequency of stained cohort (%)</b>
<b>Gender</b>	Male	266 (58)	197(59)
	Female	199 (42)	137(41)
<b>Age (years)</b>	Median	72	72
	Range	58-93	57-93
<b>Status</b>	Alive	169(37)	114(34)
	Dead	293(63)	220(66)
<b>Tumour Grade</b>	Well differentiated	29 (6)	23(7)
	Moderately differentiated	353 (77)	253(76)
	Poorly differentiated	71 (15)	53(16)
	Unknown	8 (2)	5(2)
<b>Tumour Site</b>	Colon	238 (52)	174(52)
	Rectum	181 (39)	129(39)
	Unknown	43 (9)	31(9)
<b>TNM Stage</b>	0 (T <sub>is</sub> )	3 (1)	2(1)
	1	69 (15)	44(15)
	2	174 (28)	110(38)
	3	155 (33)	99(34)
	4	54 (12)	31(11)
	Unknown	7 (2)	5(2)
<b>Extramural Vascular Invasion</b>	Negative	224 (48)	164(49)
	Positive	128 (28)	91(27)
	Unknown	110 (24)	79(24)
<b>Histological Type</b>	Adenocarcinoma	392 (85)	289(87)
	Mucinous carcinoma	51 (11)	34(10)
	Columnar carcinoma	4 (1)	3(1)
	Signet ring carcinoma	7 (1)	4(1)
	Unknown	8 (2)	4(1)

### 3.2.2 CC3 expression

Analysis of CC3 was possible in 334 of the total 462 cores (72%) with the remainder being lost during antigen retrieval or not demonstrating viable tumour cells in the core. Due to the large loss of cores, the clinicopathological data for the 334 samples was confirmed to be similar to the original cohort (Table 3.1). The majority of staining was seen in the nucleus of both tumour and tumour-associated stromal cells. The majority of tumours had less than 1000 cells/mm<sup>2</sup> of CC3 positive tumour cells and less than 2000 cells/mm<sup>2</sup> in tumour-associated stroma. There were 43 (13%) samples that had a low level of CC3 in tumour cells and 178 (56%) of samples that had a low level of CC3 expression in the tumour-associated stroma (Table 3.2). Examples of CC3 staining of tumour and tumour-associated stroma are demonstrated in figure 3.1.

**Table 3.2 Numbers of tumour specimens negative and positive for CC3 expression.**

Marker	Level of Expression	Number of specimens (%)
CC3	<b>Tumour</b>	
	Low	43 (13)
	High	314(87)
	Total	334(100)
	<b>Tumour-associated stroma</b>	
	Low	178(56)
	High	142(44)
	Total	320(100)
	MHC-II	<b>Tumour</b>
Negative		386(94)
Positive		27(6)
Total		413(100)
<b>Tumour-associated stroma</b>		
Negative		213(51)
Positive		202(49)
Total		415(100)



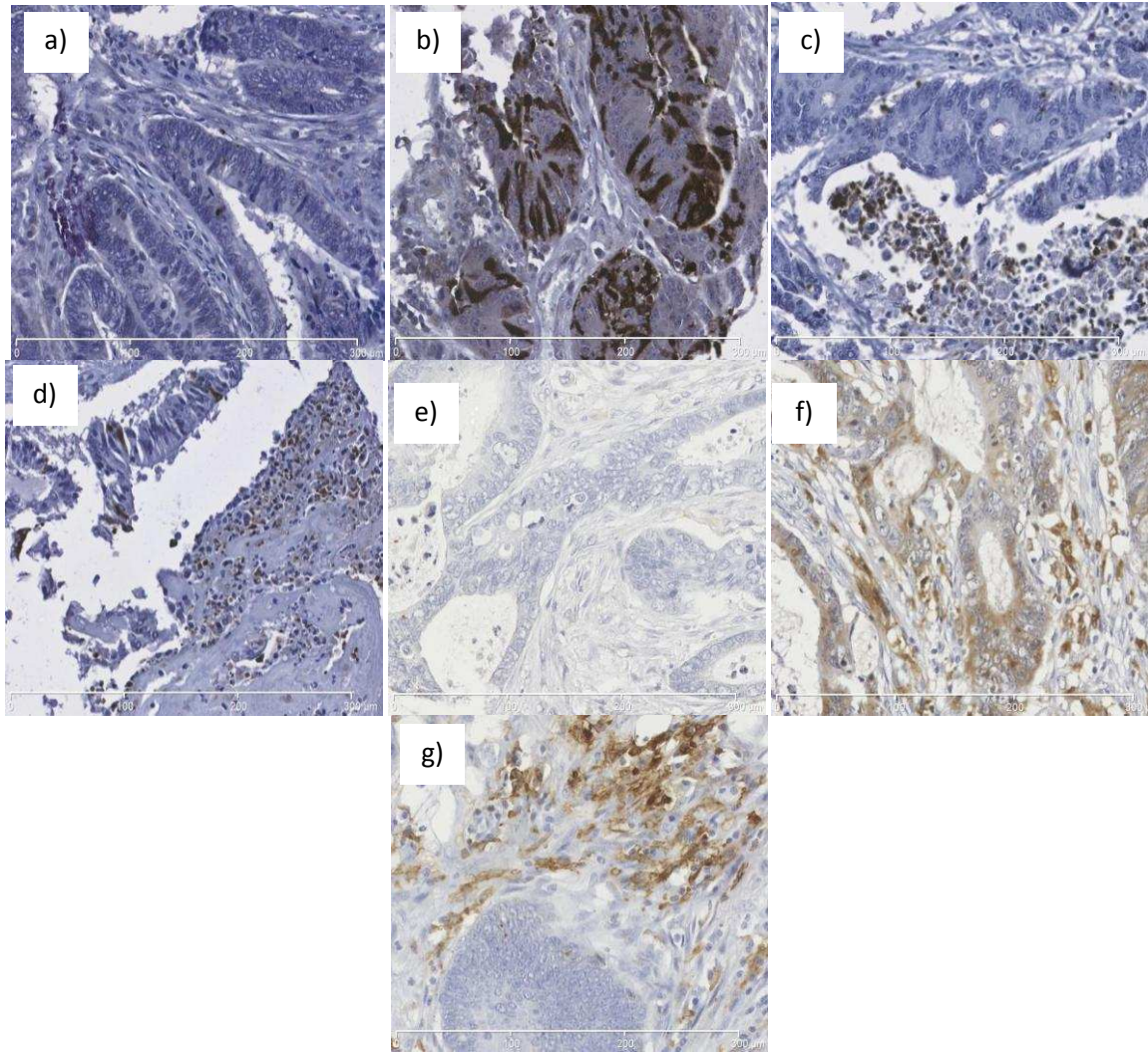


**Figure 3.1 Representations of positive and negative staining with CC3 and MHC-II.** Samples depicting both negative tumour and tumour-associated stromal cells (a), only positive tumour cells (b), only positive tumour-associated stromal cells (c), and both positive tumour and tumour-associated stromal cells (d) of CC3. Negative staining of both tumour and tumour-associated stroma (e), positive tumour and tumour associated stroma (f) and positive tumour associated stroma only MHC-II staining (g). All at X20 original magnification.

### **3.2.3 Markers of apoptosis and inflammation: Bcl2, p53, CD3, CD68, CD16 and MHC-II expression**

This array has previously been stained for the presence of stromal and intratumoural T cells using the CD3 marker (Simpson et al., 2010). Similarly the presence of macrophages or NK cells was enumerated using the CD68 or CD16 markers (Simpson et al., 2010). Expression of Bcl-2 and p53 have previously been reported (Watson et al., 2005). As a marker of IFN- $\gamma$  induced activation, expression of MHC-II on tumour cells and stroma associated cells was measured. It was possible to measure MHC-II expression in 413 of the total 462 cores (89%) with the remainder being lost during antigen retrieval or not demonstrating viable tumour cells in the core. Examples of MHC-II staining of tumour and tumour-associated stroma are demonstrated in figure 3.1. The majority of cores were negative for MHC-II expression in tumour cells (386 negative, 27 positive). 213 cores were negative for tumour-associated stroma staining, with 202 showing positive staining for MHC-II (Table 3.2). Of the cores stained with MHC-II, 286 were stained successfully with CC3.

### **3.2.4 Relationship between CC3 expression and standard clinicopathological variables**

The relationship between CC3 expression in the tumour and tumour-associated stroma and standard clinicopathological variables and markers of immune activation was measured using the Pearson  $\chi^2$  test. Expression of CC3 in the tumour associated significantly with TNM stage and distant metastases ( $p=0.047$ ,  $0.005$  respectively; Table 3.3). There was no correlation between the expression of CC3 in tumour-associated stroma with any standard clinicopathological variables, including stage (Table 3.3).

**Table 3.3 Univariate analysis of patient and tumour in relationship to active caspase 3 expression in tumour and tumour-associated stroma.** CC3 staining of tumour and tumour-associated stroma was correlated with standard clinicopathological variables using the  $\chi^2$  test. Values <0.05 are accepted to be significant.

Variable	$\chi^2$ test ( <i>p</i> value)			
	CC3 expression		MHC-II expression	
	Tumour	Tumour-associated stroma	Tumour	Tumour-associated stroma
Gender	0.832	0.579	0.116	0.656
Tumour Site	0.729	0.364	0.757	0.058
Tumour Type	0.110	0.470	0.518	0.577
Tumour Grade	0.196	0.266	<b>0.036</b>	0.190
Duke's Stage	<b>0.026</b>	0.298	0.157	0.706
TNM Stage	0.047	0.462	<b>0.007</b>	0.969
Distant Metastases	<b>0.005</b>	0.188	0.237	0.989
Extramural vascular invasion	0.775	0.368	0.249	<b>0.049</b>
Stromal MHC-II expression	0.151	<b>0.020</b>	-	-
Tumoural MHC-II expression	<b>0.008</b>	0.347	-	-
CD3- Intratumoural	0.557	0.525	<b>0.002</b>	<b>0.002</b>
CD3- Tumour-associated stroma	0.821	0.569	<b>0.001</b>	<b>0.001</b>
CD16	0.762	0.490	<b>0.002</b>	<b>0.004</b>
CD68	0.631	0.313	0.865	<b>&lt;0.001</b>
p53	0.616	0.919	0.069	0.394
Bcl-2	0.681	0.290	0.362	0.145

### 3.2.5 Relationship between MHC-II expression and standard clinicopathological variables

The relationship between MHC-II expression in tumour and tumour-associated stroma and standard clinicopathological variables was measured using the Pearson  $\chi^2$  test. Expression of MHC-II in the tumour associated significantly with TNM stage and tumour grade ( $p=0.007$  and  $0.036$  respectively; Table 2). There was no correlation between the expression of MHC-II in tumour-associated stroma with any standard clinicopathological variables, including stage (Table 3.3).

### **3.2.6 Relationship between CC3 expression and markers of immune activation and apoptosis**

The immune system and in particular the presence of T cells, has been shown to have strong prognostic significance in colorectal cancer. The relationship between CC3 expression in tumour and tumour-associated stroma and markers of immune activation was therefore measured using the Pearson  $\chi^2$  test. Expression of CC3 in the tumour associated significantly with MHC-II expression in tumour cells ( $p=0.008$ ; Table 3.3) but not with the number of CD68, CD16 or CD3 positive cells or Bcl-2 or p53. There was no correlation between the expression of CC3 in tumour-associated stroma with the number of CD68, CD16 or CD3 positive cells or Bcl-2 or p53. However, there was a significant correlation with stromal expression of MHC-II ( $p=0.020$ ; Table 3.3).

### **3.2.7 Relationship between MHC-II expression and markers of immune activation and apoptosis**

IFN- $\gamma$ , produced by NK cells, NKT and T cells has been shown to play a central role in immune surveillance. It induces MHC-II expression on tumour cells and upregulates expression on stromal cells. The relationship between MHC-II expression in the tumour and tumour-associated stroma and markers of immune activation was measured using the Pearson  $\chi^2$  test. Expression of MHC-II in the tumour associated significantly with expression of CD3 T cells either within the tumour ( $p=0.002$ ; Table 3.3) or within the stroma ( $p=0.001$ ; Table 3.3) and expression of CD16 positive cells (macrophage and NK cells;  $p=0.002$ ; Table 3.3) but not with the number of CD68 positive cells or Bcl2 or p53. Expression of MHC-II in the tumour associated stroma was significantly associated with expression of CD3 T cells either within the tumour ( $p=0.002$ ; Table 3.3) or within the stroma ( $p=0.001$ ; Table 3.3), expression of CD16 positive cells (macrophage and NK cells;  $p=0.004$ ; Table 3.3) and with the number of CD68 positive cells (macrophages;  $p=0.001$ ; Table 3.3) but not with Bcl2 or p53.

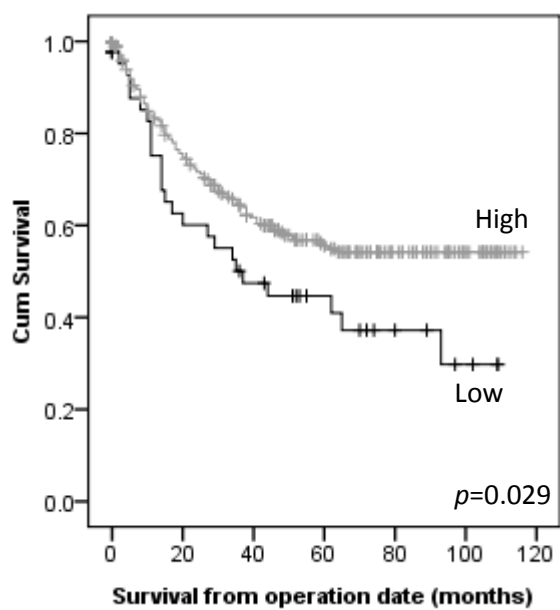
### 3.2.8 Relationship between CC3 expression and survival

Kaplan-Meier plots were used to analyse the relationship between low and high expression of CC3 and disease-specific survival. Figure 3.2a and table 3.4 demonstrate that patients with a higher level of tumour CC3 expression have a greater mean survival ( $p=0.029$ ; 73 months) than those with a lower level of CC3 expression (53 months). This is echoed in the tumour-associated stroma with a higher expression having a greater mean survival ( $p=0.009$ , 79 mean months versus 63 months; Fig 3.2b). When tumour cell expression of CC3 cells was compared to tumour-associated stromal cell expression, patients that show low expression of CC3 in the tumour and tumour-associated stroma had the worst survival (43 months), with patients with high tumour CC3 expression/high tumour-associated stromal CC3 displaying the best survival (80 months;  $p=0.009$ ). Patients with high tumour and low tumour-associated stromal CC3 expression or patients with low tumour and high tumour associated-stroma CC3 expression had a similar survival (66 and 71 months respectively; Fig 3.2c).

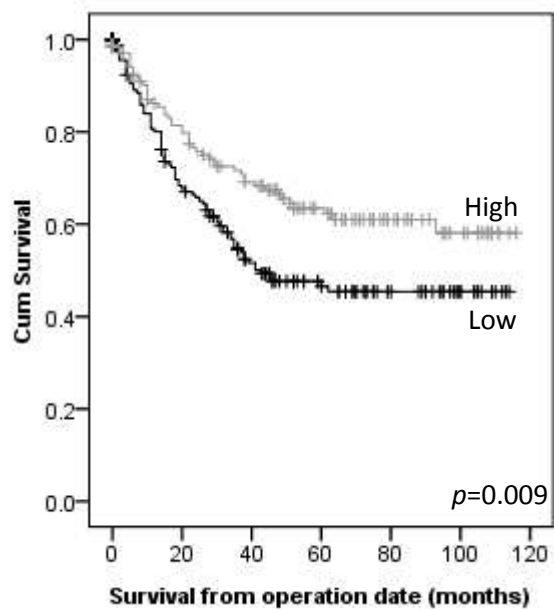
**Table 3.4 Mean survival of patients.**

Marker	Level of expression	Mean survival (months)
CC3	<b>Tumour</b>	
	Low	53
	High	73
	<b>Tumour-associated stroma</b>	
	Low	63
	High	79
	<b>Tumour versus tumour-associated stroma</b>	
	Low tumour/low tumour-associated stroma (0)	43
	Low tumour/high tumour-associated stroma (1)	71
	High tumour/low tumour-associated stroma (2)	66
High tumour/high tumour-associated stroma (3)	80	
MHC-II	<b>Tumour</b>	
	Low	71
	High	85
	<b>Tumour-associated stroma</b>	
	Low	69
High	75	

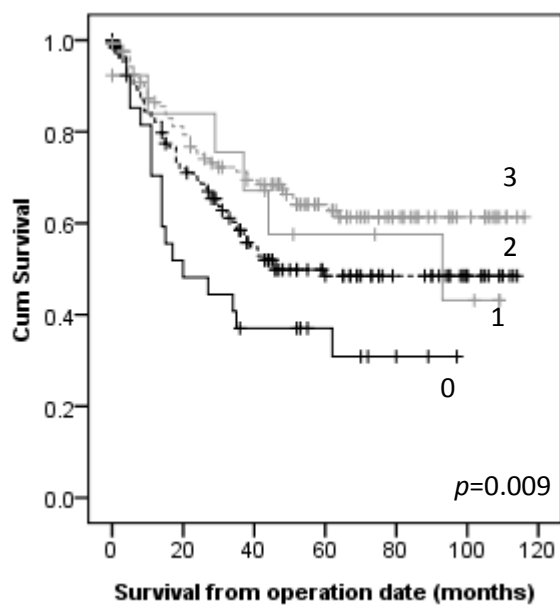
a)



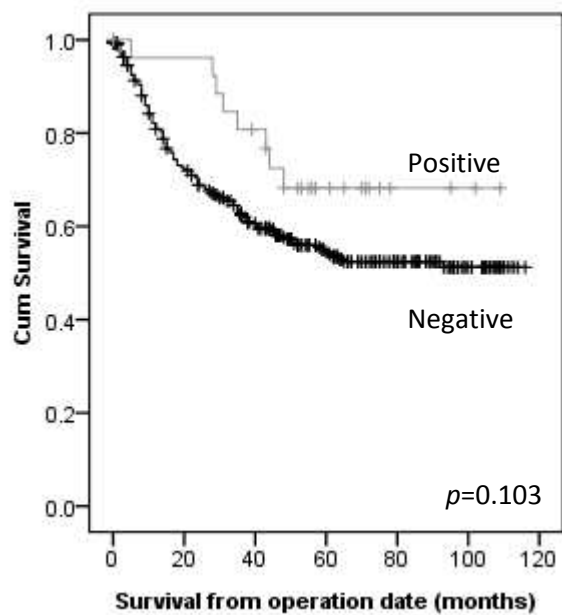
b)



c)



d)



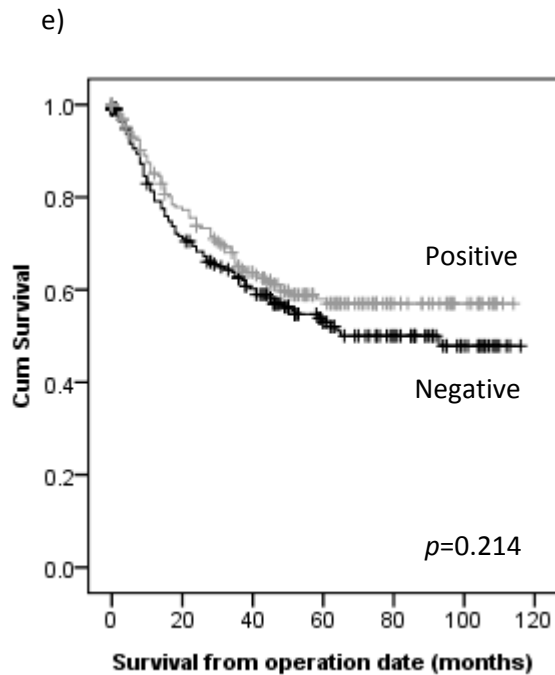


**Figure 3.2 Kaplan-Meier plot for disease-specific survival relative to CC3 and MHC-II expression.** a) CC3 low-expression in tumour cells (Low) vs. CC3 high-expression in tumour cells (High);  $p=0.029$ . b) Low CC3 expression in tumour-associated stroma (Low) vs. high CC3 high expression in tumour-associated stroma (High).  $p = 0.009$ . c) Groups of CC3 low-expression in both tumour and tumour-associated stroma (0), CC3 low-expression in tumour, high expression in tumour-associated stroma (1), CC3 high-expression in tumour, low expression in tumour-associated stroma (2) and CC3 high-expression in both tumour and tumour-associated stroma (3)  $p = 0.009$ . Where Tumour low/high = 0-60/61-max cells/mm<sup>2</sup> and tumour-associated stroma low/high = 0-104/max cells/mm<sup>2</sup>. d) MHC-II negative-expression in tumour cells (Negative) vs. MHC-II positive-expression in tumour cells (Positive;  $p=0.029$ ). e) Negative MHC-II expression in tumour-associated stroma (Negative) vs. positive MHC-II positive expression in tumour-associated stroma (Positive;  $p=0.009$ ).

### 3.2.9 Relationship between MHC-II expression and survival

Kaplan-Meier plots were used to analyse the relationship between negative and positive expression of MHC-II and DSS. Figures 3.2d, e and table 3.4 demonstrate that the level of MHC-II expression in either the tumour or tumour-associated stromal cells had no significant influence on patient survival ( $p=0.103$  and  $0.214$ ).

### 3.2.10 Multivariate analysis of CC3 expression and standard clinicopathological variables

In order to determine the relative influences of CC3 and other patient and tumour variables known to affect prognosis, a multivariate analysis was performed using the Cox proportional hazards model. The variables included were those that have been shown to be significantly related to DSS on

univariate analysis (extramural vascular invasion and TNM stage). In this model, extramural vascular invasion ( $p < 0.001$ ) and TNM stage ( $p = 0.005$ ) were seen to retain independent prognostic significance (Table 3.5a.). Low expression of CC3 in tumour-associated stroma was also seen to be an independent prognostic marker (CI 95% 0.359-0.823,  $p = 0.004$ ). Previous studies in our group have shown that both the presence of intra-tumoural T cells (ITTC) and reduced MHC-I expression are independent prognostic factors (Simpson et al., 2010). Multivariate analysis was therefore performed to see if tumour-associated stroma CC3 expression was independent of these factors and TNM stage and extramural vascular invasion. Analysis showed that only tumour-associated stroma CC3 expression ( $p = 0.005$ ) and TNM stage ( $p < 0.001$ ) retained their independent prognostic significance (Table 3.5b).

**Table 3.5 Cox multivariate regression analysis of variables in relation to disease specific survival.** Multivariate analysis using the Cox proportional hazards model for CC3 in tumour-associated stroma, extramural vascular invasion and TNM (a) and for ITCC and MHC-I expression (b).

a)

Variable		Hazard Ratio	95% CI	p value
Extramural vascular invasion	Negative	1		
	Positive	1.191	1.191-2.728	0.005
TNM Stage	0-II	1		
	III-IV	0.267	0.165-0.432	<0.001
CC3 tumour-associated stroma expression	Low	1		
	High	0.544	0.359-0.823	0.004

b)

Variable		Hazard Ratio	95% CI	p value
Extramural vascular invasion	Negative	1		
	Positive	0.638	0.394-1.034	0.068
TNM Stage	0-II	1		
	III-IV	3.733	2.141-6.506	<0.001
ITCC	Low	1		
	High	1.310	0.825-2.080	0.253
MHC-I	Low	1		
	High	0.549	0.219-1.376	0.201
CC3 tumour-associated stroma expression	Low	1		
	High	0.490	0.299-0.804	0.005



### 3.3 Discussion

Cancer is a complex interaction of transformed epithelial and associated stromal cells. Perturbation of this complex relationship can lead to tumour cell apoptosis. However, resistance to apoptosis has been shown to be a key factor in tumour progression. Colorectal cancer can become resistant to apoptosis by a wide variety of mechanisms including mutation of apoptotic regulators, upregulation of anti-apoptotic molecules and down regulation of pro-apoptotic molecules (Yang et al., 2009). CC3 expression was therefore used to determine the level of apoptosis in both the tumour and the associated stroma cells in a large, representative cohort of colorectal cancer patients from the UK. In this study we have shown that high levels of CC3 both within tumour cells and within the tumour-associated stroma correlates with good prognosis. Furthermore, CC3 expression within stromal cells was an independent prognostic marker.

The value of apoptosis as a prognostic marker remains unclear due largely to the contradictory results of previous studies (Koornstra et al., 2003). The majority of early studies used transferase-mediated nick end labelling (TUNEL) to detect fragmented DNA in apoptotic cells. The TUNEL method has two main disadvantages; firstly the labelling of DNA fragments also marks necrotic and autolytic cells (Gown & Willingham, 2002) and secondly, the method requires pre-treatment steps, which needs careful optimization and may be source of variation between studies. Our findings are in concurrence with studies that assessed apoptosis by measuring caspase-3 activity. A low level of CC3 activity in the tumour was shown to result in a greater risk of recurrence in a cohort of 117 stage III rectal cancer patients (de Heer et al., 2007). A lower level of caspase-3 activation, measured by western blots, in the tumours of 60 colorectal cancer significantly correlated with a greater risk of recurrence (Jonges et al., 2001). It has also been shown that the level of caspase-3 like protease activity increased with cancer progression (Leonardos et al., 1999) . As shown in this study, Koelink et al., found that a greater than median level of caspase activity (measured by the level of caspase-3-

degraded cytokeratin 18 product, the M30 antigen) in tumour-associated stroma, correlated with increased survival in a cohort of 211 colorectal cancer patients (Koelink et al., 2009).

It is logical that a higher level of CC3 in the tumour would predict a better prognosis, as a greater level of apoptosis would suggest a less aggressive tumour. We have also shown that this correlates with the level of MHC-II on tumour cells. This may be related to the expression of IFN- $\gamma$  as this is the only cytokine that can upregulate expression of MHC-II on epithelial cells (Giroux et al., 2003). It has been shown that transformation induces stress related molecules which are recognised by innate immune cells with the subsequent release of IFN- $\gamma$  (Dunn et al., 2005). The strong correlation between MHC-II on tumours and CD3, CD16 and CD68 expression suggests that IFN- $\gamma$  may be produced by NK cells, M1 macrophages or T cells. The correlation between CC3 and MHC-II suggests that IFN- $\gamma$  may be responsible for the tumour cell apoptosis and good prognosis. This is supported by previous studies showing that the stress related protein MICA (Watson et al., 2006c) and ITTC are markers of good prognosis in colorectal cancer (Simpson et al., 2010).

As the tumour becomes increasingly resistant to immune control, the balance in the stroma may be tipped in favour of cells enhancing angiogenesis and metastases. The strong association with stromal apoptosis and stromal cell MHC-II expression suggests that one of these key cells may be macrophages which constitutively express MHC-II. Studies have shown that M2 macrophages can express a range of proteases that remodel the ECM and can express angiogenic factors, such as VEGF, that promote tumour metastasis (Pollard, 2004). The tumour also secretes stroma-modulating factors, including basic fibroblast growth factor (bFGF), TGF- $\beta$  and members of the VEGF family (Fukumura et al., 1998). These factors disrupt the normal tissue homeostasis and act in both a paracrine and autocrine fashion and lead to the remodelling of the ECM, activation of angiogenesis and the transdifferentiation of fibroblasts into CAFs. CAFs have been shown to be present in colorectal tumour progression (Adegboyega et al., 2002; Tsujino et al., 2007). CAFs in turn act in a pro-tumour manner by secreting growth factors and additional proteases that stimulate tumour growth, migration, angiogenesis and progression. A study demonstrated that CAFs can also promote

progression of non-tumourigenic prostatic epithelial cells, leading to tumour growth (Olumi et al., 1999). A study has shown that TGF- $\beta$  promotes expression of fibroblast activation protein (FAP) on CAFs and that this expression promotes the proliferation, migration and invasion of the ovarian cancer cell line HO-8910PM *in vitro* (Chen et al., 2009). More recently, it has been shown that a FAP-expressing, mesenchymal-originated, stromal cell can suppress the immune system in a murine tumour microenvironment and when removed, cytokine mediated killing of the tumour was observed (Kraman et al., 2010). Thus, cancers with low levels of CC3 in both the tumour itself and its associated stroma are most aggressive and lead to a poor prognosis (median survival 43 months). However, if the tumour grows too rapidly, it could outcompete the stroma for nutrients and oxygen resulting in stromal death and consequently tumour death. Thus tumours with high CC3 levels in both their tumour and stroma have less aggressive tumours and better prognosis (median survival 80 months).

The independent significance of apoptosis in tumour-associated stroma in colorectal cancer suggests that tumour microenvironment targeted therapy may be beneficial. An example is bevacizumab which binds to VEGF, blocking the VEGF expressed by the tumour from binding to VEGFR on vascular endothelium, promoting angiogenesis. Bevacizumab, a VEGF-A-specific humanized mAb, blocks binding of VEGF to VEGFR and is approved for treatment in colorectal, breast and non-small cell lung cancers (Shih & Lindley, 2006). VEGFRs have also been targeted, with ramucirumab, a fully human mAb targeted at VEGFR2 showing inhibition of vascularisation in a phase I trial (Spratlin et al., 2010). It has recently been demonstrated that a DNA vaccine directed against the CAF marker FAP significantly suppressed primary tumour and pulmonary metastases in a murine model, with no significant side effects (Wen et al., 2010).

In conclusion, our study has shown that high expression of CC3 in tumours correlates with good prognosis and with the expression of MHC-II on tumour cells. This suggests that IFN- $\gamma$  and therefore immune cells may have a role to play in controlling colorectal cancer growth. High expression of CC3 in tumour-associated stroma was also associated with good prognosis and is an independent

prognostic factor in colorectal cancer. This may be because apoptosis of the tumour-associated stroma reduces the level of pro-tumour signals and therefore the tumour has reduced proliferation, migration, angiogenesis and metastasis. This study further highlights the importance of tumour-associated stroma in colorectal cancer as a possible new therapeutic target.

The complex way in which a tumour protects itself from the immune system can result in an inflammatory, pro-tumour phenotype of immune effector cells in the tumour microenvironment, which suggests that mAb-induced immune mediated mechanisms of tumour death may not always be possible. Therefore the ability of a mAb to induce direct cell death may be vital in tumours with an immune suppressed environment.

## Chapter 4 Characterisation of Lewis y/b mAb specificity and *in vitro* functionality

### 4.1 Introduction

Studies have shown that epithelial-derived tumours have an increased level of glycans compared with normal tissue, making them good tumour markers and potential therapeutic targets (Dabelsteen, 1996; Hakomori, 1985; Kannagi et al., 2008). Many of the mAbs targeting these glycans show direct non-apoptotic killing activity against tumours *in vitro* (Kelly et al., 2006). SC104 mAb has been shown to bind and directly kill colorectal tumours and inhibit growth *in vivo* (Durrant et al., 2006). F77, an anti-prostate cancer mAb, has been shown to bind a glycolipid on the surface of prostate cancer cells and inhibit growth *in vivo* (Zhang et al., 2010a). RAV12 is a chimeric mAb that has been shown to bind a minimal epitope of Gal $\beta$ 1-3GlcNAc $\beta$ 1-3Gal on the N-linked carbohydrate antigen RAAG12, which is expressed on 90% of intra-abdominal tumours. RAV12 has been shown to directly kill the colorectal cancer cell line Colo 205 *in vitro* by oncosis as well as anti-tumour activity in a phase I study (Burriss et al., 2010; Coberly et al., 2009; Loo et al., 2007). BR96, an anti-Lewis-y mAb has been shown to cause cellular cytotoxicity in Lewis y-positive cells *in vitro* as well as mediating ADCC and CDC (Hellstrom et al., 1990). We have previously described 692/29, a mouse IgG<sub>3</sub> mAb whose antigenic target is a unique but shared epitope on both Lewis b and Lewis y. Binding of the mAb inhibits growth of colorectal tumours *in vivo* by an uncharacterised mechanism. The Lewis y and Lewis b antigens are tetrasaccharides and are extensions of the H blood group galactose-glucosamine. Although both are mostly expressed throughout foetal development and are gradually lost after birth, Lewis y and Lewis b can be expressed on normal cells in the GI tract at low levels (Sakamoto et al., 1986; Sakamoto et al., 1989). Tumours have been shown to overexpress both Lewis y and Lewis b, making them good targets for mAb therapy (Abe et al., 1986; Itzkowitz, 1992; Kim et al., 1986). As glycans, Lewis y and Lewis b can be expressed on GSLs as well as glycoproteins on the cell surface. GSLs have been shown to be functional molecules that can effect tumour cell growth,

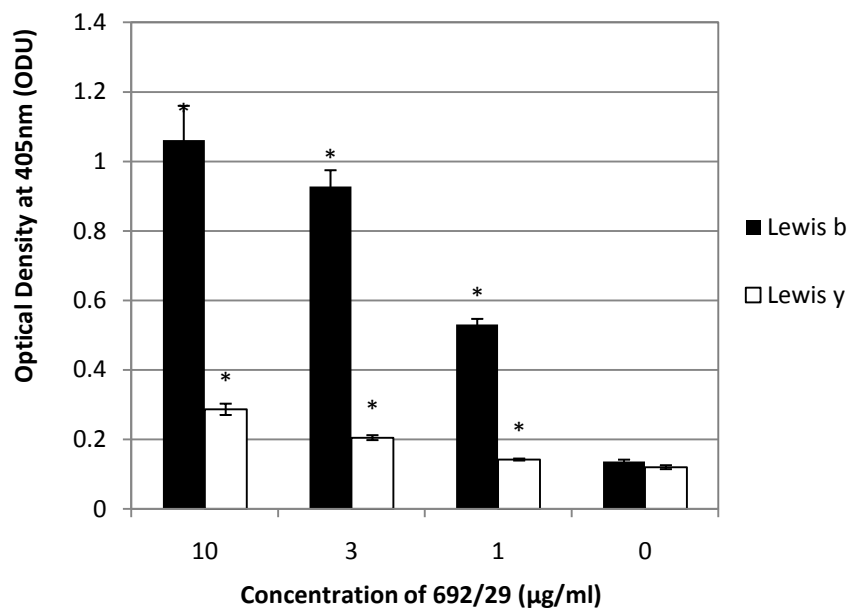
adhesion, metastasis and proliferation (Hakomori Si, 2002). This has lead to a number of trials targeting these functional glycans with mAb therapy (Kelly et al., 2006; Saleh et al., 2000).

In this study we sought to investigate the fine specificity of Lewis y and Lewis b mAbs to their antigen/s and the effect that this had on *in vitro* binding and functionality. This may determine whether the ability to bind both Lewis y and Lewis b could be of therapeutic benefit.

## 4.2 Results

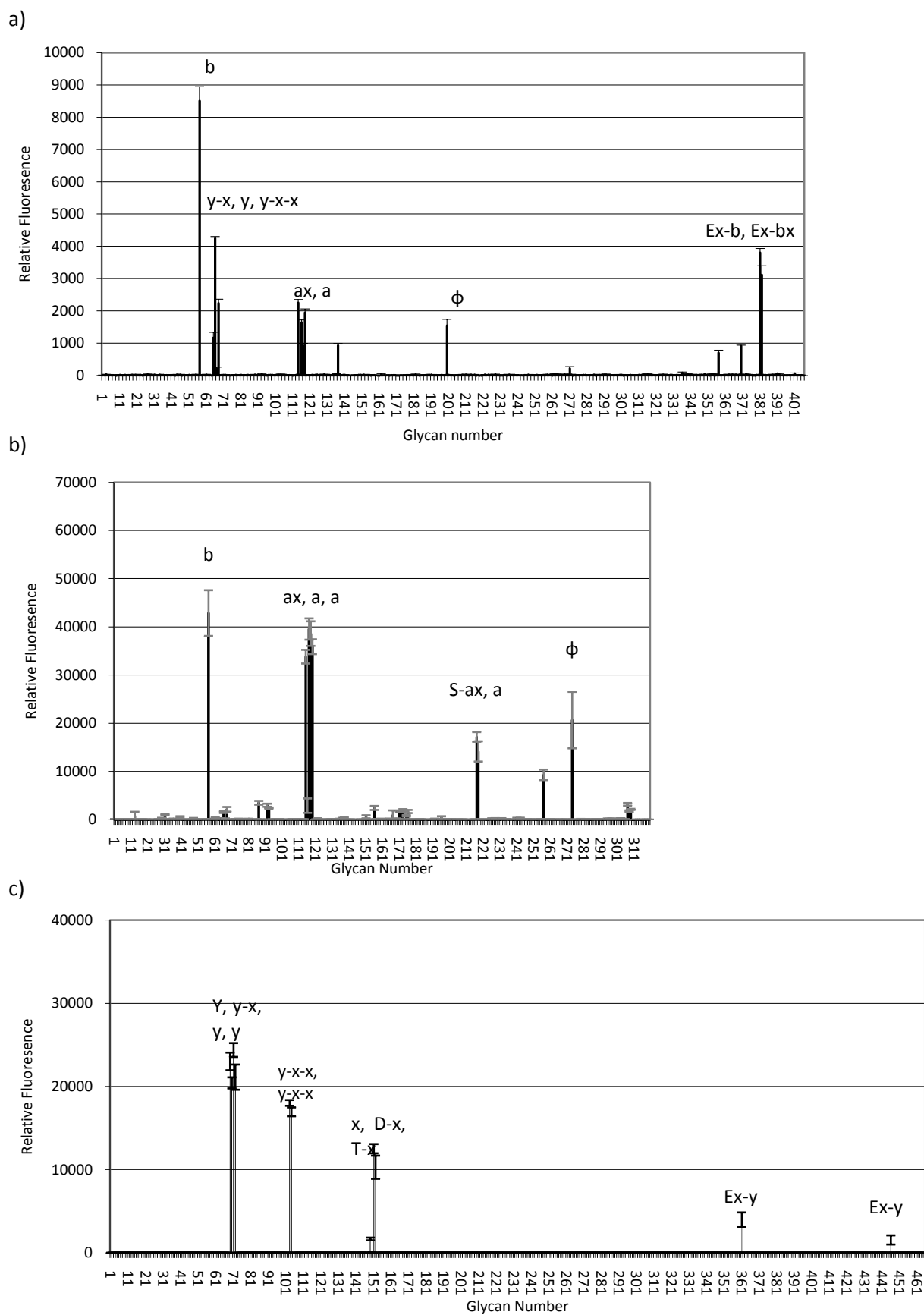
### 4.2.1 Defining the epitopes recognised by the Lewis y/b antibodies using the Consortium for Functional Glycomics glycan array

Studies have shown that due to the subtleties observed in antibody binding to tumour cells and the high level of similarity between some carbohydrate groups, including blood group antigens, many antibodies have been found to cross-react with other related carbohydrates (Manimala et al., 2007). The recognition of Lewis y as a good therapeutic target has led to the production of a number of anti-Lewis y mAbs. Despite being presented as Lewis-y specific mAbs, some have been shown to cross-react with other blood group antigens. To confirm that 692/29 could bind to both Lewis y and Lewis b, the mAb was screened against Lewis y and Lewis b glycans by ELISA. Figure 4.1 shows that 692/29 binds to both Lewis y and Lewis b glycans. In order to clarify their fine specificity the anti-Lewis y/b mAb 692/29 and the anti-Lewis y mAb BR96 were assessed and compared to the published specificity data for 2-25 LE (an anti-Lewis b mAb) from the Consortium for Functional Glycomics. Binding of 692/29 to the array reflects that seen with the ELISA, with the mAb binding most strongly to Lewis b, glycans containing Lewis b and also to tri-Lewis y and its variants (Fig 4.2a). Analysis of the 2-25 LE binding data shows strong binding to Lewis b, with some cross-reactivity to Lewis a and Lewis a-x. Weak binding can also be seen against sialyl Lewis a-x, with no binding to Lewis y (Fig 4.2b). BR96 shows strong binding to Lewis y as well as a range of Lewis y variants (Lewis y-x, Lewis y-x-x) and more weakly to Lewis x. BR96 does not bind to Lewis b (Fig 4.2c). A representation of the glycans and their structures bound by each mAb is displayed in Table 4.1.



**Figure 4.1 Binding of 692/29 to Lewis b and Lewis y antigens.** 100µl 10µg/ml Lewis b-HSA and Lewis y-HSA were incubated on an ELISA plate before blocking and the addition of 10-1µg/ml 692/29. Binding of 692/29 probed with anti-IgG-HRP. Error bars representing standard deviation of quadruplicate wells are included for all data points. \* indicates significant binding where  $p < 0.05$ . Data is representative of 2 separate experiments.



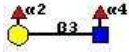
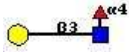


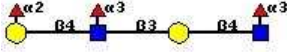
**Figure 4.2. The fine specificity differs between the anti-Lewis y and Lewis b mAbs.** The binding of 692/29 (a), 2-25 LE (b) and BR96 (c) to the Consortium for Functional Glycomics glycan array. Where a=Lewis a, b=Lewis b, y=Lewis y, x=Lewis x, D- = Di, T- = Tri, S- = sialyl, Ex- = extended, φ denotes a mannose containing glycan, and y-x= Lewis y-Lewis x.

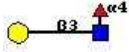
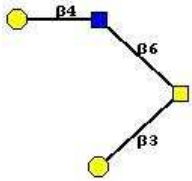
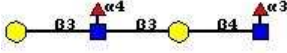
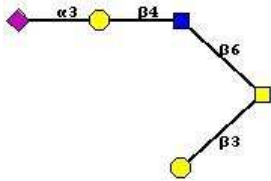
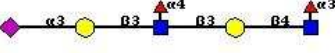
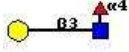
**Table 4.1 Details of glycan binding by 692/29 (a), 2-25 LE (b) and BR96 (c) to the glycan array.** A blue squares represents glucosylamine, yellow circles represents galactose, red triangles represent fucose, green circles represent mannose and purple diamond represents sialic acid. Sp denotes the length of spacer between glycan and slide. Percentage of best binder refers to the level of binding in relation to the glycan bound best by each mAb.

a)

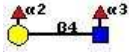
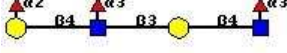
Glycan No.	Glycan	Name	Percentage of best binder (%)	Structure
57	Fuca1-2Galb1-3(Fuca1-4)GlcNAcb-Sp8	Lewis b	100	
66	Fuca1-2Galb1-4(Fuca1-3)GlcNAcb1-3Galb1-4(Fuca1-3)GlcNAcb1-3Galb1-4(Fuca1-3)GlcNAcb-Sp0	Lewis y-x-x	50	
381	Fuca1-2Galb1-3(Fuca1-4)GlcNAcb1-3(Galb1-4)GlcNAcb1-6)Galb1-4Glc-Sp21	Lewis x-containing glycan	45	
382	Fuca1-2Galb1-3(Fuca1-4)GlcNAcb1-3(Galb1-4(Fuca1-3)GlcNAcb1-6)Galb1-4Glc-Sp21	Lewis b-x containing glycan	37	
114	Galb1-3(Fuca1-4)GlcNAcb1-3Galb1-4(Fuca1-3)GlcNAcb-Sp0	Lewis a-x	27	
68	Fuca1-2Galb1-4(Fuca1-3)GlcNAcb-Sp8	Lewis y	26	
118	Galb1-3(Fuca1-4)GlcNAcb-Sp8	Lewis a	23	
116	Galb1-3(Fuca1-4)GlcNAcb-Sp0	Lewis a	19	
200	Fuca1-3(Galb1-4)GlcNAcb1-2Mana1-3(Fuca1-3(Galb1-4)GlcNAcb1-2Mana1-6)Manb1-4GlcNAcb1-4GlcNAcb-Sp20	Lewis a-containing glycan	18	

Glycan No.	Glycan	Name	Percentage of best binder (%)	Structure
57	Fuca1-2Galb1-3(Fuca1-4)GlcNAcb-Sp8	Lewis b	100	
117	Galb1-3(Fuca1-4)GlcNAc-Sp8	Lewis a	92	

65	Fuca1-2Galb1-4(Fuca1-3)GlcNAcb1-3Galb1-4(Fuca1-3)GlcNAcb-Sp0	Lewis y-x	14	
----	--------------------------------------------------------------	-----------	----	---------------------------------------------------------------------------------------

118	Galb1-3(Fuca1-4)GlcNAcb-Sp8	Lewis a	90	
119	Galb1-3(Galb1-4GlcNAcb1-6)GalNAca	Type-2 containing glycan	84	
114	Galb1-3(Fuca1-4)GlcNAcb1-3Galb1-4(Fuca1-3)GlcNAcb-Sp0	Lewis a-x	79	
274	Galb1-3(Neu5Aca2-3Galb1-4GlcNAcb1-6)GalNAca-Sp14	Sialylated Type-2 containing glycan	48	
217	Neu5Aca2-3Galb1-3(Fuca1-4)GlcNAcb1-3Galb1-4(Fuca1-3)GlcNAcb-Sp0	Sialyl Lewis a-x	40	
218	Galb1-3(Fuca1-4)GlcNAcb-Sp0	Lewis a	33	

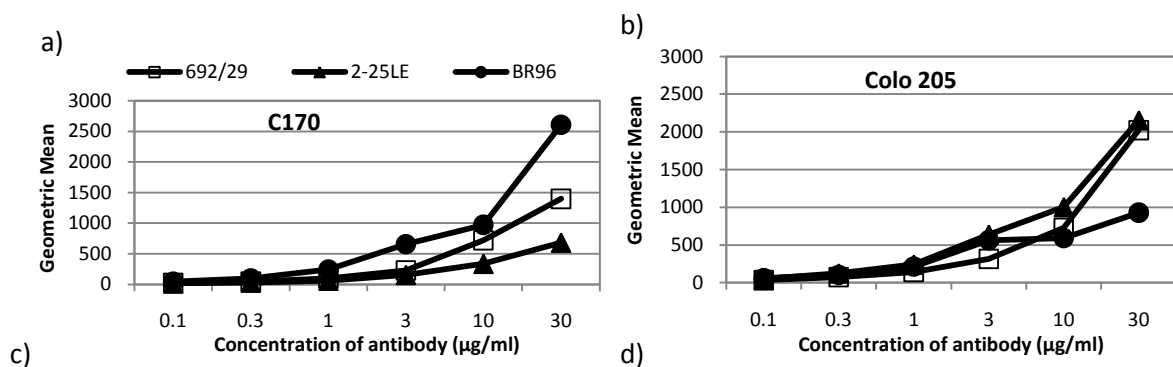
c)

Glycan No.	Glycan	Name	Percentage of best binder (%)	Structure
71	Fuca1-2Galβ1-4(Fuca1-3)GlcNAcβ-Sp0	Lewis y	100	
69	Fuca1-2Galβ1-4(Fuca1-3)GlcNAcβ1-3Galβ1-4(Fuca1-3)GlcNAcβ-Sp0	Lewis y-x	94	

72	Fuca1-2Galβ1-4(Fuca1-3)GlcNAcβ-Sp8	Lewis y	87	
70	Fuca1-2Galβ1-4(Fuca1-3)GlcNAcβ1-3Galβ1-4(Fuca1-3)GlcNAcβ1-3Galβ1-4(Fuca1-3)GlcNAcβ-Sp0	Lewis y	84	
103	Galα1-3(Fuca1-2)Galβ1-4(Fuca1-3)GlcNAcβ-Sp0	Lewis y-x-x	74	
104	Galα1-3(Fuca1-2)Galβ1-4(Fuca1-3)GlcNAcβ-Sp8	Lewis y-x-x	70	
151	Galβ1-4(Fuca1-3)GlcNAcβ1-4Galβ1-4(Fuca1-3)GlcNAcβ-Sp0	Di-Lewis X	51	
152	Galβ1-4(Fuca1-3)GlcNAcβ1-4Galβ1-4(Fuca1-3)GlcNAcβ1-4Galβ1-4(Fuca1-3)GlcNAcβ-Sp0	Tri-Lewis X	42	
361	Fuca1-2Galβ1-4(Fuca1-3)GlcNAcβ1-2Manα1-3(Fuca1-2Galβ1-4(Fuca1-3)GlcNAcβ1-2Manα1-6)Manβ1-4GlcNAcβ1-4GlcNAcβ-Sp20	Extended Lewis y	16	
149	Galβ1-4(Fuca1-3)GlcNAcβ-Sp0	Lewis X	7	
446	Fuca1-2Galβ1-4(Fuca1-3)GlcNAcβ1-2(Fuca1-2Galβ1-4(Fuca1-3)GlcNAcβ1-4)Manα1-3(Fuca1-2Galβ1-4(Fuca1-3)GlcNAcβ1-2Manα1-6)Manβ1-4GlcNAcβ1-4GlcNAcβ-Sp12	Extended Lewis y	6	

#### 4.2.2 Binding characteristics of anti-Lewis y/b mAbs on a range of antigen positive cell lines

In order to establish whether the subtlety in antigen recognition observed on the glycan array between the three mAbs related to a difference in binding characteristics to cells *in vitro*, 692/29 (Lewis y/b), 2-25 LE (Lewis a/b) and BR96 (Lewis y) were screened against a range of Lewis y and Lewis b positive cell lines (Fig 4.3a-h). All of the cell lines bound all three mAbs although to varying amounts, with the exception of MKN45. There were clear differences in antigen expression across the different cell lines, with C170 and Colo 205 expressing the greatest level of the Lewis y and b antigens. C170 expressed more Lewis y and Colo 205 more Lewis b. Several of the cell lines were Lewis b (2-25 LE) negative (OVCAR-3, OAW28, SW480) but demonstrated positive staining for the Lewis y antigen with BR96 and 692/29. MKN45 was the only cell line that was negative for both Lewis y and b antigens. Most cell lines with Lewis y antigen show similar levels of 692/29 and BR96 binding (OVCAR-3, SW480, HT29). However, both C170 and OAW28 cells show distinct binding of 692/29 and BR96, which may reflect the subtle differences in structures recognised by the mAbs on the glycan array. In both C170 and OAW28, BR96 binds at a higher level than 692/29, which may reflect a higher affinity for the Lewis y antigen. Interestingly, in all cells lines and irrespective of the level of antigen, antibody binding was not seen to saturate, even at 30µg/ml.



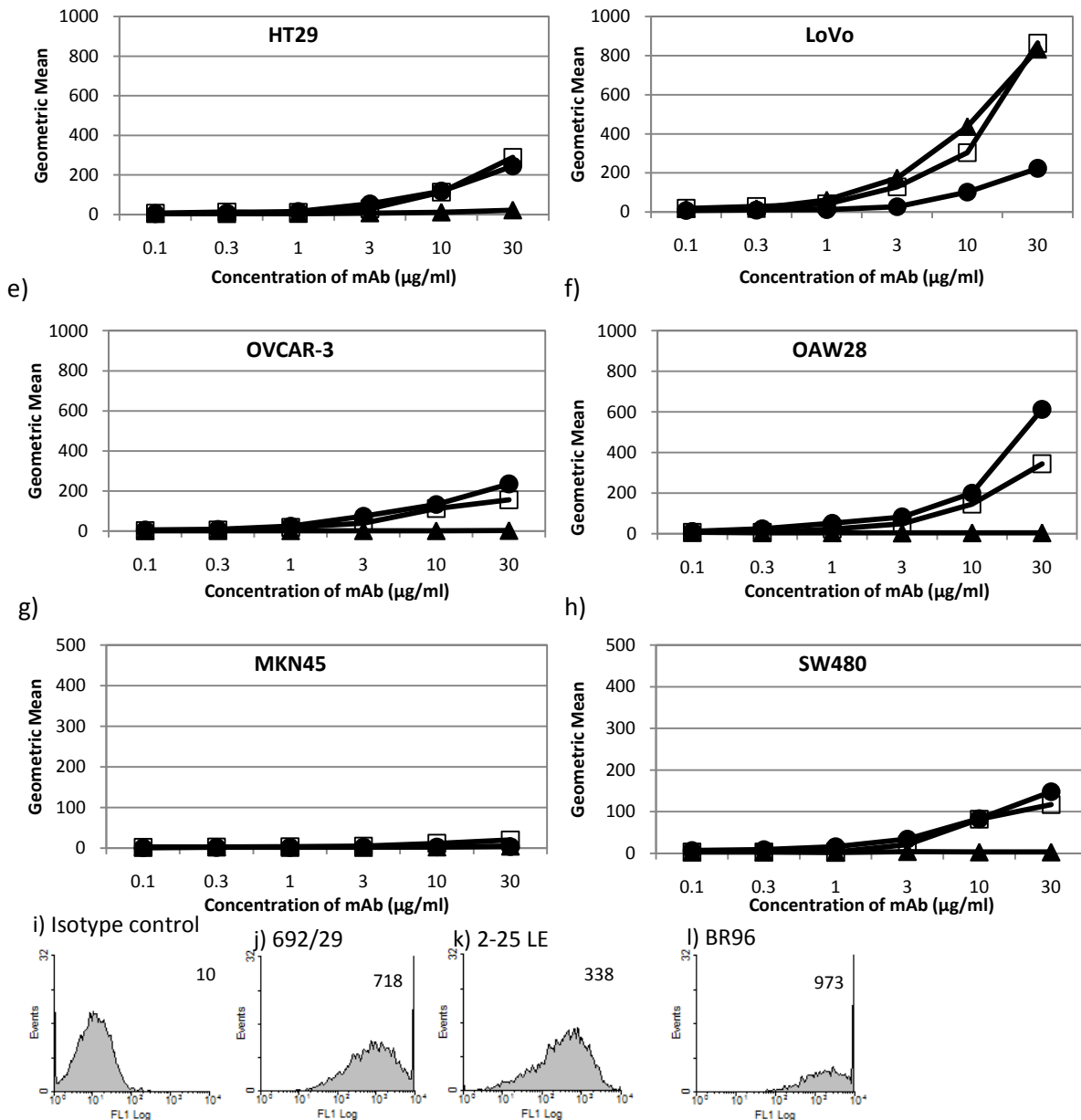


**Figure 4.3 Differences in binding pattern relate to a difference in *in vitro* cell line binding.** C170 (a), Colo 205 (b), HT29 (c), LoVo (d) OVCAR-3 (e), OAW28 (f), MKN45 (g) and SW480 (h) cells were incubated with 0.1-30μg/ml 692/29, BR96 and 2-25 LE. Examples of binding of 10μg/ml irrelevant IgG (i), 692/29 (j), 2-25 LE (k) and BR96 (l) histograms to C170 cells. All cell lines were plated at  $1 \times 10^5$  cells per well and incubated with the mAbs. Binding of mAbs to the cells was probed with an anti-mouse IgG-FITC mAb before analysing the cells by flow cytometry. An irrelevant IgG mAb was used as a negative control (geometric mean 10). Data is representative of at least 3 experiments.

#### 4.2.3 Determining self-binding (homophilic binding) of the Lewis antibodies.

In each of the cell lines used the anti-Lewis mAbs failed to show antigen saturation, as observed with similar concentrations of anti-CD46 and CD59 mAbs (Fig 4.4). Concentrations as high as 30μg/ml were still showing increases in fluorescence levels. This unusually high level of binding of antibodies

has been observed before in homophilic binding antibodies, where mAbs bind to antigen and homophilically to themselves. To investigate the possibility of homophilic binding, C170 cells were incubated with 100µg/ml of unlabelled anti-Lewis mAb. After brief washing this was followed by the addition of FITC-labelled mAb. Despite the large amount of unlabelled mAb, both 692/29 and BR96 FITC-conjugated mAbs were still able to bind to the cells to the same extent as when no unlabelled mAb was present (Fig 4.5). However, some inhibition of 2-25LE FITC-conjugated binding was observed. These results suggest that at low antibody concentrations the antibody binds to antigen but at higher concentrations may also binds to itself. It is possible that binding of one antibody results in the exposure of other antigenic sites on the cell surface. This possibility was examined by titrating the mAbs on paraformaldehyde fixed and fresh cells. No difference in binding was observed between fixed and fresh cells (Fig 4.6). It has been reported that some homophilic mAbs can also cross react, homophilically, with others. In order to test this possibility the two antibodies recognising Lewis y (BR96 and 692/29) were assayed cytometrically, on the cell line was shown to only expresses Lewis y, OAW28 (Fig 4.3). Cells were incubated with a 100µg/ml concentration of BR96-FITC, washed and then incubated with 1-10µg/ml 692/29-biotin, before detecting with streptavidin-PE/Cy5. Figure 4.7a shows that despite incubating cells with a high level of BR96-FITC, suggesting the coating of Lewis y antigens on the cell surface, 692/29-biotin was still able to bind to the cells, as detected by streptavidin PE/Cy5. Figure 4.7b shows that BR96-FITC is not displaced from the cells and is still present. To study binding of BR96 to 692/29, the reverse was undertaken; with figure 4.7c showing that BR96-FITC binding is not inhibited by 100µg/ml 692/29-biotin, with both mAbs being detected on the cells (Fig 4.7d).



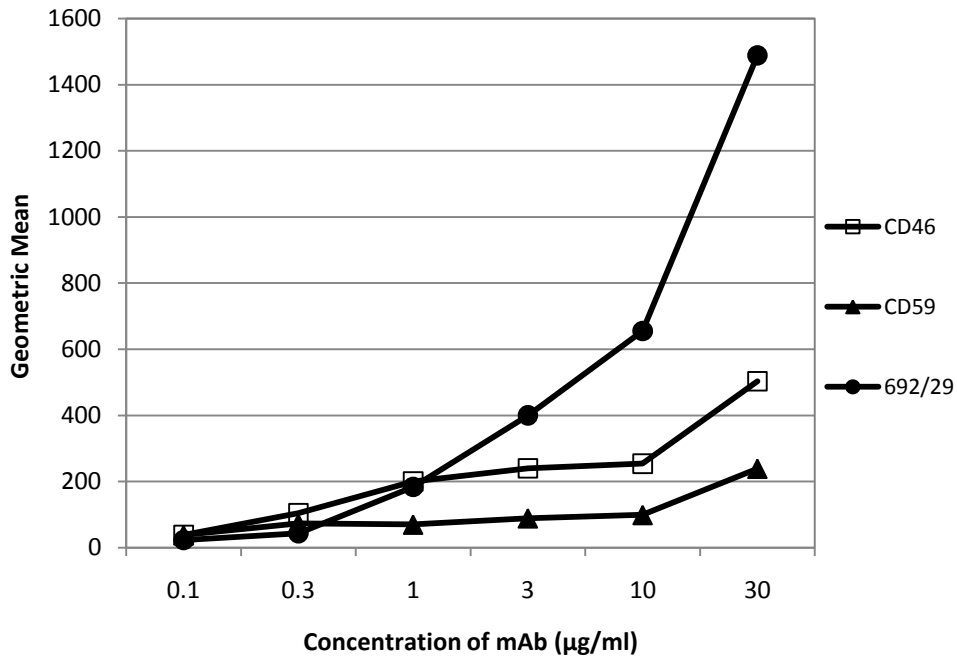


**Figure 4.4 Saturation of CD46 and CD59 binding to Colo 205 cells.** Colo 205 cells were plated at  $1 \times 10^5$  cells per well and incubated with 0.1-30 µg/ml CD46, CD59 or 692/29. Binding of the mAbs was probed with an anti-mouse IgG-FITC mAb before analysing the cells by flow cytometry. An irrelevant IgG mAb was used as a negative control (geometric mean 10). Data is representative of at least 3 experiments.

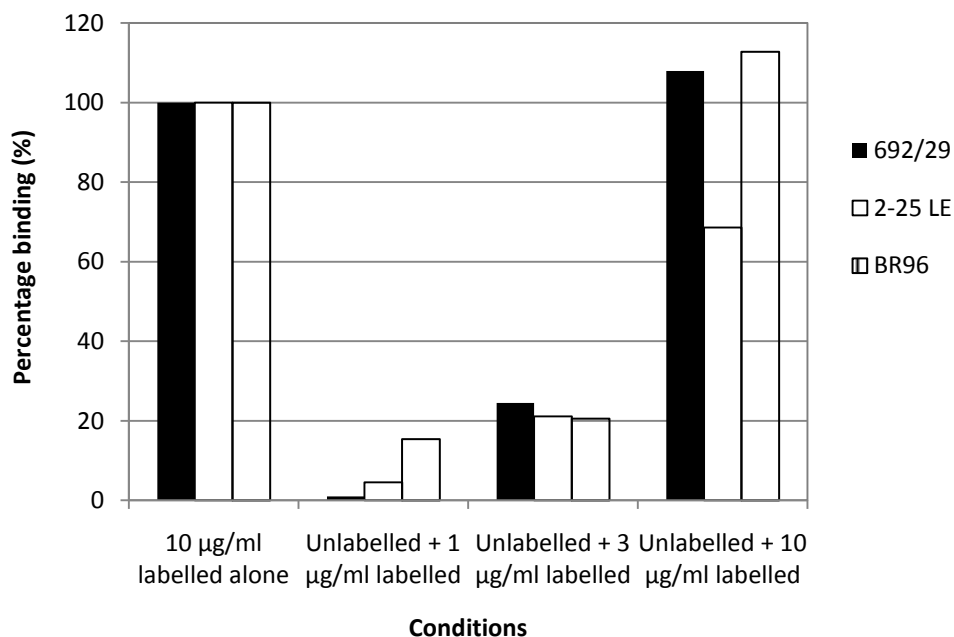


**Figure 4.5 Saturation of C170 cells with mAbs does not inhibit the binding of additional labelled 692/29 and BR96 mAb.** C170 cells were plated at  $1 \times 10^5$  cells round-bottomed well plates and saturated with 100 µg/ml unlabelled 692/29, BR96 and 2-25 LE. The cells were washed and the resuspended cells were treated with increasing concentrations (1, 3 and 10 µg/ml) either on top of unlabelled mAb or 10 µg/ml labelled mAb was added to cells alone (far left column). The cells were then analysed by flow cytometry. Results are expressed as a percentage of binding of 10 µg/ml FITC-labelled antibody alone. Data is representative of at least 3 experiments.

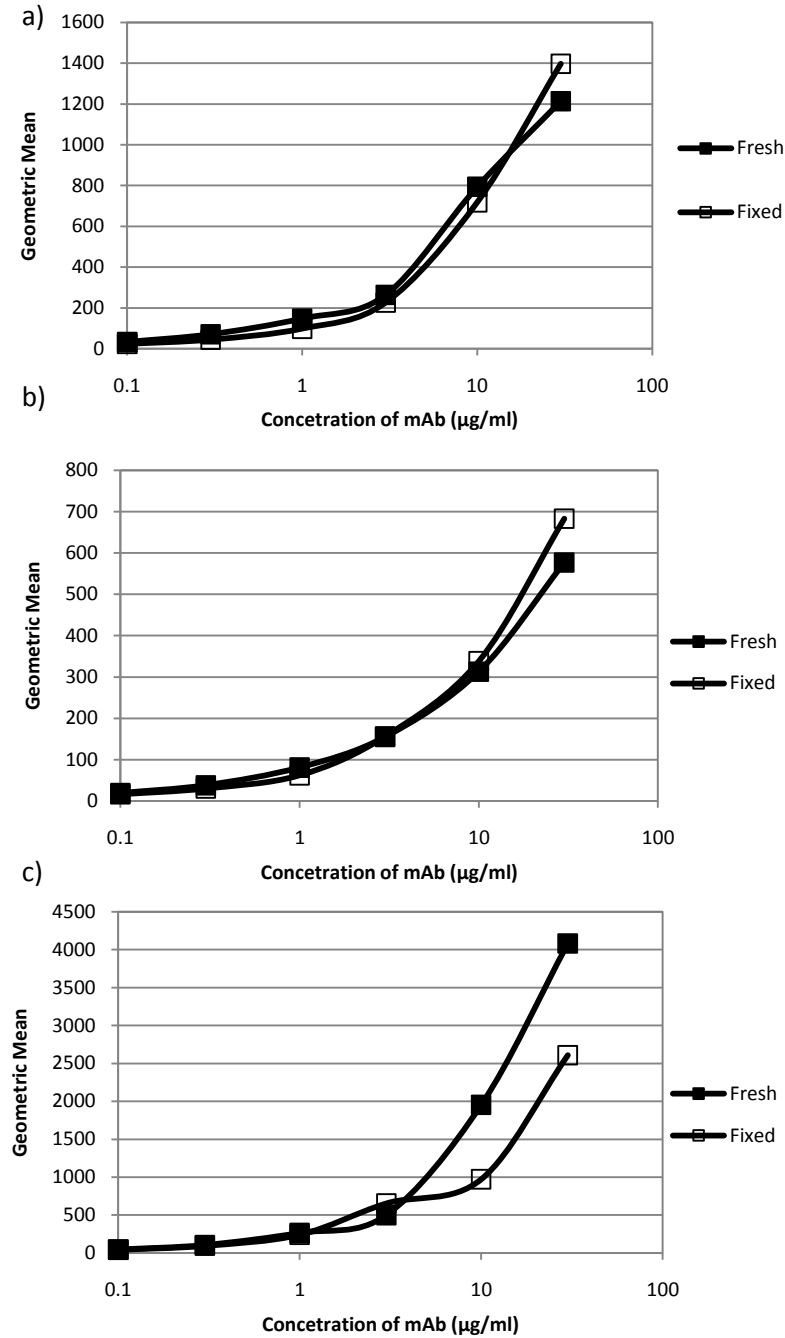


**Figure 4.6 Fixing cells does not decrease the level of mAb binding to C170 cells.** C170 cells were fixed for 15mins on ice in 1% formaldehyde before 0.1-30µg/ml 692/29 (a), 2-25 LE (b) or BR96 (c) was added to the fixed or fresh cells. Binding of mAb was detected with anti-mouse IgG FITC before analysing the cells by flow cytometry. Data is representative of at least 3 experiments.

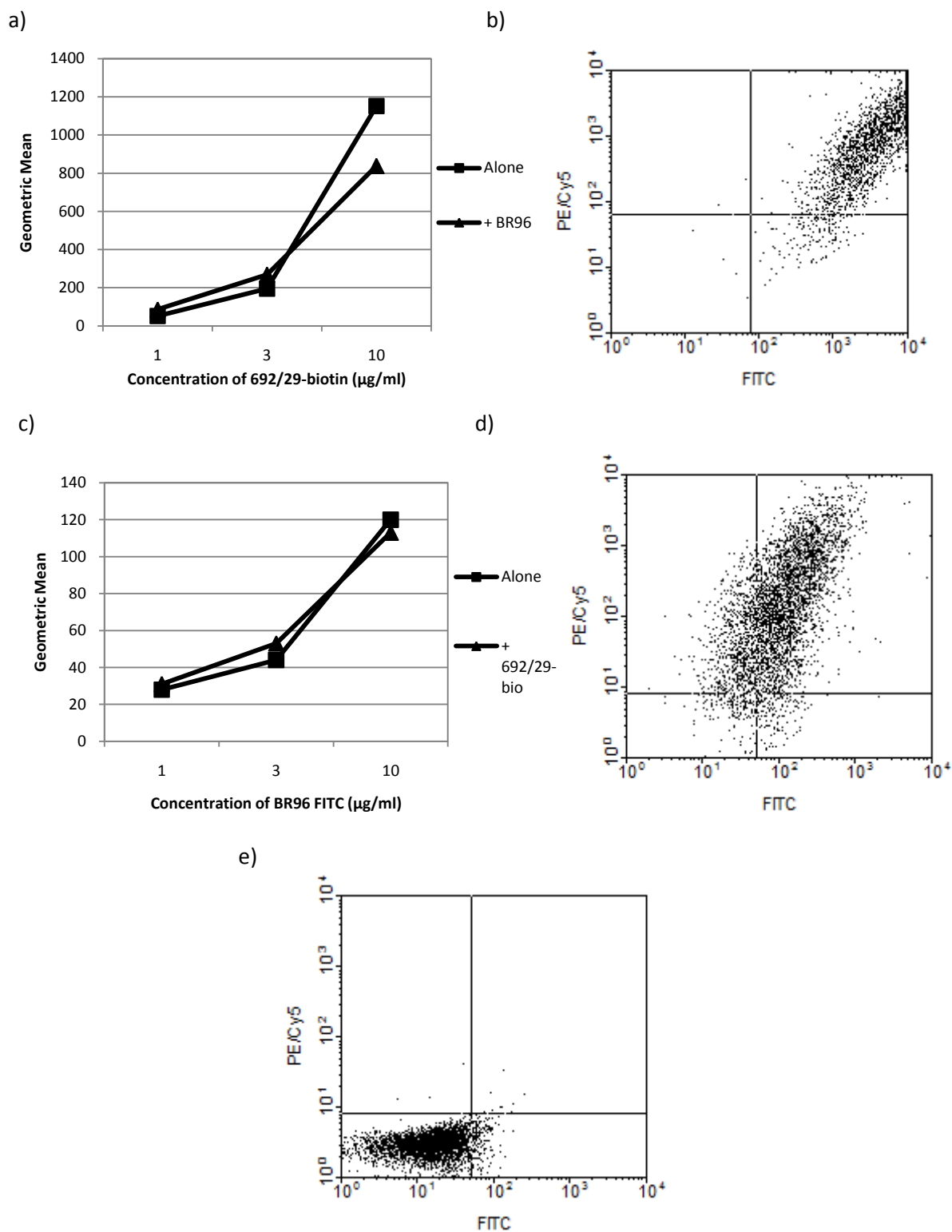
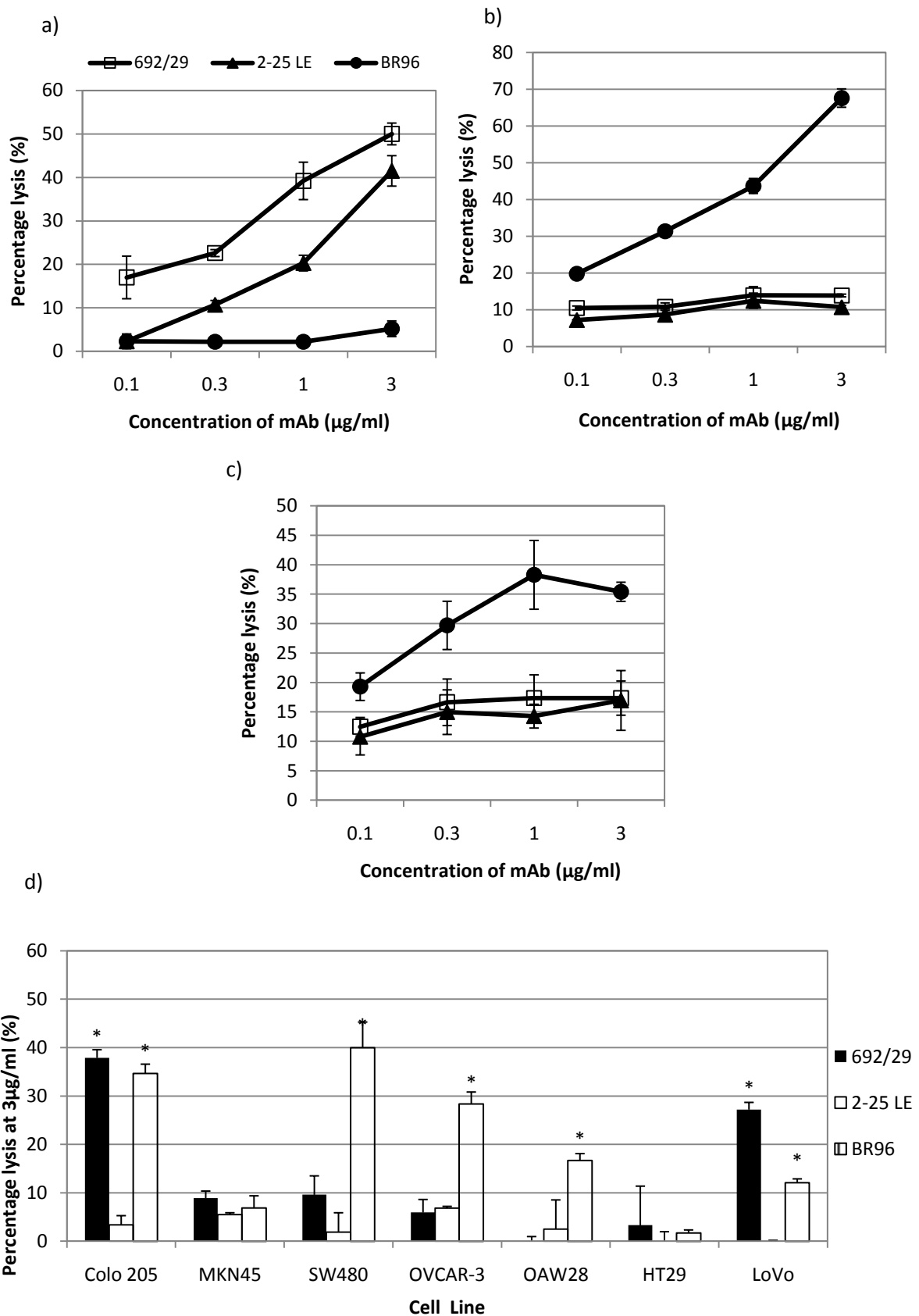


**Figure 4.7 Cross-reactivity of 692/29 with BR96.** OAW28 cells were incubated with 100µg/ml BR96-FITC before being incubated with 1, 3 and 10µg/ml 692/29-biotinylated. Cells were then probed for 692/29-biotin binding with streptavidin-PE/Cy5. Binding of 692/29-biotin is not inhibited by the pre-incubation of cells with BR96-FITC (a) which can be seen as both mAbs are present on the cells (b) The reverse was undertaken, incubating OAW28 cells with 100µg/ml 692/29-biotin before adding 1-10µg/ml BR96-FITC. The presence of 692/29-biotin was detected by streptavidin PE/Cy5. Binding of BR96-FITC is not inhibited by 692/29-biotin (c) with both mAbs still present on the cells (d) when compared to the negative control (e). Data is representative of at least 3 experiments.

#### 4.2.4 Induction of ADCC and CDC in cancer cells by 692/29, BR96 and 2-25 LE

The strong binding of the mAbs to cell lines should result in either ADCC in the presence of effector cells or CDC in the presence of complement. The ability of 692/29, BR96 and 2-25 LE to induce ADCC and CDC *in vitro* was tested using Lewis y/b positive target cells and either PBMCs isolated from human blood (ADCC) or serum isolated from human blood (CDC). Figure 4.8 shows that 692/29 is able to induce ADCC in cell lines that display a high level of binding (Colo 205), but is unable to induce ADCC in cells with lower levels of binding (OVCAR3, OAW28). 2-25 LE is also able to induce ADCC in Colo 205 cells but not in the cell lines that fail to express Lewis b (OVCAR3, OAW28). BR96 is able to induce ADCC in OAW28, and OVCAR3 cells despite the fact that it binds quite weakly to the latter cell line (Fig 4.8a-c).

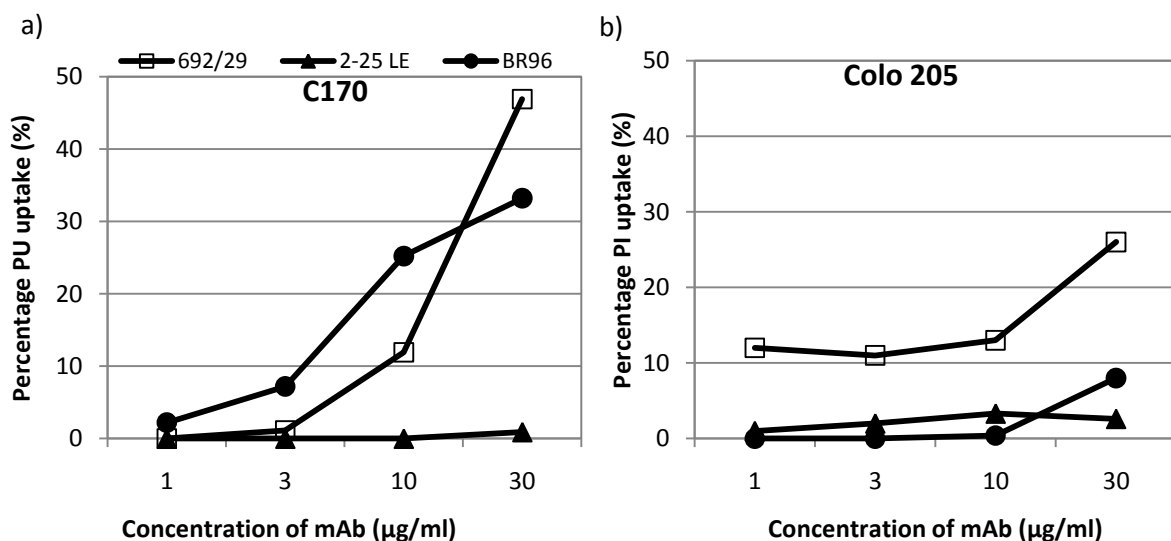
Figure 4.8e shows that 692/29 is able to induce CDC in Colo 205 and LoVo cells but not in the weak binding cell lines; SW480, OVCAR3, OAW28, MKN45 or HT29. In contrast, BR96 is able to induce CDC in Colo 205, LoVo, OAW28, SW480, and OVCAR-3, despite the fact that it binds quite weakly to the latter two lines. It does however fail to induce CDC in the very low and negative cell lines HT29 and MKN45. CDC induced by 2-25 LE is restricted to Colo 201 cells.



**Figure 4.8 ADCC and CDC assays.** Titration of anti-Lewis y and b mAbs on Colo 205 (a), OAW28 (b), OVCAR-3 (c) and a histogram showing the levels of CDC lysis observed in a range of colorectal and ovarian cancer cells (d). Cells were incubated with 692/29 2-25 LE and BR96 along with either PBMCs extracted from human blood (a, b, c) or 10% human serum (d) for 4 hours at 37°C. Cell lysis was measured by Cr<sup>51</sup> release. All data points have error bars, but may be obscured by marker. \* represents  $p < 0.05$ .

#### 4.2.5 Induction of cell death in colorectal cancer cells by 692/29, BR96 and not 2-25 LE

BR96 has previously been shown to induce membrane permeability, causing PI uptake. To determine if the differences in antigen recognition influenced the direct killing of the Lewis mAbs, they were incubated with a panel of cell lines expressing different levels of antigen. Membrane perturbation was assessed using PI uptake. 692/29 induces PI uptake in C170, Colo 205, LoVo and OVCAR-3. Little PI uptake was observed in cells with low levels of Lewis y/b expression; HT29 and OAW28 cells (Fig 4.9). BR96 induces PI uptake in C170, Colo205, HT29 and LoVo cells, despite binding weakly to HT29 (Fig 4.9). 2-25 LE fails to induce PI uptake in any of the cell lines, despite showing strong binding to C170 and Colo 205. Histograms of PI uptake are shown for C170 and summarised as percentage uptake for all cell lines (Fig 4.9g-j). In order to confirm PI uptake corresponded to cell death C170 cells were incubated with 692/29 for 5 days and cell number measured. Initially the number of cells decreased overnight before continuing to grow at the same rate as untreated cells (Fig 4.10a). Figure 4.10b and c shows that the surviving cells expressed similar levels of antigen to untreated cells after the 5 days and were not resistant to killing as they were susceptible to a new dose of 692/29.



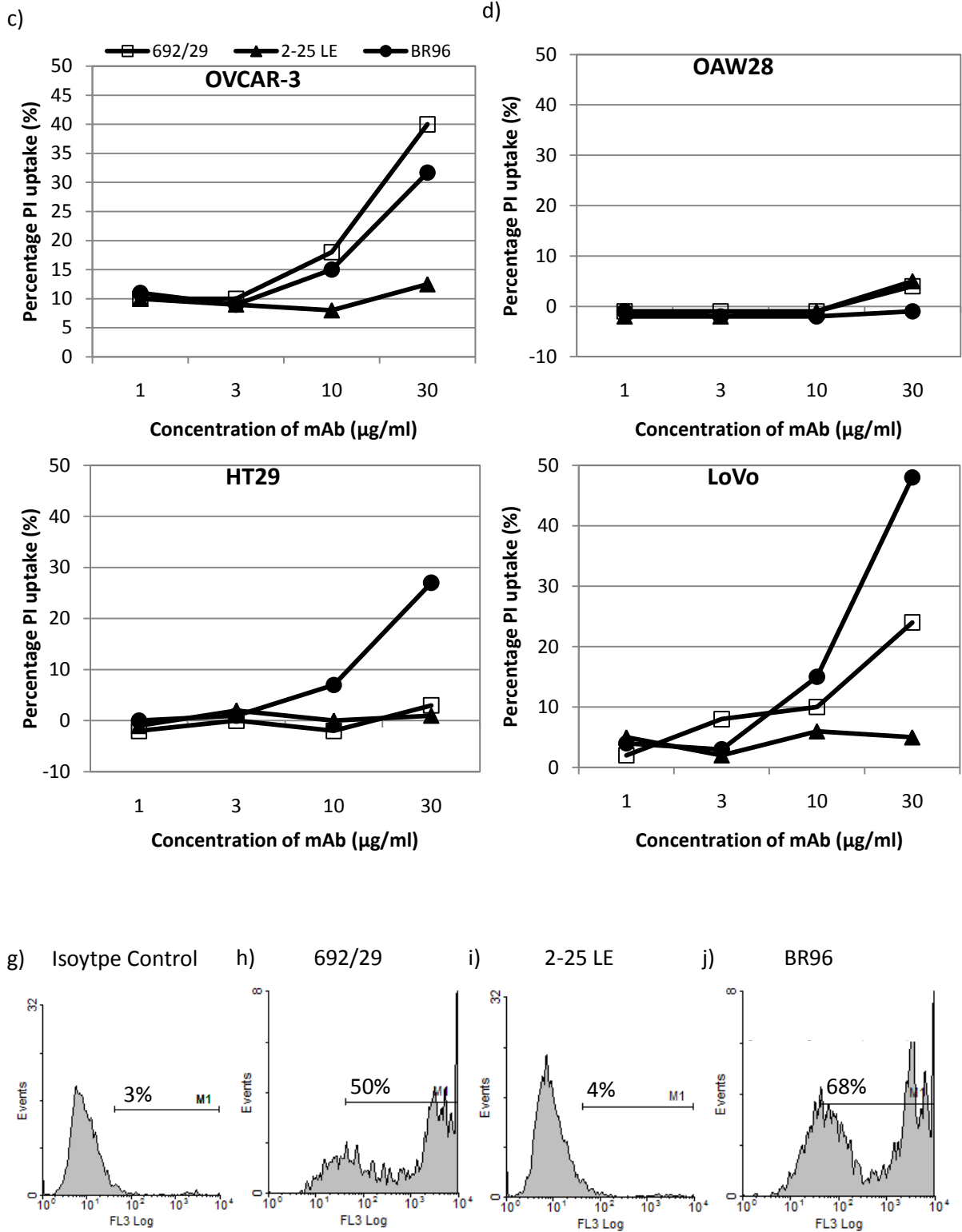


**Figure 4.9 Both 692/29 and BR96 induce direct cell death in a range of cell lines with 2-25 LE unable to induce direct cell death.** C170 (a), Colo 205 (b), OVCAR-3 (c), OAW28 (d), HT29 (e) and LoVo (f) cells were incubated with 0-30µg/ml 692/29, BR96, 2-25 LE or an isotype control overnight at 37°C. 1µg PI was added to each well 30mins before harvesting cells and detecting fluorescence by flow cytometry. Histograms of C170 uptake of PI after incubation with isotype control (g), 692/29 (h), 2-25 LE (i) and BR96 (j). Data is representative of at least 3 experiments.

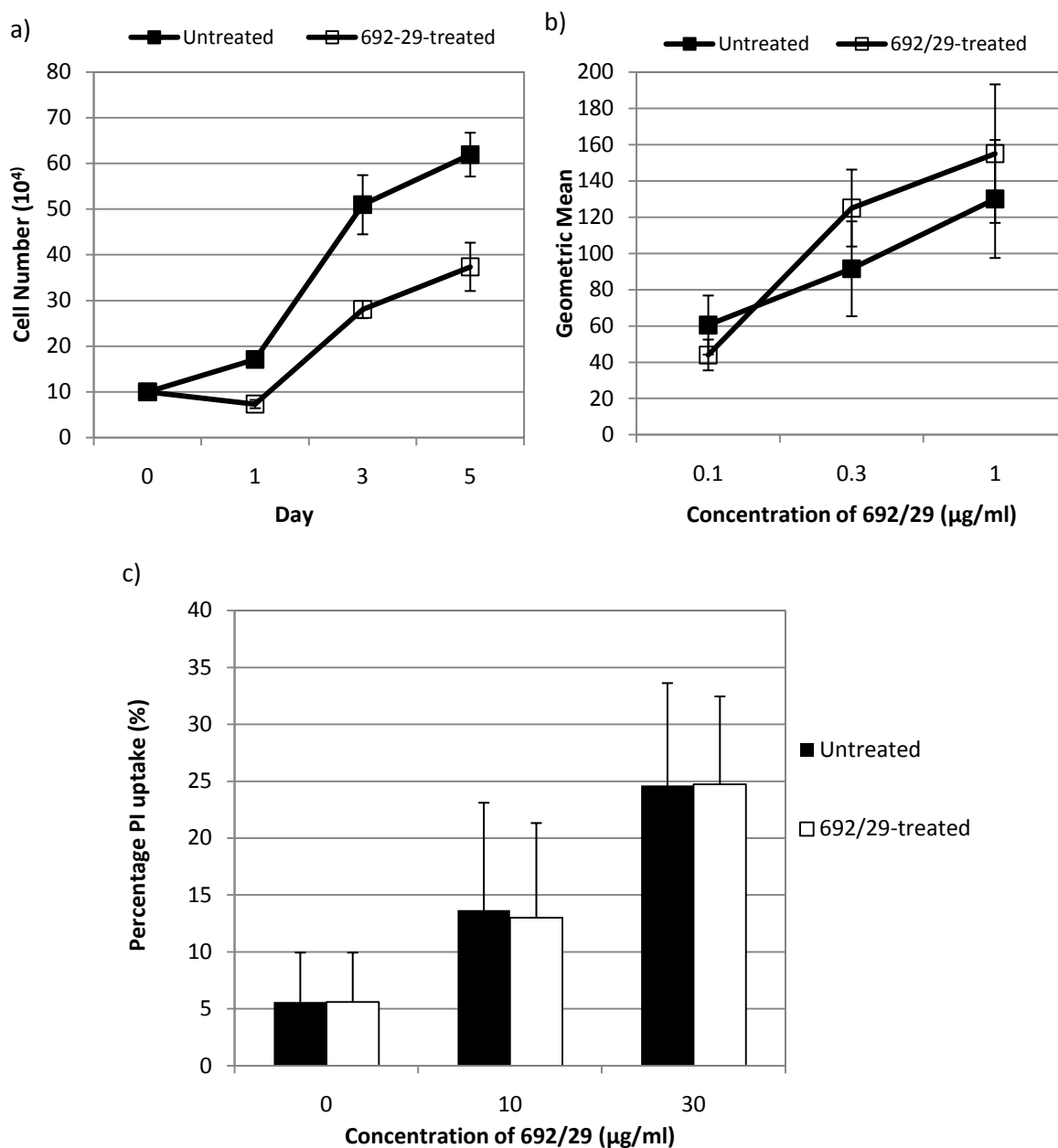


**Figure 4.10** 692/29 induces cell death of C170 cells over 5 days and the resulting cells express the same level of antigen as untreated cells which can then subsequently killed by 692/29. Cells were incubated with 30 $\mu\text{g/ml}$  692/29 and incubated at 37 $^{\circ}\text{C}$  for 5 days. Cell numbers were assessed on days 0, 1, 3 and 5 using a trypan blue assay (a). Binding of 692/29 to 692/29-treated and untreated cells was compared by screening cells with 0.1, 0.3, 1 $\mu\text{g/ml}$  692/29 and binding probed with rabbit anti-mouse IgG-FITC (b). 692/29-treated and untreated cells were incubated overnight with a fresh dose of 10, 30 $\mu\text{g/ml}$  692/29. PI was then added to cells before analysing by flow cytometry (c). Data is the average of at 3 separate experiments, with error bars present, but may be obscured by data points.



#### 4.2.6 Cross-linking the IgG<sub>1</sub> mAb 2-25 LE does not induce direct cell death

The anti-Lewis b mAb 2-25 LE demonstrated highest binding to Colo 205 and LoVo cell lines but fails to induce PI uptake and cell death. IgG<sub>3</sub>s reportedly have the ability to dimerise which may promote the killing observed with 692/29 and BR96. As 2-25 LE is an IgG<sub>1</sub>, it and 692/42, an IgG<sub>1</sub> isotype recognising the same epitope on Lewis y and Lewis b as 692/29 (unpublished data), was screened for killing with and without the addition of rabbit anti-mouse and goat anti-rabbit cross-linking antibodies. Figure 4.11 shows that the addition of cross-linking antibodies increases the killing seen with 692/42 (IgG<sub>1</sub>), but did not further enhance 692/29 (IgG<sub>3</sub>) or promote killing with 2-25 LE (IgG<sub>1</sub>).

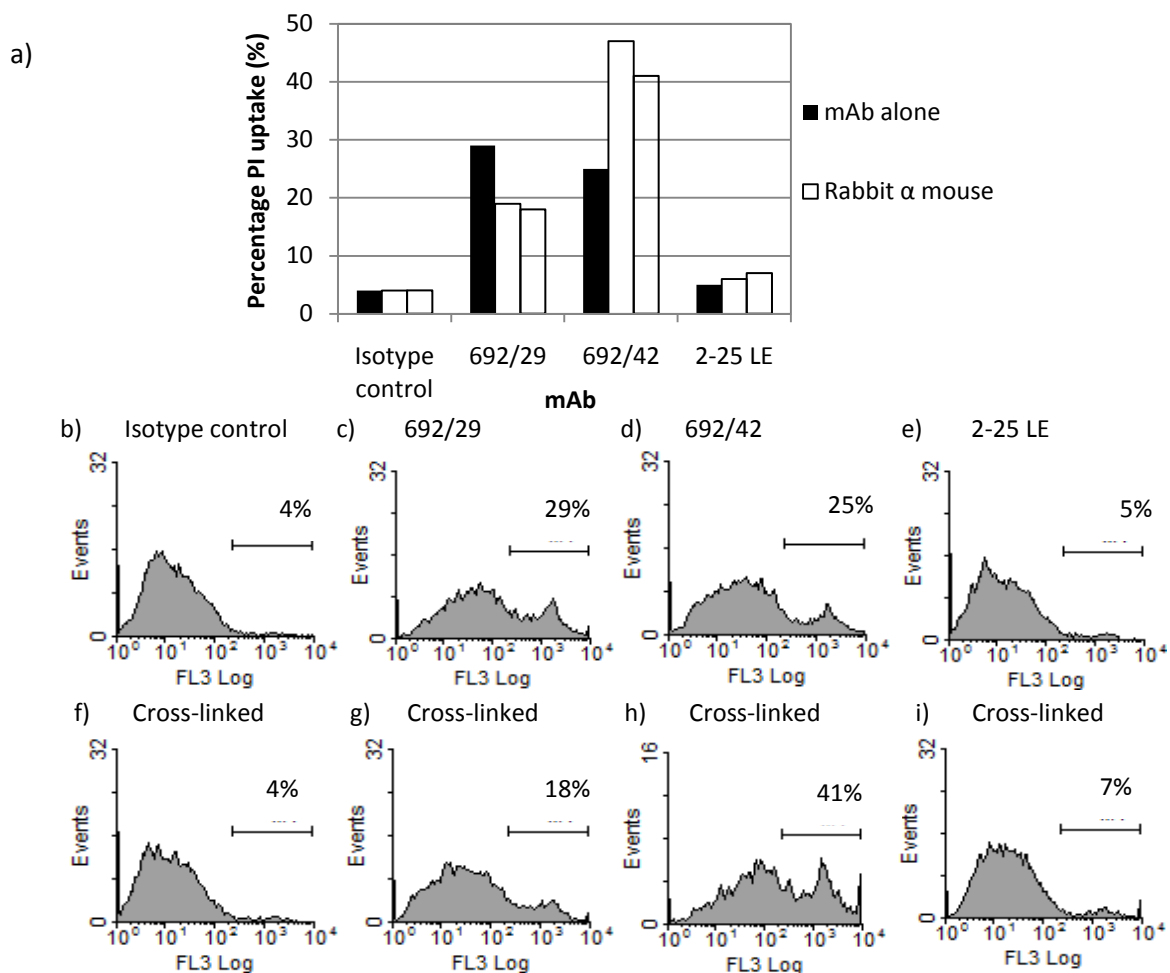


**Figure 4.11. Cross-linking the IgG<sub>1</sub> 2-25LE does not induce cell death in Colo 205 cells.** Colo 205 cells were incubated with 30µg/ml 692/29, 692/42 and 2-25LE either alone, or with rabbit anti-mouse or rabbit anti-mouse and goat anti-rabbit mAbs. Cells were then incubated overnight and PI uptake was measured (a). PI uptake in cells incubated with irrelevant IgG control (b), 692/29 (c), 692/42 (d) and 2-25 LE (e) or with rabbit anti-mouse and goat anti-rabbit Ig (f, g, h and i). Results representative of two independent experiments.

#### **4.2.7 692/29 and BR96 induce cell death via an alternative mechanism to apoptosis**

A number of anti-glycan mAbs, including BR96, have been shown to cause PI uptake by membrane perturbation, independently of apoptosis. To investigate whether 692/29 also caused cell death independently of apoptosis, cells were incubated with mAbs in the presence or absence of a pan caspase inhibitor, z-FMK-vad. Figure 4.12 shows that despite the addition of 20 $\mu$ M z-FMK-vad, only low levels of inhibition of cell death were observed with 692/29 or BR96, while anti-Fas mediated killing of Jurkat cells was almost completely inhibited by z-FMK-vad. To further investigate if the cell death was mediated on metabolically active cells, mAb induce death was measured after incubation of C170 cells at 22 $^{\circ}$ C and 4 $^{\circ}$ C. Figure 4.13 shows that 692/29 and BR96 could induce uptake of PI at both 22 and 4 $^{\circ}$ C (Fig 4.13a and b).

The induction of PI uptake in the presence of a pan caspase inhibitor and at both 22 and 4 $^{\circ}$ C, suggested that the mechanism of direct cell death was not of the type I, caspase-mediated apoptosis but may be related to oncosis, type II or type III caspase-independent mechanisms. Oncosis is associated with plasma membrane damage, caused by the formation of large pores in the membrane. Therefore, FITC-conjugated dextran beads ranging from 3kMW to 500kMW in size were used to study the size of pore formation induced by 692/29 and BR96. Anti-Fas mediated killing of Jurkat cells displayed uptake of only the smaller sized beads, compared to the membrane disruption with saponin that showed no discrimination in bead uptake (Fig 4.14). Similarly, figure 4.14 shows that the 3, 40 and 500k MW dextran beads were able to diffuse into 692/29 and BR96 treated cells, leading to an increased level of fluorescence when compared to the untreated and 2-25 LE-treated controls. This suggests that the size of pores formed on the cell surface by 692/29 and BR96 are larger than 500K MW.

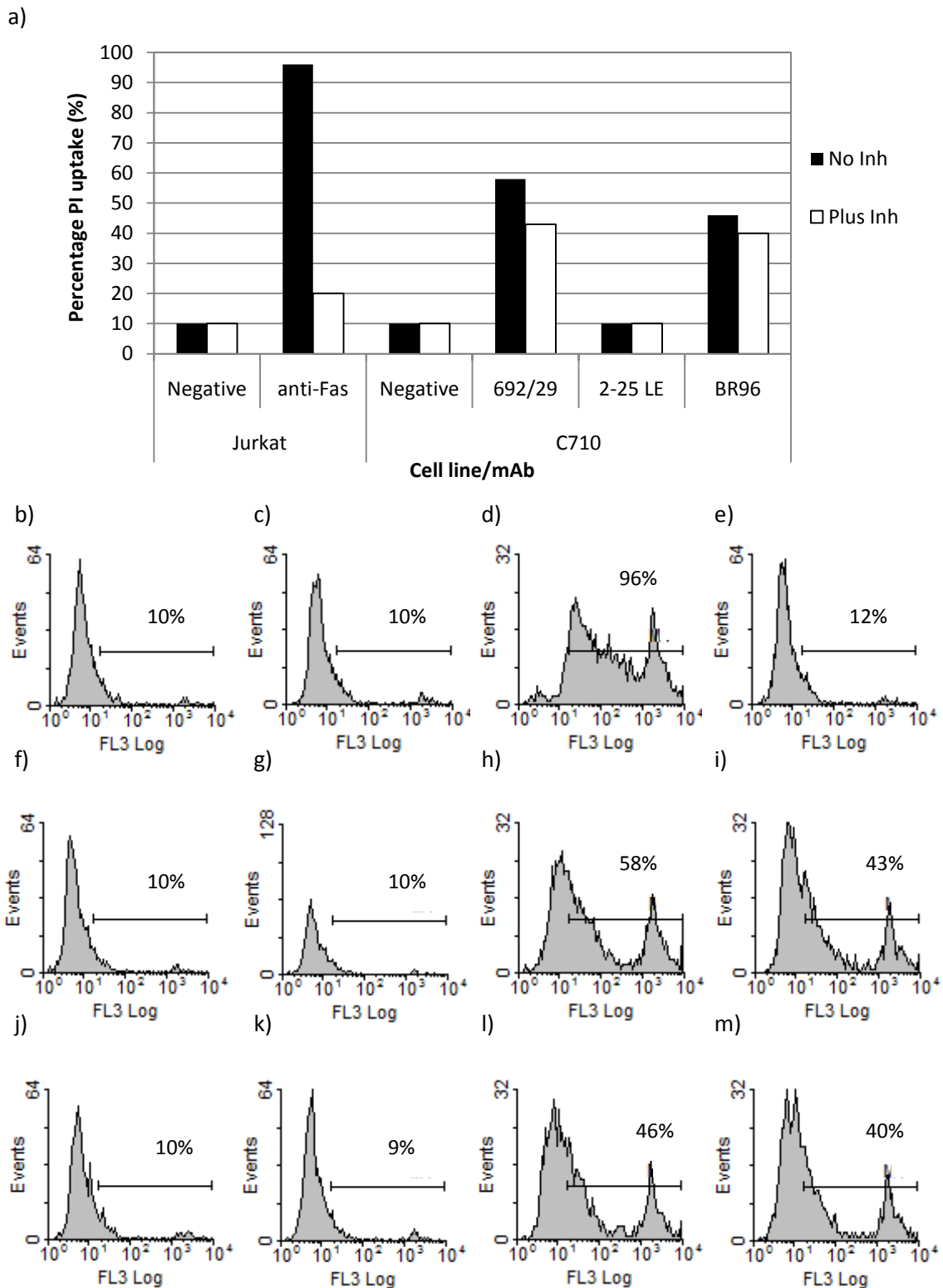


**Figure 4.12 692/29 and BR96 mediated killing of C170 cells is not inhibited by pan caspase inhibitor.** C170 cells were incubated with 30 $\mu$ g/ml 692/29, 2-25 LE and BR96 with and without a pan caspase inhibitor overnight at 37 $^{\circ}$ C, 5% CO $_2$ . Jurkat cells were incubated with 500 $\mu$ g/ml anti-Fas as a positive control. PI was added to all cells before fluorescence was detected by flow cytometry. Histograms are shown depicting IgM isotype control incubated with Jurkat cells without (b) and with pan caspase inhibitor (c), or with anti-Fas mAb without (d) and with pan caspase inhibitor (e), IgG isotype control incubated with C170 cells without (f) and with pan caspase inhibitor (g), C170 cells incubated with 692/29 (h), 2-25 LE (i) and BR96 (l) without inhibitor and with pan caspase inhibitor (i, k and m). Data is representative of at least 3 experiments.

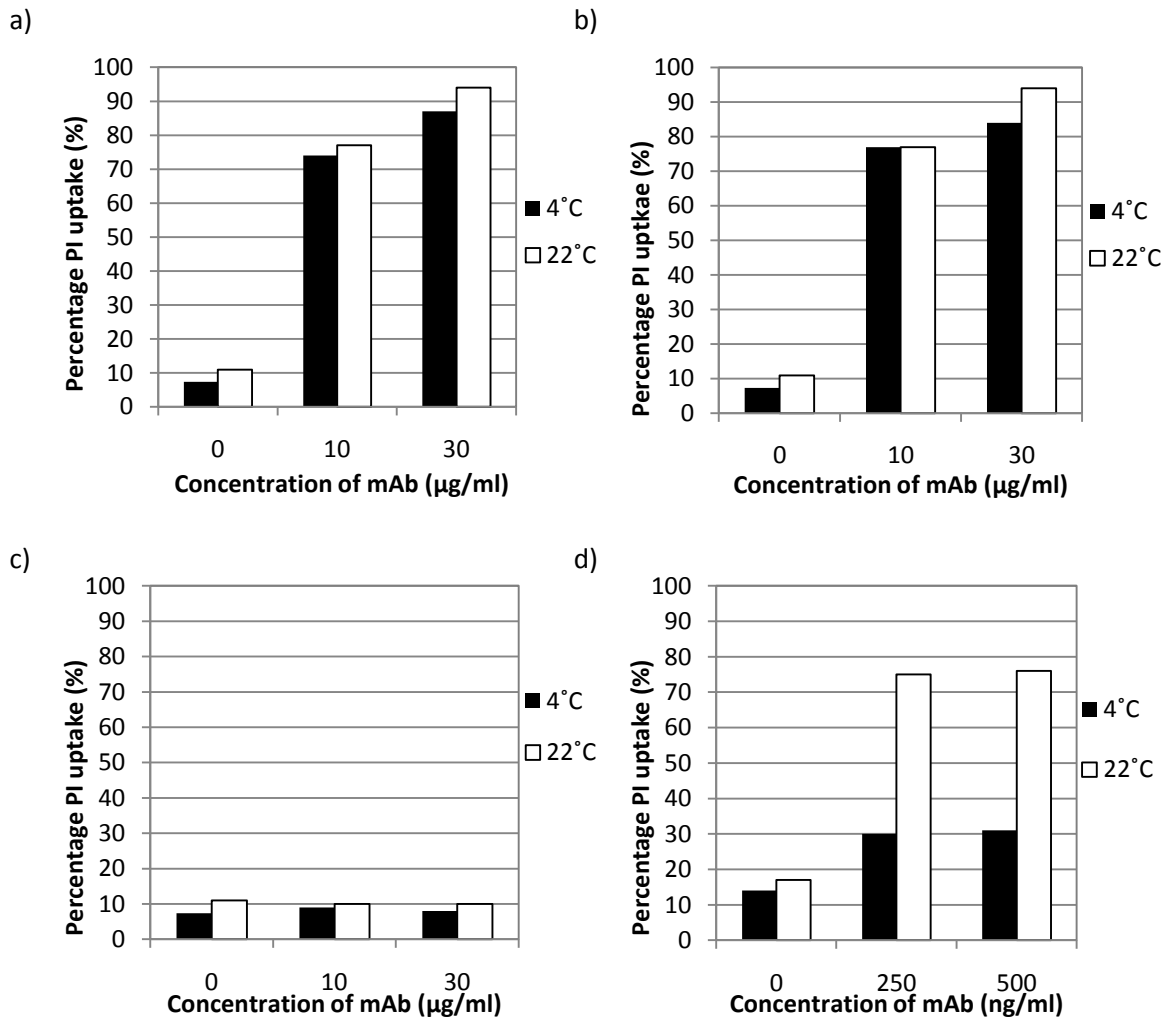


**Figure 4.13 692/29 and BR96 kill C170 cells at both 4 and 22°C.**  $5 \times 10^4$  C170 cells were incubated with 10 and 30 µg/ml of 692/29 (a), BR96 (b) or 2-25 LE (c) overnight at 4°C or 22°C or  $5 \times 10^4$  Jurkat cells were incubated with 0, 250 and 500 ng/ml anti-Fas mAb overnight at 4°C or 22°C (d). PI was added to the cells before analysing the percentage of dead cells using flow cytometry. Irrelevant-IgG was used as a negative control. Data is representative of at least 3 experiments.

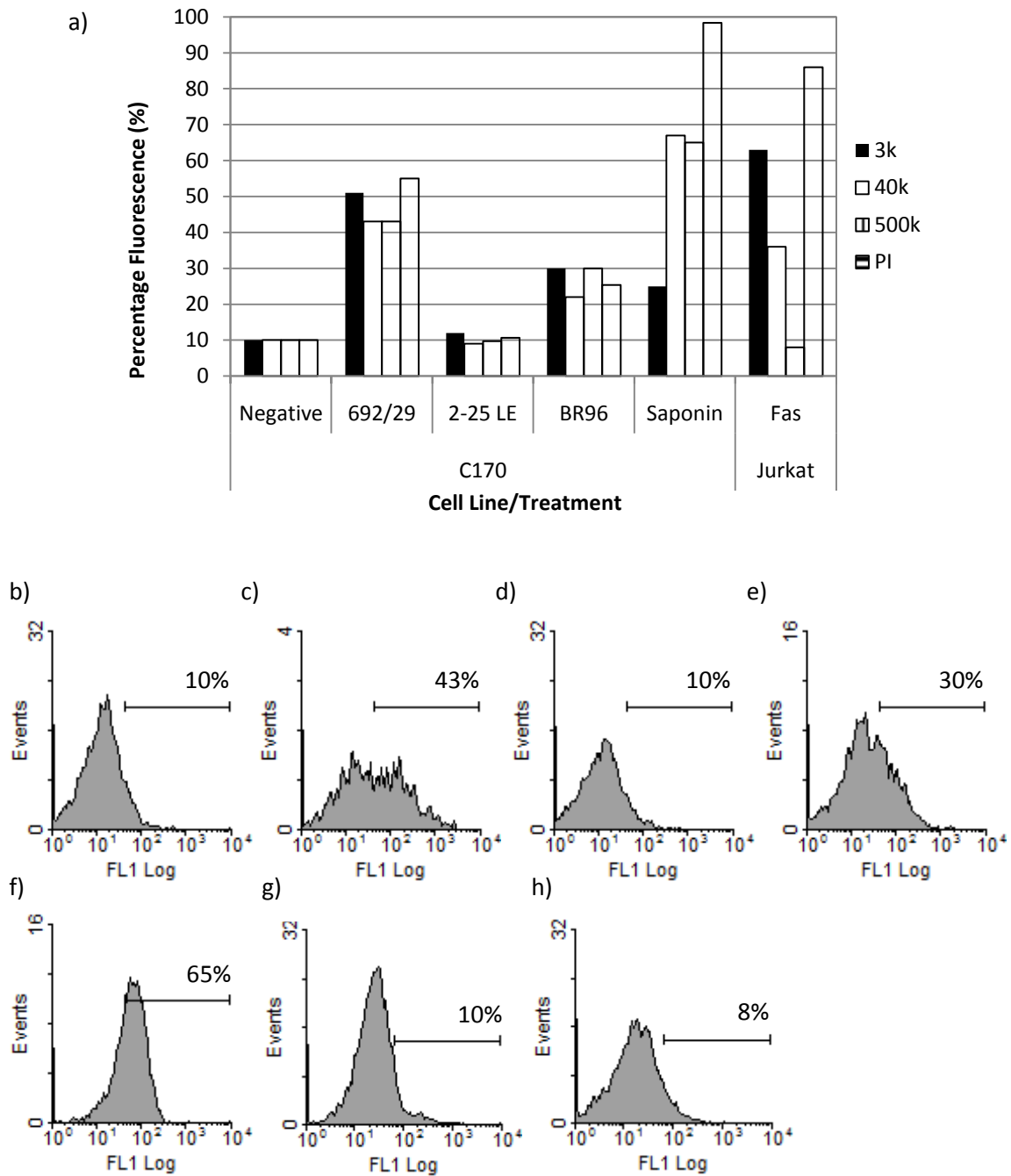


**Figure 4.14 Uptake of dextran beads upon 692/29, 2-25 LE and BR96 treatment.** C170 cells were incubated with 30 $\mu$ g/ml mAb and 3, 40 and 500K MW dextran-FITC beads or PI overnight before measuring uptake using flow cytometry. 30min treatment with 0.4% saponin was used as a positive control. Anti-Fas treatment of Jurkat cells overnight was used as a negative control for 500k MW dextran uptake (a). Histograms depict uptake of 500K MW dextran-FITC in C170 cells incubated with irrelevant IgG (b), 692/29 (c), 2-25 LE (d), BR96 (e) and 0.4% saponin (f) or Jurkat cells incubated with irrelevant Ig (g) or 500ng/ml anti-Fas (h). Data is representative of at least 3 separate experiments.

### 4.3 Discussion

One major value of mAbs as therapeutic agents is their ability to bind to a specific epitope, which can lead to specific targeting of the mAb *in vivo* and to less toxicity compared to conventional therapeutics, such as chemotherapy and radiotherapy. A further advantage is a mAbs ability to recruit the immune system to kill target cells, either by ADCC or CDC. Furthermore, as described previously, mAbs have also been shown to cause cytotoxicity directly, without the need of immune effector cells.

Lewis antigens have been proven to be over-expressed on a range of tumours making them good tumour markers (Abe et al., 1986; Hakomori, 1985; Itzkowitz, 1992; Madjd et al., 2005; Masayuki et al., 1995; Sakamoto et al., 1986; Sakamoto et al., 1989). MAbs recognising these haptens were therefore assessed for their therapeutic potential. As more recent studies have shown that the cross reactivity of anti-glycan mAbs has been underestimated (Manimala et al., 2007), the specificity of binding of 692/29 and BR96 was confirmed on the Consortium for Functional Glycomics glycan array. These results were compared to array binding data for 2-25 LE obtained from the Consortium database. The array confirmed that BR96 binds to its described antigen Lewis y but also reacts with a range of Lewis y variants (Lewis y-x, Lewis y-x-x) and more weakly to Lewis x and that 2-25 LE binds to Lewis b, with cross-reactivity with Lewis a and a-x. 629/29 binds most strongly to Lewis b and glycans containing Lewis b and also to tri-Lewis y and its variants. This is an interesting and novel feature as Lewis y or b mAbs have previously been described, including BR96 and 2-25 LE, but only one has been reported to bind both antigens (Brodin et al 1987). However, this mAb has haemagglutinating properties suggesting it cross-reactivity with H antigen and so would not be useful therapeutically. Furthermore, it has been shown that two independently produced anti-Lewis y mAbs (BR96 and 3S193) bind to structurally similar epitopes of Lewis y, and do not cross-react with b, suggesting a convergence of antigen binding to one more immunogenic epitope (Ramsland et al., 2004). 692/29 has previously been shown to bind to both Lewis y and b on a high percentage of

ovarian, colorectal, and gastric cancers (Durrant et al., 1993); Unpublished data. In order to observe whether the fine specificity of the Lewis y/b mAbs influenced binding to cells, the mAbs were screened against a range of colorectal and ovarian cancer cell lines. This revealed that the binding differed between the mAbs, despite cells being antigen positive, suggesting that the *in vivo* distribution of the mAbs may also differ. This would explain the lack of gastrointestinal binding with 692/29 (Unpublished data) when compared to BR96, which bound strongly to large intestine and caused dose limiting toxicity (Saleh et al., 2000).

Each mAb bound to a range of colorectal cancer cell lines without saturation being reached, suggesting they may bind in a homophilic manner. This was confirmed when the presence of 100µg/ml unlabelled mAb did not inhibit the binding of further mAb. Furthermore, incubation of OAW28 cells (Lewis b negative, Lewis y positive) with 100µg/ml of 692/29, did not inhibit binding of FITC-conjugated BR96 to the cells, suggesting that BR96 may have the ability to not only bind to itself, but also to 692/29. These results do not exclude the possibility that there was very high levels of Lewis y that could not be saturated even with very high levels of mAb. However, 100µg/ml of mAb contains  $\sim 2 \times 10^{13}$  molecules of antibody. If this fails to saturate there must be a very high frequency of the epitope. It may be more likely that multiple mAb molecules were bound to each glycan. Conversely, the presence of Lewis y on glycolipids and glycoproteins and the high level of unsaturable binding may suggest a very high level of Lewis y on cancer cells, which would be therapeutically beneficial.

It has been observed that mouse IgG<sub>3</sub> mAb have a tendency to aggregate in solution (Grey et al., 1971) and that this is due to Fc-Fc interaction, causing dimerisation. They may therefore aggregate on the cell surface. However, 2-25 LE is an IgG<sub>1</sub> and also displays properties of homophilic binding. Furthermore, binding of antibodies via the CDR regions has been reported, increasing the binding antibodies avidity for the antigen. Evidence of this phenomenon has been seen in both mouse and human anti-PC mAbs (Halpern et al., 1991; Kang et al., 1987). Their studies show that both mouse

and human mAbs purified from sera can bind to PC and also to each other (including mouse mAb-human mAb and human mAb-mouse mAb binding). They found that this self-binding could be inhibited by the binding of a peptide to the CDR2 (Halpern et al., 1991) and that this is due to a conserved sequence in the variable region (Kang et al., 1987). This group also conjugated the variable region sequence responsible for homophilic binding to non-homophilic antibodies, including an anti-CD20 mAb, showing greater inhibition of growth and cell death than with non-conjugated anti-CD20 mAb (Zhao et al., 2002).

ADCC and CDC assays were carried out against cells that have high and low expression of the Lewis y/b antigens using 692/29 and BR96. BR96 was able to induce ADCC and CDC on cells with both high and low levels of antigen expression, whereas 692/29 and 2-25 LE were more selective only mediating ADCC and CDC on cells with high antigen expression. As both Lewis y and Lewis b is expressed at low levels on normal cells this would predict a better therapeutic index for 692/29 and 2-25 LE than BR96 which may mediate immune directed killing of normal cells. BR96 failed in clinical studies due to mAb mediated GI toxicity (Tolcher et al., 1999).

In order to further characterise the mechanism of direct cytotoxicity the mAbs were incubated with a range of cell lines and PI uptake was measured. This confirmed that both BR96 and 692/29 had the ability to induce PI uptake in cells directly, whereas 2-25 LE did not. BR96 was able to induce PI uptake in cells that it showed weak binding, whereas, 692/29 was only able to induce PI uptake in cells with a high expression of Lewis y/b.

As all three mAbs displayed homophilic binding properties, the lack of killing by 2-25 LE to cells with high levels of antigen suggest that homophilic characteristics are not the main cause of direct cell death. Both 692/29 and BR96 are IgG<sub>3</sub> that have the ability to dimerise, whereas 2-25 LE is an IgG<sub>1</sub>. To test if the ability of the IgG<sub>3</sub> mAbs to cross-link was responsible for direct killing, 2-25 LE was cross-linked using rabbit anti-mouse Ig and goat anti-rabbit Ig mAbs. This showed that despite cross-linking, 2-25 LE was unable to induce direct cell death, implying that the mechanism of cell death is



not dependent on the ability of IgG<sub>3</sub> to cross-link, but may be antigen dependent. This suggests that Lewis b may not present on a functional glycolipid or glycoprotein that is capable of inducing cell death.

Previous studies had shown that BR96 was able to induce rapid cell death due to mAb recycling (Garrigues et al., 1993). It was suggested that this was not caused by apoptosis. Therefore cells were incubated at 4 and 22°C, as 4°C has been suggested to be lower than the temperature required for apoptosis to occur. Studies have shown that at temperatures lower than 15°C Bax is unable to insert into the mitochondrial membrane, inhibiting its ability to cause cytochrome C release, and therefore the activation of caspases in neutrophils (Pryde et al., 2000). Incubation of C170 cells at 4°C with 692/29 and BR96 failed to inhibit their ability to cause PI uptake. Furthermore, PI uptake was not inhibited by a pan caspase inhibitor, suggesting that both mAbs are able to induce cell death independently of apoptosis. In contrast, anti-Fas induced only low level apoptosis at 4°C and much higher levels at 37°C which were inhibited by the pan caspase inhibitor.

Previous studies have shown that mAbs can induce the caspase-independent cell death pathway, oncosis. For example, RAV12, which binds the carbohydrate antigen RAAG12, binds 90% of intra-abdominal tumours and has been shown to induce oncosis and inhibit growth of tumour xenografts (Loo et al., 2007). Also, the anti-porimin mAb, has been shown to cause oncosis in Jurkat cells (Zhang et al., 1998). mAb 84, that binds to the glycoprotein, podocalyxin-like protein 1 (PODXYL) has been shown to induce pore formation and oncosis in human embryonic stem cells using a range of different sized FITC-conjugated dextran beads (Tan et al., 2009). More recently, sera from patients treated with an anti-idiotypic mAb mimicking the GSL Neu5Gc-GM3, has the ability to induce the production of human anti-Neu5Gc-GM3 mAbs that induce oncosis in a leukemic cell line (Hernandez et al., 2011). One of the hallmarks of oncosis is the formation of large pores that are unique to oncosis and not seen in apoptosis. Therefore the level of fluorescence of cells after incubation with 692/29 and BR96 and various sized dextran beads was tested. Both 692/29 and BR96 mAbs

produced pores large enough to allow 500,000 MW dextran beads into the treated cells suggesting that both BR96 and 692/29 have the ability to mediate oncosis in Lewis y positive cells.

When both the immune mediated killing and direct killing were taken into consideration our results would suggest that 692/29 may be the more therapeutically valuable mAb. It binds to a wide range of cells expressing either Lewis y or b and causes direct cell death as well as ADCC and CDC in tumour cells over expressing Lewis y and b antigens. However, it fails to kill low expressing cells and may therefore have less toxicity to low expressing normal cells.

In conclusion, our study suggests that mAbs directed at the same antigen, display subtle differences in binding *in vitro*, which may affect tissue distribution *in vivo*. Furthermore, the differences in binding due to affinity or antigen density result in different effector functions, which may lead to increased toxicity *in vivo*. This can lead to the improved therapeutic benefit of mAbs recognising more than one glycan, such as the Lewis y/b mAb described in this study.

The ability of 692/29 and BR96, both anti-glycan mAbs to cause direct cell death in antigen positive cell lines warrants further investigation into another mAb produced in house, 505/4, that has been shown to bind to a glycan epitope.

## Chapter 5 Characterisation of the functional properties of an anti-glycan mAb

### 5.1 Introduction

As previously described, it has been widely reported that glycans on cancer cells undergo significant changes during transformation (Dabelsteen, 1996; Hakomori, 1985; Kannagi et al., 2008). This has led to certain glycans being used as tumour markers and therapeutic targets. Aberrant fucosylation of glycan-containing glycolipids or glycoproteins, leads to the increase in fucosylated glycans on the tumour cell surface, resulting in the overexpression of glycans such as Lewis x and Lewis a (Moriwaki & Miyoshi, 2010). For example, both Lewis a and sialyl Lewis a glycans are expressed at higher levels on tumour cells than on normal cells, making them good targets for monoclonal antibody (mAb) therapy (Kannagi et al., 2008). Furthermore, a large number of anti-glycan mAbs are capable of inducing direct cell death in cancers, such as the Lewis y specific mAbs 692/29 and BR96, described in the previous chapter and the previously mentioned F77 and RAV12 mAbs (Coberly et al., 2009; Zhang et al., 2010a).

Previous immunisation with a range of colorectal cancer cell lines lead to the production of an anti-colorectal glycolipid cancer mAb, 505/4 (unpublished data). CA19.9 is a mAb recognising sialyl Lewis a (also known as CA19.9 [carbohydrate antigen 19.9]; (Magnani et al., 1982)). Sialyl Lewis a has been shown to be overexpressed in a range of cancers, including colorectal (Yamada et al., 1997), breast (Jeschke et al., 2005) and ovarian (Charpin et al., 1982; Magnani et al., 1982). It is used as a serum marker in a range of cancers, including colorectal cancer to measure a patient's response to therapy (Nakagoe et al., 2001). 7LE is a commercial anti-Lewis a mAb.

In this study, we aim to further characterise the antigen, cell distribution and functional properties of the murine 505/4 mAb, as well as comparing the mAb with other colorectal cancer anti-glycan mAbs (CA19.9 and 7LE).

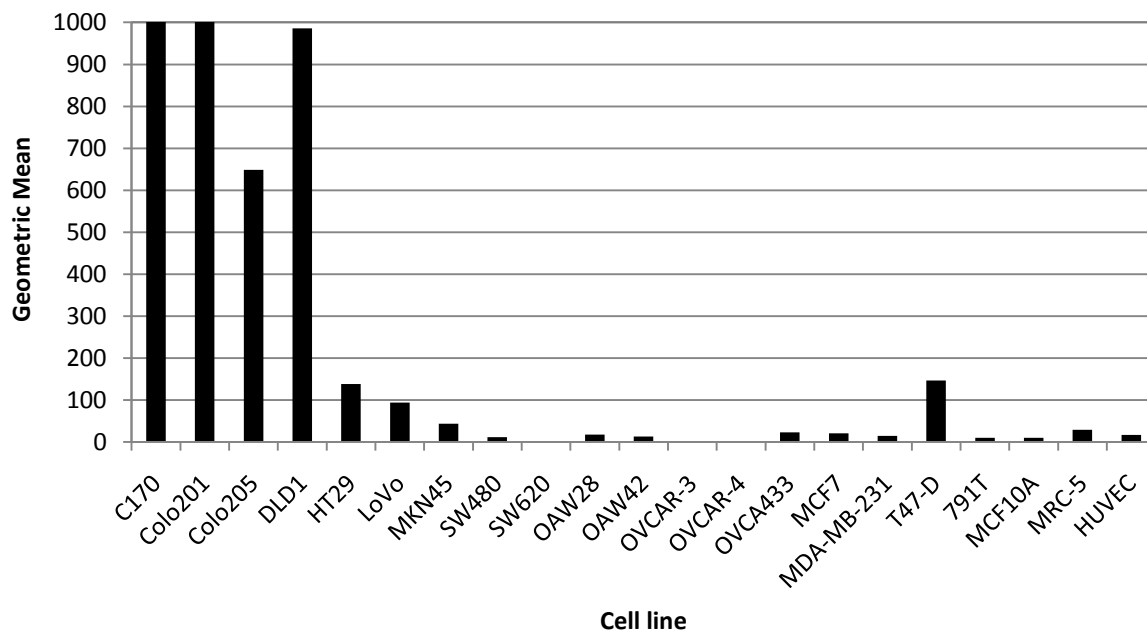
## 5.2 Results

### 5.2.1 Analysis of 505/4 therapeutic value by normal and colorectal cancer distribution

505/4 was produced by immunising mice with a range of colorectal cancer cell lines and was screened for strong binding to the cell surface of colorectal cell lines. 505/4 was incubated with a range of colorectal, ovarian, breast cancer cell lines, as well as normal human umbilical endothelial cell and fibroblast cell lines. Figure 5.1 shows that 505/4 binding was restricted to colorectal cell lines. Binding was also seen on the breast carcinoma cell line T47-D, but not to any other breast cancer cell lines or to the normal human umbilical vein endothelial cells (HUVEC).

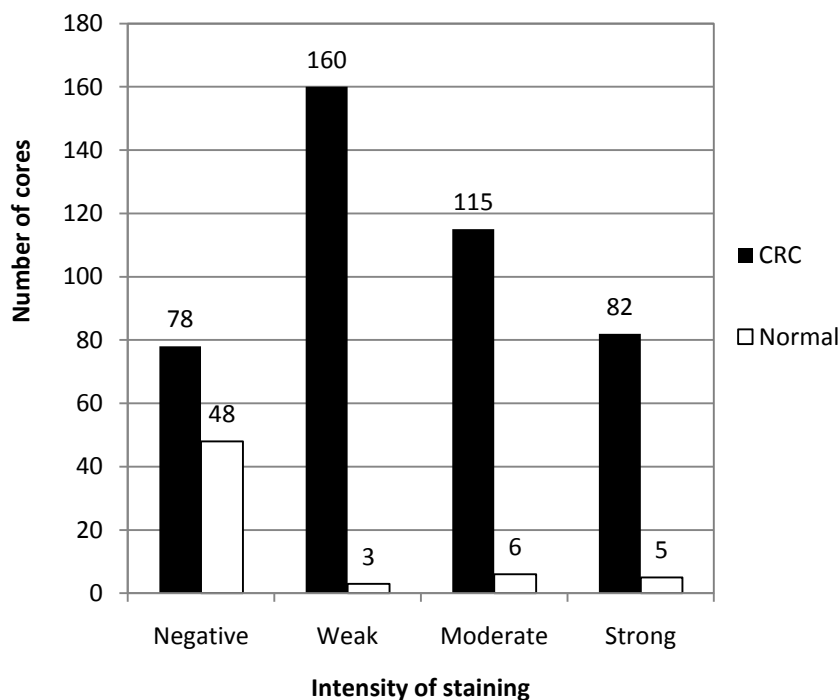
In order to assess the therapeutic value of 505/4, the mAb was stained on a colorectal TMA consisting of 462 tumours. 505/4 bound to 82% of colorectal tumours stained, 37% stained weakly, 26% stained moderately and 19% stained strongly, with the remaining 18% showing no binding (Fig 5.2a). Representative examples of negative, weak, moderate and strong staining are shown in figure 5.2b-e).

Although mAbs bind in a specific manner to their antigen, with less toxicity than traditional therapies, such as chemotherapy, they can cause toxicity by binding antigen expressed on normal tissue. Therefore, 505/4 was assessed for binding to normal tissue by immunohistochemistry. No staining was recorded in normal human brain, heart, prostate, testis, uterus, ovary, oesophagus, duodenum, ileum, jejunum, skeletal muscle, placenta or spleen (Table.5.1). 505/4 showed weak binding to gallbladder, cervix and rectum. Moderate staining was seen against breast, liver, tonsil and thymus with strong binding only seen to colon (Table 5.1). Figures 5.3b-g show examples of negative staining on brain (b) and heart (c), weak staining on lung (d), moderate staining to pancreas (e) and breast (f) and strong staining to colon (g). Despite binding to normal liver tissue by immunohistochemistry, 505/4 did not show binding to fresh hepatocytes, suggesting binding seen on normal liver tissue sections, may be to intracellular antigens (Fig 5.3).



**Figure 5.1 505/4 binds to a range of colorectal cell lines.** Cell lines were plated at  $1 \times 10^5$  cells per well and incubated with  $5 \mu\text{g/ml}$  505/4. Binding of 505/4 to the cells was probed with an anti-mouse IgG-FITC mAb before analysing the cells by flow cytometry. An irrelevant IgG mAb was used as a negative control (geometric mean 5). Data is representative of at least 3 experiments.

a)





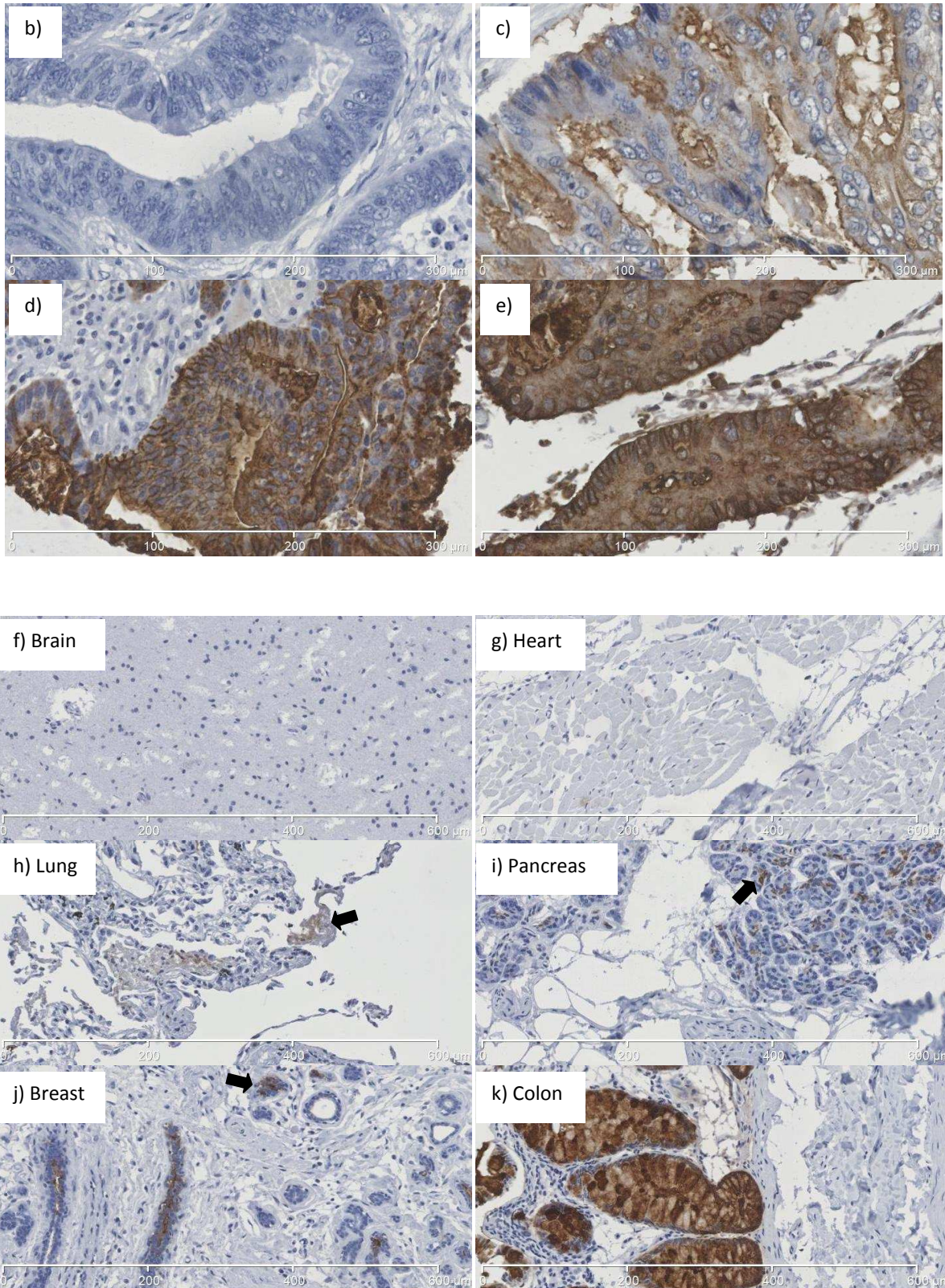


**Figure 5.2 Binding of 505/4 to colorectal tumours and normal tissues.** 504/4 was screened for binding on an array of colorectal cancers from a cohort of 462 patients and an array of 29 normal tissues by immunohistochemistry (a). Binding was visualised with DAB. Representatives of negative (b), weak (c), moderate (d) and strong (e) staining to colorectal tumours. Representatives of negative (f, g), weak (h), moderate (i, j) and strong (k) staining of the normal array are displayed at x10 original magnification. Black arrows indicate areas of staining.

**Table 5.1 Summary of 505/4 binding to a panel of normal tissues using paraffin-fixed sections.** Intensity of staining is shown as 0, 1, 2 or 3, relating to negative, weak, moderate or strong binding.

Tissue Type	Age	Gender	Intensity of staining
Placenta	29	F	0
Placenta	29	F	0
Oesophagus	23	M	0
Oesophagus	23	M	0
Rectum	24	F	0
Rectum	24	F	1
Gallbladder	24	M	3
Gallbladder	24	M	1
Skin	83	F	0
Skin	83	F	0
Adipose	26	M	0
Adipose	26	M	0
Heart	27	M	0
Heart	27	M	0
Skeletal	26	M	0
Skeletal	26	M	0
Bladder	36	F	0
Bladder	36	F	0
Ileum	62	M	0
Ileum	62	M	0
Spleen	30	M	0
Spleen	30	M	0
Brain	68	M	0
Brain	68	M	0
Jejunum	56	M	0
Jejunum	56	M	0
Stomach	66	M	0
Stomach	66	M	0
Breast	27	F	2
Breast	27	F	2
Kidney	56	M	0
Kidney	56	M	0
Testis	32	M	0
Testis	32	M	0
Cerebellum	73	F	0
Cerebellum	73	F	0
Liver	30	M	2
Liver	30	M	2
Thymus	28	M	2
Thymus	28	M	0
Cervix	30	F	0
Cervix	30	F	1
Lung	24	M	0
Lung	24	M	0
Smooth Muscle	23	M	0
Smooth Muscle	23	M	0
Colon	28	M	3
Colon	28	M	3
Ovary	50	F	0

Ovary	50	F	0
Tonsil	28	F	2
Tonsil	28	F	0
Diaphragm	26	M	0
Diaphragm	26	M	0
Pancreas	50	M	2
Pancreas	50	M	3
Uterus	40	F	0
Uterus	40	F	0
Duodenum	24	M	0
Duodenum	24	M	0
Thyroid	26	M	0
Thyroid	26	M	0

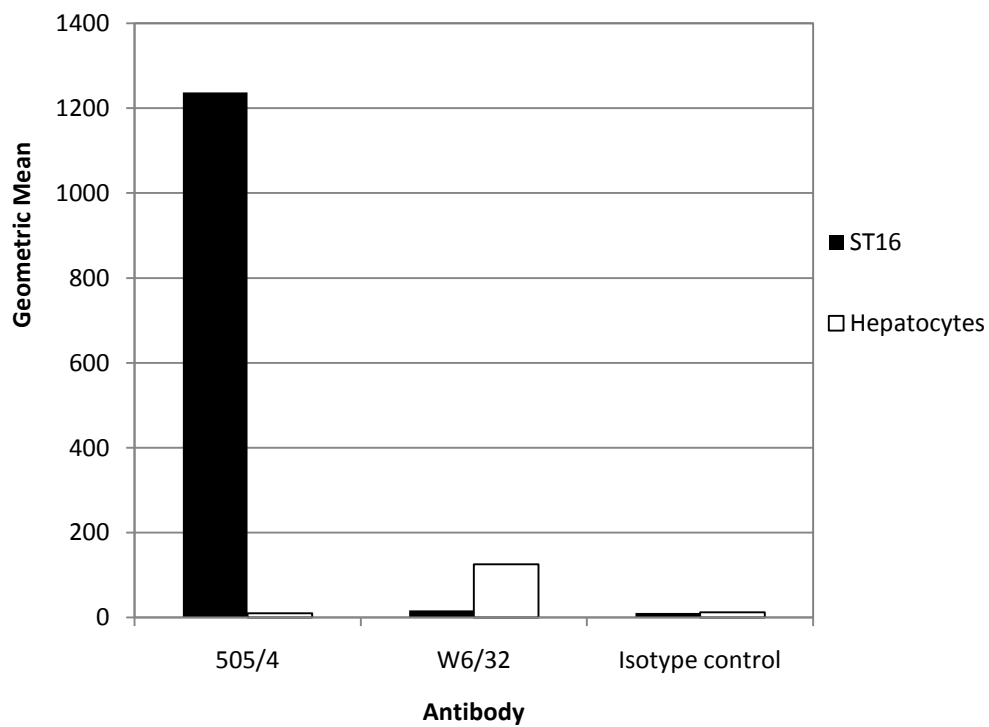


**Figure 5.3 Binding of 505/4 to the gastric cell line ST16 but not to fresh hepatocytes.** 5µg/ml 505/4, W6/32 or IgG<sub>1</sub> isotype control was incubated with either 1x10<sup>5</sup> ST16 cells or hepatocytes for 60min. Binding of primary antibody was probed with rabbit anti-mouse IgG-FITC before analysing fluorescence by flow cytometry. Data is representative of 3 separate experiments.



## 5.2.2 Characterisation of 505/4 antigen

To test whether the 505/4 antigen was present on glycolipids, 505/4 binding to C170 glycolipid extract was tested. Glycolipid was extracted from C170 cells using chloroform: methanol. The extracted layers were bound to an ELISA plate and 505/4 was screened. Figure 5.4a shows that 505/4 binds to the charged C170 glycolipid layer and to the protein layer, but not to either the neutral glycolipid layer or OVCA 433 glycolipid. 791T/36, an anti-CD55 mAb was used as a negative control, with F002, an anti-ovarian cancer glycolipid mAb produced in house used as a positive control. To confirm the specificity of 505/4 for a glycan C170 cells were treated with sodium periodate ( $\text{NaIO}_4$ ) to oxidise any cell surface glycans. 791T/36, a mAb directed against the protein antigen CD55, was resistant to  $\text{NaIO}_4$  treatment, whereas 505/4 binding was lost upon  $\text{NaIO}_4$  treatment (Fig 5.4b).

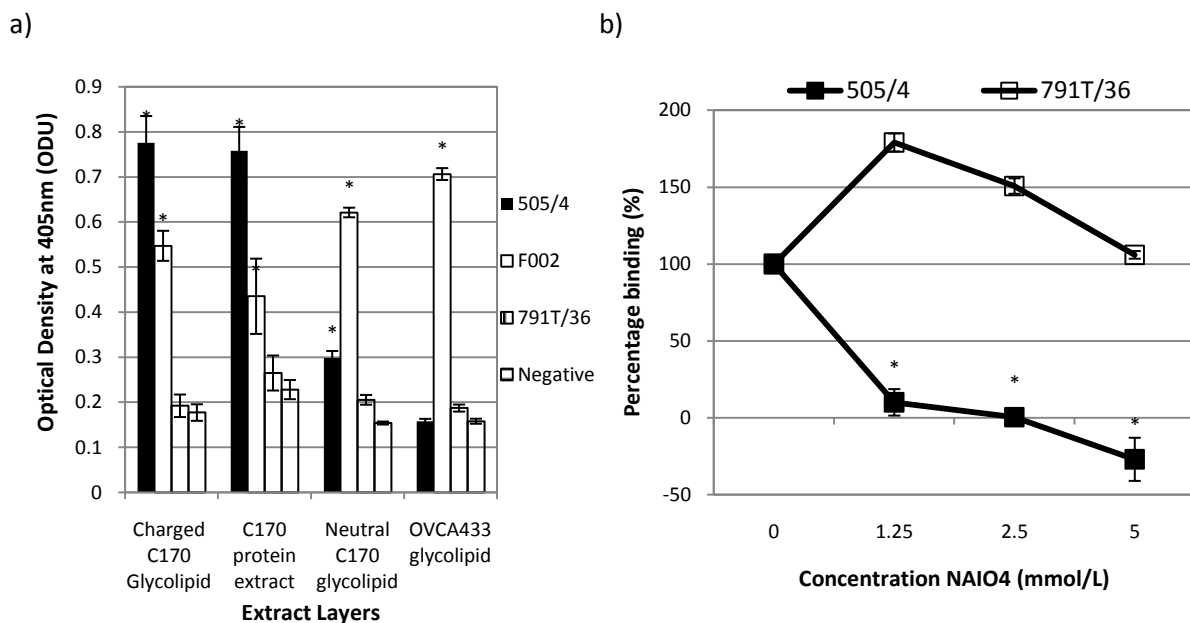


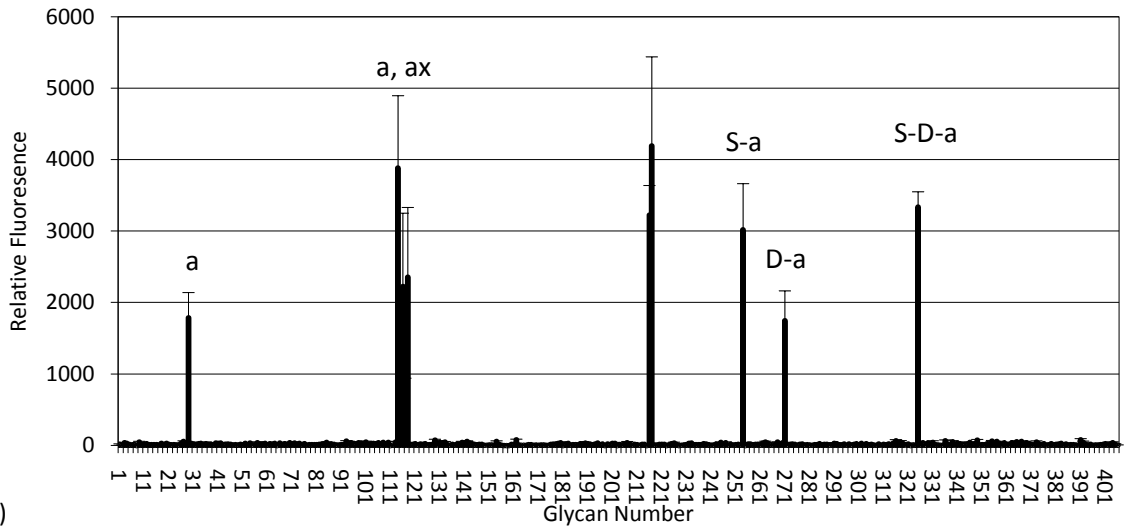
**Figure 5.4** 505/4 binds to a glycan epitope on both charged glycolipid and glycoprotein on a range of colorectal cancer cell lines. a) Glycolipid extract was carried out using 2:1 chloroform: methanol on C170 cells. The resulting layers were dried on ELISA plates before probing with 505/4. The anti-glycolipid mAb F002 was used as a positive control against OVCA 433 glycolipid, with the anti-CD55 mAb 791T/36 being used as a negative control. b) An ELISA plate coated with fixed C170 cells were incubated with 0, 0.125, 0.25 or 5mmol/L sodium periodate. Treated cells were then incubated 505/4 and mAb binding was probed with anti-IgG-HRP. ABTS colour change was used to assess the level of mAb binding. \* depicts  $p < 0.05$ . Results are representative of at least 2 experiments, error bars representing the standard deviation of quadruplicate wells are present for each data point, but may be obscured by marker.

### **5.2.3 Analysis of 505/4, CA19.9 and 7LE binding to the Consortium for Functional Glycomics array**

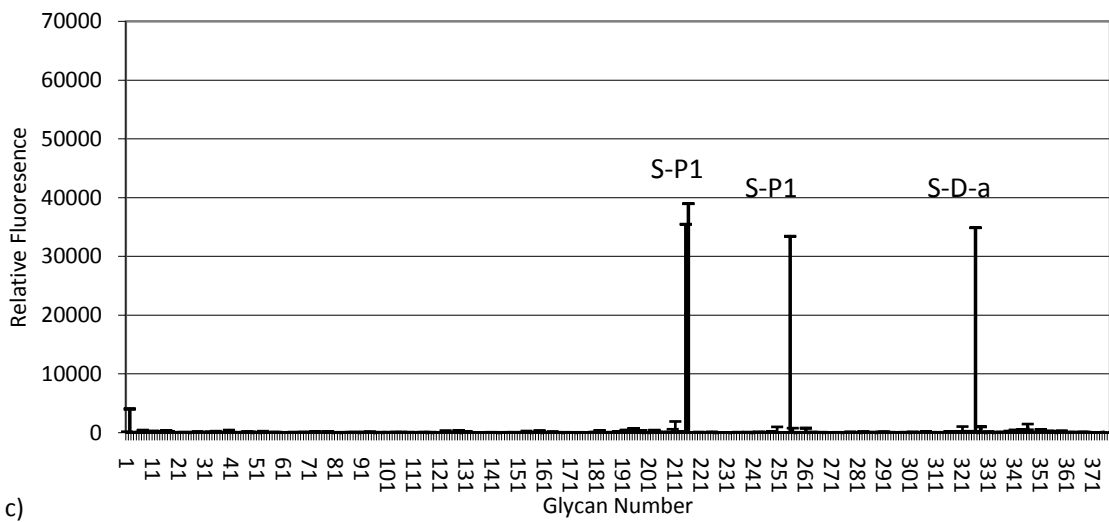
As the sodium periodate treatment and glycolipid ELISA suggested that 505/4 was binding to a glycan, the exact antigen was determined by screening 505/4 against a panel of 406 synthetic and naturally occurring glycans using the Consortium for Functional Glycomics' array. Figure 5.5a shows that binding of 505/4 to the glycan array was limited to Lewis a and its variants. Including sialyl di-Lewis a, sialyl Lewis a (both human and mammalian sialic acids,), Lewis a, Lewis a-x and di-Lewis a. Table 5.2a demonstrates that the 505/4 bound most efficiently with the sialylated versions of the glycans.

In order to compare 505/4 with other anti-Lewis a mAbs, the anti-Lewis a mab 7LE and anti-sialyl Lewis a mAb CA19.9 were acquired. The specificity of 7LE and CA19.9 was confirmed by obtaining array binding data from the Consortium for Functional Glycomics database. CA19.9 bound to sialylated precursor of Lewis a, sialylated Type 1 precursor whereas 505/4 did not. CA19.9 also bound to sialyl di-Lewis a (Fig 5.5b, table 5.2b) with both the human and mammalian version of sialic acid. 7LE bound specifically to Lewis a and its precursors (Fig 5.5c, Table 5.2c). It seemed to recognise a terminal Gal that is neither sulphated nor attached to sialic acid and prefers a non charged core of 2-4 sugars.

a)



b)



c)

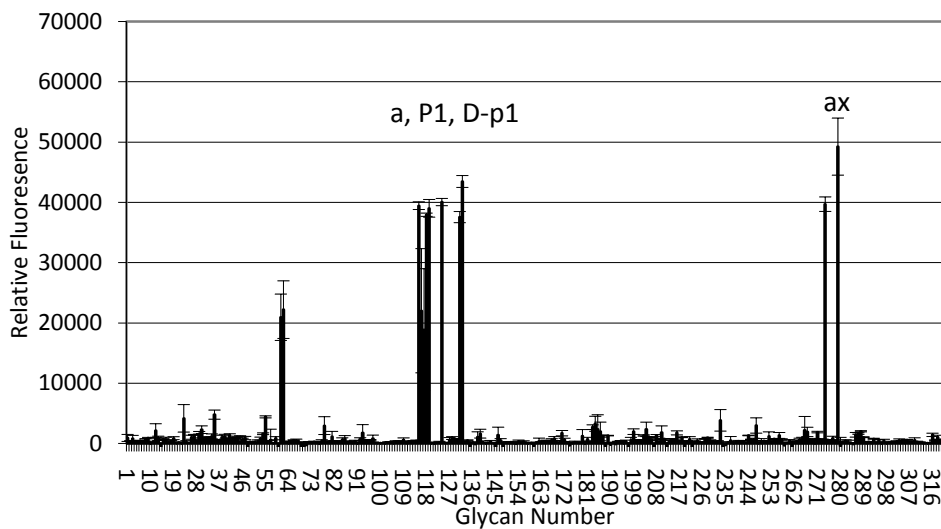


**Figure 5.5 Glycan array binding data for 505/4 (a), CA19.9 (b) and 7LE (c).** 505/4 shows specificity for sialyl Lewis a and its variants, including sialyl di-Lewis a (S-D-a), sialyl Lewis ax (S-ax) and sialyl di- Lewis ax (S-D-ax). It also binds to the non-sialylated variants of these glycans (Lewis a [a], Lewis ax [ax], and di-Lewis a [ax]). CA19.9 binds to sialylated type 1 precursor (sP1) and sialyl di-Lewis a. 7LE shows specificity to Lewis a and to di-Lewis a as well as binding to type 1 precursor (P1).

**Table 5.2 Describes the glycans that 505/4 (a), CA19.9 (b) and 7LE (c) bind to on the Glycome Consortium glycan array, the level of binding and the structures of the glycans.** A blue squares represents glucosylamine, yellow circles represents galactose, red triangles represent fucose, green circles represent mannose and purple diamond represents sialic acid. Sulphation is represented by SO<sub>3</sub> and Sp denotes the spacer between glycan and glass slide.

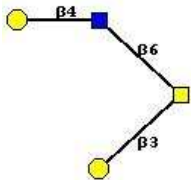
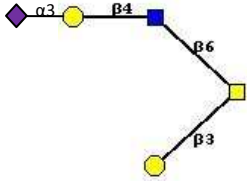
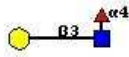
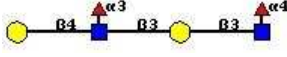
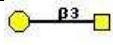
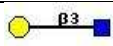
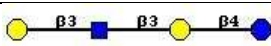
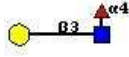
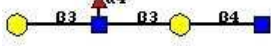
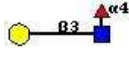
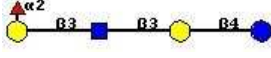
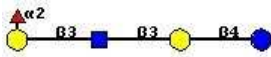
a)

Glycan No.	Glycan	Name	Percentage of best binder (%)	Structure
325	Neu5Aca2-3Galb1-3(Fuca1-4)GlcNAcb1-3Galb1-3(Fuca1-4)GlcNAcb-Sp0	Sialyl Di-Lewis a	100	
216	Neu5Aca2-3Galb1-3(Fuca1-4)GlcNAcb-Sp8	Sialyl Lewis a	97	
254	Neu5Gca2-3Galb1-3(Fuca1-4)GlcNAcb-Sp0	Sialyl Lewis a	90	
114	Galb1-3(Fuca1-4)GlcNAcb1-3Galb1-4(Fuca1-3)GlcNAcb-Sp0	Lewis a-x	68	
118	Galb1-3(Fuca1-4)GlcNAcb-Sp8	Lewis a	58	
29	[3OSO3]Galb1-3(Fuca1-4)GlcNAcb-Sp8	3'-Sulfo Lewis a	54	
271	Galb1-3(Fuca1-4)GlcNAcb1-3Galb1-3(Fuca1-4)GlcNAcb-Sp0	Di- Lewis a	52	
116	Galb1-3(Fuca1-4)GlcNAcb-Sp0	Lewis a	49	

b)

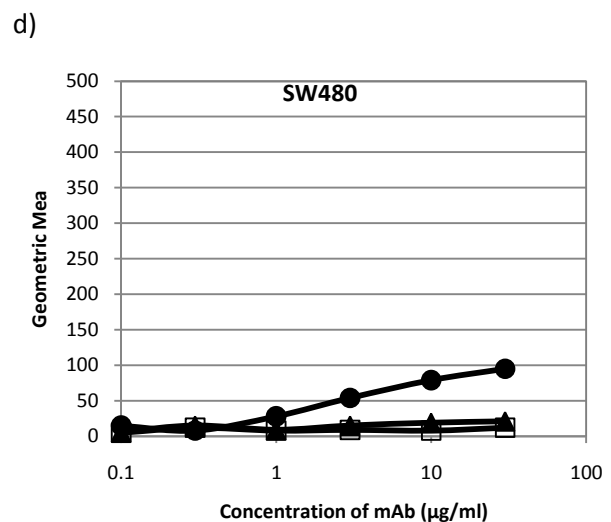
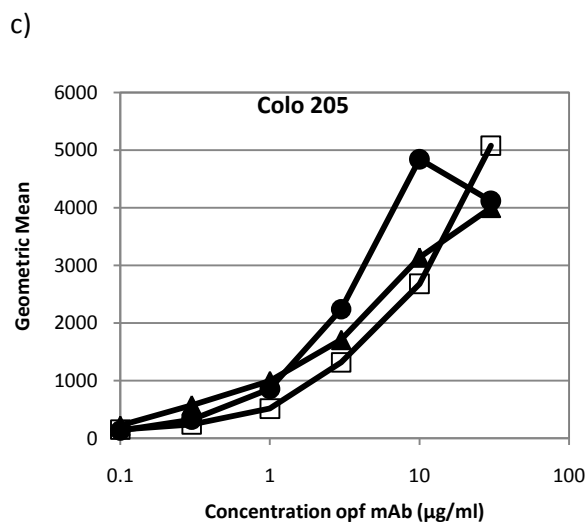
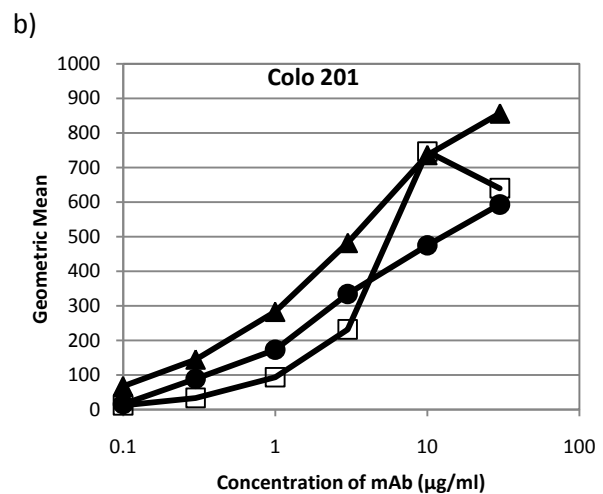
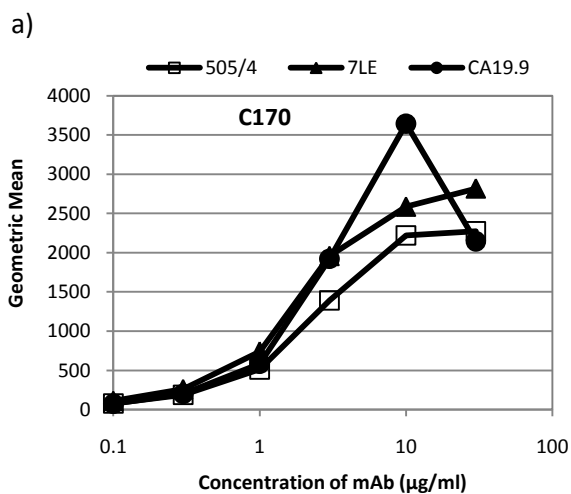
Glycan No.	Glycan	Name	Percentage of best binder (%)	Structure
215	Neu5Aca2-3Galb1-3[6OSO3]GlcNAC-Sp8	Sialylated, sulfo Type-1 precursor	100	
325	Neu5Aca2-3Galb1-3(Fuca1-4)GlcNAcb1-3Galb1-3(Fuca1-4)GlcNAcb-Sp0	Sialyl Di-Lewis a	98	
255	Neu5Gca2-3Galb1-3GlcNAcb-Sp0	Sialylated Type-1 precursor	94	

c)

Glycan No.	IUPAC	Name	Percentage of best binder (%)	Structure
119	Galb1-3(Galb1-4GlcNAcb1-6)GalNAca-Sp8	Type-2 precursor containing glycan	100	
274	Galb1-3(Neu5Aca2-3Galb1-4GlcNAcb1-6)GalNAca-Sp14	Sialylated Type-2 precursor containing glycan	93	
118	Galb1-3(Fuca1-4)GlcNAcb-Sp8	Lewis a	87	
279	Galb1-4(Fuca1-3)GlcNAcb1-3Galb1-3(Fuca1-4)GlcNAcb-Sp0	Lewis x-a	82	
124	Galb1-3GalNAca-Sp8	Galactose disaccharide	81	
132	Galb1-3GlcNAcb-Sp0	Type-1 precursor	79	
131	Galb1-3GlcNAcb1-3Galb1-4Glc-Sp10	Type-1 precursor containing glycan	78	
117	Galb1-3(Fuca1-4)GlcNAc-Sp8	Lewis a	65	
115	Galb1-3(Fuca1-4)GlcNAcb1-3Galb1-4GlcNAcb-Sp0	Extended Lewis a	44	
116	Galb1-3(Fuca1-4)GlcNAcb-Sp0	Lewis a	40	
61	Fuca1-2Galb1-3GlcNAcb1-3Galb1-4Glc-Sp10	Extended Type I H antigen	26	
62	Fuca1-2Galb1-3GlcNAcb1-3Galb1-4Glc-Sp8	Extended Type I H antigen	24	
311	Mana1-2Mana1-2Mana1-3(Mana1-2Mana1-6(Mana1-2Mana1-3)Mana1-6)Mana-Sp9	Mannose-rich glycan	17	

## 5.2.4 Analysis of 505/4, CA19.9 and 7LE colorectal cell line binding

In order to establish whether subtle differences in antigen specificity related to *in vitro* distribution, the mAbs were compared for binding to a panel of colorectal cancer cell lines. The mAbs all showed similar levels of binding to C170 (Fig 5.6a), Colo 201 (b) and Colo 205 (c). However only CA19.9 bound to SW480, HT29 and MKN45 cell lines, suggesting binding of sialyl Type I precursor by CA19.9 and not sialyl di-Lewis a.



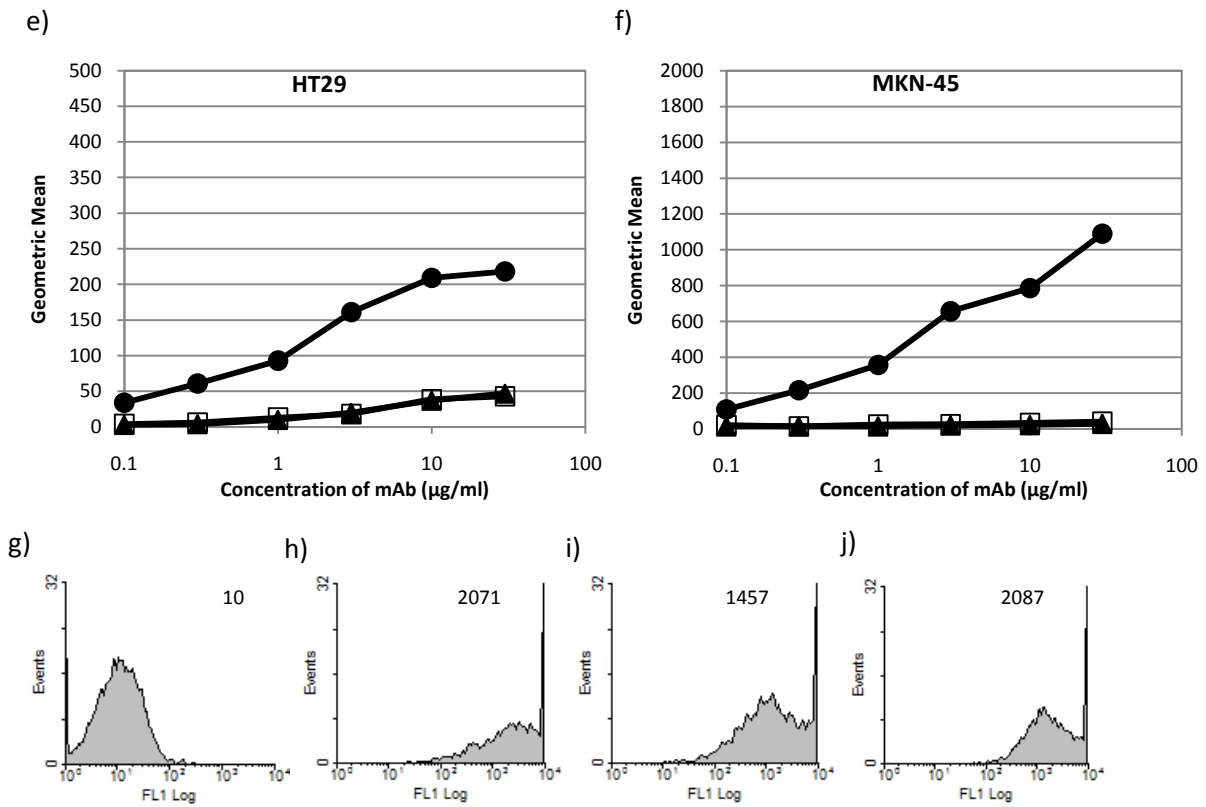


**Figure 5.6** 505/4, 7LE and CA19.9 bind to a range of colorectal cell lines. C170 (a) Colo 201 (b) Colo 205 (c), SW480 (d), HT29 (e) and MKN-45 (f) cells were incubated with 0.1-30 $\mu\text{g/ml}$  505/4, 7LE or CA19.9 and probed for binding with FITC-labelled rabbit anti-mouse IgG. Cells were then analysed for binding using flow cytometry. Examples of 10 $\mu\text{g/ml}$  irrelevant IgG (g), 505/4 (h), 7LE (i) and CA19.9 (j) binding histograms to C170 cells. Data is representative of at least 3 separate experiments.

### 5.2.5 Direct killing ability of 505/4, 7LE and CA19.9 mAbs

Several anti-glycan mAbs have the ability to induce direct cell killing, including the anti-Lewis y and Lewis b mAbs discussed previously in this thesis. Therefore, all three mAbs were assessed for their ability to kill cells without immune effector cells or complement. Figure 5.7 shows that all three mAbs have the ability to cause PI uptake in colorectal cancer cells. All three mAbs bind equally to C170 and Colo 201 cells (data not shown) but 505/4 and CA19.9 mAbs kill more effectively. In contrast, SW480 cells which bind very weakly to CA19.9 and not to 505/4 or 7LE are not killed. Of interest is Colo 205 which is a metastatic tumour derived from the same patient as Colo 201. This line is bound and killed by 505/4 and CA19.9 but is not directly killed by 7LE. To confirm that PI uptake equates to cell death, C170 cells were incubated with 505/4 for 5 days and the number of cells on days 0, 1, 3 and 5 were measured. Figure 5.8a showed that the uptake of PI does indeed reflect cell death, as the cell numbers significantly decreased from day 0 to day 1 when compared to a control well ( $p=0.038$ ). However, the remaining viable cells then grew out at the same rate as untreated cells. When these cells were reanalysed for 505/4 binding they expressed similar levels of antigen to untreated cells (Fig 5.8b) and were equally susceptible to killing (Fig 5.8c). This suggested that the cells that were killed by 505/4 in the initial exposure had a lower level of antigen, possibly due to alteration of antigen expression throughout the cell cycle, as when they regrew they were susceptible to killing.



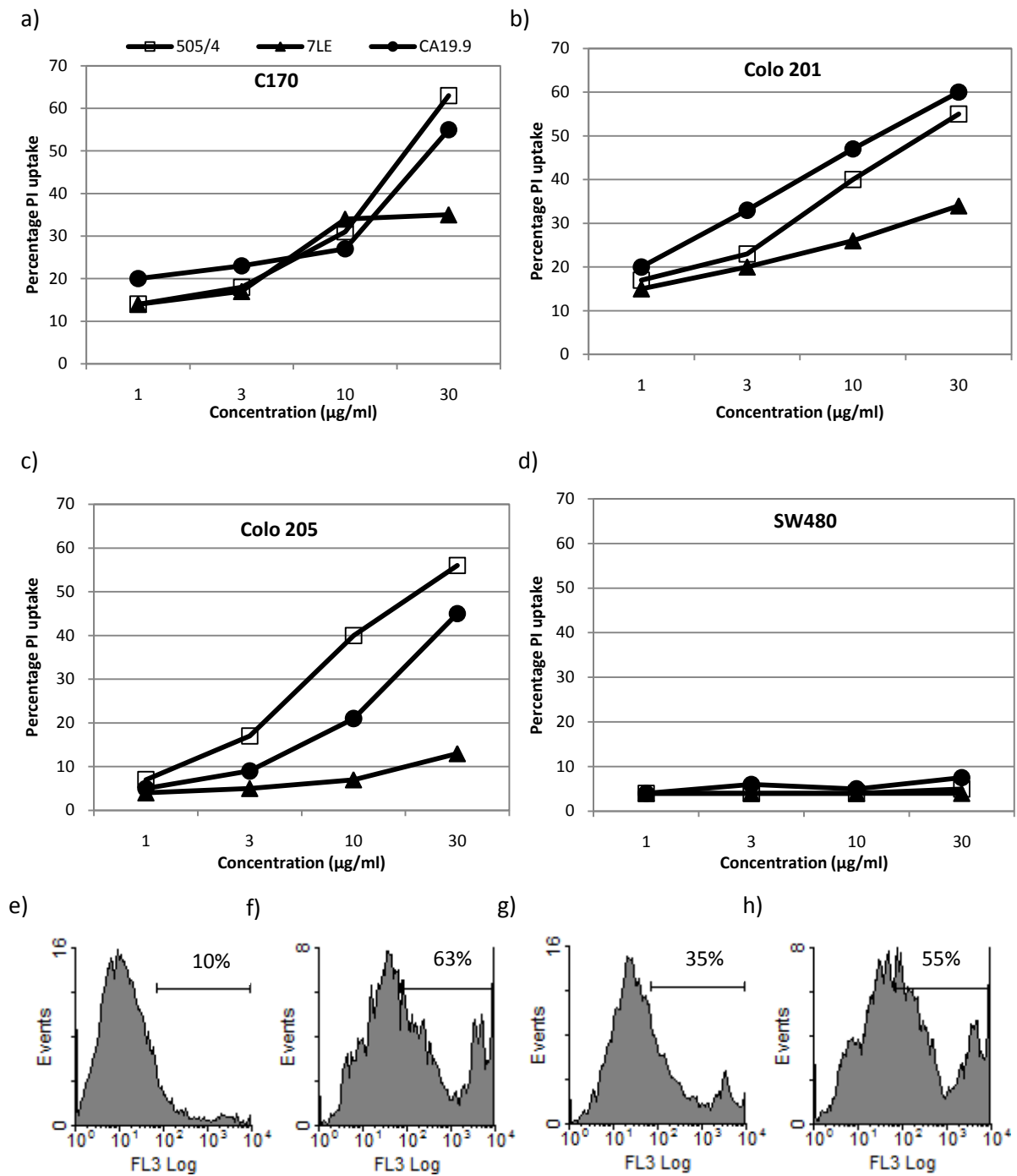


**Figure 5.7** The three anti-Lewis a mAbs tested induce direct cell death in a range of cell. C170 (a), Colo 201 (b), Colo 205 (c) and SW480 (d) cells were incubated overnight at 22°C with 505/4, 7LE and CA19.9 or isotype control before analysing PI uptake by flow cytometry. Histograms showing uptake of PI after isotype control (e), 505/4 (f), 7LE (g) or CA19.9 (h) incubation. All data are representative of at least 3 experiments.

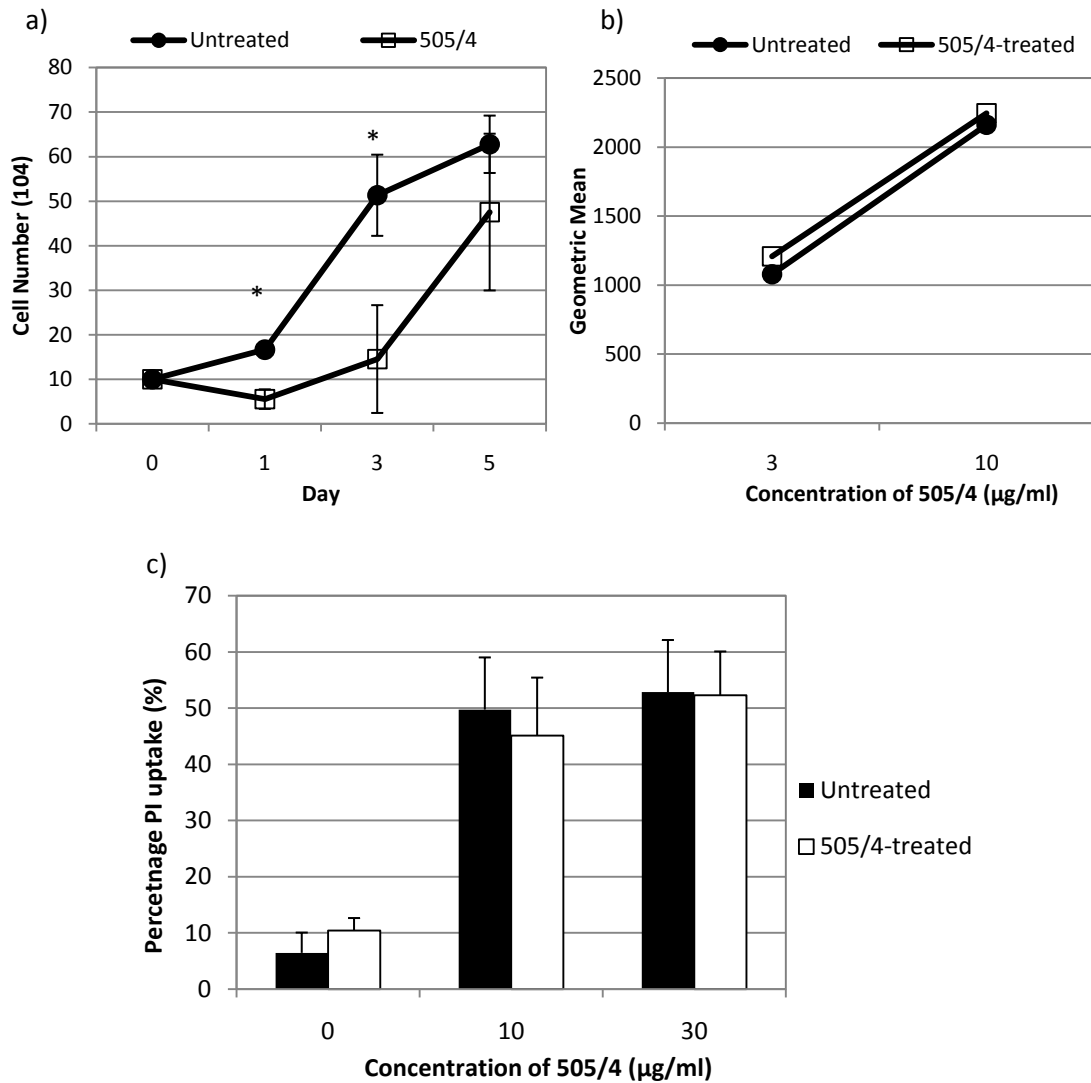


**Figure 5.8 505/4 induces cell death of C170 cells over 5 days and the resulting cells express the same level of antigen as untreated cells which can then subsequently killed by 505/4.** Cells were incubated with 30µg/ml 505/4 and incubated at 37°C for 5 days. Cell numbers were assessed on days 0, 1, 3 and 5 using a trypan blue assay.  $p=0.038$  (a). Binding of 505/4 to 505/4-treated and untreated cells was compared by screening cells with 3 and 10µg/ml 505/4 and binding probed with rabbit anti-mouse IgG-FITC (b). 505/4-treated and untreated cells were incubated overnight with a fresh dose of 10, 30µg/ml 505/4. PI was then added to cells before analysing by flow cytometry (c). Data is the average of 3 separate experiments.

## 5.2.6 Mechanism of killing of colorectal cancer cells by 505/4, 7LE and CA19.9mAbs

The number of anti-glycan mAbs inducing direct cell death in target cells independently of apoptosis prompted investigation of the mechanism of Lewis a/sialyl Lewis a-mediated cell death. PI uptake was therefore measured over a time course between 0 and 26 hours of incubation with 505/4. Figure 5.9 shows that maximum PI uptake was observed in C170 cells after only 2 hours. Furthermore, when C170 cells were incubated with 505/4, 7LE and CA19.9, PI uptake was observed at both 22 and 4°C (Fig 5.10) suggesting that the mechanism of cell death was unlikely to be apoptosis. Jurkat cells treated with anti-Fas induced apoptosis at 37°C which was inhibited 90% using a pan caspase inhibitor, z-FMK-vad, whereas, the addition of the pan caspase inhibitor did not inhibit PI uptake mediated by 505/4, CA19.9, CA19.9 or 7LE (Fig 5.11). As other glycan antibodies can kill via oncosis, uptake of different size dextran beads was also investigated. Anti-Fas mediate killing of Jurkat cells showed a graded effect on dextran bead uptake, favouring the smaller 3k MW beads. Conversely, 505/4, CA19.9 and 7LE mediated the uptake of 500k MW beads (Fig 5.12).

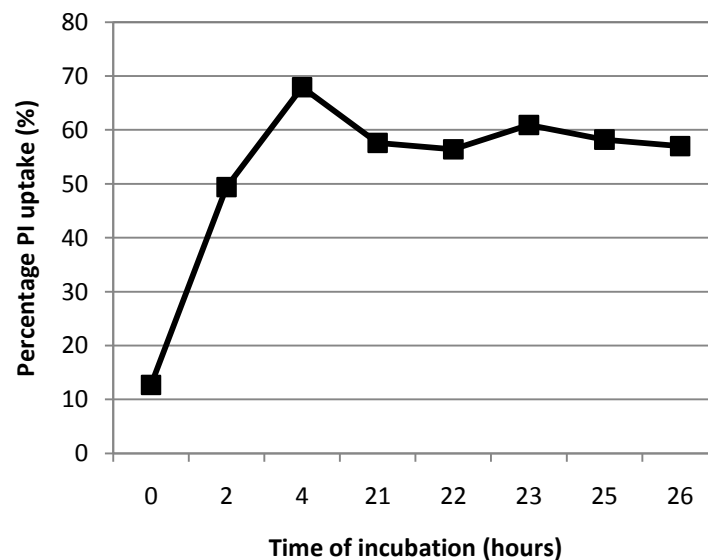


**Figure 5.9 505/4 induces PI uptake in C170 cells within 2 hours.** C170 cells were incubated with 30µg/ml 505/4 between 0 and 26 hours, propidium iodide was added and uptake measured after 30min using flow cytometry. Data is representative of at least 3 separate experiments.

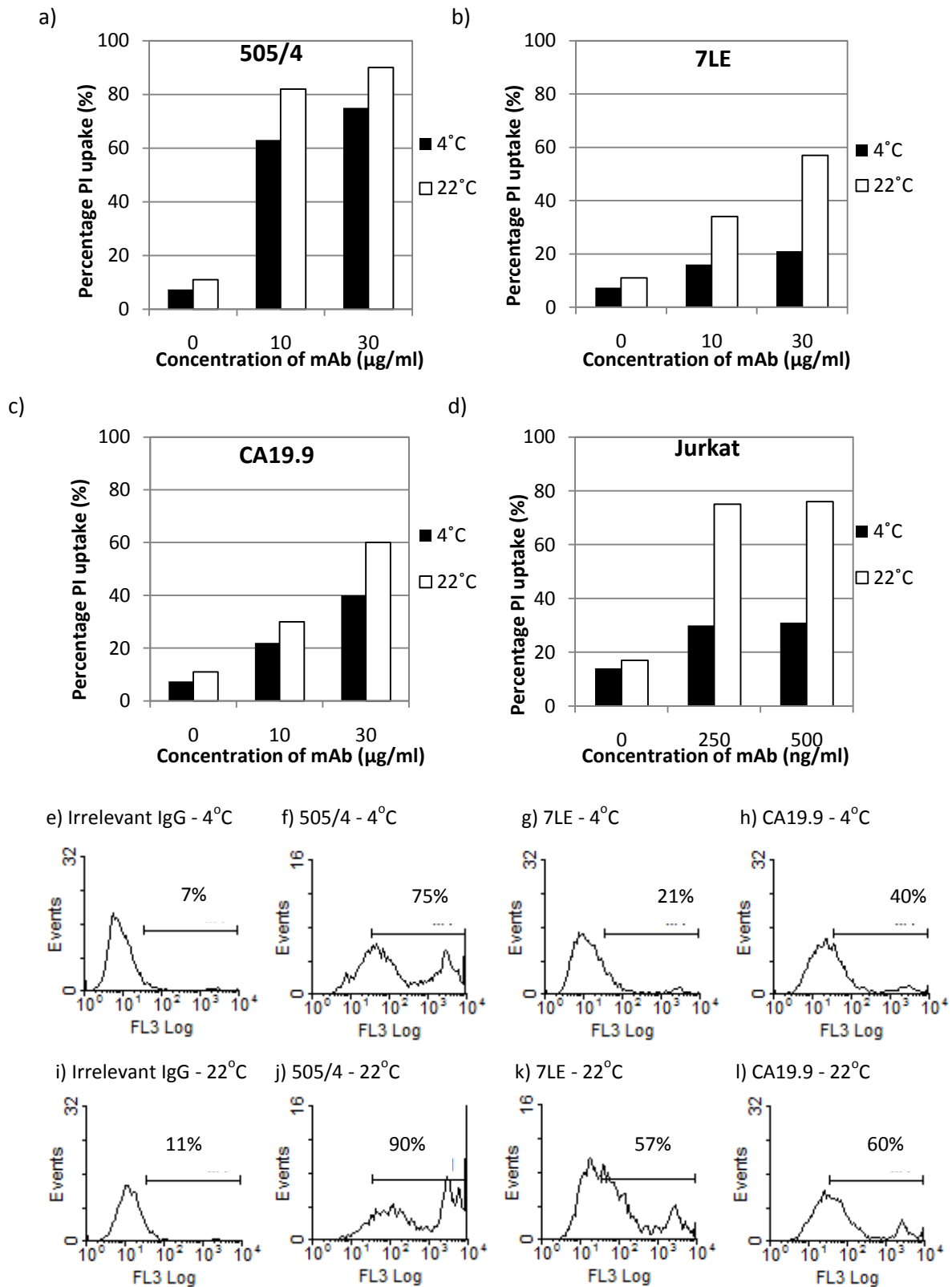


**Figure 5.10** 505/4, 7LE and CA19.9 kill C170 cells at both 4 and 22°C.  $5 \times 10^4$  C170 cells were incubated with 10 and 30 μg/ml of 505/4 (a), 7LE (b) or CA19.9 (c) overnight at 4°C or 22°C or  $5 \times 10^4$  Jurkat cells were incubated with 0, 250 and 500 ng/ml anti-Fas mAb overnight at 4°C or 22°C (d). PI was added before analysing the percentage of dead cells using flow cytometry. Irrelevant-IgG was used as a negative control. Histograms representing C170 cells incubated overnight at either 4°C (e, f, g, h) or 22°C (i, j, k, l) with 30 μg/ml of irrelevant IgG (e, i) 505/4 (f, j), 7LE (g, k) or CA19.9 (h, l). Data is representative of at least 3 separate experiments.

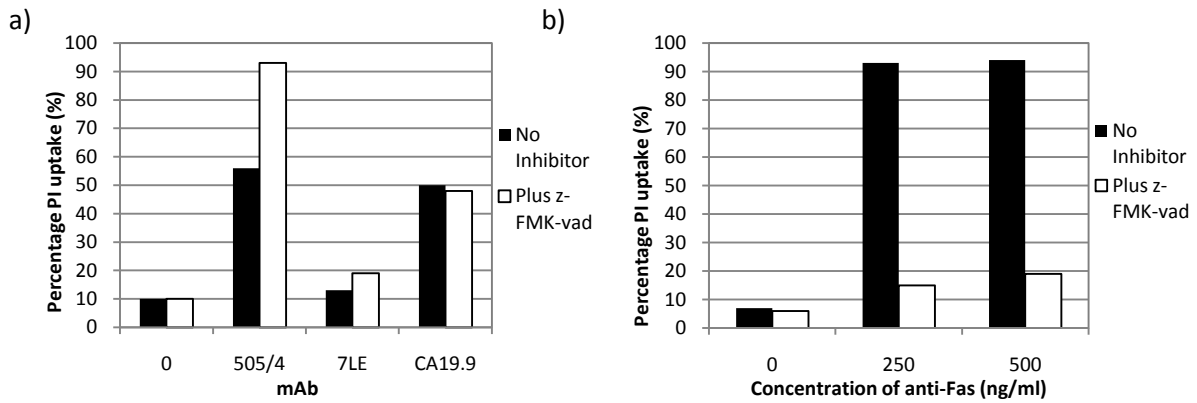


**Figure 5.11 505/4, 7LE and CA19.9 killing of C170 cells is not inhibited by pan caspase inhibitor.** C170 cells were incubated with z-FMK-vad and 10 or 30 $\mu$ g/ml mAb for 24hrs in the presence or absence of 20 $\mu$ M z-FMK-vad pan-caspase inhibitor (a). Jurkat cells were incubated with 250 or 500ng/ml anti-Fas mAb for 24hrs in the presence or absence of 20 $\mu$ M z-FMK-vad pan-caspase inhibitor (b). Data is representative of at least 3 separate experiments.

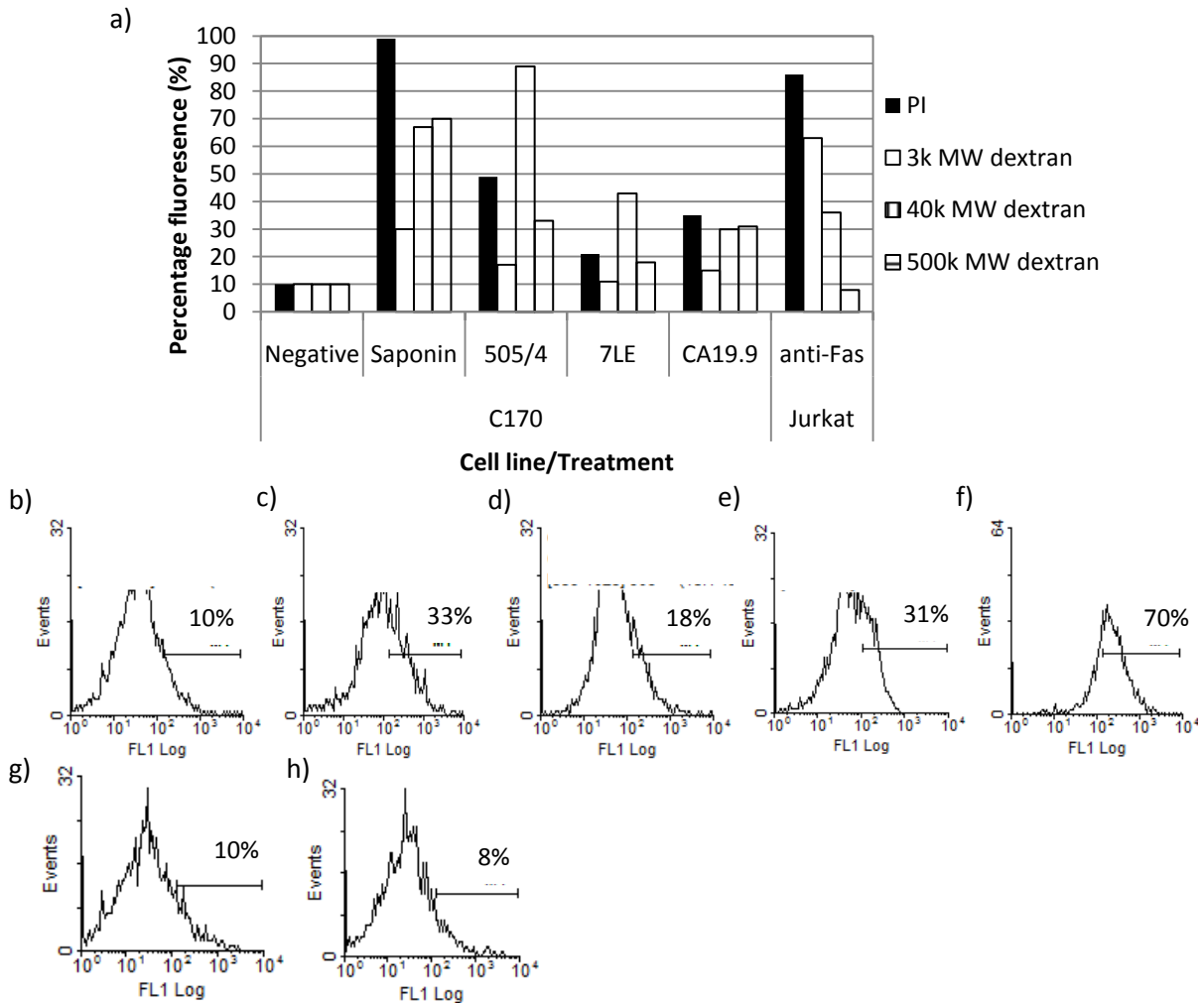


**Figure 5.12 505/4, CA19.9 and 7LE mediate uptake of 500K MW dextran beads in C170 cells.** C170 cells were incubated with 30 $\mu$ g/ml mAb and 3, 40 and 500K MW dextran-FITC beads or PI overnight before measuring uptake using flow cytometry. 30min treatment with 0.4% saponin was used as a positive control. Jurkat cells were treated with 500ng/ml anti-Fas mAb overnight as an apoptosis control. Histograms depicting 500k MW dextran-FITC uptake in C170 cells after incubation with irrelevant IgG (b), 505/4 (c), 7LE (d), CA19.9 (e) and 0.4% saponin (f) or uptake in Jurkat cells after incubation with irrelevant IgG (g) or anti-Fas (h).

### 5.3 Discussion

The ability of anti-Lewis y and Lewis b mAbs to bind to unique epitopes on shared antigens, resulting in a different *in vivo* distribution and *in vitro* function as well as their ability to cause direct cell death of antigen positive cells prompted the investigation into the therapeutic value and specific antigen of 505/4; a mAb produced by our group and compare it's *in vitro* activity to other mAbs directed at similar antigens. Characterisation of cancer cell line binding showed specific binding to colorectal cancer cell lines. Therefore, 505/4 was screened on an array of 462 colorectal tumours by immunohistochemistry, with binding seen against 80% of tumours. To assess the possibility of 505/4 binding to normal tissues *in vivo*, the mAb was screened on 29 normal tissues by immunohistochemistry. This revealed minimal binding of 505/4 to normal tissues, with only strong staining seen against colon, with moderate staining observed against liver. This could be pose a problem for *in vivo* distribution. Therefore, 505/4 was tested for binding to fresh, normal hepatocytes, with no cell surface binding seen. This implies that the staining seen against normal liver sections by immunohistochemistry may not represent binding seen *in vivo*. While characterising 505/4, it was shown that it bound to both glycolipid and glycoprotein purified from cells that expressed the antigen, suggesting that it recognised a carbohydrate epitope. Further support for this hypothesis was provided by loss of binding of 505/4 when screened on sodium periodate-treated cells. Sodium periodate destroys cell surface carbohydrate moieties by oxidation, without altering protein and lipid structure (Stevenson et al., 2004). To determine the specific antigen, 505/4 was screened against a panel of 406 synthetic and natural glycans provided by the Consortium for Functional Glycomics. This revealed that 505/4 binds to sialyl di-Lewis a and its variants, including sialyl Lewis a and dimeric Lewis a, which has been shown to be a tumour-associated epitope (Stroud et al., 1991). 505/4 also bound to sialyl Lewis a where the sialic acid was non-human derived (NeuGc). This sialic acid has been studied as a possible target for therapy (Fernandez et al., 2010; Fuentes et al., 2010; Hernandez et al., 2011) due to its absence from normal human tissue as humans are genetically unable to produce it and has been shown to be expressed in tumours (Chou

et al., 1998; Devine et al., 1991; Oliva et al., 2006). It is thought that some cancers have a greater ability to incorporate the NeuGc from the diet into glycans through a scavenger pathway (Bardor et al., 2005; Gabri et al., 2009). A possible advantage and explanation of tumour cells expressing NeuGc may be due to immunosuppression, with the ability of NeuGc to downregulate CD4 on T cells in the tumour environment being observed in murine and human T cells (de Leon et al., 2006).

The overexpression of sialyl Lewis a on a variety of digestive tract cancers, coupled with its low normal tissue expression, the suitability of 505/4 as an anti-cancer agent was assessed *in vitro*. Furthermore, due to the effect that antigen specificity had on the *in vitro* effects of anti-Lewis y and Lewis b mAbs, an anti-sialyl Lewis a mAb (CA19.9) and an anti-Lewis a mAb (7LE) were assessed alongside 505/4. Before studying these mAbs their glycan specificity was confirmed using the Consortium for Functional Glycomics glycan array. Array binding data for 7LE was obtained from the Consortium database and CA19.9 was screened. The array showed that the CA19.9 mAb used in this study bound to sialyl di-Lewis a, but also bound to the sialylated type 1 precursor with both human and non-human derived sialic acids, but not to dimeric Lewis a. The data also showed that 7LE bound to Lewis a, as described as well as to the type 1 precursor and Lewis a-x. The difference in fine specificity is reflected in cell binding with only CA19.9 binding to SW480, HT29 and MKN45, suggesting they express sialylated Type 1 precursor but not sialyl di Lewis a or Lewis a.

Due to the large proportion of anti-glycan mAbs displaying anti-tumour activity in the absence of complement or effector cells, 505/4, 7LE and CA19.9 were assessed for their ability to kill colorectal cells *in vitro* without the need for complement or effector cells. Interestingly, all three mAbs elicited direct cell death of colorectal cancer cell lines but 505/4 and CA19.9 mAbs kill more effectively suggesting that they are more potent or that sialyl di-Lewis a and Lewis a containing lipids/proteins can mediate cell killing but that the latter are more efficient. In contrast, SW480 cells which bind very weakly to CA19.9 and not to 505/4 or 7LE are not killed suggesting that sialylated Type 1 precursor glycolipids/proteins do not kill or that the level of binding is too weak for direct killing. Of

interest is Colo 205 which is a metastatic tumour derived from the same patient as Colo 201. This line binds and is killed by 505/4 and CA19.9 but is not directly killed by 7LE. As binding of 7LE is inhibited by sialylation of the Lewis a glycan, this suggests that the metastatic cell line has a greater level of sialylation and is more susceptible to killing by mAbs that recognise this modification. In order to clarify uptake of PI as cell death, 505/4 was incubated with C170 cells over 5 days, with the number and viability of cells observed throughout. A decrease in cell number and viability was observed, followed by an increase over the 5 days. The surviving cells were also susceptible to 505/4 treatment. The survival of some cells could be due to the uptake of mAb after binding, therefore, surviving cells may grow in the absence of mAb and be susceptible to another dose of mAb. This would be useful *in vivo* as treatment with 505/4 may not produce a subset of mAb-resistant cells that could avoid further mAb treatment.

Both 505/4 and CA19.9 mAbs may cause cell death in colorectal cancer cells independently of apoptosis. All three mAbs were shown to induce direct cell death at temperatures as low as 4°C, although the level of 7LE-mediated killing is reduced at 4°C, compared with 22°C, suggesting that 7LE may kill via apoptosis. Further to this, 7LE-mediated killing was inhibited by the pan-caspase inhibitor z-FMK-vad, whereas, killing with 505/4 and 7LE was not inhibited. The ability of 505/4 and CA19.9 to induce uptake of 500k MW dextran beads suggests that the mAbs induced large pore formation on the cell surface of the target cells. Treatment of Jurkat cells with anti-Fas activating mAb, which kills cells by apoptosis, was unable to induce uptake of the largest beads. 7LE-mediated uptake of 500k MW beads was minimal, further suggesting that 7LE mediates cell death in a mechanism distinct from that of 505/4 and CA19.9. A lower level of 3k MW bead uptake compared to PI was observed, which is a smaller molecule (668 MW) in 505/4 and CA19.9-treated cells and may be due to the ability of the 3K MW beads to move in and out of the treated cells more freely, as once PI enters a cell it collates to the DNA, therefore is inhibited from exiting the cell. Large pore formation is indicative of oncosis, an apoptosis-independent cell death mechanism. Oncosis has been shown to be induced by other mAbs, including mAb 84, which also demonstrated the uptake of



large molecular weight dextran beads (Tan et al., 2009). The ability to induce apoptosis-independent cell death may be therapeutically beneficial in tumours resistant to apoptosis. Furthermore, oncosis leads to the release of inflammatory intracellular components, providing tumour antigens. For example, the release of the danger molecule pattern (DAMP) proteins, heat shock protein 70 (Hsp70) and high mobility group box 1 (HMGB1) in the UVC treated renal cell carcinoma cell line K1 results in Hsp70 chaperoning antigenic peptides to iDC and the maturation of DCs by both HMGB1 and Hsp70 and presentation of tumour associated antigens (Brusa et al., 2008). Oncosis-mediated necrosis can also result in the release of mitochondrial antigens, such as mitochondrial DNA rich in cytosine-phosphate-guanosine sites dinucleotides that can be recognised by TLR9 in specific immune cells (Zhang et al., 2010b). As well as the release of intracellular tumour antigens, cells dying by necrosis, but not apoptosis, also secrete IL-6, resulting in the attraction of other immune cells to the tumour microenvironment, such as neutrophils and macrophages, that could enhance the anti-tumour response (Vanden Berghe et al., 2006). An example of this is the recognition that chemotherapy induced cell death can elicit an immune response against dying tumour cells and that the immune response is required for the optimal therapeutic effect of the chemotherapy (van der Most et al., 2008). However, as discussed in a previous chapter, the development of a pro-inflammatory tumour microenvironment may lead to the polarisation of immune cells towards a tissue repair and remodelling state, therefore benefiting the tumour (Sica et al., 2008; Tesniere et al., 2008; Vakkila & Lotze, 2004).

Recently, a human anti-sialyl Lewis a mAb was produced using PBMCs isolated from a breast cancer patient undergoing sialyl Lewis a-keyhole limpet hemocyanin (KLH) treatment (Sawada et al., 2011). This mAb has shown specific binding to sialyl Lewis a alone and promisingly induces ADCC and CDC of antigen positive cell lines as well as anti-tumour activity in a xenograft model.

In conclusion, the murine mAb 505/4 has been shown to bind to sialyl Lewis a / di-sialyl Lewis a and comparison of 505/4 with other anti-Lewis a-related mAbs revealed distinct specificities between mAbs. Specifically the lack of 505/4 binding to Type 1 precursors suggests that it may have a better

distribution *in vivo*. 505/4 bound to a high proportion of colorectal cancer tumours, with limited binding to normal tissues when tested by IHC. Analysis of functionality revealed sialyl Lewis a /sialyl di Lewis a as a targets for mAb-mediated direct cell death, with 505/4 and CA19.9 having the ability to induce direct cell death via an oncosis-like mechanism. The lower level of direct cell death caused by 7LE suggests that sialylated versions of Lewis a may be better targets for therapy. The ability for anti-Lewis a mAbs to induce oncotic cell death may be an important therapeutic factor, which may increase the immune anti-tumour response due to the release of tumour antigens.

Interestingly, the investigation of anti-Lewis y/b and sialyl Lewis a-related mAbs has revealed that these mAbs have the ability to cause rapid cell death in antigen positive cell lines in a complement and effector cell independent manner. This is also true of other anti-glycan mAbs, suggesting that glycans are good targets for functional mAbs that may be more effective in an immunosuppressive tumour microenvironment.

## Chapter 6 The production of monoclonal antibodies targeted against ovarian cancer glycolipid

### 6.1 Background

Although, several promising glycolipid mAbs have been produced they are few in number compared to mAbs recognising protein antigens, yet the complexity of glycome exceeds the proteome. Therefore, it is our aim to develop a novel platform for the generation, selection and evaluation of anti-ovarian cancer glycolipid mAbs.

Glycolipids are T cell independent antigens (TI) as they cannot be presented to T cells on MHC-II, but are processed by B cells and presented on CD1d, an MHC-class 1-like molecule. Studies have shown that TI antigens multivalently cross-link, mlg, giving B cells a primary signal which results in proliferation (Mond et al., 1995; Tolar et al., 2009). However, Ig affinity maturation and production requires further signals including ligation of CD40 and production of cytokines, which can be provided by helper T cells (Ahonen et al., 2002; Kawabe et al., 1994). As glycolipids are TI antigens, presented on CD1d and not MHC-II, the T cell help can be provided by CD40 ligand on NK and NKT cells and not T cells (Blanca et al., 2001; Leadbetter et al., 2008). NK cells can activate resting B cells to produce Ig in a contact-dependent manner, through CD40-CD40L interaction (Blanca et al., 2001). Glycolipid presented on CD1d can stimulate NKT cells to produce IL-4 and IFN- $\gamma$ , causing Ig production in B cells (Huang et al., 2004). Despite the emergence of mAbs as potent anti-cancer drugs, no mAbs have been approved for the treatment of ovarian cancer and as described previously, treatment still centres on chemotherapy. For this reason, our aim was to develop a platform for the production of anti-ovarian cancer glycolipid mAbs using whole cells, purified glycolipid and NKT/NK adjuvants to immunise mice and screen for novel glycolipid antibodies.

## 6.2 Results

### 6.2.1 Glycolipid extracted from C170 cells binds both 692/29 and 505/4 mAbs

In order to establish whether immunisation protocols yielded anti-glycolipid antibodies, a method of screening mouse sera and hybridoma supernatant for anti-glycolipid Ig was needed.

To this end glycolipid was extracted using a ratio of 2:1 chloroform: methanol from the colorectal cell line C170. This was then centrifuged, resulting in the formation of three phases: a phase of sialylated glycolipids (layer 2), a plug of denatured glycoproteins (layer 1) and a final phase of neutral glycolipid lipids (layer 3) (Fig 6.1a). The mouse antibodies 505/4 and F002 have been shown to bind glycolipid and were used, along with the anti-CD55 (protein antigen) mAb 791T/36 to determine the constituents of each phase. Figure 6.1b shows that antigens in all three layers were amenable to detection by both anti-glycolipid mAbs, showing that all three layers adhere firmly to the plastic plates, but not by antibodies which recognise protein conformation (791T/36).

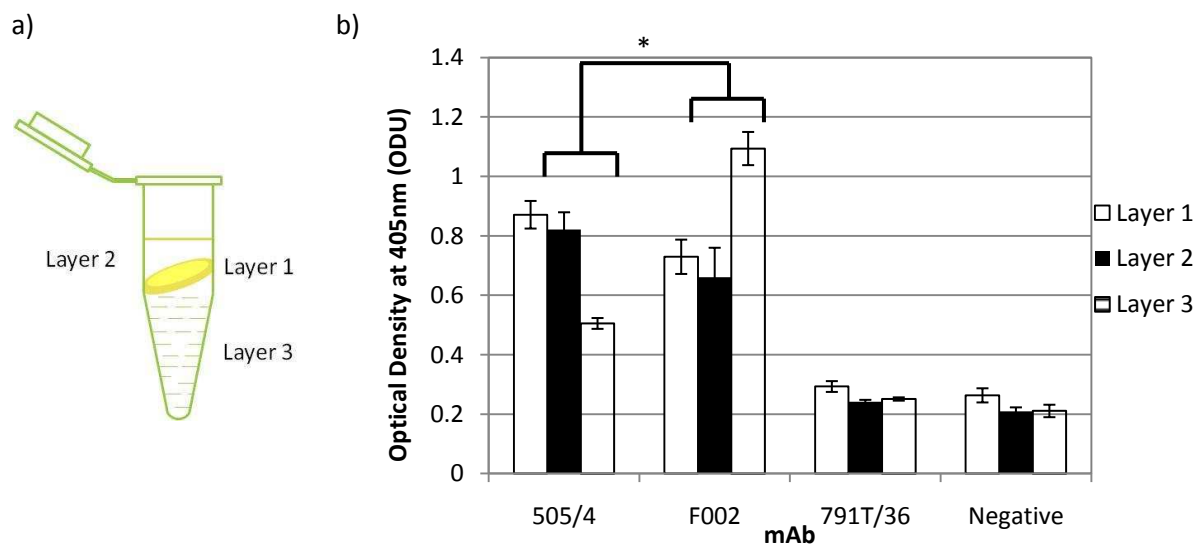
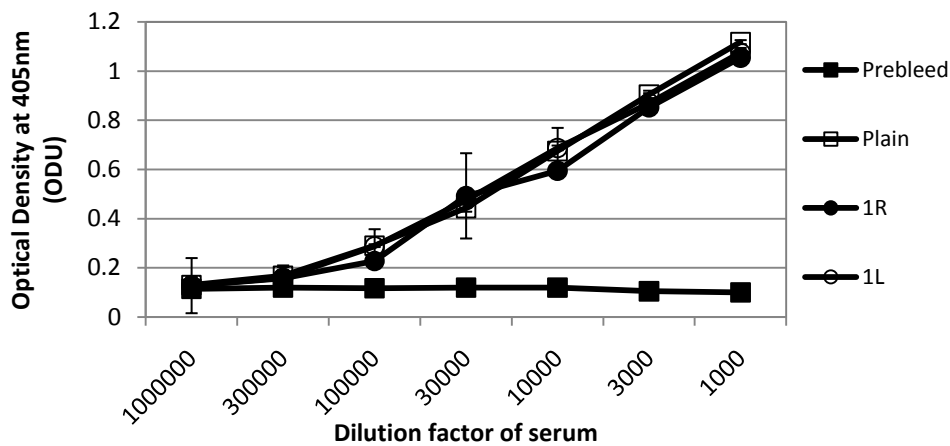


**Figure 6.1 Production and validation of glycolipid extract.** Glycolipid was extracted from C170 cells using 2:1 chloroform: methanol before mixing overnight and centrifugation that resulted in three layers (a). The layers were dried and resuspended in either PBS (layers 2 and 3) or DMSO (layer 1) before plating on a 96 well flexi-plate. Glycolipid was dried down before screening with the anti-glycolipid mAbs 505/4 and F002 and the anti-protein mAb 791T/26 (b). Error bars representing standard deviation of quadruplicate wells are present but may be obscured by data bars. Data is representative of at least 3 separate experiments. \* represents  $p < 0.05$ .

## 6.2.2 Immunisation of BALB/c mice with ovarian cancer cells

Immunisation with whole cancer cells has also been shown to produce antibodies against tumour antigens. In order to ascertain whether anti-ovarian glycolipid antibodies can be produced by this immunisation approach, BALB/c mice were immunised with three different ovarian cell lines. When sera from immunised mice were screened (Fig 6.2a and b) there was a strong response against the ovarian cancer cell line OVCA 433 (end point titre 1:100,000) but no response to OVAC 433 glycolipid, suggesting that the predominant response was not against glycolipid.

a)



b)

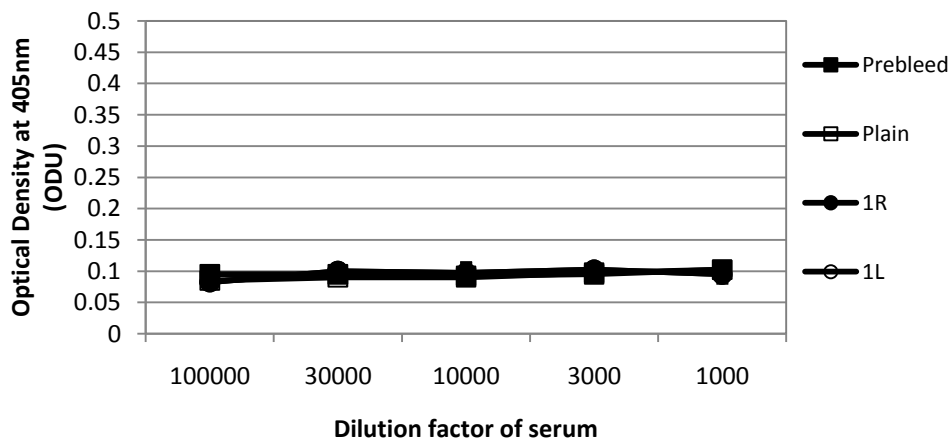


**Figure 6.2 Screening of cell-immunised mouse sera (3358340) to OVCA 433 cells (a) and OVCA-433 glycolipid extract (b) by ELISA** a) OVCA 433 cells were grown to confluency in a 96 well plate (a) or OVCA 433 glycolipid extract was dried onto a 96 flexi-plate (b). Plates were blocked before incubating with serial dilutions of mouse serum and probed with anti-mouse immunoglobulin-HRP before adding ABTS substrate. Error bars representing standard deviation are present, but may be obscured by marker.

### **6.2.2 Fusion (F012) of OVCA 433 immunised mouse splenocytes yields anti-ovarian cancer glycolipid hybridomas**

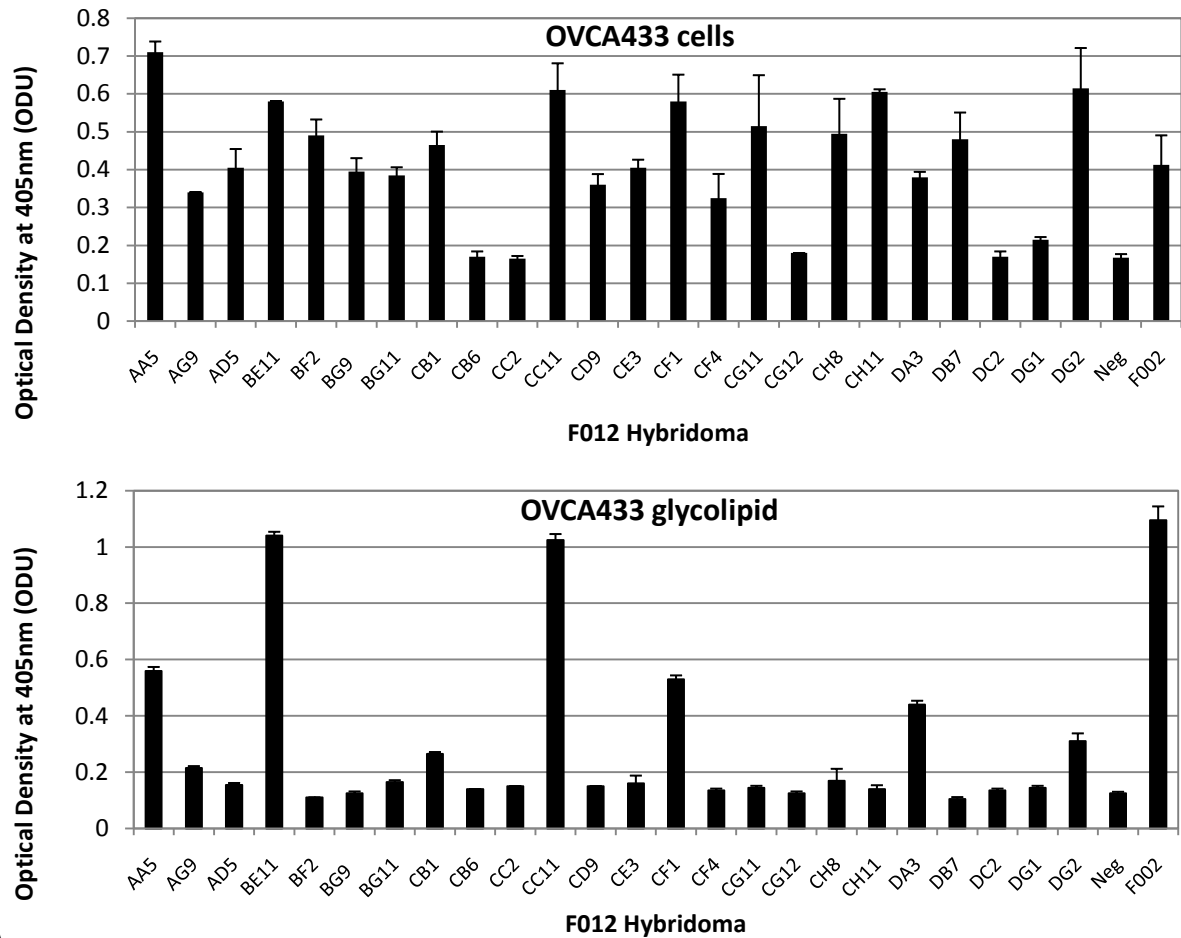
To confirm that there was not an anti-ovarian cancer glycolipid response; the splenocytes from a mouse that displayed a response to ovarian cancer cells were fused with NS0 cells to produce hybridomas.

Hybridoma supernatants were screened by ELISA for binding to ovarian cancer cells (OVCA 433; Fig 6.3a) and to OVCA 433 glycolipid extract (Fig 6.3b). Figure 6.3a shows that 20 hybridomas produce anti-OVCA 433 cell antibodies (OD >0.2), with 9 binding to OVCA 433 glycolipid extract (F012 – AA5, AG9, BE11, CB1, CC11, CE3, CF1, DA3, DG2; Fig 6.3b). This suggests that there was an anti-glycolipid response which was not detected by the glycolipid ELISA screen of mouse sera. This may have been related to the method of detection of anti-sera used in the two assays. Mouse sera were screened for IgG responses whereas the hybridomas were screened for all Ig isotypes.

MAbs binding to cells and glycolipid have potential therapeutic value. However, if they cross react with glycolipids expressed on the surface of normal blood cells they will be absorbed in the blood and never reach the tumour. Positive mAbs were therefore screened for binding to human PBMCs. Figure 6.3c shows that the supernatant from hybridomas AA5, CF1 and DG2 bound to PBMCs. W6/32, an anti-MHC mAb was used as a positive control.

After further analysis using an antibody isotype kit, the remaining 6 anti-glycolipid antibodies were found to be IgM antibodies (data not shown). These antibodies are less effective in a therapeutic setting as their size precludes their extravasation from the blood vessels and therefore the hybridomas were not cloned.

a)



b)

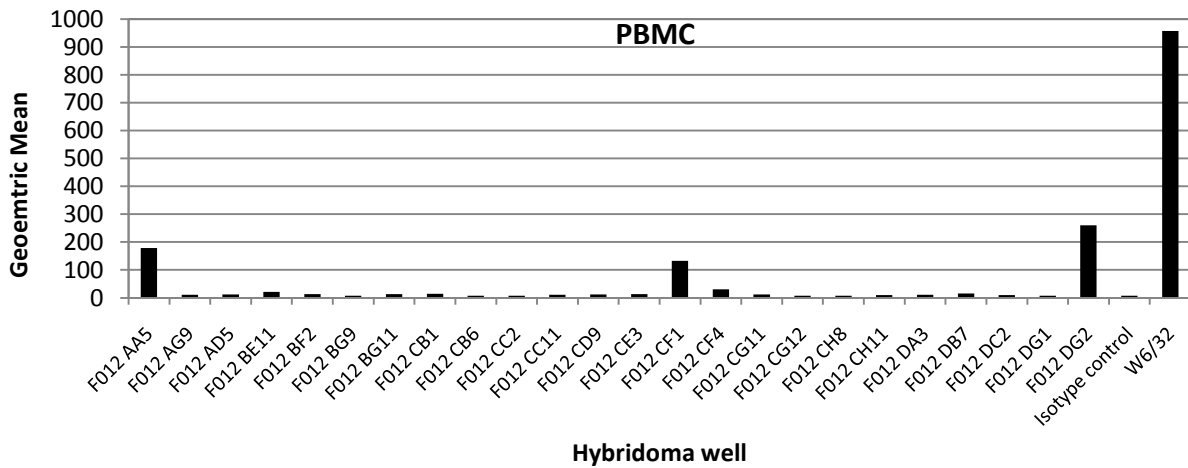


**Figure 6.3 Binding of F012 hybridoma supernatant to OVCA 433 cells (a) and glycolipid (b) and to peripheral blood mononuclear cells (PBMCs) (c).** a) OVCA 433 cells (a) were grown to confluency in a 96 well plate or OVCA 433 glycolipid (b) was extracted as described, then dried onto 96 well flexi-plates. Both plates were blocked before incubating with hybridoma supernatant and probed with anti-mouse Ig-HRP before adding ABTS substrate. The plate was then read at 405nm. Error bars representing standard deviation of quadruplicate wells are present, but may be obscured by data bar. c) PBMCs were isolated from whole blood and incubated with hybridoma supernatant, probed with anti-mouse Ig-FITC and binding analysed by flow cytometry. F002 was used as a positive control for ovarian cancer cell line whole cell and glycolipid binding (a) with W6/32 binding as a positive control for PBMC binding.

### 6.2.3 Immunisation with the mAb TIB 207 depletes mouse T cells *in vivo*

In order to reduce the antibody response to protein antigen in the whole cell immunisation and perhaps favour an anti-glycolipid response, BALB/c mice were depleted of CD4 helper cells with TIB 207 mAb prior to immunisation with cells. A blood sample was collected prior to the TIB 207 immunisations and 6 days subsequent to the last immunisation. Total PBMCs were purified from each blood sample and probed with anti-CD4-FITC (Fig 6.4a, b and c) or without mAb (Fig 6.4d, e, f). The level of CD4 positive cells was calculated by subtracting the percentage of CD4+ cells (red histograms) from the control (green histograms) and compared to the undepleted mouse. Figure 6.3g shows that both mice 1R and 1L had a lower level of CD4 positive cells than the untreated mouse, suggesting that the TIB 207 mAb had depleted CD4 cells.

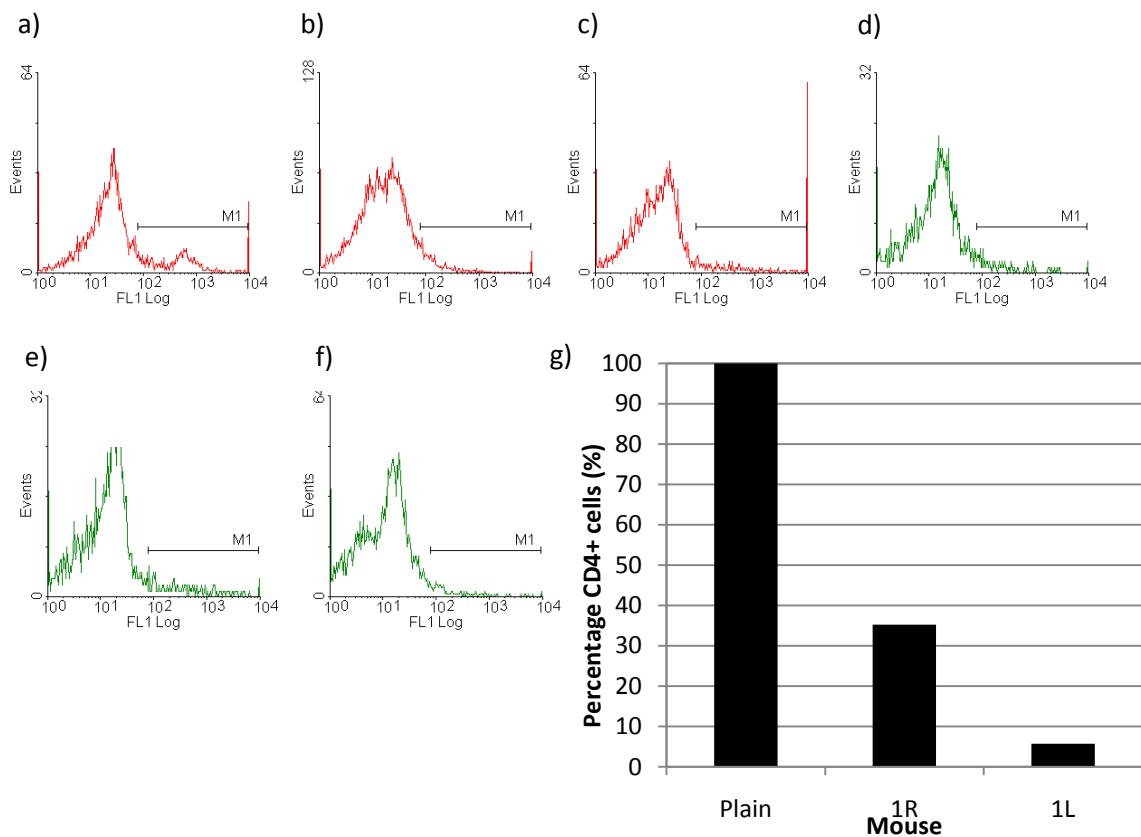


**Figure 6.4 TIB 207 mediated depletion of mouse CD4 cells.** Mice were immunised with 200 $\mu$ l of PBS (Plain; a, d) or 200 $\mu$ g TIB 207 mAb (1R and 1L; b, e, c, f) and bled on day 7. Histograms in red show level of CD4 positive cells (M1), with negative controls in green histograms. Levels of CD4 depletion compared to the non-immunised mouse are shown (g). Data representative of 2 independent experiments.



## 6.2.4 Depletion of CD4 cells is ineffective at increasing the anti-ovarian cancer glycolipid response

Following the depletion of CD4 cells, a group of mice were immunised with three different ovarian cancer cell lines. The sera was analysed for antibody response by titrating on OVCA 433 cells. Figure 6.5a suggests that the depletion of CD4+ cells had an effect on the anti-ovarian cancer cell response, with only mouse 1L showing an Ig response to OVCA 433 cells. The titre of this response (end point titre 1:30,000) was less than achieved with the ovarian cancer cell alone immunisation (Fig 6.3a). However, a reduction in the anti-cell response did not generate a greater anti-ovarian cancer glycolipid response with none of the three mice showing an Ig response when screened against OVCA 433 glycolipid extract (Fig 6.5b).

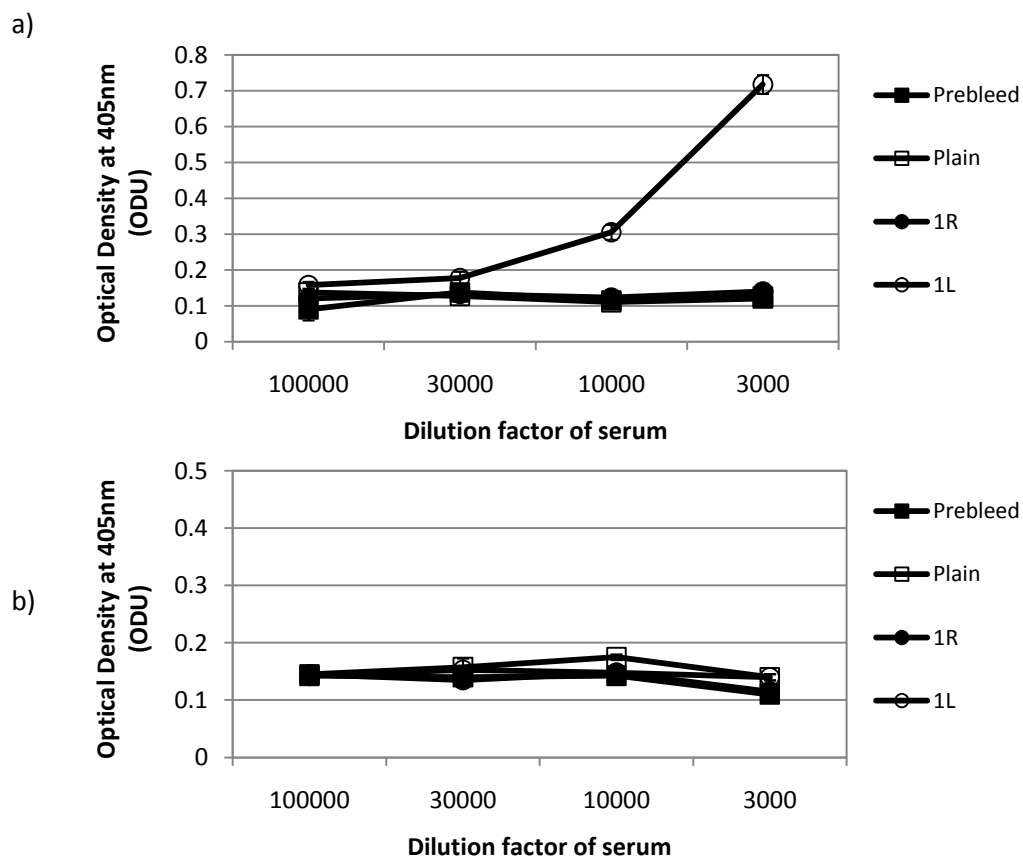


**Figure 6.5 Binding of TIB 207, OVCA 433 cell immunised mouse serum (3676379) against OVCA 433 cells and OVCA 433 glycolipid.** OVCA 433 cells were grown to confluency in a 96 well plate (a) or OVCA 433 glycolipid extract was dried onto a 96 flexi-plate (b). Plates were blocked before incubating with serial dilutions of mouse serum and probed with anti-mouse Ig-HRP before adding ABTS substrate. Error bars representing standard deviation of quadruplicate wells are present, but may be obscured by marker.

## 6.2.5 Fusion (F013) of TIB-207/OVCA 433 immunised mouse splenocytes yields anti-ovarian cancer cell but not anti-glycolipid hybridomas

Although, the serum did not give an IgG anti-glycolipid response (Fig 6.5b), the splenocytes were harvested from 1L and fused (fusion named F013) to further investigate the antibody response, yielding 15 hybridomas. Of these, 12 secreted antibodies that bound to at least one of the three immunised cell lines (Fig 6.6a). One of these bound to PBMCs (4D1; Fig 6.6a). Of the 15 hybridomas, none bound to ovarian cancer glycolipid (Fig 6.6b). The 3 most positive hybridomas were taken forward and cloned were (3H1, 3C9 and 2B8). This was based on their ability to bind a range of cell lines, a lack of binding to PBMCs. However, due to their inability to bind glycolipid, F013 2B8, 3C9 and 3H1 were not investigated further in this thesis.

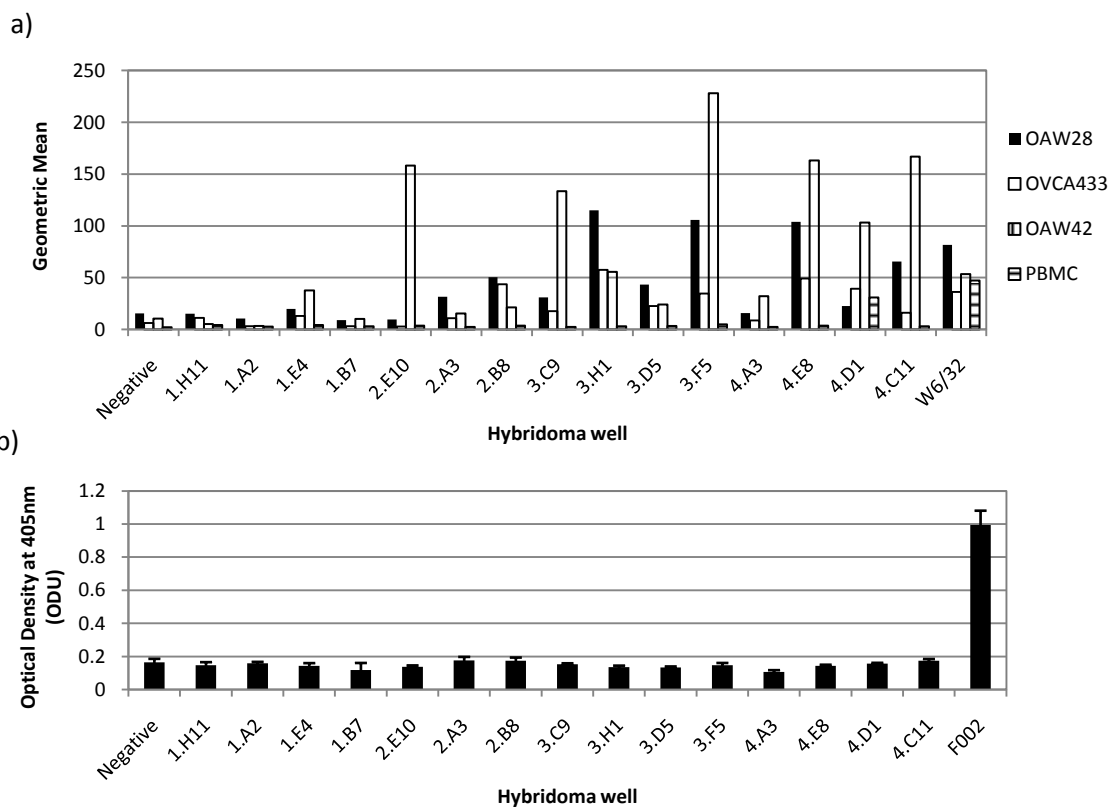


**Figure 6.6 Screening of F013 hybridoma supernatant for binding to OAW28, OVCA 433, OAW42 and PBMCs by indirect immunofluorescence and analysed by flow cytometry (a) and OAW42 glycolipid by ELISA (b).** a) Supernatant was taken from wells with colonies and incubated with OAW28, OVCA 433, OAW42 and PBMCs. Binding was probed for with anti-mouse IgG-FITC and analysed by flow cytometry (FL1). b) OAW42 glycolipid was dried onto 96 well flexi-plate, incubated with hybridoma supernatant. Binding was probed with anti-mouse IgG-HRP and ABTS substrate was added. The plate was then read at 405nm. Error bars representing standard deviation of quadruplicate wells are present, but may be obscured by data bars. W6/32 was used as a positive control against whole cells and F002 in the glycolipid screen.

### 6.2.7 Immunisation of BALB/c mice with an NK cell adjuvant

Screening of T cell depleted mice revealed a possible reduction in anti-cell response, but this did not in turn reveal a greater anti-ovarian cancer glycolipid response. Glycolipids are classed as type II TI antigens and it has been shown that in order to produce an *in vivo* antibody response to these antigens, non-T cell help is required by B cells. Poly(I:C) is a synthetic analogue of double-stranded RNA that mimics a viral infection and acts *in vivo* by activating NK cells via the toll-like receptor 3. Activation of NK cells has been shown to provide T cell independent help to B cells in the production of antibodies to TI antigens, such as glycolipid, through the activation of CD40.

The CD4 cells of BALB/c mice were depleted as previously described, before being immunised three times with the ovarian cancer cell lines OVCA 433, OAW28 and OAW42 along with an NK cell adjuvant, poly(I:C). Serum was purified from a blood sample taken six days subsequent to the last immunisation. Figure 6.7 shows that there is a slight IgG response by mouse 1R against OVCA 433 cells, but this was a low titre (1:3000).

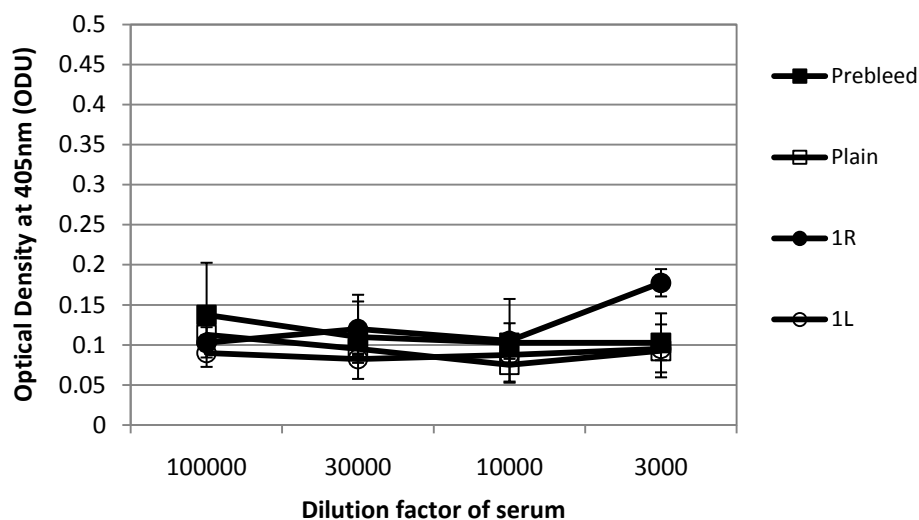


**Figure 6.7 Binding of OVCA 433 cell and poly(I:C) immunised mice serum (3673323) against OVCA 433 cells.** OVCA 433 cells were grown to confluency in a 96 well plate. Plates were blocked before incubating with serial dilutions of mouse serum and probed with anti-mouse Ig-HRP before adding ABTS substrate. F002 was used as a positive control (O.D. = 0.48). Error bars representing standard deviation of quadruplicate wells are present, but may be obscured by marker.

### 6.2.9 Immunisation of colorectal cancer glycolipid extract does not give an anti-glycolipid response

As there was no anti-glycolipid response to ovarian cancer cells immunisation despite T cell depletion and NK cell help, it was decided to try an immunise directly with glycolipids. As mAbs had previously been made recognising colorectal glycolipid extracted from C170 cells this was the initial choice of immunogen.

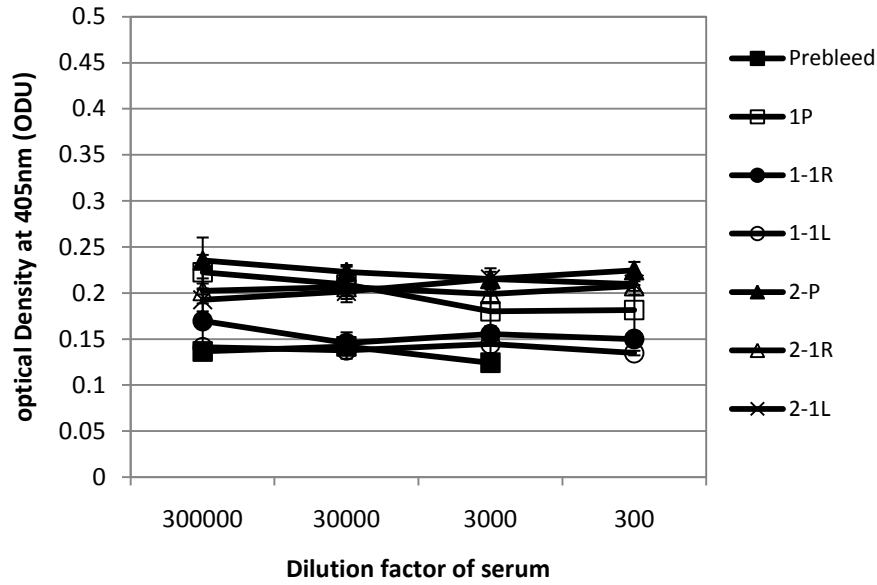
Using the validated glycolipid (Section 6.2.1), two groups of mice were immunised with C170 glycolipid layer 2. Group 1 received intraperitoneal injections of C170 layer 2 glycolipid alone on days 1 and 7 followed by a boost with  $1 \times 10^7$  C170 cells on day 14. Group 2 received subcutaneous injections of C170 glycolipid layer 2 with complete Freund's adjuvant on day 1, followed by C170 glycolipid layer 2 with incomplete Freund's adjuvant on day 7 and a boost of  $1 \times 10^7$  C170 cells and incomplete Freund's adjuvant on day 14 (Table 6.1).

Blood samples were taken and sera isolated before testing by ELISA against C170 glycolipid and C170 cells using a polyclonal rabbit anti-mouse Ig HRP. Figure 6.8 shows that immunisation of glycolipid did not result in either an anti-C170 cell (Fig 9a) or anti-C170 glycolipid response (Fig 6.8b).

**Table 6.1 Immunisation with C170 layer 2 glycolipid.**

Group	Day		
	1	7	14
1	C170 glycolipid layer 2-IP	C170 glycolipid layer 2-IP	C170 cells-IP
2	C170 glycolipid layer 2 & complete Freund's adjuvant-SC	C170 glycolipid layer 2 & incomplete Freund's adjuvant-SC	C170 cells & incomplete Freund's adjuvant-SC

a)



b)

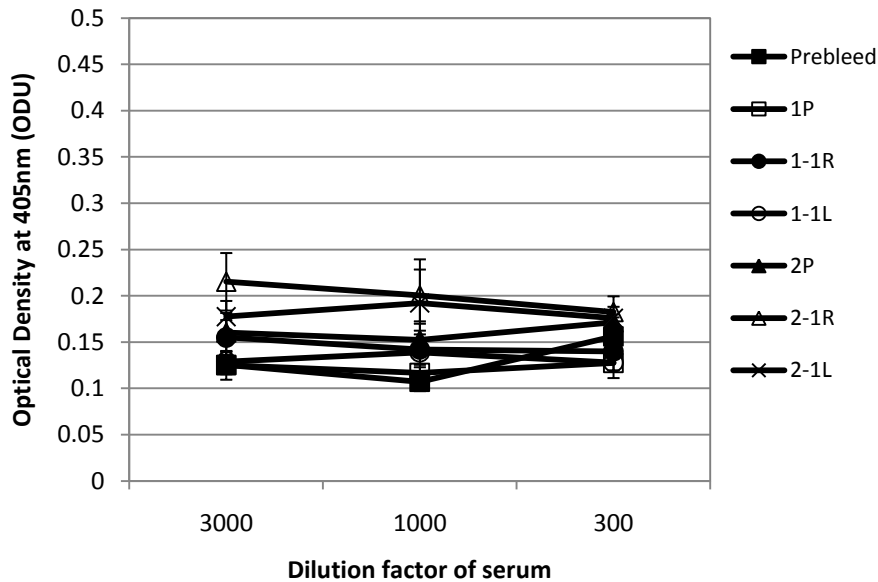


**Figure 6.8 Binding of C170 glycolipid immunised mouse serum (3582907) against C170 cells (a) and C170 glycolipid (b).** C170 cells were grown to confluency in a 96 well (a) or C170 glycolipid extract was dried onto a 96 flexi-plate (b). Plates were blocked before incubating with serial dilutions of mouse serum and probed with anti-mouse Ig-HRP before adding ABTS substrate. Error bars representing standard deviation of quadruplicate wells are present, but may be obscured by marker.

### **6.2.10 Ovarian cancer cell glycolipid immunisation**

In order to clarify whether the lack of Ig response to C170 glycolipid (Fig 6.8) was cell type specific ovarian cancer cell glycolipid extract was immunised. Figure 6.9a shows that F002 bound to ovarian cancer glycolipid layer 2, with the anti-colorectal glycolipid mAb 505/4 and the anti-protein mAb 791T/36 not binding. This allowed the use of ovarian cancer cell glycolipid as an immunogen, using F002 as a control in screening assays.

On day 0 prebleeds were taken from a group of three mice followed by an intraperitoneal injection of layer 2 glycolipid from the equivalent of  $1 \times 10^6$  OVCA 433 cells. On days 7, 14 and 21 mice received injections of OAW42, OVCAR-3 and OVCAR-4 derived glycolipid respectively. After a further 7 days mice were bled. Figure 6.9b shows that all three mice show a minimal response against OVCAR-3, OVCAR-4 and OAW42 cells. When sera (1/10) were screened against OVCA 433 glycolipid extract, binding was seen in all three mice (Fig 6.9c) but only at this high dilution, therefore the splenocytes from these mice were not fused.

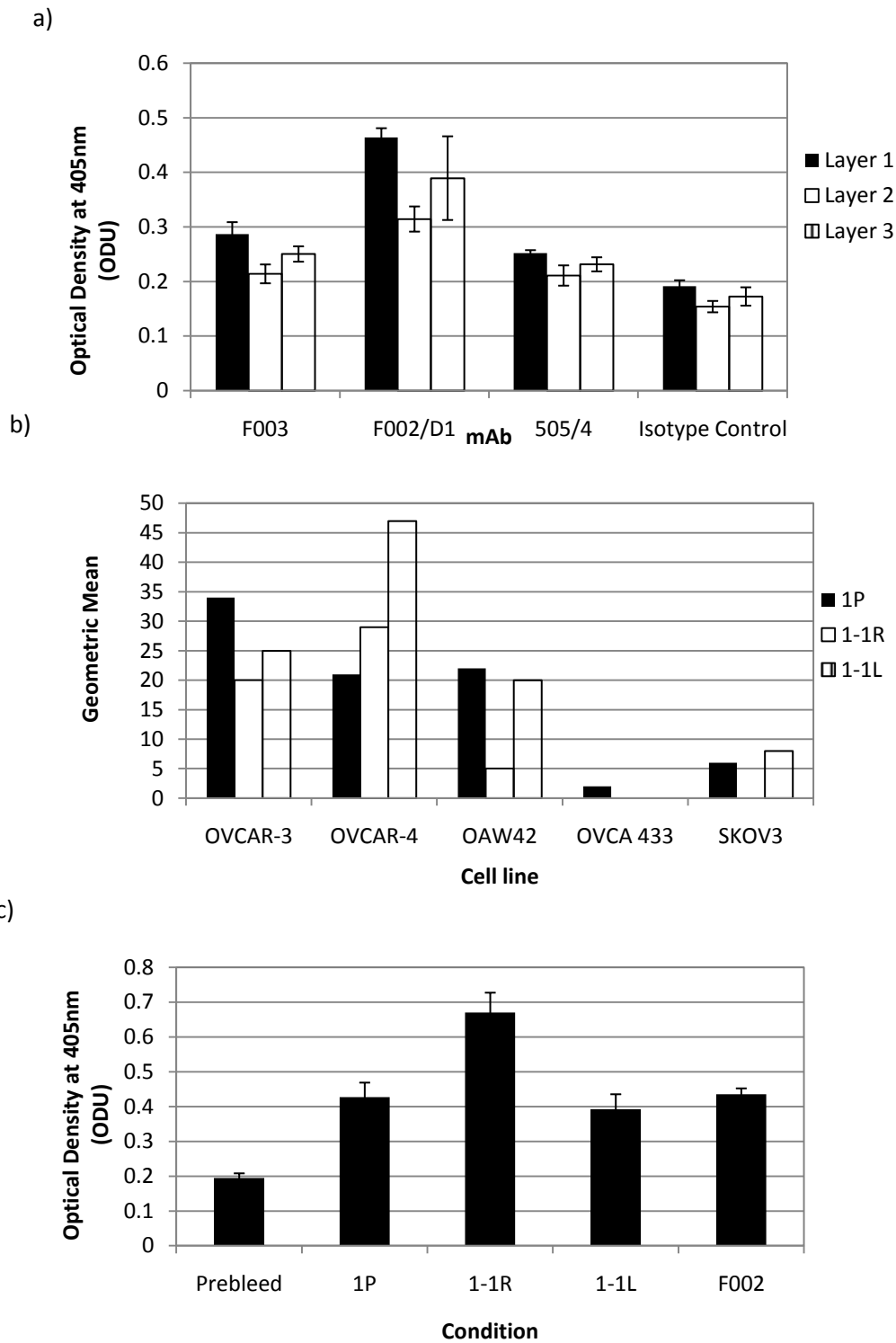


**Figure 6.9 Characterisation of F002 binding to glycolipid (a) and binding of ovarian cancer cell glycolipid immunised mouse serum (3673323) against a panel of ovarian cancer cell lines, either fresh or formaldehyde-fixed (b) and OVCA 433 glycolipid (c).** a)  $1 \times 10^5$  OVCAR-3, OVCAR-4, OAW42, OVCA 433 and SK-OV3 cells were incubated with  $50 \mu\text{l}$  1:100 serum from 1P, 1-1R and 1-1L final bleeds or  $50 \mu\text{l}$   $5 \mu\text{g}/\text{ml}$  F002 before probing binding with anti-IgG-FITC mAb. OVCA 433 glycolipid extract was dried onto a 96 flexi-plate. Plates were blocked before incubating with 1:100 mouse sera and probed with anti-mouse Ig-HRP before adding ABTS substrate. F002 was used as a positive control against both cells (Geometric mean=205) and glycolipid (O.D.=0.44). Error bars representing standard deviation of quadruplicate wells are present, but may be obscured by marker or data bar.

### 6.2.11 Preparation of ovarian cancer glycolipid-containing liposomes for immunisation

The lack of response to both C170 and ovarian cancer cell glycolipid *in vivo* suggests that glycolipid alone is not potent enough as an antigen for immunisation.

To increase the potency of cancer glycolipid *in vivo* it was incorporated into liposomes allowing the concentration of glycolipid at one point to be increased. The glycolipid extracted from a range of ovarian cancer cell lines (OVCA) was dried down with DPC, PC and cholesterol before resuspending in PBS to create liposomes (help with liposome composition was provided by Dr M Garnett, School of Pharmacy, University of Nottingham). To further enhance the immunogenicity of the liposomes the NKT cell agonist  $\alpha$ GalCer was incorporated into the liposomes. To determine the correct ratio of components mice were immunised with liposomes that contained a range of ovarian cancer cell glycolipid extract, with and without  $\alpha$ GalCer, summarised in Table 6.2.

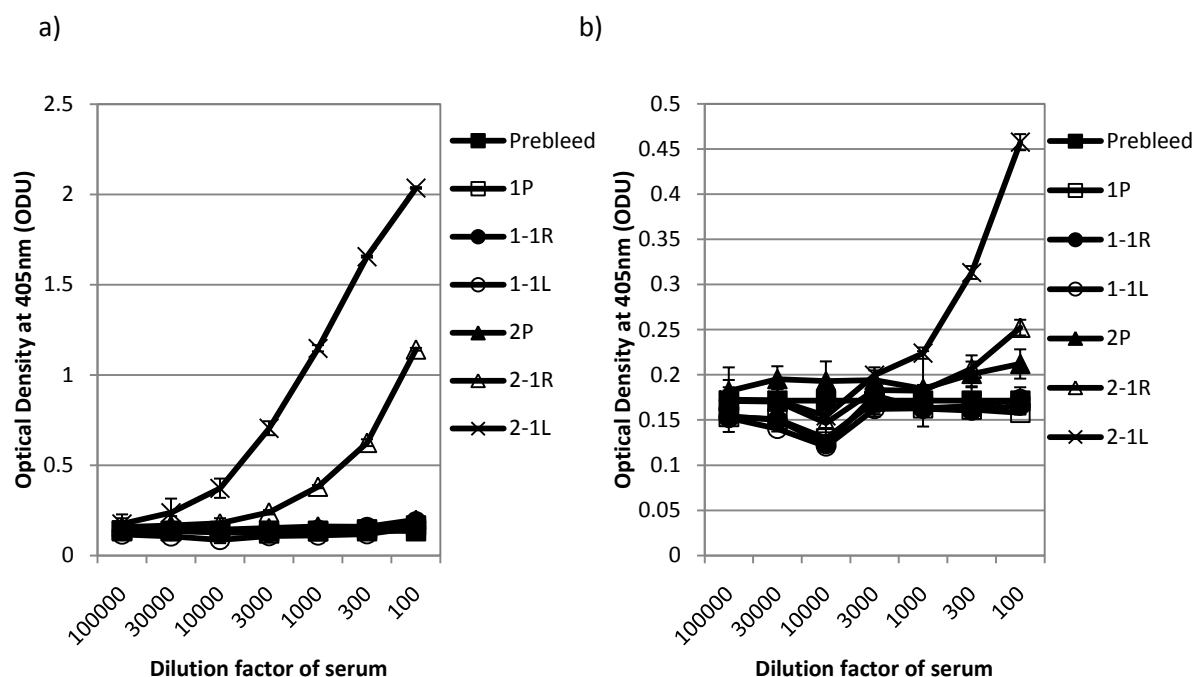
**Table 6.2 Immunisation details for OVCA glycolipid-containing liposomes and  $\alpha$ -galactosylceramide.** OVCA denotes glycolipid extracted from OVCA 433, OAW28, OAW42, SK-OV3 OVCAR-3 and OVCAR-4 cells.  $\alpha$ -galactosylceramide is abbreviated to  $\alpha$ GalCer.

Mouse	Immunisation
1P	90% OVCA glycolipid
1-1R	90% OVCA glycolipid + $\alpha$ GalCer
1-1L	10% OVCA glycolipid
2P	10% OVCA glycolipid + $\alpha$ GalCer
2-1R	2.5% OVCA glycolipid + OVCAR-4 cell boost
2-1L	2.5% OVCA glycolipid + $\alpha$ GalCer+ OVCAR-4 cell boost



### 6.2.12 Immunisation with OVCA glycolipid-containing liposomes with $\alpha$ GalCer

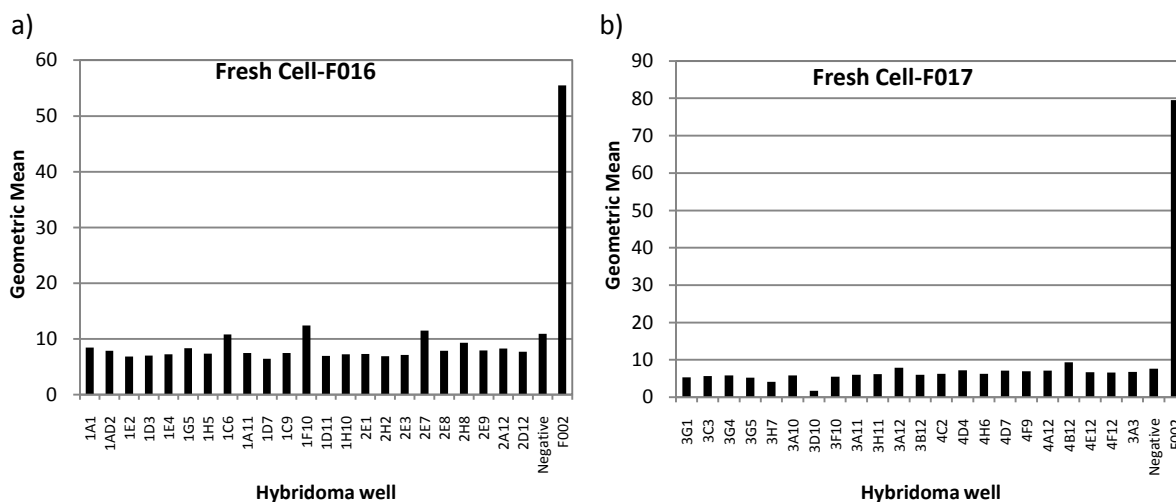
Six mice were immunised with liposomes (Table 6.2) on days 1 and 7 before blood samples were taken on day 14. The sera was then isolated and screened for mouse IgG binding against OVCA 433 whole cells and OVCA 433 glycolipid extract (Fig 6.10). Screening revealed that mice immunised with liposomes containing the lowest level of glycolipid (2.5%; mice 2-1R and 2-1L) gave the best anti-OVCA 433 cell response (Fig 6.10a), with the responses titrating out at 1:30,000 and 1:3,000 (2-1L and 2-1R respectively). Addition of  $\alpha$ GalCer seemed to enhancing the titre in mouse 2-1L compared to 2-1R. Both 2-1R and 2-1L also gave an anti-OVCA 433 glycolipid response (Fig 6.11b). The 2-1L response titrated out at 1:1000 and 2-1R at 1:300 (Fig 6.10b).



**Figure 6.10 Binding of OVCA glycolipid-containing liposomes immunised mouse serum (3694211) against OVCA 433 cells (a) and OVCA 433 glycolipid (b).** a) OVCA 433 cells were grown to confluency in a 96 well plate (a) or OVCA 433 glycolipid extract was dried onto a 96 well flexi-plate (b). Plates were blocked before incubating with serial dilutions of mouse blood sera and probed with anti-mouse IgG-HRP before adding ABTS substrate. Error bars are included, but may be covered by symbols. W6/32 was used as a positive control for binding to cells (O.D. = 0.86). F002 was used as a positive control for OVCA 433 glycolipid binding (O.D.=4.2). Error bars representing standard deviation of quadruplicate wells are present, but may be obscured by marker.

### 6.2.13 Fusion of splenocytes from mice 2-1R and 2-1L

Due to the positive response to OVCA 433 glycolipid, the splenocytes from mice 2-1R and 2-1L were isolated and fused with NS0 cells giving rise to F016 (2-1L derived) and F017 (2-1R derived) fusions. The supernatant from the resulting hybridomas was screened against whole fresh and fixed OVCA 433 cells for IgG binding using a FITC-conjugated anti-mouse IgG mAb before analysing the cells by flow cytometry. This revealed that none of the hybridomas secreted IgG against OVCA 433 cells (data not shown). Hybridoma supernatant was then screened against whole fresh and fixed OVCA 433 cells for total Ig binding using a FITC-conjugated anti-mouse Ig mAb before analysing the cells by flow cytometry. Figure 6.12 shows that a sample of positive wells from F016 (Fig 6.11a) and a sample of positive wells from F017 (Fig 6.11b) do not secrete Ig that binds to fresh OVCA 433 cells. However, after fixing OVCA 433 cells with formaldehyde, binding of IgM from the same hybridomas can be seen (Fig 6.11c, d), suggesting F016 and F017 secrete IgM directed against intracellular antigens. Furthermore, IgM binding to OVCA 433 glycolipid was seen to 16 hybridomas from the F016 fusion and 4 of the F017 fusion, suggesting that tumour glycolipid incorporated into liposomes is able to induce an anti-glycolipid response (Fig 6.11e, f). Results are summarised in Table 6.3.



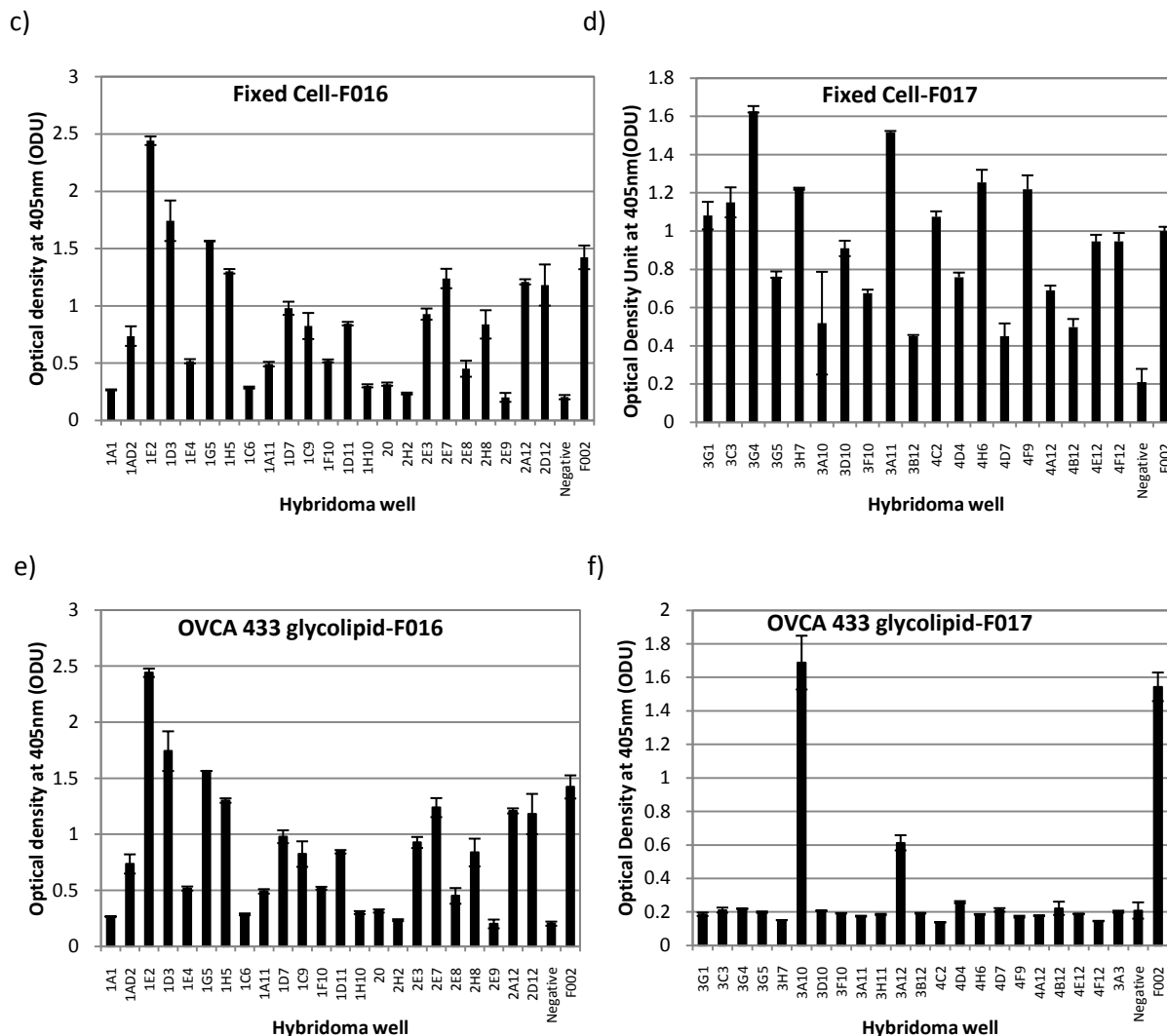


**Figure 6.12 Screening of F016 and F017 hybridoma supernatant for binding to fresh and fixed OVCA 433.** Splenocytes were extracted from mice 2-1L and 2-1R and fused, giving rise to F016 and F017 respectively. Spent supernatant from F016 (a, c, e) and F017 (b, d, f) hybridomas was taken from wells with colonies and incubated with fresh (a, b) or fixed (c, d) OVCA 433 cells or OVCA 433 glycolipid layer 2 (e, f). Binding to fresh cells (a, b) was probed for with anti-mouse Ig-FITC and analysed by flow cytometry (FL1). Binding to fixed cells and OVCA 433 glycolipid layer 2 was analysed by ELISA. OVCA 433 cells were grown to confluence in a 96 well plate before being fixed or OVCA 433 glycolipid layer 2 was plated and dried. The cells or glycolipid were then incubated with hybridoma supernatant. Binding was probed with anti-mouse IgM-HRP and ABTS substrate was added. The plate was then read at 405nm. F002 was used as a control for binding to fresh and fixed cells as well as OVCA 433 glycolipid layer 2. Error bars representing standard deviation of quadruplicate wells are present, but may be obscured by marker.

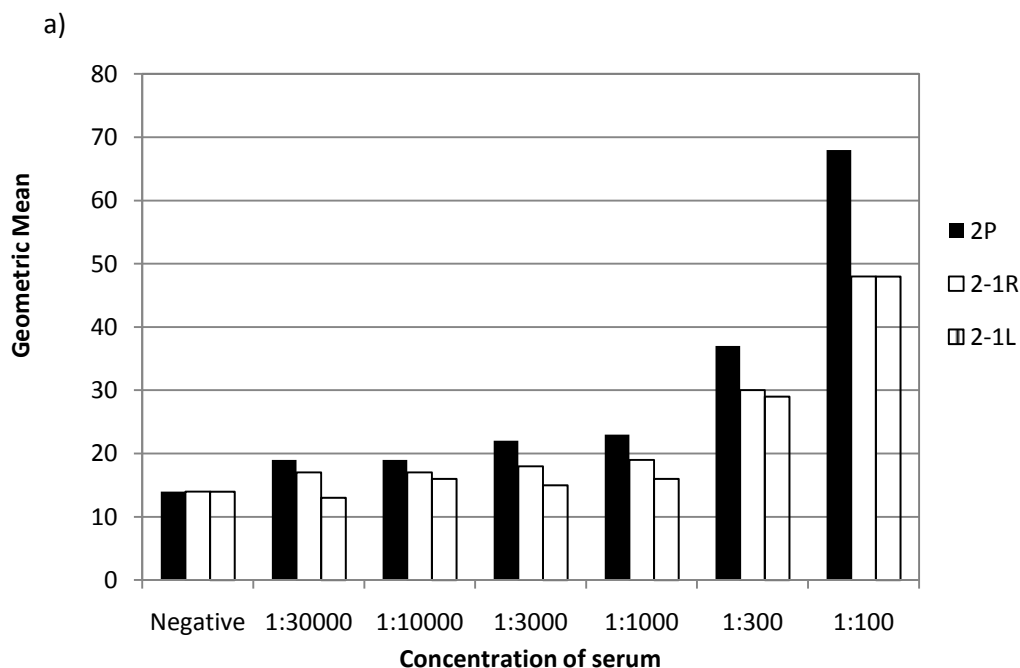
**Table 6.3 Summary of F016 and F017 hybridomas.**

Assay	F016	F017
Binding to fixed OVCA 433 cells (Ig)	67	41
Binding to fresh cells	0	0
IgM binding to OVCA 433 glycolipid	16	4

#### 6.2.14 Immunisation with 2.5% OVCA glycolipid and $\alpha$ GalCer containing liposomes boosted with OVCAR-4 cells

Despite seeing an IgG response in bleeds from mice 2-1R and 2-1L (immunised with 2.5% OVCA glycolipid and  $\alpha$ GalCer liposomes, the resulting hybridomas secreted only IgM directed at intracellular glycolipid antigen. In order to encourage class switching of Ig from IgM to IgG, mice were immunised with 2.5% OVCA glycolipid and  $\alpha$ GalCer containing liposomes on days 1 and 7, followed by a whole cell boost on day 14. Blood samples were then taken on day 21. Sera were isolated from the blood before screening against fresh OVCAR-4 cells. An anti-mouse IgG-FITC mAb was used to detect the mouse IgG before analysing by flow cytometry. All three mice showed an IgG response that titrated out at 1:1000 (Figure 6.12a).

As the previous immunisations produced hybridomas that secreted IgM specific for mostly intracellular mAbs, the serum was tested against a range of cell lines, fresh and fixed. Figure 6.12b shows that serum from all three mice bound to both OVCAR-3 and OVCAR-4 cells, with the greatest level of binding of 2-1L against fresh OVCAR-4 cells. Interestingly, on the contrary to the previous immunisations, cell fixation did not have a great affect on the level of binding. Low levels of binding are seen with the serum from all three mice against OAW28, OVCA 433 and SK-OV3 cells.



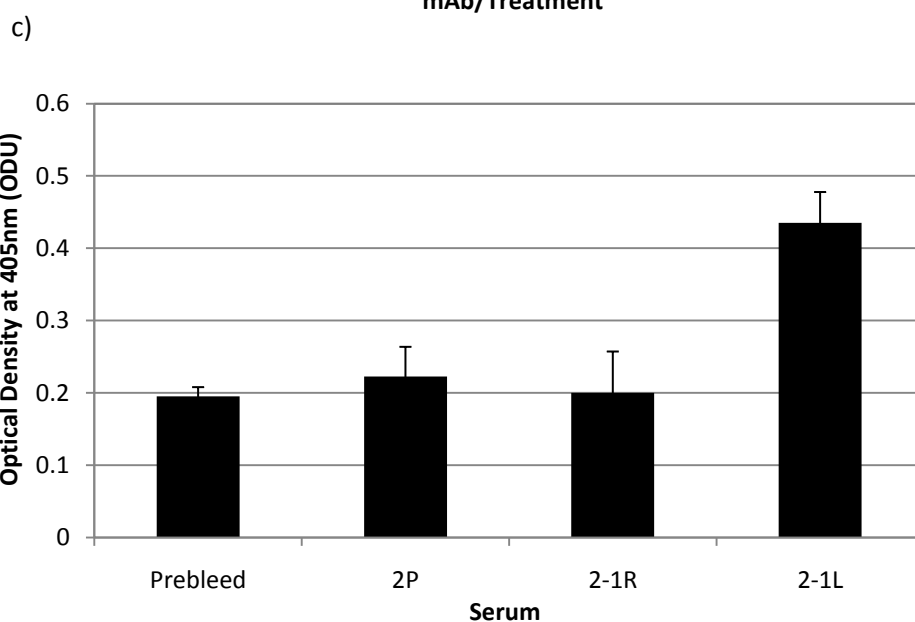
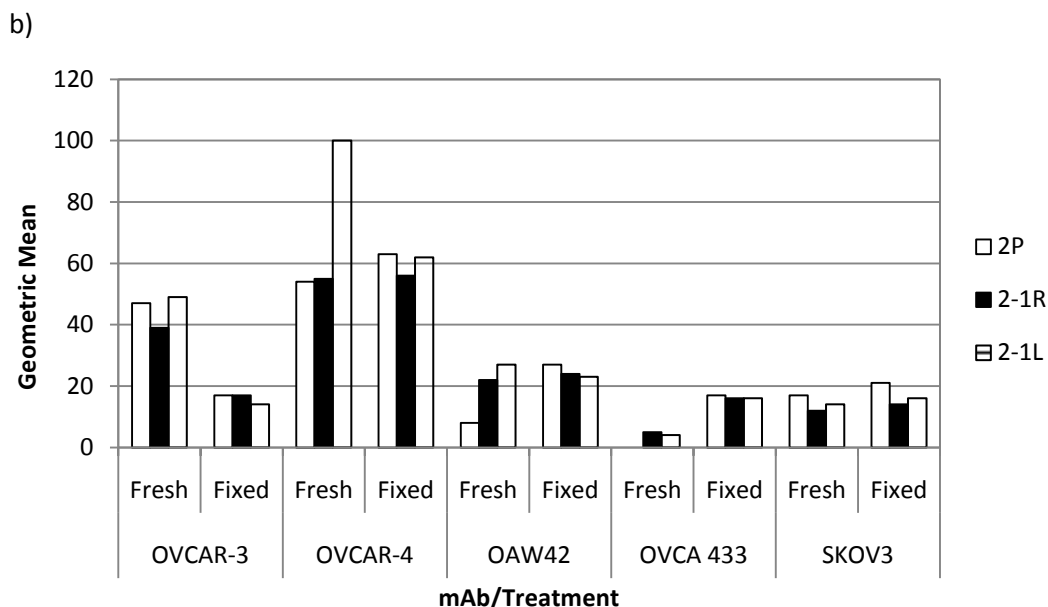


**Figure 6.12 Binding of OVCA-glycolipid immunised and 2.5% OVCA glycolipid and  $\alpha$ GalCer-containing liposomes mouse serum (3713725) to OVCAR-4 cells (a) or fresh and fixed OVCAR-3, OVCAR-4, OAW42, OVCA 433 and SK-OV3 cells (b) and OVCA 433 glycolipid (c).** a) Serum from mice immunised with 2-5% OVCA glycolipid and  $\alpha$ GalCer-containing liposomes (2-P, 2-1R and 2-1L) was titrated against OVCAR-4 cells and probed for antibody binding with anti-mouse IgG-FITC (Serum from mouse 1L from T cell depleted immunisation used as a positive control – Geometric mean = 362). b) Serum from 2.5% OVCA glycolipid and  $\alpha$ GalCer-containing liposomes mouse serum (2P, 2-1R, 2-1L) was diluted to 1:100 and incubated with fresh or formaldehyde-fixed OVCAR-3, OVCAR-4, OAW42, OVCA 433 and SK-OV3 cells before incubation with anti-mouse IgG-FITC. Cells were then analysed by flow cytometry. F002 was used as a positive control. c) Serum from 2.5% OVCA glycolipid and  $\alpha$ GalCer-containing liposomes mouse serum (2P, 2-1R, 2-1L) was diluted to 1:100 and incubated with OVCA glycolipid before binding was probed with anti-mouse IgG-HRP. ABTS substrate was added before reading at 405nm. Error bars representing standard deviation of quadruplicate wells are present, but may be obscured by marker. F002 was used as a positive control (O.D. = 0.43).

### 6.2.15 Fusion of splenocytes from 2-1L and initial screening

AS the serum from mouse 2-1L displayed both an anti-ovarian cancer cell and ovarian cancer glycolipid response, with a greater level of binding seen against fresh cells, the splenocytes were harvested and fused to create hybridomas (F019). The resulting hybridomas were screened for IgG binding to fresh OVCAR-4 cells (data not shown). Of the positive wells, 9 bound to fresh OVCAR-4 cells (Table 6.4). F019/1A7, F019/1D3 and F019/1D10 all showed binding to OVCAR-3, OVCAR-4 and SK-OV3, however F019/1D10 bound PBMCs (Table 6.4). Therefore, F019/1A7 and F019/1D3 were taken forward for further screening. Both F019/1A7 and F019/1D3 bound to the ovarian cancer cell lines OVCA 433 and OAW42 and also to the colorectal cell line C170. Both did not show any binding to HUVEC (Table 6.4).

**Table 6.4. Summary of F019 hybridomas that bind OVCA 433 cells.** Wells with colonies were first screened against OVCA 433 cells. Those positive for binding to OVCA 433 cells were screened against PBMCs, OVCAR-4, OVCAR-3 and SK-OV3 cells and probed for with anti-mouse IgG-FITC. Cells were incubated with hybridoma supernatant before probing with anti-mouse IgG-FITC. Numbers represent the geometric mean fluorescence when the cells were analysed by flow cytometry. W6/32 was used as a positive control.

Hybridoma well	PBMCs	OVCAR-4	OVCAR-3	SKOV-3	HUVEC	OVCA 433	OAW42	C170
<b>F019/1A7</b>	32	226	314	141	23	67	566	112
<b>F019/1B4</b>	30	47	43	119				
<b>F019/1D3</b>	28	172	291	108	20	70	744	95
<b>F019/1D10</b>	67	290	404	259				
<b>F109/1F7</b>	20	54	185	55				
<b>F019/2C1</b>	30	19	21	62				
<b>Negative</b>	28	9	8	6	5	8	9	6
<b>W6/32</b>	1005	772	793	7347				

### 6.2.16 Further characterisation and cloning of F019/1A7 and F019/1D3

Due to the pan-cancer cell line reactivity of F019/1A7 and F019/1D3 and the lack of binding to PBMC and HUVEC, the hybridomas were cloned. Each hybridoma was plated at 3, 1 and 0.3 cells/well across 3 96 well plates. Once colonies were present, supernatant from the 0.3 cell/well plate with 30 colonies per plate was screened against OVCAR-4 cells. Positive wells were picked from the F019/1A7 and F019/1D3 96 well plate and grown in 48 well plates before a second round of cloning. The 0.3 cell per well plate was then screened against OVCAR-4 cells. All wells from F019/1A7 were positive, therefore 1 well was picked and was expanded. Wells from F019/1D3 were either positive, or weak with small colonies, therefore, positive wells from F019/1D3 were transferred to 48 well plates before re-cloning. The supernatant was again screened against OVCAR-4 cells with all wells being positive. One well was then picked and expanded. The supernatant from F019/1A7 and F019/1D3 was collected and purified. Isotyping of the mAbs revealed that both F019/1A7 and F019/1D3 were IgG<sub>1</sub> (data not shown). The F019/1A7 mAb was validated by titrating across the cell lines that F019/1A7 previously bound (OVCAR-4 and OAW42). Figure 6.13 shows that purified F019/1A7 has retained its ability to bind to both cell lines, saturating the antigen between 3 and 10µg/ml (Fig 6.13a). The mAb was then screened on a wider range of cell lines. F019/1A7 binds to all ovarian cancer cell lines tested as well as to the colorectal cell lines Colo 201, Colo 205, HT29 and LoVo but did not bind to the gastric cell line CaCO2 (Fig 6.13b). To ensure that F019/1A7 bound to glycolipid, glycolipid was extracted from a range of cell lines, dried onto an ELISA plate before incubating with F019/1A7. Binding of F019/1A7 was seen to OAW42 glycolipid, but not to any other cell lines tested (Fig 6.13c). As a further test for glycolipid binding, F019/1A7 was screened by immune dot blot against glycolipid extract layers from C170, OAW42, OVCAR-4 and OVCAR-3 cells with F019/1A7 binding restricted to layer 2 and layers 2 and 3 of OAW42 cells (Fig 6.13d).

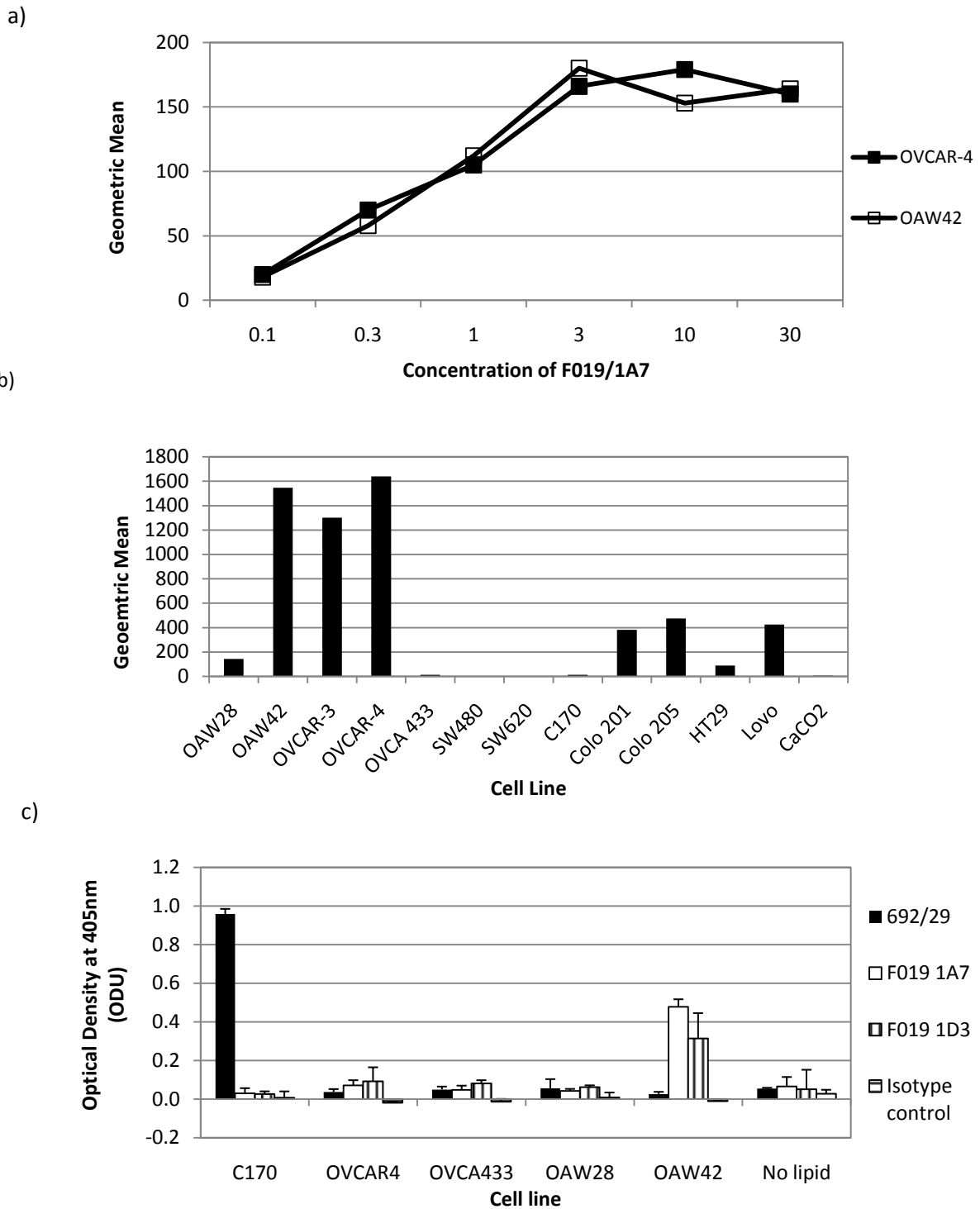


**Figure 6.13 Titration of F019/1A7 on ovarian cancer cells (a), binding of F019/1A7 after cloning to a range of ovarian and colorectal cell lines (b) and glycolipid from a range of cell lines by ELISA (c).** a)  $1 \times 10^5$  OAW42 and OVCAR-4 cells per well were incubated with 0.1-30µg/ml F019/1A7 before probing for mAb binding with rabbit anti-mouse IgG-FITC. Cells were analysed by flow cytometry. b)  $1 \times 10^5$  cells were incubated with purified F019/1A7 at 10µg/ml before probing with rabbit anti-mouse IgG-FITC. Cells were then analysed using flow cytometry (FL1). c) Glycolipid was extracted from C170, OVCAR-4, OVCA 433, OAW28 and OAW42 cell lines and plated at 1:100, left to dry before blocking and the addition F019/1A7 and F019/1D3 mAb. 692/29 binding to C170 glycolipid was used as a positive control with an irrelevant IgG used as a negative control. Binding was detected with rabbit anti-mouse IgG-HRP/ABTS. Error bars representing standard deviation of quadruplicate wells are present, but may be obscured by marker.



### 6.2.17 Screening of F019/1A7 against ovarian cancer tissue array

To establish how ubiquitously the F019/1A7 antigen is expressed, a TMA consisting of 360 ovarian cancer cases was stained with F019/1A7. Of the cohort of 364 patients' age ranged from 24-90 years old, with a mean age of 62 years old. The mean survival from diagnosis was 61 months. Of the 364 tumours, 95(27%) were FIGO (International Federation of Obstetricians and Gynaecologists) stage 1, with 38(11%) being stage 2, 175(48%) being stage 3 and 40(12%) unknown. In order of lethality, the proportion of type of the 364 tumours was 19 (5%) borderline, 25 (7%) clear cell OVCA, 35 (10%) mucinous OVCA, 42 (12%) endometrioid OVCA, 178 (49%) serous OVCA 54 (15%) undifferentiated with 5 (1%) being other OVCA and 4 (1%) of an unknown type. Figure 6.14a-d shows examples of the level of staining seen on the ovarian. Staining was mainly seen in the cytoplasm. Of the 362 tumours, 234 tumour samples were stained, with 128 lost during staining or no viable tumour was present in the core. Of the 234 tumours stained, F019/1A7 bound to 88% of tumours, with strong binding seen to 51(22%) of tumours. 63(27%) showed moderate staining with 91(39%) and 29(12%) of tumours staining weakly or not at all, respectively (Fig 6.14e).

The relationship between F019/1A7 binding and standard clinicopathological variables was measured using the Pearson  $\chi^2$  test. Binding of F019/1A7 in the tumour associated significantly with TNM stage and distant metastases ( $p=0.047$ ,  $0.005$  respectively; Table 6.6). Binding of F019/1A7 correlated with tumour type (both histological and in relation to lethality;  $p=0.014$  and  $0.003$  respectively) as well as with tumour grade ( $p=0.033$ ). No correlation was seen with FIGO stage however ( $p=0.052$ ), or with age ( $p=0.894$ ; Table 6.6). When the level of F019/1A7 binding is split into low (negative and low) and high (moderate and strong) groups of binding, the group with high binding have a significantly worse prognosis than patients with low level of F019/1A7 binding ( $p=0.005$ ; Fig 6.15), although this was not found to be independent of stage or grade.

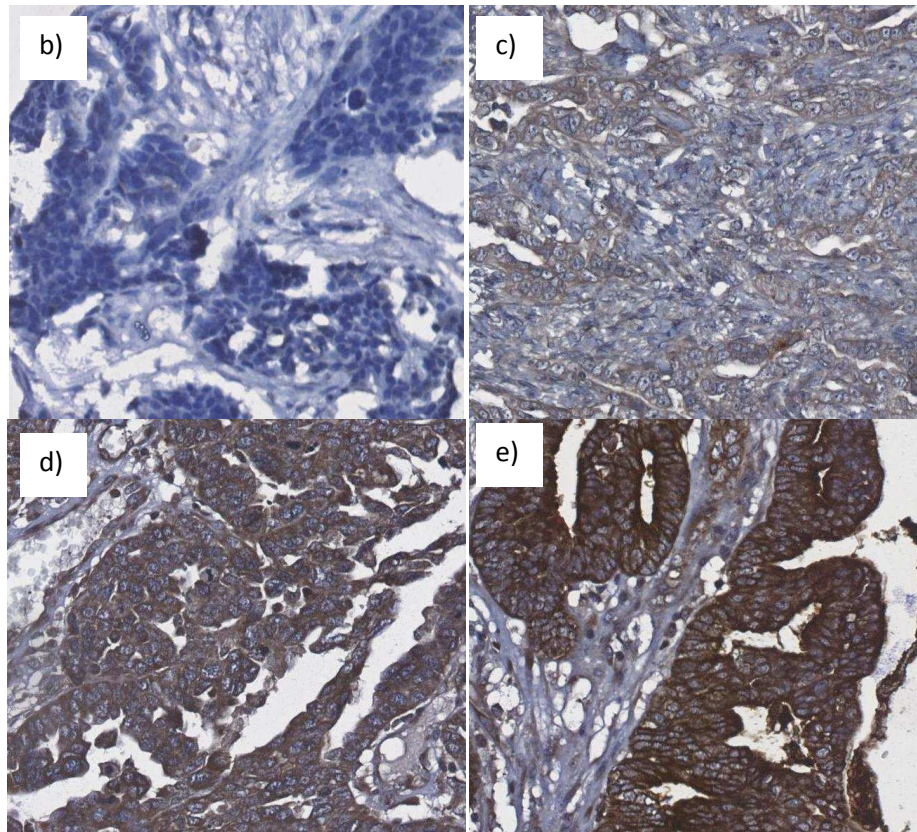
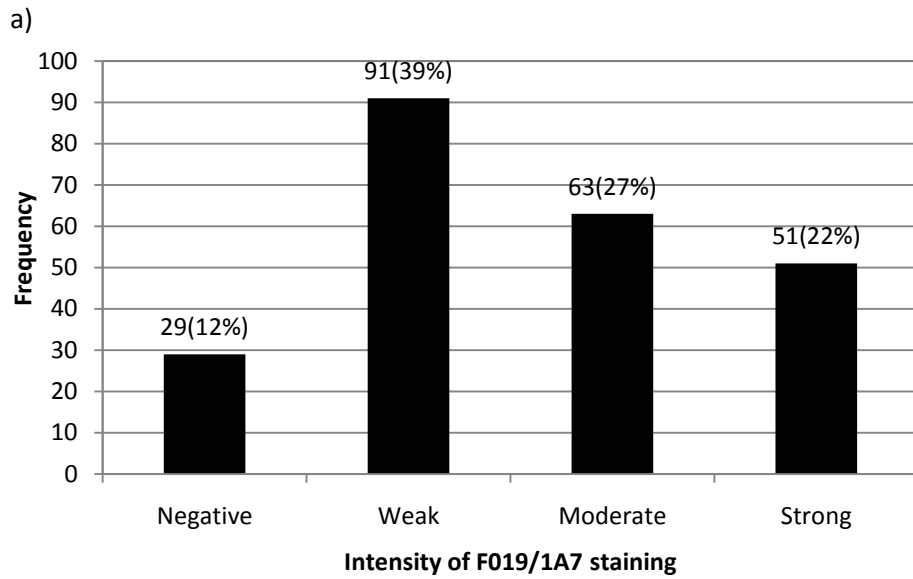


**Figure 6.14 Examples of F019/1A7 staining of ovarian cancer and F019/1A7 staining levels.** An ovarian TMA consisting of 362 tumour samples was stained with F019/1A7 and visualised with DAB (brown). Frequencies of negative, weak, moderate and strong staining on the ovarian cancer TMA; 22% of the cores were strong with 27% being moderate. Only 12% of the cores were negative for F019/1A7 staining. The remaining 39% stained weakly with F019/1A7. Annotations denote number of cores. The TMA was scored a negative (b), weak (c), moderate (d) or strong (e) staining independently by two observers, magnification X20 original magnification.

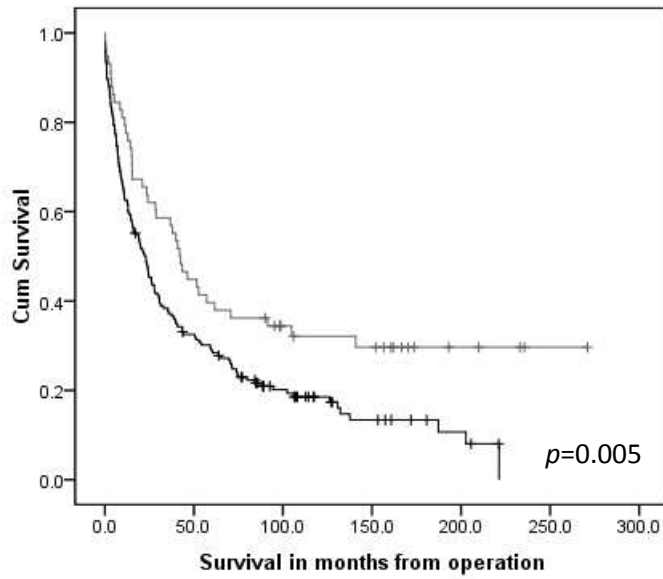


**Figure 6.15 Kaplan-Meier plot of survival.** Analysis of survival in patients with either low (grey) or high (black) levels of F019/1A7 expression.  $p=0.005$ .

**Table 6.6 Pearson  $\chi$  squared tests of F019/1A7 with other patient variables.**

Variable	$\chi^2$ Test ( $p$ value)
Age	0.894
Histological Type	0.014
Tumour Grade	0.033
FIGO Stage	0.052
Types of OVCA in order of lethality in this series	0.003

### **6.2.18 Staining of normal tissue array with F019/1A7**

To be an effective therapeutic mAb, F019/1A7 would need to bind specifically to its antigen on tumour cells and have minimal binding to normal tissues. In order to investigate the level of binding to normal tissue, the mAb was stained on a tissue microarray consisting of 59 cores, representing samples of 38 types of tissue (Table 6.6). During staining the core of bronchus tissue (core no. 14) was lost. No staining of F019/1A7 was seen against 7 of 59 cores. The majority of cores (25) showed weak staining, with 11 and 15 showing moderate and strong staining respectively (Fig 6.16). Of the tissues stained, F019/1A7 bound breast, gallbladder, pancreas, kidney, oesophagus, stomach, appendix, colon, rectum, kidney, endometrium, adrenal gland and thyroid most strongly. Moderate staining was seen against subcutis, spleen, lymph node, heart and liver. Weak staining was seen against skin, nasal mucosa, salivary gland, tonsil, duodenum, small bowel, bladder, prostate, seminal vesicle, testis, cervix, salpinx, placenta and thymus. No staining was seen against brain or umbilical cord. Examples of F019/1A7 staining intensity can be seen in figure 6.17. To ascertain if the staining on the normal tissues was cell surface and therefore accessible to mAbs, normal hepatocytes, HUVECs and PBMCs cells were stained by indirect immunofluorescence and analysed by flow cytometry. Figure 6.18 shows that the staining on normal hepatocytes was very weak, and was 10 fold lower than seen on ovarian tumour lines and no binding was seen to HUVECs (Fig 6.18; passage<6). Furthermore, no binding was seen against freshly isolated human PBMCs (Fig 6.19).

**Table 6.6 List of normal tissues on microarray, tissue type and staining intensity of F019/1A7 with 505/4 staining a positive control.**

Core Number	Organ	Associated lesion Tissue type	Tissue type <sup>2</sup>	F019/1A7 intensity <sup>3</sup>	505/4 intensity
1	Skin	Breast cancer	B	1	-
2	Skin breast cancer	Breast cancer	B	1	-
3	Subcutis	Fatty abdomen	A	2	-
4	Breast	Breast cancer	C	0	-
5	Breast	Breast cancer	C	3	-
6	Spleen	Stomach cancer	B	2	0
7	Spleen	Stomach cancer	B	1	0
8	Lymph node	Stomach cancer	B	1	0
9	Lymph node	Stomach cancer	B	2	0
10	Skeletal	Muscle angiosarcoma	B	2	0
11	Nasal mucosa	Chronic sinusitis	A	1	-
12	Lung	Metastatic cancer of lung (from stomach)	B	1	0
13	Lung	Lung cancer	C	1	0
14	Bronchus	Lung cancer	C	-	0
15	Heart	No abnormal finding	A	1	-
16	Salivary gland	Oropharyngeal cancer	B	1	-
17	Liver	Hepatocellular carcinoma	C	2	1
18	Liver	Stomach cancer	B	2	0
19	Liver	Hepatocellular carcinoma	C	2	0
20	Gallbladder	Rectal cancer	B	3	0
21	Pancreas	Stomach cancer	B	3	0
22	Pancreas	Pancreas islet cell tumour	C	2	0
23	Tonsil	Chronic tonsillitis	A	1	0
24	Oesophagus	Oesophageal cancer	C	1	-
25	Oesophagus	Oesophageal cancer	C	3	0
26	Stomach	Body stomach cancer	C	3	1
27	Stomach	Body stomach cancer	C	3	1
28	Stomach	Antrum stomach cancer	C	2	1
29	Stomach	Smooth muscle stomach cancer	C	1	0
30	Duodenum	Ampulla of Vater cancer	C	1	0
31	Small bowel	Pseudomyxoma peritonei	B	2	-
32	Small bowel	Colonic diverticulosis	A	1	0
33	Appendix	Metastatic cancer of ovary (from stomach)	B	2	2
34	Colon	Rectal cancer	C	3	3
35	Colon	Colon cancer	C	3	-
36	Rectum	Rectal cancer	C	3	2
37	Kidney	Cortex renal cell carcinoma	C	3	2
38	Kidney	Cortex renal cell carcinoma	C	3	1
39	Kidney	Medulla renal cell carcinoma	C	3	1

<sup>2</sup> Tissue type denotes the following categories; A Normal tissue from a non-cancer patient; B Normal tissue from a cancer patient, but the cancer involves unrelated organ; C Normal tissue adjacent to the cancer

<sup>3</sup> Levels of intensity are classified as 0- negative, 1- weak, 2- moderate and 3- strong. – denotes that scoring was not possible for that core.

40	Urinary bladder	Invasive bladder carcinoma	C	3	-
41	Prostate	Bladder cancer	B	2	0
42	Prostate	Bladder cancer	B	2	0
43	Seminal vesicle	Bladder cancer	B	2	-
44	Testis	Prostate cancer	B	2	0
45	Endometrium	Proliferative benign ovarian neoplasm	A	1	0
46	Endometrium,	Secretory ovarian cancer	B	2	-
47	Myometrium	Adenomyosis	A	1	0
48	Uterine cervix	Leiomyoma	A	1	0
49	Salpinx	Cervix cancer	B	2	-
50	Ovary	Ovary cancer	C	3	-
51	Placenta	Mature placenta	A	1	0
52	Placenta	Mid-trimester placenta	A	1	0
53	Umbilical cord	Mature placenta	A	1	-
54	Adrenal gland	Renal cell carcinoma	B	2	2
55	Thyroid	Thyroid cancer	C	3	-
56	Thymus	Lymphoid hyperplasia	A	1	0
57	Brain	White matter no abnormal finding	A	1	0
58	Brain	Gray matter no abnormal finding	A	1	0
59	Cerebellum	No abnormal finding	A	1	0

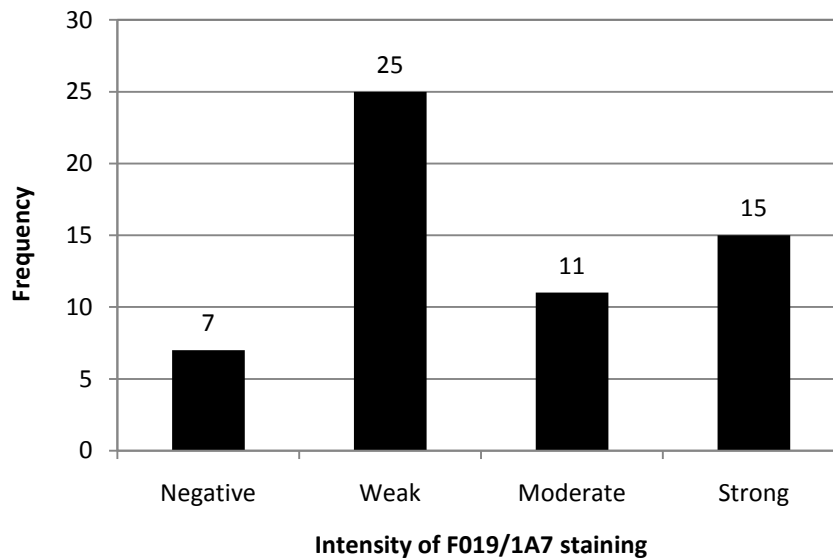


**Figure 6.16 Histogram of F019/1A7 staining intensity across normal tissues.** Of the 58 cores stained 7 showed no binding of F019/1A7. F019/1A7 bound 25 cores with weak intensity with 11 cores staining moderately. 15 cores showed strong staining of F019/1A7.



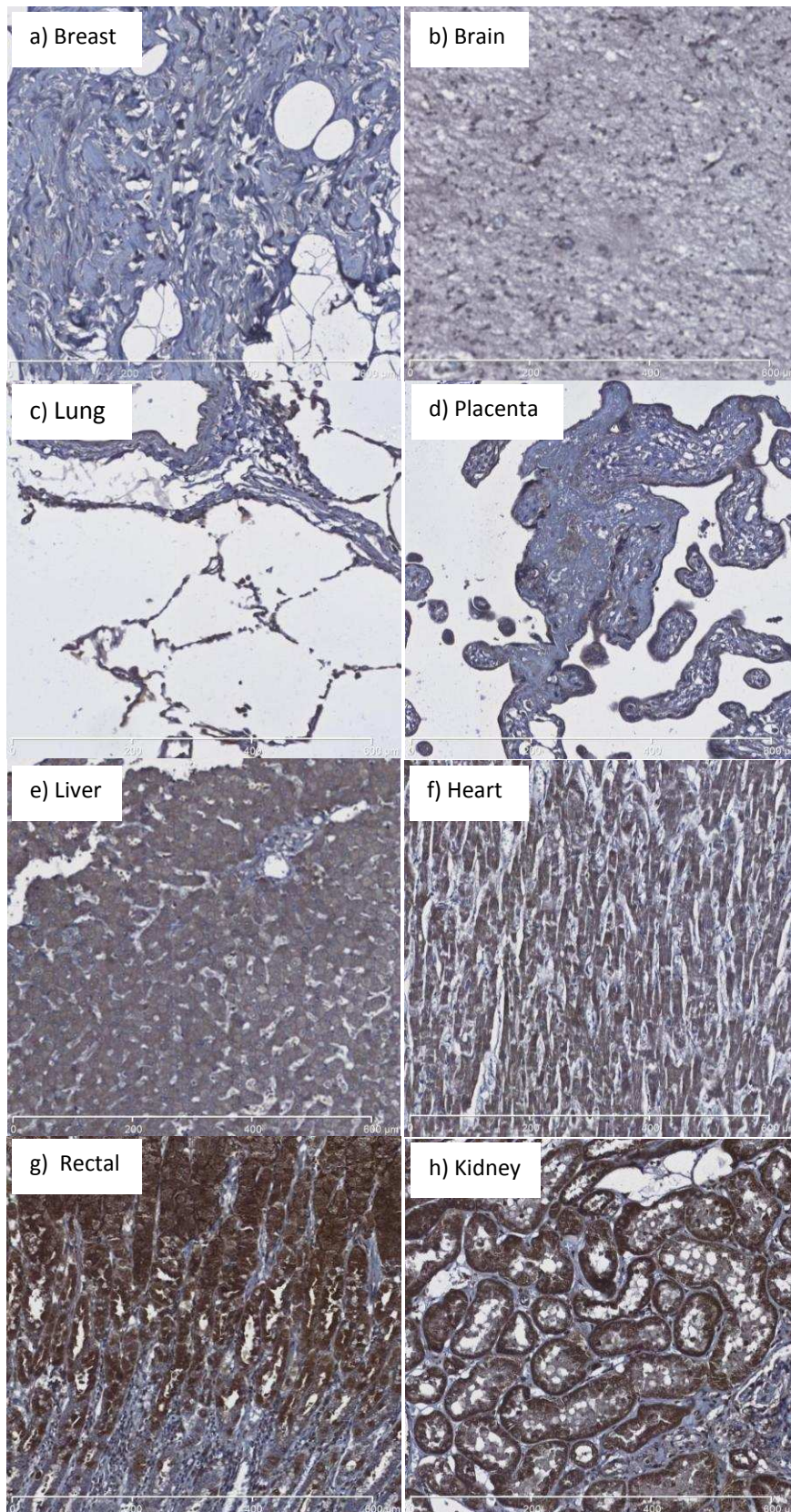


**Figure 6.17 Examples of F019/1A7 staining intensity across normal tissues.** Examples of negative staining can be seen against breast (a) and brain (b), with weak staining seen against lung (c) and placenta (d). Moderate staining is shown against liver (e) and heart (f) tissue. Strong staining can be seen against rectal (g) and kidney (h) tissue.

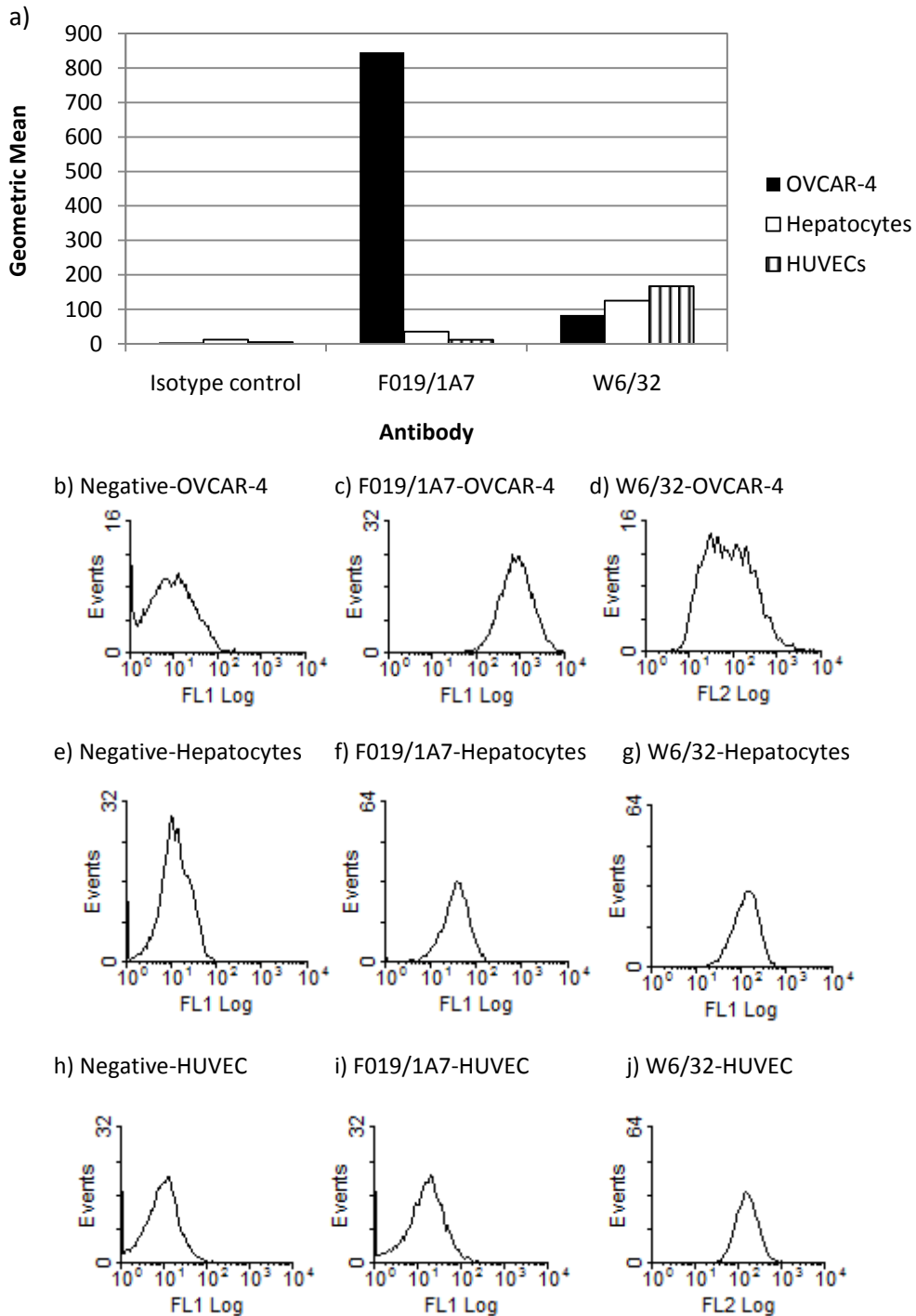


**Figure 6.18 Analysis of F019/1A7 binding to a range of normal cells.** a)  $1 \times 10^5$  human hepatocytes, HUVECs or OVCAR-4 cells were incubated with  $5 \mu\text{g/ml}$  F019/1A7 or  $10 \mu\text{g/ml}$  W6/32-PE. F019/1A7 binding was probed with anti-mouse IgG-FITC. Cells were then analysed for W6/32-PE or anti-mouse IgG-FITC binding by flow cytometry. Histograms are displayed representing isotype control binding to OVCAR-4 (b), hepatocytes (e) and HUVECs (h), F019/1A7 binding to OVCAR-4 (c), hepatocytes (f) and HUVECs (i), W6/32 binding to OVCAR-4 (d), hepatocytes (g) and HUVECs (j). Data representative of at least 2 separate experiments.



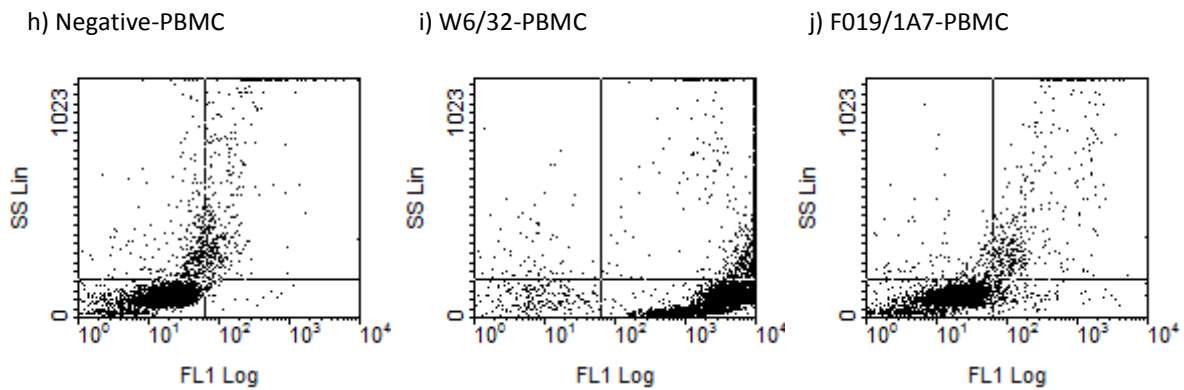
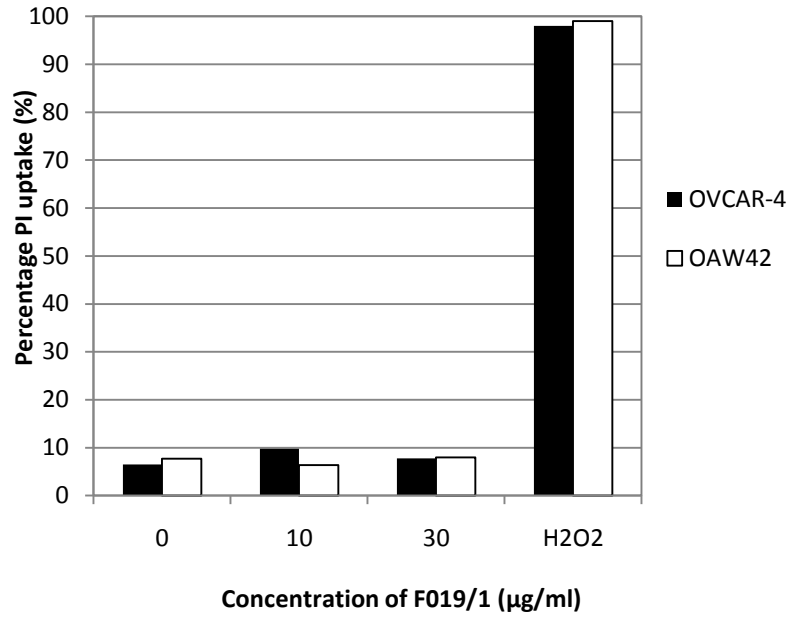


**Figure 6.19 F019/1A7 does not bind to PBMCs.** PBMCs were isolated from human blood and  $1 \times 10^5$  cells per well were incubated with irrelevant IgG (a), W6/32 (b) or  $5 \mu\text{g/ml}$  F019.1 (c). Data is representative of at least 3 separate experiments.

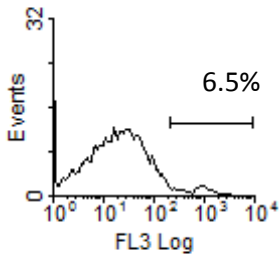
### 6.2.19 Evaluation of direct killing with F019/1A7

The ability for mAbs to induce cytotoxicity *in vivo* relies upon the mAb being able to induce cancer cell death through more than one mechanism. In order to ascertain whether F019/1A7 has the ability to induce ovarian cancer cell death directly,  $1 \times 10^5$  OVCAR-4 and OAW42 cells were incubated with 0, 10 and  $30 \mu\text{g/ml}$  F019/1A7 in 10% NBS supplemented RPMI overnight at  $37^\circ\text{C}$ . The induction of cell death was measured by PI uptake and by counting the number of cells. Figure 6.20a shows that despite the addition of  $30 \mu\text{g/ml}$  F019/1A7, no cell death has occurred. This is mirrored in the cell counts, which show that the cells incubated with F019/1A7 have grown at the same rate as those incubated with media alone (Fig 6.20 f, g).

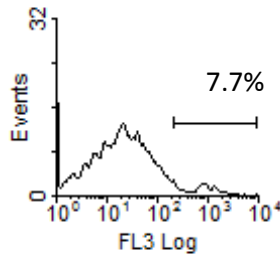
a)



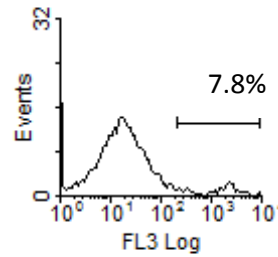
b) Negative-OVCAR-4



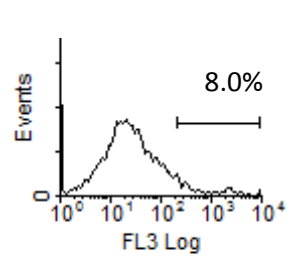
c) F019/1A7-OVCAR-4



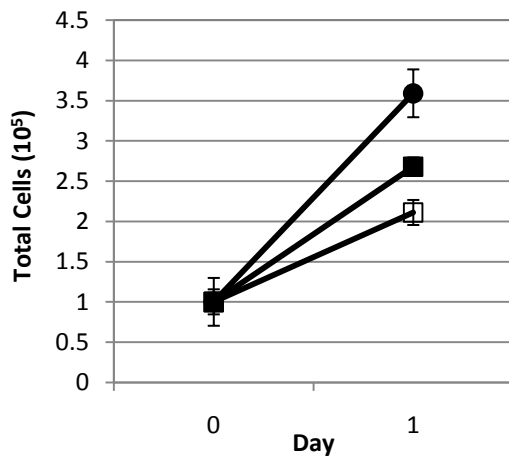
d) Negative-OAW42



e) F019/1A7-OAW42



f)



g)

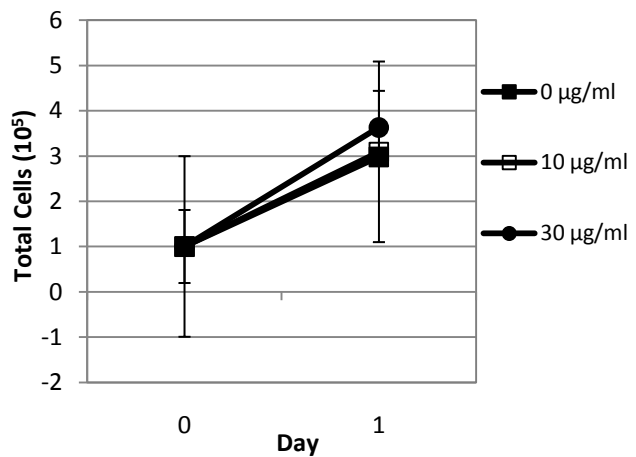


**Figure 6.20 Measurement of F019/1A7 direct cytotoxicity against OVCAR-4 and  $1 \times 10^5$  OAW42 cells.** OVCAR-4 and OAW42 cells were incubated with 10 and 30 µg/ml F019/1A7 or 0.5% H<sub>2</sub>O<sub>2</sub> overnight at 37°C. After 30mins of PI incubation, cells were analysed by flow cytometry (a). Histograms showing negative controls for OVCAR-4 (b) and OAW42 (d) as well as histograms representing 30 µg/ml F019/1A7 incubated with OVCAR-4 (c) and OAW42 cells (e). After overnight incubation of F019/1A7 counts of OVCAR-4 (f) and OAW42 (g) cells were taken using trypan blue. Error bars are present on each data point representing standard deviation of 3 repeat experiments, but may be obscured by the marker.

### 6.2.20 F019/1A7 cytotoxicity at different temperatures and with cross-linking

As direct cell death has been seen at temperatures lower than 37°C with other mAbs, 1x10<sup>5</sup> OVCAR-4 and OAW42 cells were incubated with 0, 10 and 30µg/ml F019/1A7 in 10% NBS supplemented RPMI overnight at RT (approximately 22°C). The induction of cell death was measured by PI uptake and by counting the number of cells. Figure 6.21a shows that despite a reduction in temperature, the addition of 30µg/ml F019/1A7 has not induced cell death.

As F019/1A7 is an IgG<sub>1</sub>, it is unable to dimerise via the Fc receptor, which may have an effect on its ability to cause direct cell death. OVCAR-4 cells were incubated with F019/1A7, a rabbit anti-mouse Ig mAb and a goat anti-rabbit Ig mAb to encourage cross-linking of mAbs on the cell surface. Cells were incubated overnight at 37°C before measuring PI uptake and analysing the cells with flow cytometry. Figure 6.21b shows that despite the addition of cross-linking mAbs, no increase in cell death was seen.

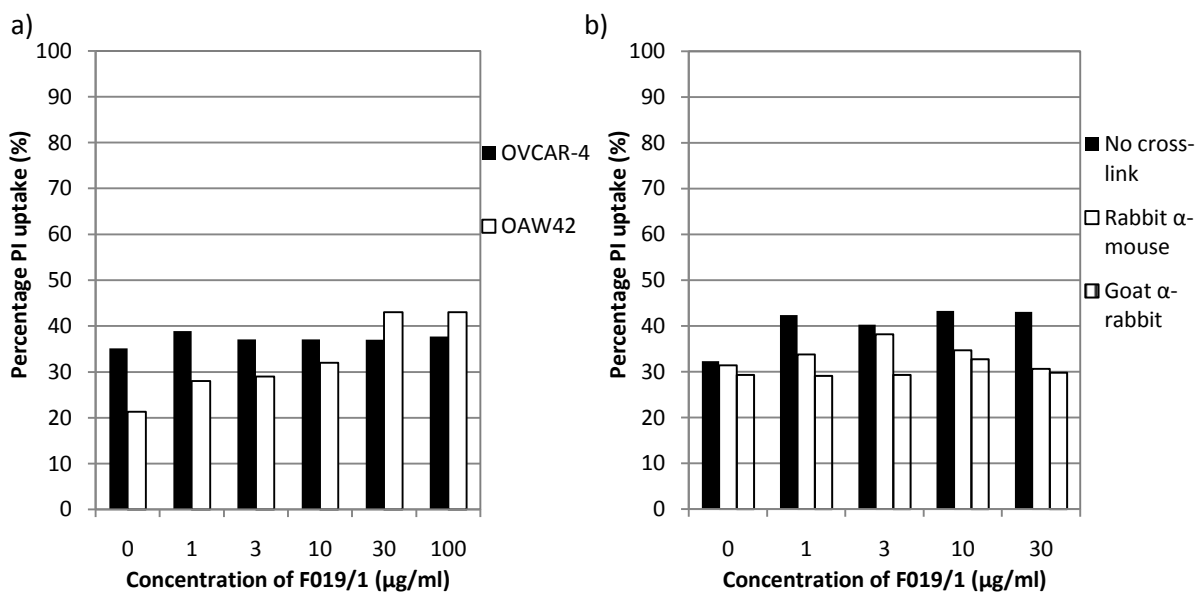


**Figure 6.19 Measurement of F019/1A7 cytotoxicity at room temperature and when incubated with cross-linking mAbs.** PI uptake was measured after overnight incubation of OVCAR-4 and OAW42 cells with F019/1A7 at RT (a). PI uptake was measured after incubation of OVCAR-4 cells with F019/1A7 and rabbit anti-mouse Ig and goat anti-rabbit Ig mAbs at 37°C. Data representative of at least 3 experiments.

### 6.2.21 Ability of F019/1A7 to induce ADCC in target cells with cross-linking

A number of studies have shown the importance of a mAb to induce ADCC in target cells *in vivo*. Therefore, F019/1A7 was assessed for its ability to cause cell death in OVCAR-4 cells. Figure 6.20 shows that even at a concentration of 30µg/ml, F019/1A7 is unable to induce PBMC-mediated cell lysis. However, with the addition of a rabbit anti-mouse antibody, cross-linked F019/1A7 is able to induce cell lysis (Fig 6.22).

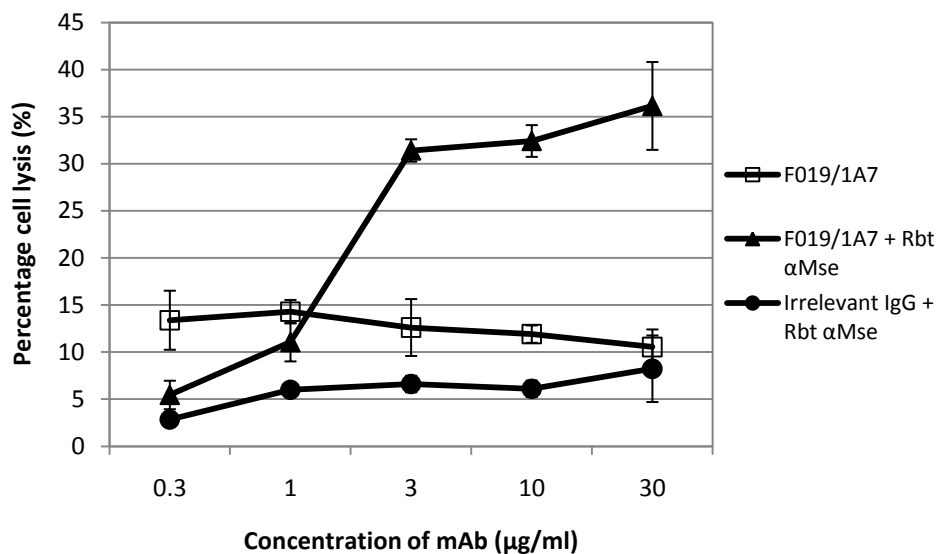


**Figure 6.22 F019/1A7 mediated ADCC of OVCAR-4 cells after cross-linking with rabbit anti-mouse Ig.**  $1 \times 10^5$   $\text{Chr}^{51}$  labelled OVCAR-4 cells were incubated with PBMCs isolated from human blood with either F019/1A7 or irrelevant IgG with or without rabbit anti-mouse Ig for 4 hours. Cell lysis was measured as a percentage of maximum – spontaneous  $\text{Cr}^{51}$  release. Error bars representing standard deviation of triplicate wells are present but may be obscured by data points. Data is representative of at least 2 experiments.

## 6.3 Discussion

In order to produce new ovarian anti-glycolipid mAbs, mice were immunised with whole cancer cells. It is well known that this is a good method for producing mAbs against cancer cells. The screening of mouse sera against whole ovarian cancer cells showed that immunisation with whole ovarian cancer cells gave a very strong antibody response. The resulting fusion yielded 3 anti-glycolipid mAbs that displayed good tumour selectivity, but were of the IgM isotype. IgM are too large for efficient tumour targeting, due to their inability to extravasate and were not further developed. These results suggested that although an anti-glycolipid antibody response was being induced they were not receiving the correct cytokine milieu to affinity mature and subclass switch to an IgG response. In order to increase the level of antibodies directed at non-protein targets, T cells were depleted in mice using an anti-CD4 mAb, in order to reduce the level of T cell help for B cell response to protein antigens and with the aim of allowing more of a T cell independent response. Despite drastic reduction in the number of T cells, antibodies against cells and not to the glycolipid extract were still produced, resulting in no anti-glycolipid mAbs. T cell-independent help has been shown to be provided by NK and iNKT cells increasing the level of B cell proliferation and IgG antibody production against TI antigens (Leadbetter et al., 2008; Mond et al., 1995). Studies have shown that poly(I:C), a synthetic homologue of double-stranded RNA is a potent stimulator of NK cells *in vivo* (Miyake et al., 2009; Wulff et al., 2010). Used as an adjuvant it has the ability to stimulate NK cells to interact with B cells either directly or indirectly (by producing IFN $\gamma$  and IL-4) which would provide a second signal to B cells (the first being Ig receptor clustering on the B cell surface (Mond *et al.*, 1979; Iber & Gruhn, 2006). This would stimulate B cells to produce antibodies and proliferate. In order to increase the T cell independent response immunisations included poly(I:C) along with whole ovarian cancer cells after CD4 depletion.

Although glycolipids were present in whole cell immunisations, protein antigens elicited the greatest response *in vivo*. Despite depleting T cells and the addition of an NK cell adjuvant to provide T cell

independent antigen help to B cells, a mouse anti-glycolipid response was not observed. Therefore, in order to create anti-glycolipid mAbs and remove the possibility of anti-protein mAbs being generated with whole cell immunisation, glycolipid was extracted from whole cancer cells for immunisation using a chloroform: methanol extraction. Previous studies have utilised immunisation of glycans to produce an antibody response to these antigens. An example being the sialyl Lewis x-keyhole limpet (KHL) conjugate immunised with a saponin adjuvant, which gave rise to both an IgM and an IgG immune response in mice (Ragupathi et al., 2009). Colorectal cancer cell derived glycolipid was first used for immunisation due to the ability to use both 505/4 and 692/29 as positive controls for glycolipid binding in screening assays. Immunising with colorectal cancer-glycolipid alone to increase the level of mAbs to glycolipid proved unsuccessful with no response to either glycolipid or whole cells. With the in-house characterisation of an anti-ovarian cancer glycolipid mAb, F002, it was possible to immunise with ovarian cancer glycolipid extract, using F002 as a positive control in screening assays. Immunisation with ovarian cancer glycolipid was undertaken to ensure that the lack of response to colorectal cancer glycolipid observed was not tissue specific, however, no response to either cell or glycolipid extract was observed. Studies have shown that activation of B cells requires the clustering of BcRs upon antigen binding (Mond et al., 2005; Barral et al., 2008). This along with our results suggested that glycolipid alone is unable to stimulate B cells to proliferate or produce antibodies. In order to increase the chance of BcR clustering, ovarian cancer cell glycolipid was incorporated into liposomes. This has previously been reported when isoglobotetraosylceramide, a tumour-associated glycolipid, was inserted into liposomes which resulted in an array of anti-cancer cell antibodies (Brodin et al., 1986). As well as tumour-associated glycolipid,  $\alpha$ GalCer was also incorporated into the liposomes to provide stimulation of NKT cells.  $\alpha$ GalCer, a glycosphingolipid originally isolated from the marine sponge *Agelas mauritanus*, is a potent stimulator of NKT cells due to its long half-life and strong binding to the iNKT TCR (Sidobre et al., 2004). It has been shown to be presented by the  $\beta$ 2-microglobulin-associated class I-like molecule, CD1d, to NKT cells, leading to their activation *in vivo* (Leadbetter et al., 2008; Naidenko et

al., 2000). The activation of NKT cells would lead to the production of IL-4 and IFN $\gamma$ , stimulating B cells in the absence of T cell help (Barral et al., 2008; Huang et al., 2004). Ovarian cancer cell glycolipid was incorporated into liposomes yielding an immune response to ovarian cancer cells. Liposomes with 2.5% ovarian cancer glycolipid alone stimulated a response to both cells and glycolipid with an improved response with the addition of  $\alpha$ GalCer. Fusions yielded IgM antibodies that bound to fixed but not fresh cells suggesting that the response was to intracellular antigens and CSR had not been achieved. Immunisation with 2.5% ovarian cancer glycolipid and  $\alpha$ GalCer was repeated with the addition of a whole cell boost in order to encourage class switching from IgM to IgG. This yielded an IgG response and the splenocytes were fused. The resulting hybridomas yielded F019/1A7 and F019/1D3 that bound to fresh ovarian cancer cells as well as glycolipid and not to PBMCs or HUVEC. Both F019/1A7 and F019/1D3 bound to a range of ovarian cancer cell lines but not OVCA 433 cells and less strongly to a range of colorectal cell lines, including Colo 201, Colo 205 and LoVo. Cell line distribution suggested that F019/1A7 and F019/1D3 were in fact binding to the same antigen so F019/1A7 was taken forward. Despite binding to OVCAR-3, OVCAR-4, OAW28 and OAW42 cells, anti-glycolipid ELISA revealed that F019/1A7 only bound to OAW42 glycolipid extract. However, subsequent work and increased sensitivity of the anti-glycolipid screen has shown that F019/1A7 does bind to glycolipid extracted from F019/1A7 antigen positive cell lines (unpublished data). To study whether the F019/1A7 functions similarly to the anti-glycolipid mAbs 692/29 and 505/4, the direct killing activity of F019/1A7 was assessed. No direct cell death activity was observed when F019/1A7 was incubated overnight with OVCAR-4 or OAW42 cells, with no increase in PI uptake or decrease in cell number observed. Further characterisation of F019/1A7 revealed an inability of the mAb to induce ADCC or CDC in ovarian cancer cells. However, with the addition of a cross-linking antibody, cell lysis was observed. This inability to induce ADCC without a cross-linking agent may be due to low affinity of the mAb. It has been shown that a large proportion of T1 antigen-directed mAbs have a low level of hypermutation (Stein, 1992; Toellner et al., 2002), therefore have not been affinity matured. This has since been confirmed by sequencing F019/1A7 which had a

low level of mutation from germline (unpublished data). Random site mutagenesis may increase the affinity of F019/1A7, increasing its effector functions. In order to determine the distribution that could be expected *in vivo*, F019/1A7 was screened on 362 samples of ovarian cancer tissue by TMA. This revealed that F019/1A7 bound to 88% of the ovarian tumours stained, with only 12% showing no staining. This suggests that F019/1A7 could bind to a high proportion of ovarian tumours *in vivo*, with binding to all types and grades of ovarian cancer. However, screening of F019/1A7 against a panel of normal tissue by TMA showed that the mAb bound to a range of normal tissues. This may make F019/1A7 unsuitable for therapy. However, F019/1A7 was screened against fresh, normal hepatocytes and PBMCs with minimal binding seen, despite binding moderately to liver and weakly to tonsil on the TMA. The disparity between the two results may be due to F019/1A7 binding to intracellular antigen on the TMA, which would be inaccessible therapeutically. Furthermore, if F019/1A7 binds to a carbohydrate moiety on glycolipids and glycoproteins, incomplete synthesised glycans can be present in the ER and Golgi apparatus of normal tissues and may be bound by F019/1A7, but once completely synthesised and presented on the cell surface, F019/1A7 may no longer bind. In cancer, the carbohydrate antigen may not be completely synthesised, allowing it to be bound by F019/1A7. Another factor to take into account is whether IHC binding reflects *in vivo* binding. EGFR is overexpressed on a range of epithelial-derived tumours and despite the presence of EGFR on normal cells, the chimeric, anti-EGFR mAb cetuximab shows restricted toxicity to the skin (Busam et al., 2001; Gullick, 1991). Interestingly, the level of F019/1A7 staining showed an inverse correlation with survival, with lower levels of staining predicting a better survival. F019/1A7 also correlated with tumour grade and type. These results and the ability of F019/1A7 to bind to glycolipid pose the question of whether its antigen is a carbohydrate involved in adhesion or metastasis, leading to decreased survival with more expression. Similar examples are mucin-4 and Lewis y which are involved in the adhesion and metastasis of ovarian cancers (Li et al., 2011; Ponnusamy et al., 2010).



Despite the binding of F019/1A7 to normal tissue, the method of incorporating liposomes with ovarian cancer glycolipid and  $\alpha$ GalCer has shown that anti-glycolipid mAbs can be produced. Further development of the immunisation protocol may yield promising, tumour-specific mAbs, with the ability to bind glycolipid, with the possibility of mAbs causing direct cell death as observed with other anti-glycan mAbs. One way in which to increase the efficacy of the immunisation protocol may be to alter the immunisation schedule. Studies have shown that repeated immunisation with  $\alpha$ GalCer could lead to NKT cell anergy, with a decrease in cytokine production and reduced proliferation of NKT cells (Parekh et al., 2005; Uldrich et al., 2005). However, these studies use soluble  $\alpha$ GalCer, whereas a more recent study has shown that immunising repeatedly with nanoparticle formulated  $\alpha$ GalCer leads to repeated activation of NKT cells, without any observed energy (Thapa et al., 2009). This model would be closer to our model which uses  $\alpha$ GalCer incorporated into liposomes. More important are effects of  $\alpha$ GalCer on the dynamics of NKT cells, with studies showing a nearly complete loss of NKT cells due to transient expression of the iNKT cell receptor, followed by reappearance after 24-48 hours, before proliferation of NKT cells to 10-times their normal levels after 3 days, before reducing to normal levels by day 6-9 (Uldrich et al., 2005). Immunisation with  $\alpha$ GalCer-containing liposomes 3 days before immunising with tumour glycolipid-containing liposomes could make most use of the activated NKT cells. Modification of the glycolipid extraction method may lead to a better immunogen. For example, isolation and glycolipid extraction of the plasma membrane or lipid rafts may provide a more limited immunogen directed at more functional glycolipids. TI antigens lack T cell help, resulting in a predominantly IgM response, with low somatic hypermutation, resulting in a low affinity response. This is evidenced by the low level of mutation observed in the sequence of F019/1A7. Adjuvants could be used to increase class switching and somatic hypermutation, resulting in higher affinity mAbs. One example is the administration of anti-CD40 mAb alongside the immunogen. The anti-CD40 mAb could substitute T cell help, providing a second signal to the B cells. Evidence from a study immunising mice with bacterial pathogens and an anti-CD40 mAb displayed an increased antigen-specific antibody response to the pathogen with

an increase in class switching to IgG, showing that the anti-CD40 mAb could substitute for T cell (Dullforce et al., 1998).

In conclusion, anti-glycolipid antibodies are proven to bind tumour cells specifically and can induce direct killing of those cells. This study outlines a series of immunisation methods with the aim of producing anti-glycolipid mAbs. Cell based immunisations produce a good anti-tumour cell response, but only an IgM anti-glycolipid response. Glycolipid is a poor immunogen if immunised alone, however if incorporated into liposomes along with  $\alpha$ GalCer and immunised followed by a whole cell boost, an IgG anti-glycolipid response can be observed. This study has shown that fusion of responding splenocytes can be fused and cloned, producing anti-glycolipid mAbs that have the ability to bind to a large proportion of ovarian cancers, with binding not restricted to one type or grade of cancer. Unfortunately, the mAb produced in this instance bound to a range of normal tissue, although the significance of this on *in vivo* effect could be further assessed. Further development of the technique may yield more specific mAbs, with the ability to bind to cancer glycolipid and cause cancer cell death either independently or in combination with human PBMCs or complement.

## Chapter 7 Final Discussion

### What is the therapeutic potential of mAbs?

The growth of mAb production for therapeutic use has seen great success with 22 mAbs being approved for treatment in the last 25 years. These mAbs have revolutionised the treatment of cancer, greatly increasing the response rate compared to standard therapy alone. Examples include rituximab and cetuximab which are used in first-line treatments of cancer (Coiffier et al., 2002; NICE, 2009; Van Cutsem et al., 2009). Success of therapeutic mAbs is owed to their ability to bind their target with high affinity and functionality and their generally lower toxicity than traditional therapies. The number of mAbs entering clinical trials is increasing each year and they have a higher approval success rate compared to new small-molecule drugs; chimeric and humanised mAbs have an FDA approval rate of 26 and 18% respectively, with small-molecule drugs having a FDA-approval rate of 11%; (Reichert & Pavolu, 2004; Reichert, 2011; Reichert et al., 2005). These factors show that mAb therapy remains an important area of research.

### Why target glycolipids?

Glycolipids have been shown to be overexpressed on the surface of many tumour types (Hakomori & Zhang, 1997; Hakomori, 2008). Studies have shown that glycolipids are good targets for mAb therapy (Durrant et al., 2006; Loo et al., 2007; Zhang et al., 2010a). All mAbs approved to date, have protein targets, illustrating that membrane glycolipids are a potential area for novel mAb target discovery. Furthermore, studies into the functional role of glycolipids has shown that they form glycosynapses on the cell membrane and associate with functional proteins that effect a wide range of cellular processes, such as cell adhesion, growth and proliferation (Hakomori, 2008). In addition, a remarkable number of mAbs generated against glycolipids have the ability to induce direct cell death in target cells without the need for effector cells or complement (Alvarez-Rueda et al., 2007; Chou et al., 1998; Hellstrom et al., 1990; Loo et al., 2007; Zhang et al., 2010a; Zhong et al., 2001).

The premise of this thesis therefore, was to further characterise two anti-cancer associated glycolipid-targeted murine mAbs produced in-house. One aspect of this was to assess whether their ability to cause direct cell death would be useful by evaluating the level of apoptosis in colorectal cancer. Furthermore, this thesis set out to develop a platform for the production of anti-cancer associated glycolipid mAbs. By combining these two areas, this thesis aimed to determine whether cancer-associated glycolipid targeted mAbs would be viable therapeutics.

### **What are the ideal antigens?**

In both the characterisation of existing mAbs and the development of new mAbs, the criteria for a therapeutically valuable mAb remain the same. The properties of such a mAb can be distilled into two main properties; efficacy and safety. The most important factor in mAb production/characterisation is the target antigen and its specificity which relates to both efficacy and safety. Ideally the target antigen would be expressed at high levels on the cell surface and be specific to cancer cells, thereby reducing toxicity caused by binding normal cells. Desirably, the target antigen would be expressed on a high percentage of tumours and not be limited to one subset (e.g. type or grade) of the target cancer. Even more desirable would be the expression of the antigen on a range of cancers originated in different sites. An example of this is the use of cetuximab in the treatment of both colorectal and head and neck cancers (Blick & Scott, 2007). In this thesis two anti-glycolipid mAbs have been characterised and compared to mAbs with similar target antigens. 505/4 and 692/29 have been shown to bind to both glycolipids and glycoproteins. Analysis by glycan array binding (Consortium For Functional Glycomics) revealed that 505/4 binds to the sialyl Lewis a glycan and other related molecules, with 692/29 binding to a unique epitope on both Lewis y and Lewis b glycans. Lewis antigens are good targets as they are overexpressed on a range of cancers and are expressed at low levels of expression normal tissues. *In vitro* distribution studies showed that 505/4 bound to 90% of colorectal cancer tissues and had limited binding to normal tissues. *In*

*vitro* cell line analysis of 692/29 showed a good distribution across the majority of colorectal and some ovarian cancer cell lines, suggesting that both mAbs could have good *in vivo* distribution.

As well as tumour-specificity, a mAb would have a functional effect, killing the cancer cells by a variety of mechanisms, as most approved mAbs cause tumour cell death by more than one mechanism.

### **Functionality of the anti-tumour mAb**

The ability to induce cytotoxicity by more than one mechanism increases the efficacy of a mAb, for example through the induction of ADCC, CDC, inhibition of angiogenesis, blocking intracellular signalling and induction of direct cell death. A good example of this is the anti-CD20 mAb rituximab which is one of the most successful mAbs in cancer therapy. Rituximab has been shown to eliminate CD20+ B cells via three different mechanisms; ADCC, CDC and direct cell death (Pescovitz, 2006). ADCC has been shown to be a key factor in antibody-mediated cytotoxicity in a number of approved mAbs. For example, cancers can become resistant to trastuzumab treatment and this has been shown to be mediated by an increased resistance to perforin and granzyme-mediated cell death, suggesting that resistance to ADCC significantly reduces the efficacy of trastuzumab *in vivo* (Kawaguchi et al., 2009). Evidence has also shown that the FcγRIIIa receptor 158V allotype displays a higher affinity for human IgG1 and increased ADCC (Koene et al., 1997) and rituximab-mediated response was greater in patients with this polymorphism than those without, highlighting the importance of ADCC as an effector function (Cartron et al., 2002). As well as inducing cellular cytotoxicity via effector cells mAbs can cause the formation of MAC complexes on target cells by activating the complement cascade. The anti-CD20 mAbs rituximab and ofatumumab have been shown to induce potent CDC, contributing to their *in vivo* efficacy (Lin, 2010; Pescovitz, 2006).

As well as the traditional mechanisms of action described above, mAbs can have antigen-associated effects. An example of this is the growth inhibition seen in cells that have been blocked with

trastuzumab. By binding HER2 trastuzumab has the ability to block intracellular signalling involved in cell growth, proliferation and apoptosis (Delord et al., 2005). By binding to all isoforms of VEGF, often overexpressed by tumours and tumour-associated stromal cells (Fukumura et al., 1998; Hicklin & Ellis, 2005), bevacizumab blocks binding of VEGF to its receptor, VEGFR, therefore inhibiting angiogenesis, resulting in a reduction in tumour growth (Shih & Lindley, 2006).

As well as potently inducing ADCC and CDC rituximab has also been shown to induce direct cell death in target cells, although the mechanism by which this occurs has been disputed. Conflicting evidence suggest a role of translocation of CD20 into lipid rafts bound by anti-CD20 mAbs resulting in signalling via p38 MAP-kinase (Cardarelli et al., 2002; Pedersen et al., 2002). However, other studies have suggested that rituximab-mediated cell death is independent of caspases and lipid raft translocation (Chan et al., 2003; Daniels et al., 2008).

A greater number of effector mechanisms, however, do not necessarily result in a better therapeutic response. An example is the fully human IgG2 mAb panitumumab, which binds to EGFR with a very high affinity and is a good competitive inhibitor of EGF (Yang et al., 2001). If it were engineered as an IgG1 in order to induce ADCC, it may induce toxicity to normal cells due to its high affinity for the antigen (Cohenuram & Saif, 2007). Although studies into the mechanism of action of rituximab have shown an important role for CDC, a study investigating the importance of ADCC demonstrated that rituximab-mediated C3b deposition on CD20+ cells inhibited the interaction between NK cells and the Fc region of rituximab, therefore inhibiting ADCC (Wang et al., 2008). Defucosylation of IgG can lead to an increase in ADCC *in vitro*, therefore creating classes of IgG that could induce ADCC and not CDC (IgG2 and IgG4; (Niwa et al., 2005)). The engineering of a defucosylated, IgG2 or IgG4, anti CD20-specific mAb capable of mediating potent ADCC and not CDC, may increase efficacy *in vivo* of anti-CD20 mAbs.

Both 505/4 and 692/29 show direct killing activity, with evidence suggesting that this is independent of apoptosis. This may be of therapeutic value, especially as a hallmark of tumour development is

resistance to apoptosis (Fulda, 2009). Results of this thesis suggest that tumours with a lower level of caspase-3 activation significantly correlate with a worse prognosis. Therefore, 505/4 and 692/29 may be able to improve survival rates in a group that have a worse prognosis.

Both 505/4 and 692/29 bind to highly expressed antigens on cancer cells, with minimal binding to normal cells and the ability to cause direct cell death. Interestingly, other mAbs tested in this thesis directed against Lewis y, Lewis a and sialyl Lewis a have been able to induce direct cell death in an apoptosis-independent manner (BR96 and CA19.9). Other mAbs have also been shown to cause similar toxicity. RAV12, a chimeric mAb recognises a minimal epitope of Gal $\beta$ 1-3GlcNAc $\beta$ 1-3Gal (a Lewis antigen precursor) on the N-linked carbohydrate antigen RAAG12 and induces oncosis of target cells. RAV12 has been shown to induce oncosis in colorectal cancer cell lines (Loo et al., 2007). F77, a chimeric mAb has been shown to induce oncosis by binding a prostate cancer-specific glycolipid (Zhang et al., 2010a). These studies as well as this thesis show a trend for anti-Lewis mAbs to induce oncosis-like cell death in target cells, suggesting that Lewis antigens have a functional role on the cell surface, as part of an altered glycoprotein or glycolipid. The mechanism of direct cell death caused by anti-glycan mAbs is as yet undiscovered.

The anti-glycan mAbs described above have all been shown to kill independently of apoptosis, with an oncosis-like mechanism being a common theme. BR96 and the recently described human anti-sialyl Lewis a mAb, 5B1, have both been shown to be internalised upon binding to antigen on the target cell (Garrigues et al., 1993; Sawada et al., 2011). Furthermore, BR96 has been shown to be degraded by lysosomes once internalised (Garrigues et al., 1993). These observations may suggest that binding of mAb to the cell surface causes cellular stress or activates an intracellular pathway, leading to the formation of an autophagosome, which is then degraded by the lysosome. This would facilitate the uptake of PI or dextran beads observed in this study and the degradation of BR96 observed previously, although it does not account for the cellular swelling observed after mAb treatment. One of the hallmarks of oncosis is the depletion of ATP, leading to Na<sup>+</sup> and Ca<sup>2+</sup> intake, followed by cellular and organelle swelling (Eguchi et al., 1997; Majno & Joris, 1995). Anti-glycan mAbs may

initiate oncosis through the internalisation of mAb and membrane, prompting the cell to synthesise more membrane components, such as cholesterol, sphingomyelin, ceramide, in an ATP-dependent manner. This could lead to the depletion of ATP, resulting in cellular swelling and ultimately cell death. The calpain family of proteins are  $\text{Ca}^{2+}$ -dependent proteases that have been shown to be activated in oncosis (Liu et al., 2004). Increased cytoplasmic levels of  $\text{Ca}^{2+}$  leads to the activation of calpains, which have a number of substrates. These include components of the actin cytoskeleton-plasma membrane junction. Calpain-mediated proteolysis of these proteins can lead to increased plasma membrane permeability (Liu & Schnellmann, 2003). The binding of anti-glycan mAbs may lead to the influx of  $\text{Ca}^{2+}$  and calpain activation, followed by cytoskeleton-associated plasma membrane permeability.

Further investigation into the mechanism by which anti-glycan mAbs induce apoptosis-independent cell death is warranted.

The mAbs 505/4 and 692/29 were compared to other mAbs directed at similar antigens, whose binding was first analysed on a glycan array. Upon *in vitro* comparison sialyl Lewis a, Lewis a and Lewis y-directed mAbs all mediated direct cell death in the absence of effector cells or complement. 2-25 LE, directed at Lewis b failed to induce direct cell death, despite binding at similar levels. This suggests that Lewis y, Lewis a and sialyl Lewis a, but not Lewis b, in this instance, are functional targets for mAb therapy with mAb binding initiating direct cell death. The specificity of 692/29 to both Lewis y and Lewis b may relate to better *in vivo* efficacy than that seen with the BR96-doxirubicin mAb conjugate (Tolcher et al., 1999). In this study, BR96 showed cytotoxic effects against cell lines with high and low levels of antigen by ADCC, CDC and direct cytotoxicity, compared to 692/29 that showed cytotoxicity only in cell lines with a high expression of Lewis y/b.

## Human mAbs

In order to transfer into the clinic, chimerising or humanising the mAbs would further increase their efficacy. Producing chimerised, IgG1 versions of the mAbs in a *FUT8* knockout could increase the



ability of the mAbs to induce ADCC *in vivo*, as well as reduce immunogenicity, increasing their *in vivo* half-life. An interesting feature of all anti-Lewis mAbs tested in this thesis was the ability for them to bind cells at very high levels, without saturating the antigen. Furthermore, the mAbs had the ability to bind to cells that have already been incubated with a high concentration of mAb. These are properties of homophilic mAbs, which have been previously described against glycolipid antigens (Kaminski et al., 1999). It would be important to test any chimerised or humanised mAbs for their ability to bind target cells as well as their murine counterparts, as the homophilic property of the murine mAbs may affect their *in vivo* efficacy.

The type of antibody used also has an effect on the efficacy and safety of a therapeutic mAb. The first mAbs to be used were fully murine, grown as hybridomas. However, immunogenicity and Fc incompatibility of murine mAbs reduced their *in vivo* potency. However, murine mAbs have been approved for treatment, including muromonab-CD3 and <sup>131</sup>I-tositumomab. The success of muromonab-CD3 was partly due to the fact that patients undergoing kidney transplant were also administered with immunosuppressants, reducing the HAMA response. <sup>131</sup>I-tositumomab was successful due to its radioactive isotope which allow only small amounts of mAb to be administered, with a good anti-tumour response (Cheung et al., 2009). Engineering of chimeric mAbs showed a reduced level of HAMA response, with humanised mAbs further reducing the level of immunogenicity (Hwang & Foote, 2005). Fully human mAbs have been shown to be the least immunogenic, for example panitumumab, which has shown no HAMA response and very low levels of toxicity in clinical studies (Cohenuram & Saif, 2007). Some human mAbs can still elicit an antibody response, although HAMA levels are generally low and results do depend on detection methods (Scott & De Groot, 2010).

## Serum half-life

As well as the ability to bind specifically to cancer cells and to cause cytotoxicity to those cells, mAbs need to have a long half-life in order to reach the target and have increased efficacy. As well as

increasing efficacy, a longer half-life decreases the administration frequency that could result in a decreased in HAMA/HAHA response, depending on the nature of the mAb. Engineering of the Fc region to increase affinity for the FcRn at pH 6.0, resulting in FcRn mediated recycling of the mAb into circulation could also increase the half-life of a mAb (Dall'Acqua et al., 2006).

## Other potential targets

During the characterisation of 505/4 and 692/29, this thesis investigated the level of apoptosis in a cohort of colorectal cancers. Results showed that the level of apoptosis in the tumour significantly correlated to patient survival. However, a low level of apoptosis in the tumour-associated stroma rather than the tumour itself was an independent marker of bad prognosis. The tumour microenvironment has become more and more studied over the past decade. It is accepted that tumours are able to evade immune detection by manipulating their microenvironment through the release of cytokines and other soluble factors in order to create an immunosuppressive environment as well as downregulating stress molecules on their surface (Ostman & Augsten, 2009; Watson et al., 2006c). The creation of an immunosuppressive environment involves the production of pro-tumour phenotype of a variety of cell types. The creation of cancer-associated stromal cells may be an interesting source of new mAb targets. Therapeutics aimed at the microenvironment have been tested, targeting a range of stromal elements. An example is the humanised mAb sibrotuzumab which is directed at the CAF-associated protein FAP $\alpha$  and showed good *in vivo* distribution in patients with the mAb targeted at tumour-associated stroma and minimal normal tissue binding (Scott et al., 2003), although no anti-tumour responses have been observed with sibrotuzumab *in vivo* (Hofheinz et al., 2003). However, a more recent anti-FAP mAb-maytansinoid (tubulin binding cytotoxic agent) conjugate, FAP5-DM1, showed inhibition of tumour growth in various solid tumour xenograft models (Ostermann et al., 2008) as did PF-5412, a mAb targeted at integrin $\alpha$ 1 $\beta$ 5, which is overexpressed on both tumour-associated stroma and tumour cells (Li et al., 2010). These studies show that mAb therapy targeted at tumour-associated cells could inhibit establishment of the

tumour microenvironment by recruiting immune effector cells and destruction of pro-tumour cells. Studies have shown that incubation of fibroblasts with tumour cells can lead to the transformation of fibroblasts into CAFs (Tyan et al., 2011). Extraction of *in vitro*-activated CAF glycolipid and immunisation could lead to an anti-CAF mAb response. Any resulting mAbs directed at glycolipid may have direct killing ability, as observed in other anti-glycan mAbs. Due to the close proximity of the tumour and its environment the possibility of a bi-specific mAb targeting more than one molecule could produce a potent anti-tumour response, with the previously described catumaxomab demonstrating proof of principle of this type of mAb.

As well as the characterisation of previously produced mAbs 505/4 and 692/29 this thesis set out to develop an immunisation protocol to produce anti-ovarian cancer-associated glycolipid mAbs in order to find novel tumour-associated targets for mAb therapy. Results suggested that immunisation of glycolipid alone is a weak immunogen, but by incorporating tumour glycolipid into liposomes and immunising with the NKT cell adjuvant,  $\alpha$ GalCer, anti-cancer glycolipid mAbs could be produced. The level of IgG response was lower than with whole cell immunisation and there was a tendency for IgG to be targeted to intracellular antigens. Despite this, an anti-cancer associated glycolipid mAbs was produced, with good levels of binding to a large percentage of ovarian cancer tumours. This provides a unique method for the production of mAbs targeted tumour cell glycolipids. Regrettably, F019/1A7 bound to a range of normal tissues by immunohistochemistry, although this would need to be validated in another setting. Further investigation of the immunisation protocol, using more cell surface-specific cancer-associated glycolipids and adjustments to adjuvant help may provide an immunisation protocol capable of producing mAbs directed at novel, functional cancer-specific glycolipid molecules on a range of cancers.

## Summary

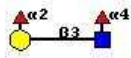
Therapeutically valuable mAbs work by employing a variety of effector functions to reduce tumour size and growth. The 692/29 and 505/4 anti-colorectal cancer mAbs were produced in house and

previously characterised to various degrees. 692/29 was shown to bind to a large proportion of colorectal tumours, with minimal binding observed to normal tissues by IHC. Preliminary antigen discovery using TLC revealed specificity for both Lewis y and Lewis b blood group antigens. 505/4 was selected as a candidate for further characterisation due to its ability to bind to a number of colorectal cell lines and colorectal cancer cell line glycolipid. Preliminary TLC analysis of antigen specificity showed binding of 505/4 to a sialyltetrasylceramide.

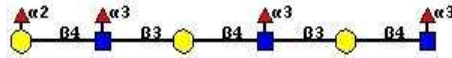
In chapters 4 and 5 the Consortium for Functional Glycomics glycan array was used to confirm the fine specificity of 692/29, with results showing binding predominantly to Lewis b as well as Lewis y-containing glycans. Furthermore, using this resource allowed the discovery of the specificity of 505/4 to sialyl Lewis a as well as sialyl di-Lewis a, with no cross-reactivity with other blood group antigens. Comparison with other anti-Lewis mAbs directed at Lewis y, Lewis b and Lewis a revealed that the fine specificity of the mAbs differed, despite apparent binding to the same antigen (Fig 7.1). Figure 6.1 shows that the anti-Lewis y and Lewis b mAbs appear to recognise different aspects of the antigens, with 2-25 LE showing specificity for the minimal epitope Gal $\beta$ 1-3GlcNAc and BR96 Gal $\beta$ 1-4GlcNAc. 505/4 shows specificity for the sialyl Lewis a glycan, with CA19.9 recognising sialylated Gal $\beta$ 1-3GlcNAc. 692/29 and 7LE, however, do not have an obvious binding specificity when the three top-binding glycans are compared. The effect of differences in fine specificity of the mAbs was assessed in this study, with varying levels of cell binding or death observed. This was most apparent with anti-Lewis y and Lewis b mAbs, with anti-sialyl Lewis a/Lewis a mAbs showing similar patterns of *in vitro* characteristics. Although there may be a difference to *in vivo* binding due to abundance or accessibility of certain glycans on the cell surface, the glycan array is a useful tool in easily identifying anti-glycan mAb targets and their fine specificity.

This study provided preliminary evidence of non-saturable mAb binding to tumour cells, termed homophilic binding, by the anti-Lewis mAbs analysed. The results suggested that despite a large number of mAb molecules, antigen saturation was not achieved. Further characterisation of this

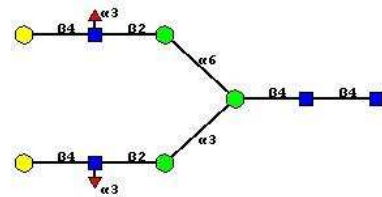
692/29



Lewis b

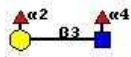


Lewis y-x-x

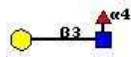


Lewis x-containing

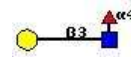
2-25 LE



Lewis b

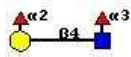


Lewis a

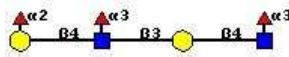


Lewis a

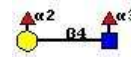
BR96



Lewis y

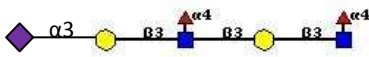


Lewis y-x

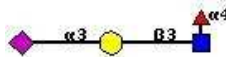


Lewis y

505/4



Sialyl di-Lewis a

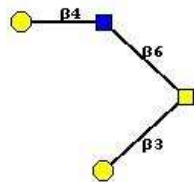


Sialyl Lewis a

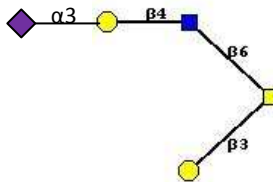


Sialyl Lewis a

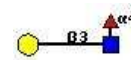
7LE



Type II precursor

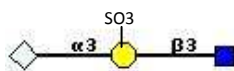


Sialylated Type II precursor

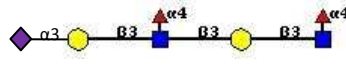


Lewis a

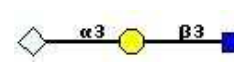
CA19.9



Sialylated, sulfo Type-1 precursor



Sialyl di-Lewis a



Sialylated Type-1 precursor

**Figure 7.1** The binding of anti-Lewis mAbs to their antigens according to The Consortium for Functional Glycomics's array binding data. The binding of 692/29, 2-25 LE, BR96, 505/4, 7LE and CA19.9 to the glycan array is represented by the glycans bound most strongly by the mAbs (Strongest-weakler binding; left to right). A blue squares represents glucosylamine, yellow circles represents galactose, red triangles represent fucose, green circles represent mannose and purple diamond represents sialic acid.

phenomenon could provide evidence of a mAb property that may be therapeutically useful, providing the mAb with a greater avidity *in vivo*. Conversely, the ability to bind homophilically may reduce the ability of the mAb to penetrate a solid tumour, resulting in a lower efficacy. Further characterisation of the mAbs using antigen to inhibit self-self binding or modelling and site-directed mutagenesis may provide further evidence for homophilic binding.

An interesting mechanism displayed by a number of approved mAbs is the ability to cause direct cell death of target cells, without the need for immune cells or complement. Previous studies with the anti-Lewis y mAb, BR96, revealed its ability to cause direct cell death of antigen positive cell lines.

This prompted the analysis of the ability of 692/29 and 505/4 to cause direct cell death. Chapters 4 and 5 of this thesis revealed that both 505/4 and 692/29 mAbs were able to induce direct cell death in antigen positive cell lines. Further to this, investigation into the mechanism of cell death suggested that both mAbs may cause direct cell death independently of apoptosis. One hallmark of oncosis is the formation of large pores on the cell surface of mAb-bound cells. Analysis using electron microscopy may provide further evidence of mAb-mediated oncosis.

Other mAbs have been shown to induce direct cell death in an apoptosis independent manner. An example being rituximab, which has been shown to induce direct cell death independently of apoptosis (Daniels et al., 2008). In order to determine the therapeutic value of a mAb's ability to induce direct cell death independently of apoptosis, this study determined the level of apoptosis in colorectal cancer using a large TMA cohort. Results in chapter 3 revealed that the level of apoptosis in the tumour-associated stroma is an independent prognostic factor for patient survival in colorectal cancer. In addition this study revealed a strong correlation of apoptosis with the immune marker MHC-II, suggesting a role of an immunosuppressive environment in tumour progression. Therefore, the ability of a mAb to induce direct cell death may be vital in tumours with an immune suppressed environment. This study demonstrated the importance of the tumour microenvironment in tumour progression. This may be a represent target for therapy either alone or combined with

anti-tumour agents. One limitation of this study is the possible variability of CC3 in different areas of a tumour. As this study used TMA technology, only one area of a tumour was assessed. Whole sections, analysing the level of apoptosis across a larger area, or a larger cohort of patients may further validate the results of this study.

Glycans and as a result, glycolipids are aberrantly expressed on the cell surface. A growing area of research has shown the importance of glycolipids on the cell surface of cells *in vitro* as part of functional sub-domains, which exist to allow optimal function of a number of membrane proteins. Disruption of membrane protein-associated glycolipids has been shown to have a functional effect. In order to take advantage of binding a functional glycolipid and perhaps discover novel, tumour-associated glycolipids, this study performed a series of investigations to improve the immunogenicity of tumour-associated glycolipid with the aim of developing a protocol for the production of anti-glycolipid mAbs. Previously anti-glycolipid mAbs have been produced from whole cell immunisations or isolated from patient serum and identified as anti-glycolipid mAbs. Chapter 6 resulted in the production of a new anti-glycolipid mAb, F019/1A7, providing proof of principle that the novel immunisation protocol incorporating tumour glycolipid into liposomes with an iNKT cell adjuvant,  $\alpha$ GalCer, can yield anti-glycolipid mAbs. A limitation of this protocol is that a small number of anti-glycolipid mAbs were produced. A direct comparison to a whole cell immunisation would allow quantification of the effectiveness of the protocol developed. Further to the work carried out in this thesis, the group have been successful in producing a number of anti-glycolipid mAbs against ovarian, pancreatic and gastric cancers, using a protocol based on the one developed in this thesis. It would be interesting to see results of further characterisation of these mAbs show good tissue distribution and any anti-tumour effects. Future development of this protocol should centre on improving the reaction of antibodies produced with cell surface antigens with a functional effect. This may be achieved by immunising with cell membrane sub-domains that may contain more functional, cell surface glycolipid molecules.

## Bibliography

- Abe, K., Hakomori, S. & Ohshiba, S. (1986). Differential expression of difucosyl type 2 chain (LeY) defined by monoclonal antibody AH6 in different locations of colonic epithelia, various histological types of colonic polyps, and adenocarcinomas. *Cancer Res*, **46**, 2639-44.
- Adams, C.W., Allison, D.E., Flagella, K., Presta, L., Clarke, J., Dybdal, N., McKeever, K. & Sliwkowski, M.X. (2006). Humanization of a recombinant monoclonal antibody to produce a therapeutic HER dimerization inhibitor, pertuzumab. *Cancer Immunol Immunother*, **55**, 717-27.
- Adegboyega, P.A., Mifflin, R.C., DiMari, J.F., Saada, J.I. & Powell, D.W. (2002). Immunohistochemical study of myofibroblasts in normal colonic mucosa, hyperplastic polyps, and adenomatous colorectal polyps. *Arch Pathol Lab Med*, **126**, 829-36.
- Ahonen, C., Manning, E., Erickson, L.D., O'Connor, B., Lind, E.F., Pullen, S.S., Kehry, M.R. & Noelle, R.J. (2002). The CD40-TRAF6 axis controls affinity maturation and the generation of long-lived plasma cells. *Nat Immunol*, **3**, 451-6.
- Alberts, B., Johnson, A., Lewis, J., Raff, M., Roberts, K., Walter, P. (2002). *Molecular biology of the cell*. Garland Science: New York, USA.
- Allan, L.L., Hoefl, K., Zheng, D.J., Chung, B.K., Kozak, F.K., Tan, R. & van den Elzen, P. (2009). Apolipoprotein-mediated lipid antigen presentation in B cells provides a pathway for innate help by NKT cells. *Blood*, **114**, 2411-6.
- Alvarez-Rueda, N., Leprieur, S., Clemenceau, B., Supiot, S., Sebille-Rivain, V., Faivre-Chauvet, A., Davodeau, F., Paris, F., Barbet, J., Aubry, J. & Birkle, S. (2007). Binding activities and antitumor properties of a new mouse/human chimeric antibody specific for GD2 ganglioside antigen. *Clin Cancer Res*, **13**, 5613s-5620s.
- Angenieux, C., Salamero, J., Fricker, D., Cazenave, J.P., Goud, B., Hanau, D. & de La Salle, H. (2000). Characterization of CD1e, a third type of CD1 molecule expressed in dendritic cells. *J Biol Chem*, **275**, 37757-64.
- Anthony, R.M. & Ravetch, J.V. (2010). A novel role for the IgG Fc glycan: the anti-inflammatory activity of sialylated IgG Fcs. *J Clin Immunol*, **30 Suppl 1**, S9-14.
- Arnold, J.N., Wormald, M.R., Sim, R.B., Rudd, P.M. & Dwek, R.A. (2007). The impact of glycosylation on the biological function and structure of human immunoglobulins. *Annu Rev Immunol*, **25**, 21-50.
- Aruffo, A., Farrington, M., Hollenbaugh, D., Li, X., Milatovich, A., Nonoyama, S., Bajorath, J., Grosmaire, L.S., Stenkamp, R., Neubauer, M. & et al. (1993). The CD40 ligand, gp39, is defective in activated T cells from patients with X-linked hyper-IgM syndrome. *Cell*, **72**, 291-300.
- Ashkenazi, A. & Herbst, R.S. (2008). To kill a tumor cell: the potential of proapoptotic receptor agonists. *J Clin Invest*, **118**, 1979-90.
- Ballou, L.R., Lauderkind, S.J., Rosloniec, E.F. & Raghov, R. (1996). Ceramide signalling and the immune response. *Biochim Biophys Acta*, **1301**, 273-87.
- Bardor, M., Nguyen, D.H., Diaz, S. & Varki, A. (2005). Mechanism of uptake and incorporation of the non-human sialic acid N-glycolylneuraminic acid into human cells. *J Biol Chem*, **280**, 4228-37.
- Barker, E., Mueller, B.M., Handgretinger, R., Herter, M., Yu, A.L. & Reisfeld, R.A. (1991). Effect of a chimeric anti-ganglioside GD2 antibody on cell-mediated lysis of human neuroblastoma cells. *Cancer Res*, **51**, 144-9.
- Barral, D.C. & Brenner, M.B. (2007). CD1 antigen presentation: how it works. *Nat Rev Immunol*, **7**, 929-41.
- Barral, P., Eckl-Dorna, J., Harwood, N.E., De Santo, C., Salio, M., Illarionov, P., Besra, G.S., Cerundolo, V. & Batista, F.D. (2008). B cell receptor-mediated uptake of CD1d-restricted antigen augments antibody responses by recruiting invariant NKT cell help in vivo. *Proc Natl Acad Sci U S A*, **105**, 8345-50.



- Barten, L.J., Allington, D.R., Procacci, K.A. & Rivey, M.P. (2010). New approaches in the management of multiple sclerosis. *Drug Des Devel Ther*, **4**, 343-66.
- Baselga, J. (2001). The EGFR as a target for anticancer therapy--focus on cetuximab. *Eur J Cancer*, **37 Suppl 4**, S16-22.
- Baselga, J., Gelmon, K.A., Verma, S., Wardley, A., Conte, P., Miles, D., Bianchi, G., Cortes, J., McNally, V.A., Ross, G.A., Fumoleau, P. & Gianni, L. (2010). Phase II trial of pertuzumab and trastuzumab in patients with human epidermal growth factor receptor 2-positive metastatic breast cancer that progressed during prior trastuzumab therapy. *J Clin Oncol*, **28**, 1138-44.
- Bate, C., Tayebi, M. & Williams, A. (2010). A glycosylphosphatidylinositol analogue reduced prion-derived peptide mediated activation of cytoplasmic phospholipase A2, synapse degeneration and neuronal death. *Neuropharmacology*, **59**, 93-9.
- Beers, S.A., Chan, C.H., James, S., French, R.R., Attfield, K.E., Brennan, C.M., Ahuja, A., Shlomchik, M.J., Cragg, M.S. & Glennie, M.J. (2008). Type II (tositumomab) anti-CD20 monoclonal antibody out performs type I (rituximab-like) reagents in B-cell depletion regardless of complement activation. *Blood*, **112**, 4170-7.
- Birch, J.R. & Racher, A.J. (2006). Antibody production. *Adv Drug Deliv Rev*, **58**, 671-85.
- Blackhall, F.H., Merry, C.L., Davies, E.J. & Jayson, G.C. (2001). Heparan sulfate proteoglycans and cancer. *Br J Cancer*, **85**, 1094-8.
- Blanca, I.R., Bere, E.W., Young, H.A. & Ortaldo, J.R. (2001). Human B cell activation by autologous NK cells is regulated by CD40-CD40 ligand interaction: role of memory B cells and CD5+ B cells. *J Immunol*, **167**, 6132-9.
- Blick, S.K. & Scott, L.J. (2007). Cetuximab: a review of its use in squamous cell carcinoma of the head and neck and metastatic colorectal cancer. *Drugs*, **67**, 2585-607.
- Boya, P., Roques, B. & Kroemer, G. (2001). New EMBO members' review: viral and bacterial proteins regulating apoptosis at the mitochondrial level. *Embo J*, **20**, 4325-31.
- Breitfeld, D., Ohl, L., Kremmer, E., Ellwart, J., Sallusto, F., Lipp, M. & Forster, R. (2000). Follicular B helper T cells express CXC chemokine receptor 5, localize to B cell follicles, and support immunoglobulin production. *J Exp Med*, **192**, 1545-52.
- Brodbeck, W.G., Mold, C., Atkinson, J.P. & Medof, M.E. (2000). Cooperation between decay-accelerating factor and membrane cofactor protein in protecting cells from autologous complement attack. *J Immunol*, **165**, 3999-4006.
- Brodin, T., Thurin, J., Stromberg, N., Karlsson, K.A. & Sjogren, H.O. (1986). Production of oligosaccharide-binding monoclonal antibodies of diverse specificities by immunization with purified tumor-associated glycolipids inserted into liposomes with lipid A. *Eur J Immunol*, **16**, 951-6.
- Brusa, D., Garetto, S., Chiorino, G., Scatolini, M., Migliore, E., Camussi, G. & Matera, L. (2008). Post-apoptotic tumors are more palatable to dendritic cells and enhance their antigen cross-presentation activity. *Vaccine*, **26**, 6422-32.
- Burris, H.A., 3rd, Rosen, L.S., Rocha-Lima, C.M., Marshall, J., Jones, S., Cohen, R.B., Kunkel, L.A., Loo, D., Baughman, J., Stewart, S.J. & Lewis, N. (2010). Phase 1 experience with an anti-glycotope monoclonal antibody, RAV12, in recurrent adenocarcinoma. *Clin Cancer Res*, **16**, 1673-81.
- Busam, K.J., Capodici, P., Motzer, R., Kiehn, T., Phelan, D. & Halpern, A.C. (2001). Cutaneous side-effects in cancer patients treated with the antiepidermal growth factor receptor antibody C225. *Br J Dermatol*, **144**, 1169-76.
- Cao, X., Zhang, Y., Zou, L., Xiao, H., Chu, Y. & Chu, X. (2010). Persistent oxygen-glucose deprivation induces astrocytic death through two different pathways and calpain-mediated proteolysis of cytoskeletal proteins during astrocytic oncosis. *Neurosci Lett*, **479**, 118-22.
- Cardarelli, P.M., Quinn, M., Buckman, D., Fang, Y., Colcher, D., King, D.J., Bebbington, C. & Yarranton, G. (2002). Binding to CD20 by anti-B1 antibody or F(ab')(2) is sufficient for induction of apoptosis in B-cell lines. *Cancer Immunol Immunother*, **51**, 15-24.

- Cartron, G., Dacheux, L., Salles, G., Solal-Celigny, P., Bardos, P., Colombat, P. & Watier, H. (2002). Therapeutic activity of humanized anti-CD20 monoclonal antibody and polymorphism in IgG Fc receptor FcγRIIIa gene. *Blood*, **99**, 754-8.
- Cavanna, B., Jiang, H., Allaria, S., Carpo, M., Scarlato, G. & Nobile-Orazio, E. (2001). Anti-GM(2) IgM antibody-induced complement-mediated cytotoxicity in patients with dysimmune neuropathies. *J Neuroimmunol*, **114**, 226-31.
- Chan, H.T., Hughes, D., French, R.R., Tutt, A.L., Walshe, C.A., Teeling, J.L., Glennie, M.J. & Cragg, M.S. (2003). CD20-induced lymphoma cell death is independent of both caspases and its redistribution into triton X-100 insoluble membrane rafts. *Cancer Res*, **63**, 5480-9.
- Chang, F., Li, R. & Ladisch, S. (1997). Shedding of gangliosides by human medulloblastoma cells. *Exp Cell Res*, **234**, 341-6.
- Chapman, P.B., Yuasa, H. & Houghton, A.N. (1990). Homophilic binding of mouse monoclonal antibodies against GD3 ganglioside. *J Immunol*, **145**, 891-8.
- Charpin, C., Bhan, A.K., Zurawski, V.R., Jr. & Scully, R.E. (1982). Carcinoembryonic antigen (CEA) and carbohydrate determinant 19-9 (CA 19-9) localization in 121 primary and metastatic ovarian tumors: an immunohistochemical study with the use of monoclonal antibodies. *Int J Gynecol Pathol*, **1**, 231-45.
- Chen, H., Yang, W.W., Wen, Q.T., Xu, L. & Chen, M. (2009). TGF-beta induces fibroblast activation protein expression; fibroblast activation protein expression increases the proliferation, adhesion, and migration of HO-8910PM [corrected]. *Exp Mol Pathol*, **87**, 189-94.
- Chen, M., Won, D.J., Krajewski, S. & Gottlieb, R.A. (2002). Calpain and mitochondria in ischemia/reperfusion injury. *J Biol Chem*, **277**, 29181-6.
- Cheong, J.W., Chong, S.Y., Kim, J.Y., Eom, J.I., Jeung, H.K., Maeng, H.Y., Lee, S.T. & Min, Y.H. (2003). Induction of apoptosis by apicidin, a histone deacetylase inhibitor, via the activation of mitochondria-dependent caspase cascades in human Bcr-Abl-positive leukemia cells. *Clin Cancer Res*, **9**, 5018-27.
- Cheresh, D.A., Honsik, C.J., Staffileno, L.K., Jung, G. & Reisfeld, R.A. (1985). Disialoganglioside GD3 on human melanoma serves as a relevant target antigen for monoclonal antibody-mediated tumor cytolysis. *Proc Natl Acad Sci U S A*, **82**, 5155-9.
- Cherukuri, A., Cheng, P.C. & Pierce, S.K. (2001a). The role of the CD19/CD21 complex in B cell processing and presentation of complement-tagged antigens. *J Immunol*, **167**, 163-72.
- Cherukuri, A., Cheng, P.C., Sohn, H.W. & Pierce, S.K. (2001b). The CD19/CD21 complex functions to prolong B cell antigen receptor signaling from lipid rafts. *Immunity*, **14**, 169-79.
- Chester, M.A. (1998). IUPAC-IUB Joint Commission on Biochemical Nomenclature (JCBN). Nomenclature of glycolipids--recommendations 1997. *Eur J Biochem*, **257**, 293-8.
- Cheung, M.C., Maceachern, J.A., Haynes, A.E., Meyer, R.M. & Imrie, K. (2009). I-Tositumomab in lymphoma. *Curr Oncol*, **16**, 32-47.
- Cheung, N.K., Kushner, B.H., Cheung, I.Y., Kramer, K., Canete, A., Gerald, W., Bonilla, M.A., Finn, R., Yeh, S.J. & Larson, S.M. (1998). Anti-G(D2) antibody treatment of minimal residual stage 4 neuroblastoma diagnosed at more than 1 year of age. *J Clin Oncol*, **16**, 3053-60.
- Cheung, N.K., Saarinen, U.M., Neely, J.E., Landmeier, B., Donovan, D. & Coccia, P.F. (1985). Monoclonal antibodies to a glycolipid antigen on human neuroblastoma cells. *Cancer Res*, **45**, 2642-9.
- Chou, H.H., Takematsu, H., Diaz, S., Iber, J., Nickerson, E., Wright, K.L., Muchmore, E.A., Nelson, D.L., Warren, S.T. & Varki, A. (1998). A mutation in human CMP-sialic acid hydroxylase occurred after the Homo-Pan divergence. *Proc Natl Acad Sci U S A*, **95**, 11751-6.
- Chu, X., Fu, X., Zou, L., Qi, C., Li, Z., Rao, Y. & Ma, K. (2007). Oncosis, the possible cell death pathway in astrocytes after focal cerebral ischemia. *Brain Res*, **1149**, 157-64.
- Clynes, R.A., Towers, T.L., Presta, L.G. & Ravetch, J.V. (2000). Inhibitory Fc receptors modulate in vivo cytotoxicity against tumor targets. *Nat Med*, **6**, 443-6.

- Cobb, B.A., Wang, Q., Tzianabos, A.O. & Kasper, D.L. (2004). Polysaccharide processing and presentation by the MHCII pathway. *Cell*, **117**, 677-87.
- Coberly, S.K., Chen, F.Z., Armanini, M.P., Chen, Y., Young, P.F., Mather, J.P. & Loo, D.T. (2009). The RAV12 monoclonal antibody recognizes the N-linked glycotope RAAG12: expression in human normal and tumor tissues. *Arch Pathol Lab Med*, **133**, 1403-12.
- Coelho, V., Krysov, S., Ghaemmaghami, A.M., Emara, M., Potter, K.N., Johnson, P., Packham, G., Martinez-Pomares, L. & Stevenson, F.K. (2010). Glycosylation of surface Ig creates a functional bridge between human follicular lymphoma and microenvironmental lectins. *Proc Natl Acad Sci U S A*, **107**, 18587-92.
- Cohen, M.H., Gootenberg, J., Keegan, P. & Pazdur, R. (2007). FDA drug approval summary: bevacizumab (Avastin) plus Carboplatin and Paclitaxel as first-line treatment of advanced/metastatic recurrent nonsquamous non-small cell lung cancer. *Oncologist*, **12**, 713-8.
- Cohen, M.H., Shen, Y.L., Keegan, P. & Pazdur, R. (2009a). FDA drug approval summary: bevacizumab (Avastin) as treatment of recurrent glioblastoma multiforme. *Oncologist*, **14**, 1131-8.
- Cohen, N.R., Garg, S. & Brenner, M.B. (2009b). Antigen Presentation by CD1 Lipids, T Cells, and NKT Cells in Microbial Immunity. *Adv Immunol*, **102**, 1-94.
- Cohenuram, M. & Saif, M.W. (2007). Panitumumab the first fully human monoclonal antibody: from the bench to the clinic. *Anticancer Drugs*, **18**, 7-15.
- Coiffier, B., Lepage, E., Briere, J., Herbrecht, R., Tilly, H., Bouabdallah, R., Morel, P., Van Den Neste, E., Salles, G., Gaulard, P., Reyes, F., Lederlin, P. & Gisselbrecht, C. (2002). CHOP chemotherapy plus rituximab compared with CHOP alone in elderly patients with diffuse large-B-cell lymphoma. *N Engl J Med*, **346**, 235-42.
- Cooper, G.M. (2000). *The cell; A molecular approach Second Edition*. Sinauer Associates.
- Coppola, D., Khalil, F., Eschrich, S.A., Boulware, D., Yeatman, T. & Wang, H.G. (2008). Down-regulation of Bax-interacting factor-1 in colorectal adenocarcinoma. *Cancer*, **113**, 2665-70.
- Cragg, M.S. & Glennie, M.J. (2004). Antibody specificity controls in vivo effector mechanisms of anti-CD20 reagents. *Blood*, **103**, 2738-43.
- Cragg, M.S., Morgan, S.M., Chan, H.T., Morgan, B.P., Filatov, A.V., Johnson, P.W., French, R.R. & Glennie, M.J. (2003). Complement-mediated lysis by anti-CD20 mAb correlates with segregation into lipid rafts. *Blood*, **101**, 1045-52.
- Craigen, J.L., Wendy, J.M. Mackus, Patrick Englebarts, Sam R Miller, Sue Speller, Louise C Chamberlain, Bill G Davis, PhD, Simon M McHugh, Ed Bullmore, Charles J Cox, Sally Wetten, Gerrard Perdock, Joost M Bakker, Jan G. J. van de Winkel, and Parren P.H.W. (2009). Ofatumumab, a Human Mab Targeting a Membrane-Proximal Small-Loop Epitope On CD20, Induces Potent NK Cell-Mediated ADCC. In *51st American Society of Hematology Annual Meeting and Exposition* New Orleans, LA.
- Crocker, P.R., Paulson, J.C. & Varki, A. (2007). Siglecs and their roles in the immune system. *Nat Rev Immunol*, **7**, 255-66.
- CRUK. (2010). Cancer in the UK: July 2010.
- Dabelsteen, E. (1996). Cell surface carbohydrates as prognostic markers in human carcinomas. *J Pathol*, **179**, 358-69.
- Dall'Acqua, W.F., Kiener, P.A. & Wu, H. (2006). Properties of human IgG1s engineered for enhanced binding to the neonatal Fc receptor (FcRn). *J Biol Chem*, **281**, 23514-24.
- Daniels, I., Turzanski, J. & Haynes, A.P. (2008). A requirement for calcium in the caspase-independent killing of Burkitt lymphoma cell lines by Rituximab. *Br J Haematol*, **142**, 394-403.
- Davis, T.A., Kaminski, M.S., Leonard, J.P., Hsu, F.J., Wilkinson, M., Zelenetz, A., Wahl, R.L., Kroll, S., Coleman, M., Goris, M., Levy, R. & Knox, S.J. (2004). The radioisotope contributes significantly to the activity of radioimmunotherapy. *Clin Cancer Res*, **10**, 7792-8.

- de Heer, P., de Bruin, E.C., Klein-Kranenbarg, E., Aalbers, R.I., Marijnen, C.A., Putter, H., de Bont, H.J., Nagelkerke, J.F., van Krieken, J.H., Verspaget, H.W., van de Velde, C.J. & Kuppen, P.J. (2007). Caspase-3 activity predicts local recurrence in rectal cancer. *Clin Cancer Res*, **13**, 5810-5.
- de Leon, J., Fernandez, A., Mesa, C., Clavel, M. & Fernandez, L.E. (2006). Role of tumour-associated N-glycolylated variant of GM3 ganglioside in cancer progression: effect over CD4 expression on T cells. *Cancer Immunol Immunother*, **55**, 443-50.
- Degenhardt, K., Mathew, R., Beaudoin, B., Bray, K., Anderson, D., Chen, G., Mukherjee, C., Shi, Y., Gelinias, C., Fan, Y., Nelson, D.A., Jin, S. & White, E. (2006). Autophagy promotes tumor cell survival and restricts necrosis, inflammation, and tumorigenesis. *Cancer Cell*, **10**, 51-64.
- Delord, J.P., Allal, C., Canal, M., Mery, E., Rochaix, P., Hennebelle, I., Pradines, A., Chatelut, E., Bugat, R., Guichard, S. & Canal, P. (2005). Selective inhibition of HER2 inhibits AKT signal transduction and prolongs disease-free survival in a micrometastasis model of ovarian carcinoma. *Ann Oncol*, **16**, 1889-97.
- Dennis, J.W., Granovsky, M. & Warren, C.E. (1999). Glycoprotein glycosylation and cancer progression. *Biochim Biophys Acta*, **1473**, 21-34.
- Devine, P.L., Clark, B.A., Birrell, G.W., Layton, G.T., Ward, B.G., Alewood, P.F. & McKenzie, I.F. (1991). The breast tumor-associated epitope defined by monoclonal antibody 3E1.2 is an O-linked mucin carbohydrate containing N-glycolylneuraminic acid. *Cancer Res*, **51**, 5826-36.
- Dhein, J., Daniel, P.T., Trauth, B.C., Oehm, A., Moller, P. & Krammer, P.H. (1992). Induction of apoptosis by monoclonal antibody anti-APO-1 class switch variants is dependent on cross-linking of APO-1 cell surface antigens. *J Immunol*, **149**, 3166-73.
- Dickerson, S.K., Market, E., Besmer, E. & Papavasiliou, F.N. (2003). AID mediates hypermutation by deaminating single stranded DNA. *J Exp Med*, **197**, 1291-6.
- Dinndorf, P.A., Andrews, R.G., Benjamin, D., Ridgway, D., Wolff, L. & Bernstein, I.D. (1986). Expression of normal myeloid-associated antigens by acute leukemia cells. *Blood*, **67**, 1048-53.
- Duckworth, C.A. & Pritchard, D.M. (2009). Suppression of apoptosis, crypt hyperplasia, and altered differentiation in the colonic epithelia of bak-null mice. *Gastroenterology*, **136**, 943-52.
- Dullforce, P., Sutton, D.C. & Heath, A.W. (1998). Enhancement of T cell-independent immune responses in vivo by CD40 antibodies. *Nat Med*, **4**, 88-91.
- Duncan, T.J., Watson, N.F., Al-Attar, A.H., Scholefield, J.H. & Durrant, L.G. (2007). The role of MUC1 and MUC3 in the biology and prognosis of colorectal cancer. *World J Surg Oncol*, **5**, 31.
- Dunn, G.P., Bruce, A.T., Sheehan, K.C., Shankaran, V., Uppaluri, R., Bui, J.D., Diamond, M.S., Koebel, C.M., Arthur, C., White, J.M. & Schreiber, R.D. (2005). A critical function for type I interferons in cancer immunoediting. *Nat Immunol*, **6**, 722-9.
- Durrant, L.G., Chapman, M.A., Buckley, D.J., Spendlove, I., Robins, R.A. & Armitage, N.C. (2003). Enhanced expression of the complement regulatory protein CD55 predicts a poor prognosis in colorectal cancer patients. *Cancer Immunol Immunother*, **52**, 638-42.
- Durrant, L.G., Harding, S.J., Green, N.H., Buckberry, L.D. & Parsons, T. (2006). A new anticancer glycolipid monoclonal antibody, SC104, which directly induces tumor cell apoptosis. *Cancer Res*, **66**, 5901-9.
- Durrant, L.G., Singhal, A., Jacobs, E. & Price, M.R. (1993). Development Of 2nd-Generation Monoclonal-Antibodies Recognizing Lewis(Y/B) Antigen By Antiidiotypic Immunization. *Hybridoma*, **12**, 647-660.
- Early, P., Huang, H., Davis, M., Calame, K. & Hood, L. (1980). An immunoglobulin heavy chain variable region gene is generated from three segments of DNA: VH, D and JH. *Cell*, **19**, 981-92.
- Eguchi, Y., Shimizu, S. & Tsujimoto, Y. (1997). Intracellular ATP levels determine cell death fate by apoptosis or necrosis. *Cancer Res*, **57**, 1835-40.
- El-Rayes, B.F. & LoRusso, P.M. (2004). Targeting the epidermal growth factor receptor. *Br J Cancer*, **91**, 418-24.
- FDA. (1997). FDA approval of Rituximab.

- FDA. (1998). Approval of Trastuzumab, Genentech (ed).
- FDA. (2002). Rituximab Approval Information - Licensing Action.
- FDA. (2004). FDA approval of Cetuximab (Erbix), Inc, I.S. (ed). FDA: Branchburg.
- FDA. (2009). FDA Approves New Treatment for Chronic Lymphocytic Leukemia. US Food and Drug Administration.
- FDA. (2010). Mylotarg (gemtuzumab ozogamicin): Market Withdrawal.
- Feizi, T. (1985). Demonstration by monoclonal antibodies that carbohydrate structures of glycoproteins and glycolipids are onco-developmental antigens. *Nature*, **314**, 53-7.
- Fernandes, D.M., Baird, A.M., Berg, L.J. & Rock, K.L. (1999). A monoclonal antibody reactive with a 40-kDa molecule on fetal thymocytes and tumor cells blocks proliferation and stimulates aggregation and apoptosis. *J Immunol*, **163**, 1306-14.
- Fernandez, L.E., Gabri, M.R., Guthmann, M.D., Gomez, R.E., Gold, S., Fainboim, L., Gomez, D.E. & Alonso, D.F. (2010). NGcGM3 ganglioside: a privileged target for cancer vaccines. *Clin Dev Immunol*, **2010**, 814397.
- Fink, S.L. & Cookson, B.T. (2005). Apoptosis, pyroptosis, and necrosis: mechanistic description of dead and dying eukaryotic cells. *Infect Immun*, **73**, 1907-16.
- Fishwild, D.M., O'Donnell, S.L., Bengoechea, T., Hudson, D.V., Harding, F., Bernhard, S.L., Jones, D., Kay, R.M., Higgins, K.M., Schramm, S.R. & Lonberg, N. (1996). High-avidity human IgG kappa monoclonal antibodies from a novel strain of minilocus transgenic mice. *Nat Biotechnol*, **14**, 845-51.
- Fong, P.C., Yap, T.A., Boss, D.S., Carden, C.P., Mergui-Roelvink, M., Gourley, C., De Greve, J., Lubinski, J., Shanley, S., Messiou, C., A'Hern, R., Tutt, A., Ashworth, A., Stone, J., Carmichael, J., Schellens, J.H., de Bono, J.S. & Kaye, S.B. (2010). Poly(ADP)-ribose polymerase inhibition: frequent durable responses in BRCA carrier ovarian cancer correlating with platinum-free interval. *J Clin Oncol*, **28**, 2512-9.
- Foss, D.L., Zilliox, M.J. & Murtaugh, M.P. (2001). Bacterially induced activation of interleukin-18 in porcine intestinal mucosa. *Vet Immunol Immunopathol*, **78**, 263-77.
- Foy, T.M., Laman, J.D., Ledbetter, J.A., Aruffo, A., Claassen, E. & Noelle, R.J. (1994). gp39-CD40 interactions are essential for germinal center formation and the development of B cell memory. *J Exp Med*, **180**, 157-63.
- Frost, J.D., Hank, J.A., Reaman, G.H., Friedrich, S., Seeger, R.C., Gan, J., Anderson, P.M., Ettinger, L.J., Cairo, M.S., Blazar, B.R., Krailo, M.D., Matthay, K.K., Reisfeld, R.A. & Sondel, P.M. (1997). A phase I/IB trial of murine monoclonal anti-GD2 antibody 14.G2a plus interleukin-2 in children with refractory neuroblastoma: a report of the Children's Cancer Group. *Cancer*, **80**, 317-33.
- Fuentes, D., Avellanet, J., Garcia, A., Iglesias, N., Gabri, M.R., Alonso, D.F., Vazquez, A.M., Perez, R. & Montero, E. (2010). Combined therapeutic effect of a monoclonal anti-idiotypic tumor vaccine against NeuGc-containing gangliosides with chemotherapy in a breast carcinoma model. *Breast Cancer Res Treat*, **120**, 379-89.
- Fujii, S., Shimizu, K., Smith, C., Bonifaz, L. & Steinman, R.M. (2003). Activation of natural killer T cells by alpha-galactosylceramide rapidly induces the full maturation of dendritic cells in vivo and thereby acts as an adjuvant for combined CD4 and CD8 T cell immunity to a coadministered protein. *J Exp Med*, **198**, 267-79.
- Fukumura, D., Xavier, R., Sugiura, T., Chen, Y., Park, E.C., Lu, N., Selig, M., Nielsen, G., Taksir, T., Jain, R.K. & Seed, B. (1998). Tumor induction of VEGF promoter activity in stromal cells. *Cell*, **94**, 715-25.
- Fulda, S. (2009). Tumor resistance to apoptosis. *Int J Cancer*, **124**, 511-5.
- Fung, J.J., Markus, B.H., Gordon, R.D., Esquivel, C.O., Makowka, L., Tzakis, A. & Starzl, T.E. (1987). Impact of Orthoclone OKT3 on liver transplantation. *Transplant Proc*, **19**, 37-44.

- Gabri, M.R., Otero, L.L., Gomez, D.E. & Alonso, D.F. (2009). Exogenous incorporation of neugc-rich mucin augments n-glycolyl sialic acid content and promotes malignant phenotype in mouse tumor cell lines. *J Exp Clin Cancer Res*, **28**, 146.
- Galli, G., Nuti, S., Tavarini, S., Galli-Stampino, L., De Lalla, C., Casorati, G., Dellabona, P. & Abrignani, S. (2003). CD1d-restricted help to B cells by human invariant natural killer T lymphocytes. *J Exp Med*, **197**, 1051-7.
- Galon, J., Costes, A., Sanchez-Cabo, F., Kirilovsky, A., Mlecnik, B., Lagorce-Pages, C., Tosolini, M., Camus, M., Berger, A., Wind, P., Zinzindohoue, F., Bruneval, P., Cugnenc, P.H., Trajanoski, Z., Fridman, W.H. & Pages, F. (2006). Type, density, and location of immune cells within human colorectal tumors predict clinical outcome. *Science*, **313**, 1960-4.
- Garnier, P., Ying, W. & Swanson, R.A. (2003). Ischemic preconditioning by caspase cleavage of poly(ADP-ribose) polymerase-1. *J Neurosci*, **23**, 7967-73.
- Garrigues, J., Garrigues, U., Hellstrom, I. & Hellstrom, K.E. (1993). Ley specific antibody with potent anti-tumor activity is internalized and degraded in lysosomes. *Am J Pathol*, **142**, 607-22.
- Gatto, D. & Brink, R. (2010). The germinal center reaction. *J Allergy Clin Immunol*, **126**, 898-907; quiz 908-9.
- Gennari, R., Menard, S., Fagnoni, F., Ponchio, L., Scelsi, M., Tagliabue, E., Castiglioni, F., Villani, L., Magalotti, C., Gibelli, N., Oliviero, B., Ballardini, B., Da Prada, G., Zambelli, A. & Costa, A. (2004). Pilot study of the mechanism of action of preoperative trastuzumab in patients with primary operable breast tumors overexpressing HER2. *Clin Cancer Res*, **10**, 5650-5.
- Gianni, L. (2008). The "other" signaling of trastuzumab: antibodies are immunocompetent drugs. *J Clin Oncol*, **26**, 1778-80.
- Gilman, A.L., Ozkaynak, M.F., Matthay, K.K., Krailo, M., Yu, A.L., Gan, J., Sternberg, A., Hank, J.A., Seeger, R., Reaman, G.H. & Sondel, P.M. (2009). Phase I study of ch14.18 with granulocyte-macrophage colony-stimulating factor and interleukin-2 in children with neuroblastoma after autologous bone marrow transplantation or stem-cell rescue: a report from the Children's Oncology Group. *J Clin Oncol*, **27**, 85-91.
- Ginzburg, L., Kacher, Y. & Futerman, A.H. (2004). The pathogenesis of glycosphingolipid storage disorders. *Semin Cell Dev Biol*, **15**, 417-31.
- Giroux, M., Schmidt, M. & Descoteaux, A. (2003). IFN-gamma-induced MHC class II expression: transactivation of class II transactivator promoter IV by IFN regulatory factor-1 is regulated by protein kinase C-alpha. *J Immunol*, **171**, 4187-94.
- Glassy, M.C., Tharakan, J.P. & Chau, P.C. (1988). Serum-free media in hybridoma culture and monoclonal antibody production. *Biotechnol Bioeng*, **32**, 1015-28.
- Golay, J., Manganini, M., Rambaldi, A. & Introna, M. (2004). Effect of alemtuzumab on neoplastic B cells. *Haematologica*, **89**, 1476-83.
- Goldenberg, M.M. (1999). Trastuzumab, a recombinant DNA-derived humanized monoclonal antibody, a novel agent for the treatment of metastatic breast cancer. *Clin Ther*, **21**, 309-18.
- Goldstein, N.I., Prewett, M., Zuklys, K., Rockwell, P. & Mendelsohn, J. (1995). Biological efficacy of a chimeric antibody to the epidermal growth factor receptor in a human tumor xenograft model. *Clin Cancer Res*, **1**, 1311-8.
- Gown, A.M. & Willingham, M.C. (2002). Improved detection of apoptotic cells in archival paraffin sections: immunohistochemistry using antibodies to cleaved caspase 3. *J Histochem Cytochem*, **50**, 449-54.
- Green, D.R. & Martin, S.J. (1995). The killer and the executioner: how apoptosis controls malignancy. *Curr Opin Immunol*, **7**, 694-703.
- Grey, H.M., Hirst, J.W. & Cohn, M. (1971). A new mouse immunoglobulin: IgG3. *J Exp Med*, **133**, 289-304.
- Gujral, J.S., Farhood, A. & Jaeschke, H. (2003). Oncotic necrosis and caspase-dependent apoptosis during galactosamine-induced liver injury in rats. *Toxicol Appl Pharmacol*, **190**, 37-46.

- Gullick, W.J. (1991). Prevalence of aberrant expression of the epidermal growth factor receptor in human cancers. *Br Med Bull*, **47**, 87-98.
- Hakomori, S. (1985). Aberrant glycosylation in cancer cell membranes as focused on glycolipids: overview and perspectives. *Cancer Res*, **45**, 2405-14.
- Hakomori, S. (2002). The glycosynapse. *Proc Natl Acad Sci U S A*, **99**, 225-32.
- Hakomori, S. & Zhang, Y. (1997). Glycosphingolipid antigens and cancer therapy. *Chem Biol*, **4**, 97-104.
- Hakomori, S.I. (2008). Structure and function of glycosphingolipids and sphingolipids: recollections and future trends. *Biochim Biophys Acta*, **1780**, 325-46.
- Hakomori, S.I. & Murakami, W.T. (1968). Glycolipids of hamster fibroblasts and derived malignant-transformed cell lines. *Proc Natl Acad Sci U S A*, **59**, 254-61.
- Hakomori Si, S.I. (2002). The glycosynapse. *Proc Natl Acad Sci U S A*, **99**, 225-32.
- Hale, G., Dyer, M.J., Clark, M.R., Phillips, J.M., Marcus, R., Riechmann, L., Winter, G. & Waldmann, H. (1988). Remission induction in non-Hodgkin lymphoma with reshaped human monoclonal antibody CAMPATH-1H. *Lancet*, **2**, 1394-9.
- Halpern, R., Kaveri, S.V. & Kohler, H. (1991). Human anti-phosphorylcholine antibodies share idiotopes and are self-binding. *J Clin Invest*, **88**, 476-82.
- Hartley, S.B., Cooke, M.P., Fulcher, D.A., Harris, A.W., Cory, S., Basten, A. & Goodnow, C.C. (1993). Elimination of self-reactive B lymphocytes proceeds in two stages: arrested development and cell death. *Cell*, **72**, 325-35.
- Hector, S. & Prehn, J.H. (2009). Apoptosis signaling proteins as prognostic biomarkers in colorectal cancer: a review. *Biochim Biophys Acta*, **1795**, 117-29.
- Hellstrom, I., Garrigues, H.J., Garrigues, U. & Hellstrom, K.E. (1990). Highly tumor-reactive, internalizing, mouse monoclonal antibodies to Le(y)-related cell surface antigens. *Cancer Res*, **50**, 2183-90.
- Hernandez-Campo, P.M., Almeida, J., Matarraz, S., de Santiago, M., Sanchez, M.L. & Orfao, A. (2007). Quantitative analysis of the expression of glycosylphosphatidylinositol-anchored proteins during the maturation of different hematopoietic cell compartments of normal bone marrow. *Cytometry B Clin Cytom*, **72**, 34-42.
- Hernandez, A.M., Rodriguez, N., Gonzalez, J.E., Reyes, E., Rondon, T., Grinan, T., Macias, A., Alfonso, S., Vazquez, A.M. & Perez, R. (2011). Anti-NeuGcGM3 Antibodies, Actively Elicited by Idiopathic Vaccination in Nonsmall Cell Lung Cancer Patients, Induce Tumor Cell Death by an Oncosis-Like Mechanism. *J Immunol*.
- Hettmer, S., McCarter, R., Ladisch, S. & Kaucic, K. (2004). Alterations in neuroblastoma ganglioside synthesis by induction of GD1b synthase by retinoic acid. *Br J Cancer*, **91**, 389-97.
- Hicklin, D.J. & Ellis, L.M. (2005). Role of the vascular endothelial growth factor pathway in tumor growth and angiogenesis. *J Clin Oncol*, **23**, 1011-27.
- Hodi, F.S., O'Day, S.J., McDermott, D.F., Weber, R.W., Sosman, J.A., Haanen, J.B., Gonzalez, R., Robert, C., Schadendorf, D., Hassel, J.C., Akerley, W., van den Eertwegh, A.J., Lutzky, J., Lorigan, P., Vaubel, J.M., Linette, G.P., Hogg, D., Ottensmeier, C.H., Lebbe, C., Peschel, C., Quirt, I., Clark, J.I., Wolchok, J.D., Weber, J.S., Tian, J., Yellin, M.J., Nichol, G.M., Hoos, A. & Urba, W.J. (2010). Improved survival with ipilimumab in patients with metastatic melanoma. *N Engl J Med*, **363**, 711-23.
- Hofheinz, R.D., al-Batran, S.E., Hartmann, F., Hartung, G., Jager, D., Renner, C., Tanswell, P., Kunz, U., Amelsberg, A., Kuthan, H. & Stehle, G. (2003). Stromal antigen targeting by a humanised monoclonal antibody: an early phase II trial of sibrotuzumab in patients with metastatic colorectal cancer. *Onkologie*, **26**, 44-8.
- Holz, G. & Dormann, P. (2007). Structure and function of glycolipids in plants and bacteria. *Prog Lipid Res*, **46**, 225-43.
- Horejsi, V. (2003). The roles of membrane microdomains (rafts) in T cell activation. *Immunol Rev*, **191**, 148-64.

- Hu, Y., Turner, M.J., Shields, J., Gale, M.S., Hutto, E., Roberts, B.L., Siders, W.M. & Kaplan, J.M. (2009). Investigation of the mechanism of action of alemtuzumab in a human CD52 transgenic mouse model. *Immunology*, **128**, 260-70.
- Huang, M.M., Borszcz, P., Sidobre, S., Kronenberg, M. & Kane, K.P. (2004). CD1d1 displayed on cell size beads identifies and enriches an NK cell population negatively regulated by CD1d1. *J Immunol*, **172**, 5304-12.
- Hurwitz, H., Fehrenbacher, L., Novotny, W., Cartwright, T., Hainsworth, J., Heim, W., Berlin, J., Baron, A., Griffing, S., Holmgren, E., Ferrara, N., Fyfe, G., Rogers, B., Ross, R. & Kabbinavar, F. (2004). Bevacizumab plus irinotecan, fluorouracil, and leucovorin for metastatic colorectal cancer. *N Engl J Med*, **350**, 2335-42.
- Hwang, W.Y. & Foote, J. (2005). Immunogenicity of engineered antibodies. *Methods*, **36**, 3-10.
- Ichikawa, S. & Hirabayashi, Y. (1998). Glucosylceramide synthase and glycosphingolipid synthesis. *Trends Cell Biol*, **8**, 198-202.
- Itzkowitz, S.H. (1992). Blood group-related carbohydrate antigen expression in malignant and premalignant colonic neoplasms. *J Cell Biochem Suppl*, **16G**, 97-101.
- Iwabuchi, K., Yamamura, S., Prinetti, A., Handa, K. & Hakomori, S. (1998). GM3-enriched microdomain involved in cell adhesion and signal transduction through carbohydrate-carbohydrate interaction in mouse melanoma B16 cells. *J Biol Chem*, **273**, 9130-8.
- Izban, K.F., Wrone-Smith, T., Hsi, E.D., Schnitzer, B., Quevedo, M.E. & Alkan, S. (1999). Characterization of the interleukin-1beta-converting enzyme/ced-3-family protease, caspase-3/CPP32, in Hodgkin's disease: lack of caspase-3 expression in nodular lymphocyte predominance Hodgkin's disease. *Am J Pathol*, **154**, 1439-47.
- James, J.S. & Dubs, G. (1997). FDA approves new kind of lymphoma treatment. Food and Drug Administration. *AIDS Treat News*, 2-3.
- Janas, E., Priest, R., Wilde, J.I., White, J.H. & Malhotra, R. (2005). Rituxan (anti-CD20 antibody)-induced translocation of CD20 into lipid rafts is crucial for calcium influx and apoptosis. *Clin Exp Immunol*, **139**, 439-46.
- Janeway, C.A., Travers, P., Walport, M., Shlomchik, M.J. (2001). *Immunobiology: The Immune System in Health and Disease*. Garland Science: New York.
- Jeschke, U., Mylonas, I., Shabani, N., Kunert-Keil, C., Schindlbeck, C., Gerber, B. & Friese, K. (2005). Expression of sialyl Lewis X, sialyl Lewis A, E-cadherin and cathepsin-D in human breast cancer: immunohistochemical analysis in mammary carcinoma in situ, invasive carcinomas and their lymph node metastasis. *Anticancer Res*, **25**, 1615-22.
- Jones, P.T., Dear, P.H., Foote, J., Neuberger, M.S. & Winter, G. (1986). Replacing the complementarity-determining regions in a human antibody with those from a mouse. *Nature*, **321**, 522-5.
- Jonges, L.E., Nagelkerke, J.F., Ensink, N.G., van der Velde, E.A., Tollenaar, R.A., Fleuren, G.J., van de Velde, C.J., Morreau, H. & Kuppen, P.J. (2001). Caspase-3 activity as a prognostic factor in colorectal carcinoma. *Lab Invest*, **81**, 681-8.
- Jordanova, E.S., Gorter, A., Ayachi, O., Prins, F., Durrant, L.G., Kenter, G.G., van der Burg, S.H. & Fleuren, G.J. (2008). Human leukocyte antigen class I, MHC class I chain-related molecule A, and CD8+/regulatory T-cell ratio: which variable determines survival of cervical cancer patients? *Clin Cancer Res*, **14**, 2028-35.
- Jugdutt, B.I. & Idikio, H.A. (2005). Apoptosis and oncosis in acute coronary syndromes: assessment and implications. *Mol Cell Biochem*, **270**, 177-200.
- Kakar, S., Aksoy, S., Burgart, L.J. & Smyrk, T.C. (2004). Mucinous carcinoma of the colon: correlation of loss of mismatch repair enzymes with clinicopathologic features and survival. *Mod Pathol*, **17**, 696-700.
- Kaminski, M.J., MacKenzie, C.R., Mooibroek, M.J., Dahms, T.E., Hirama, T., Houghton, A.N., Chapman, P.B. & Evans, S.V. (1999). The role of homophilic binding in anti-tumor antibody



- R24 recognition of molecular surfaces. Demonstration of an intermolecular beta-sheet interaction between vh domains. *J Biol Chem*, **274**, 5597-604.
- Kang, C.Y., Cheng, H.L., Rudikoff, S. & Kohler, H. (1987). Idiotypic self binding of a dominant germline idiotype (T15). Autobody activity is affected by antibody valency. *J Exp Med*, **165**, 1332-43.
- Kannagi, R., Yin, J., Miyazaki, K. & Izawa, M. (2008). Current relevance of incomplete synthesis and neo-synthesis for cancer-associated alteration of carbohydrate determinants--Hakomori's concepts revisited. *Biochim Biophys Acta*, **1780**, 525-31.
- Kawabe, T., Naka, T., Yoshida, K., Tanaka, T., Fujiwara, H., Suematsu, S., Yoshida, N., Kishimoto, T. & Kikutani, H. (1994). The immune responses in CD40-deficient mice: impaired immunoglobulin class switching and germinal center formation. *Immunity*, **1**, 167-78.
- Kawaguchi, Y., Kono, K., Mimura, K., Sugai, H., Akaike, H. & Fujii, H. (2007). Cetuximab induce antibody-dependent cellular cytotoxicity against EGFR-expressing esophageal squamous cell carcinoma. *Int J Cancer*, **120**, 781-7.
- Kawaguchi, Y., Kono, K., Mizukami, Y., Mimura, K. & Fujii, H. (2009). Mechanisms of escape from trastuzumab-mediated ADCC in esophageal squamous cell carcinoma: relation to susceptibility to perforin-granzyme. *Anticancer Res*, **29**, 2137-46.
- Kawamura, Y.I., Toyota, M., Kawashima, R., Hagiwara, T., Suzuki, H., Imai, K., Shinomura, Y., Tokino, T., Kannagi, R. & Dohi, T. (2008). DNA hypermethylation contributes to incomplete synthesis of carbohydrate determinants in gastrointestinal cancer. *Gastroenterology*, **135**, 142-151 e3.
- Kelly, M.P., Lee, F.T., Smyth, F.E., Brechbiel, M.W. & Scott, A.M. (2006). Enhanced efficacy of 90Y-radiolabeled anti-Lewis Y humanized monoclonal antibody hu3S193 and paclitaxel combined-modality radioimmunotherapy in a breast cancer model. *J Nucl Med*, **47**, 716-25.
- Khan, O.A., Gore, M., Lorigan, P., Stone, J., Greystoke, A., Burke, W., Carmichael, J., Watson, A.J., McGown, G., Thorncroft, M., Margison, G.P., Califano, R., Larkin, J., Wellman, S. & Middleton, M.R. (2011). A phase I study of the safety and tolerability of olaparib (AZD2281, KU0059436) and dacarbazine in patients with advanced solid tumours. *Br J Cancer*, **104**, 750-5.
- Khazaeli, M.B., Conry, R.M. & LoBuglio, A.F. (1994). Human immune response to monoclonal antibodies. *J Immunother Emphasis Tumor Immunol*, **15**, 42-52.
- Kim, Y.S., Yuan, M., Itzkowitz, S.H., Sun, Q., Kaizu, T., Palekar, A., Trump, B.F. & Hakamori, S. (1986). Expression of Le<sup>y</sup> and extended Le<sup>y</sup> blood group-related antigens in human malignant, premalignant and non malignant colonic tissues. *Can Res*, **46**, 5985.
- Kimura, H., Sakai, K., Arao, T., Shimoyama, T., Tamura, T. & Nishio, K. (2007). Antibody-dependent cellular cytotoxicity of cetuximab against tumor cells with wild-type or mutant epidermal growth factor receptor. *Cancer Sci*, **98**, 1275-80.
- Kinoshita, T. (1991). Biology of complement: the overture. *Immunol Today*, **12**, 291-5.
- Kirkwood, J.M., Mascari, R.A., Edington, H.D., Rabkin, M.S., Day, R.S., Whiteside, T.L., Vlock, D.R. & Shipe-Spotloe, J.M. (2000). Analysis of therapeutic and immunologic effects of R(24) anti-GD3 monoclonal antibody in 37 patients with metastatic melanoma. *Cancer*, **88**, 2693-702.
- Kitatani, K., Idkowiak-Baldys, J. & Hannun, Y.A. (2008). The sphingolipid salvage pathway in ceramide metabolism and signaling. *Cell Signal*, **20**, 1010-8.
- Klos, K.S., Zhou, X., Lee, S., Zhang, L., Yang, W., Nagata, Y. & Yu, D. (2003). Combined trastuzumab and paclitaxel treatment better inhibits ErbB-2-mediated angiogenesis in breast carcinoma through a more effective inhibition of Akt than either treatment alone. *Cancer*, **98**, 1377-85.
- Knodler, L.A., Vallance, B.A., Celli, J., Winfree, S., Hansen, B., Montero, M. & Steele-Mortimer, O. (2010). Dissemination of invasive Salmonella via bacterial-induced extrusion of mucosal epithelia. *Proc Natl Acad Sci U S A*, **107**, 17733-8.
- Koelink, P.J., Sier, C.F., Hommes, D.W., Lamers, C.B. & Verspaget, H.W. (2009). Clinical significance of stromal apoptosis in colorectal cancer. *Br J Cancer*, **101**, 765-73.

- Koene, H.R., Kleijer, M., Algra, J., Roos, D., von dem Borne, A.E. & de Haas, M. (1997). Fc gammaRIIIa-158V/F polymorphism influences the binding of IgG by natural killer cell Fc gammaRIIIa, independently of the Fc gammaRIIIa-48L/R/H phenotype. *Blood*, **90**, 1109-14.
- Kohler, G. & Milstein, C. (1975). Continuous cultures of fused cells secreting antibody of predefined specificity. *Nature*, **256**, 495-7.
- Kohmura, C., Gold, H.K., Yasuda, T., Holt, R., Nedelman, M.A., Guerrero, J.L., Weisman, H.F. & Collen, D. (1993). A chimeric murine/human antibody Fab fragment directed against the platelet GPIIb/IIIa receptor enhances and sustains arterial thrombolysis with recombinant tissue-type plasminogen activator in baboons. *Arterioscler Thromb*, **13**, 1837-42.
- Koike, T., Kimura, N., Miyazaki, K., Yabuta, T., Kumamoto, K., Takenoshita, S., Chen, J., Kobayashi, M., Hosokawa, M., Taniguchi, A., Kojima, T., Ishida, N., Kawakita, M., Yamamoto, H., Takematsu, H., Suzuki, A., Kozutsumi, Y. & Kannagi, R. (2004). Hypoxia induces adhesion molecules on cancer cells: A missing link between Warburg effect and induction of selectin-ligand carbohydrates. *Proc Natl Acad Sci U S A*, **101**, 8132-7.
- Kojima, N. & Hakomori, S. (1991). Cell adhesion, spreading, and motility of GM3-expressing cells based on glycolipid-glycolipid interaction. *J Biol Chem*, **266**, 17552-8.
- Kononen, J., Bubendorf, L., Kallioniemi, A., Barlund, M., Schraml, P., Leighton, S., Torhorst, J., Mihatsch, M.J., Sauter, G. & Kallioniemi, O.P. (1998). Tissue microarrays for high-throughput molecular profiling of tumor specimens. *Nat Med*, **4**, 844-7.
- Koornstra, J.J., de Jong, S., Hollema, H., de Vries, E.G. & Kleibeuker, J.H. (2003). Changes in apoptosis during the development of colorectal cancer: a systematic review of the literature. *Crit Rev Oncol Hematol*, **45**, 37-53.
- Krajewska, M., Kitada, S., Winter, J.N., Variakojis, D., Lichtenstein, A., Zhai, D., Cuddy, M., Huang, X., Luciano, F., Baker, C.H., Kim, H., Shin, E., Kennedy, S., Olson, A.H., Badzio, A., Jassem, J., Meinhold-Heerlein, I., Duffy, M.J., Schimmer, A.D., Tsao, M., Brown, E., Sawyers, A., Andreeff, M., Mercola, D., Krajewski, S. & Reed, J.C. (2008). Bcl-B expression in human epithelial and nonepithelial malignancies. *Clin Cancer Res*, **14**, 3011-21.
- Kraman, M., Bambrough, P.J., Arnold, J.N., Roberts, E.W., Magiera, L., Jones, J.O., Gopinathan, A., Tuveson, D.A. & Fearon, D.T. (2010). Suppression of antitumor immunity by stromal cells expressing fibroblast activation protein-alpha. *Science*, **330**, 827-30.
- Kramer, K., Cheung, N.K., Humm, J.L., Dantis, E., Finn, R., Yeh, S.J., Antunes, N.L., Dunkel, I.J., Souweidane, M. & Larson, S.M. (2000). Targeted radioimmunotherapy for leptomeningeal cancer using (131)I-3F8. *Med Pediatr Oncol*, **35**, 716-8.
- Kramer, K., Gerald, W.L., Kushner, B.H., Larson, S.M., Hameed, M. & Cheung, N.K. (1998). Disialoganglioside G(D2) loss following monoclonal antibody therapy is rare in neuroblastoma. *Clin Cancer Res*, **4**, 2135-9.
- Kramer, K., Humm, J.L., Souweidane, M.M., Zanzonico, P.B., Dunkel, I.J., Gerald, W.L., Khakoo, Y., Yeh, S.D., Yeung, H.W., Finn, R.D., Wolden, S.L., Larson, S.M. & Cheung, N.K. (2007). Phase I study of targeted radioimmunotherapy for leptomeningeal cancers using intra-Ommaya 131-I-3F8. *J Clin Oncol*, **25**, 5465-70.
- Krummel, M.F. & Allison, J.P. (1995). CD28 and CTLA-4 have opposing effects on the response of T cells to stimulation. *J Exp Med*, **182**, 459-65.
- Kubota, T., Niwa, R., Satoh, M., Akinaga, S., Shitara, K. & Hanai, N. (2009). Engineered therapeutic antibodies with improved effector functions. *Cancer Sci*, **100**, 1566-72.
- Kurosaki, T. (2002). Regulation of B-cell signal transduction by adaptor proteins. *Nat Rev Immunol*, **2**, 354-63.
- Kushner, B.H., Kramer, K. & Cheung, N.K. (2001). Phase II trial of the anti-G(D2) monoclonal antibody 3F8 and granulocyte-macrophage colony-stimulating factor for neuroblastoma. *J Clin Oncol*, **19**, 4189-94.
- Lambris, J.D., Ricklin, D. & Geisbrecht, B.V. (2008). Complement evasion by human pathogens. *Nat Rev Microbiol*, **6**, 132-42.

- Lannert, H., Bunning, C., Jeckel, D. & Wieland, F.T. (1994). Lactosylceramide is synthesized in the lumen of the Golgi apparatus. *FEBS Lett*, **342**, 91-6.
- Leadbetter, E.A., Brigl, M., Illarionov, P., Cohen, N., Luteran, M.C., Pillai, S., Besra, G.S. & Brenner, M.B. (2008). NK T cells provide lipid antigen-specific cognate help for B cells. *Proc Natl Acad Sci U S A*, **105**, 8339-44.
- Ledford, H. (2011). Melanoma drug wins US approval. *Nature*, **471**, 561.
- Leonardos, L., Butler, L.M., Hewett, P.J., Zalewski, P.D. & Cowled, P.A. (1999). The activity of caspase-3-like proteases is elevated during the development of colorectal carcinoma. *Cancer Lett*, **143**, 29-35.
- Levade, T. & Jaffrezou, J.P. (1999). Signalling sphingomyelinases: which, where, how and why? *Biochim Biophys Acta*, **1438**, 1-17.
- Levine, B. & Klionsky, D.J. (2004). Development by self-digestion: molecular mechanisms and biological functions of autophagy. *Dev Cell*, **6**, 463-77.
- Li, F., Lin, B., Hao, Y., Li, Y., Liu, J., Cong, J., Zhu, L., Liu, Q. & Zhang, S. (2011). Lewis Y Promotes Growth and Adhesion of Ovarian Carcinoma-Derived RMG-I Cells by Upregulating Growth Factors. *Int J Mol Sci*, **11**, 3748-59.
- Li, G., Zhang, L., Chen, E., Wang, J., Jiang, X., Chen, J.H., Wickman, G., Amundson, K., Bergqvist, S., Zobel, J., Buckman, D., Baxi, S.M., Bender, S.L., Casperson, G.F. & Hu-Lowe, D.D. (2010). Dual functional monoclonal antibody PF-04605412 targets integrin alpha5beta1 and elicits potent antibody-dependent cellular cytotoxicity. *Cancer Res*, **70**, 10243-54.
- Li, J.C. & Li, R. (2007). RAV12 accelerates the desensitization of Akt/PKB pathway of insulin-like growth factor I receptor signaling in COLO205. *Cancer Res*, **67**, 8856-64.
- Li, P., Nijhawan, D., Budihardjo, I., Srinivasula, S.M., Ahmad, M., Alnemri, E.S. & Wang, X. (1997). Cytochrome c and dATP-dependent formation of Apaf-1/caspase-9 complex initiates an apoptotic protease cascade. *Cell*, **91**, 479-89.
- Li, Y., Williams, M.E., Cousar, J.B., Pawluczko, A.W., Lindorfer, M.A. & Taylor, R.P. (2007). Rituximab-CD20 complexes are shaved from Z138 mantle cell lymphoma cells in intravenous and subcutaneous SCID mouse models. *J Immunol*, **179**, 4263-71.
- Lin, T.S. (2010). Ofatumumab: a novel monoclonal anti-CD20 antibody. *Pharmacogenomics and Personalized Medicine*, **3** 51-59.
- Lingwood, D. & Simons, K. (2010). Lipid rafts as a membrane-organizing principle. *Science*, **327**, 46-50.
- Liszewski, M.K., Post, T.W. & Atkinson, J.P. (1991). Membrane cofactor protein (MCP or CD46): newest member of the regulators of complement activation gene cluster. *Annu Rev Immunol*, **9**, 431-55.
- Liu, X.-y., Pop, L.M. & Vitetta, E.S. (2008). Engineering therapeutic monoclonal antibodies, Vol. 222. pp. 9-27.
- Liu, X. & Schnellmann, R.G. (2003). Calpain mediates progressive plasma membrane permeability and proteolysis of cytoskeleton-associated paxillin, talin, and vinculin during renal cell death. *J Pharmacol Exp Ther*, **304**, 63-70.
- Liu, X., Van Vleet, T. & Schnellmann, R.G. (2004). The role of calpain in oncotic cell death. *Annu Rev Pharmacol Toxicol*, **44**, 349-70.
- Loo, D., Pryer, N., Young, P., Liang, T., Coberly, S., King, K.L., Kang, K., Roberts, P., Tsao, M., Xu, X., Potts, B. & Mather, J.P. (2007). The glycotope-specific RAV12 monoclonal antibody induces oncosis in vitro and has antitumor activity against gastrointestinal adenocarcinoma tumor xenografts in vivo. *Mol Cancer Ther*, **6**, 856-65.
- Los, M., Wesselborg, S. & Schulze-Osthoff, K. (1999). The role of caspases in development, immunity, and apoptotic signal transduction: lessons from knockout mice. *Immunity*, **10**, 629-39.
- Los, M.H., W. (2002). *Caspases: Their Role in Cell Death and Cell Survival*. Kluwer Academic/Plenum Publishers.

- Luo, X., Budihardjo, I., Zou, H., Slaughter, C. & Wang, X. (1998). Bid, a Bcl2 interacting protein, mediates cytochrome c release from mitochondria in response to activation of cell surface death receptors. *Cell*, **94**, 481-90.
- MacLennan, I.C., Toellner, K.M., Cunningham, A.F., Serre, K., Sze, D.M., Zuniga, E., Cook, M.C. & Vinuesa, C.G. (2003). Extrafollicular antibody responses. *Immunol Rev*, **194**, 8-18.
- Madjd, Z., Parsons, T., Watson, N.F., Spendlove, I., Ellis, I. & Durrant, L.G. (2005). High expression of Lewis y/b antigens is associated with decreased survival in lymph node negative breast carcinomas. *Breast Cancer Res*, **7**, R780-7.
- Magnani, J.L., Nilsson, B., Brockhaus, M., Zopf, D., Steplewski, Z., Koprowski, H. & Ginsburg, V. (1982). A monoclonal antibody-defined antigen associated with gastrointestinal cancer is a ganglioside containing sialylated lacto-N-fucopentaose II. *J Biol Chem*, **257**, 14365-9.
- Majno, G. & Joris, I. (1995). Apoptosis, oncosis, and necrosis. An overview of cell death. *Am J Pathol*, **146**, 3-15.
- Malisan, F. & Testi, R. (2002). GD3 ganglioside and apoptosis. *Biochim Biophys Acta*, **1585**, 179-87.
- Manimala, J.C., Roach, T.A., Li, Z. & Gildersleeve, J.C. (2007). High-throughput carbohydrate microarray profiling of 27 antibodies demonstrates widespread specificity problems. *Glycobiology*, **17**, 17C-23C.
- Mantovani, A., Sica, A. & Locati, M. (2007). New vistas on macrophage differentiation and activation. *Eur J Immunol*, **37**, 14-6.
- Marionneau, S., Cailleau-Thomas, A., Rocher, J., Le Moullac-Vaidye, B., Ruvoen, N., Clement, M. & Le Pendu, J. (2001). ABH and Lewis histo-blood group antigens, a model for the meaning of oligosaccharide diversity in the face of a changing world. *Biochimie*, **83**, 565-73.
- Masayuki, W., Tomohiro, S., Toshihito, S., Taiichi, N., Takayuki, I., Masato, I., Yasuko, S., Kyoichi, I. & Akiharu, O. (1995). Lewis Y antigen expression in hepatocellular carcinoma. An immunohistochemical study. *Cancer*, **75**, 2827-2835.
- Mathias, S., Pena, L.A. & Kolesnick, R.N. (1998). Signal transduction of stress via ceramide. *Biochem J*, **335 ( Pt 3)**, 465-80.
- Maul, R.W. & Gearhart, P.J. (2010). Controlling somatic hypermutation in immunoglobulin variable and switch regions. *Immunol Res*, **47**, 113-22.
- Mazelin, L., Bernet, A., Bonod-Bidaud, C., Pays, L., Arnaud, S., Gespach, C., Bredesen, D.E., Scoazec, J.Y. & Mehlen, P. (2004). Netrin-1 controls colorectal tumorigenesis by regulating apoptosis. *Nature*, **431**, 80-4.
- McGilvray, R.W., Eagle, R.A., Watson, N.F., Al-Attar, A., Ball, G., Jafferji, I., Trowsdale, J. & Durrant, L.G. (2009). NKG2D ligand expression in human colorectal cancer reveals associations with prognosis and evidence for immunoediting. *Clin Cancer Res*, **15**, 6993-7002.
- Medema, J.P., Scaffidi, C., Kischkel, F.C., Shevchenko, A., Mann, M., Krammer, P.H. & Peter, M.E. (1997). FLICE is activated by association with the CD95 death-inducing signaling complex (DISC). *Embo J*, **16**, 2794-804.
- Merrill, A.H., Jr., Schmelz, E.M., Dillehay, D.L., Spiegel, S., Shayman, J.A., Schroeder, J.J., Riley, R.T., Voss, K.A. & Wang, E. (1997). Sphingolipids--the enigmatic lipid class: biochemistry, physiology, and pathophysiology. *Toxicol Appl Pharmacol*, **142**, 208-25.
- Mild, G., Bachmann, F., Boulay, J.L., Glatz, K., Laffer, U., Lowy, A., Metzger, U., Reuter, J., Terracciano, L., Herrmann, R. & Rochlitz, C. (2002). DCR3 locus is a predictive marker for 5-fluorouracil-based adjuvant chemotherapy in colorectal cancer. *Int J Cancer*, **102**, 254-7.
- Miller, R.A., Maloney, D.G., Warnke, R. & Levy, R. (1982). Treatment of B-cell lymphoma with monoclonal anti-idiotypic antibody. *N Engl J Med*, **306**, 517-22.
- Mimura, Y., Church, S., Ghirlando, R., Ashton, P.R., Dong, S., Goodall, M., Lund, J. & Jefferis, R. (2000). The influence of glycosylation on the thermal stability and effector function expression of human IgG1-Fc: properties of a series of truncated glycoforms. *Mol Immunol*, **37**, 697-706.

- Mitsuzuka, K., Handa, K., Satoh, M., Arai, Y. & Hakomori, S. (2005). A specific microdomain ("glycosynapse 3") controls phenotypic conversion and reversion of bladder cancer cells through GM3-mediated interaction of alpha3beta1 integrin with CD9. *J Biol Chem*, **280**, 35545-53.
- Miyake, T., Kumagai, Y., Kato, H., Guo, Z., Matsushita, K., Satoh, T., Kawagoe, T., Kumar, H., Jang, M.H., Kawai, T., Tani, T., Takeuchi, O. & Akira, S. (2009). Poly I:C-induced activation of NK cells by CD8 alpha+ dendritic cells via the IPS-1 and TRIF-dependent pathways. *J Immunol*, **183**, 2522-8.
- Miyoshi, E., Moriwaki, K. & Nakagawa, T. (2008). Biological function of fucosylation in cancer biology. *J Biochem*, **143**, 725-9.
- Modak, S. & Cheung, N.K. (2007). Disialoganglioside directed immunotherapy of neuroblastoma. *Cancer Invest*, **25**, 67-77.
- Molina, M.A., Codony-Servat, J., Albanell, J., Rojo, F., Arribas, J. & Baselga, J. (2001). Trastuzumab (herceptin), a humanized anti-Her2 receptor monoclonal antibody, inhibits basal and activated Her2 ectodomain cleavage in breast cancer cells. *Cancer Res*, **61**, 4744-9.
- Mombaerts, P., Iacomini, J., Johnson, R.S., Herrup, K., Tonegawa, S. & Papaioannou, V.E. (1992). RAG-1-deficient mice have no mature B and T lymphocytes. *Cell*, **68**, 869-77.
- Mond, J.J., Vos, Q., Lees, A. & Snapper, C.M. (1995). T cell independent antigens. *Curr Opin Immunol*, **7**, 349-54.
- Moody, D.B., Zajonc, D.M. & Wilson, I.A. (2005). Anatomy of CD1-lipid antigen complexes. *Nat Rev Immunol*, **5**, 387-99.
- Moriwaki, K. & Miyoshi, E. (2010). Fucosylation and gastrointestinal cancer. *World J Hepatol*, **2**, 151-61.
- Mujoo, K., Cheresch, D.A., Yang, H.M. & Reisfeld, R.A. (1987). Disialoganglioside GD2 on human neuroblastoma cells: target antigen for monoclonal antibody-mediated cytotoxicity and suppression of tumor growth. *Cancer Res*, **47**, 1098-104.
- Mukohara, T., Engelman, J.A., Hanna, N.H., Yeap, B.Y., Kobayashi, S., Lindeman, N., Halmos, B., Pearlberg, J., Tsuchihashi, Z., Cantley, L.C., Tenen, D.G., Johnson, B.E. & Janne, P.A. (2005). Differential effects of gefitinib and cetuximab on non-small-cell lung cancers bearing epidermal growth factor receptor mutations. *J Natl Cancer Inst*, **97**, 1185-94.
- Munn, D.H., McBride, M. & Cheung, N.K. (1991). Role of low-affinity Fc receptors in antibody-dependent tumor cell phagocytosis by human monocyte-derived macrophages. *Cancer Res*, **51**, 1117-23.
- Muramatsu, M., Kinoshita, K., Fagarasan, S., Yamada, S., Shinkai, Y. & Honjo, T. (2000). Class switch recombination and hypermutation require activation-induced cytidine deaminase (AID), a potential RNA editing enzyme. *Cell*, **102**, 553-63.
- Musolino, A., Naldi, N., Bortesi, B., Pezzuolo, D., Capelletti, M., Missale, G., Laccabue, D., Zerbini, A., Camisa, R., Bisagni, G., Neri, T.M. & Ardizzoni, A. (2008). Immunoglobulin G fragment C receptor polymorphisms and clinical efficacy of trastuzumab-based therapy in patients with HER-2/neu-positive metastatic breast cancer. *J Clin Oncol*, **26**, 1789-96.
- Naidenko, O.V., Kozuka, Y. & Kronenberg, M. (2000). CD1-mediated antigen presentation of glycosphingolipids. *Microbes Infect*, **2**, 621-31.
- Nakagoe, T., Sawai, T., Tsuji, T., Jibiki, M., Nanashima, A., Yamaguchi, H., Kurosaki, N., Yasutake, T. & Ayabe, H. (2001). Circulating sialyl Lewis(x), sialyl Lewis(a), and sialyl Tn antigens in colorectal cancer patients: multivariate analysis of predictive factors for serum antigen levels. *J Gastroenterol*, **36**, 166-72.
- Nakamura, K., Tanaka, Y., Shitara, K. & Hanai, N. (2001). Construction of humanized anti-ganglioside monoclonal antibodies with potent immune effector functions. *Cancer Immunol Immunother*, **50**, 275-84.
- Nausch, N. & Cerwenka, A. (2008). NKG2D ligands in tumor immunity. *Oncogene*, **27**, 5944-58.

- Nelson, A.L., Dhimolea, E. & Reichert, J.M. (2010). Development trends for human monoclonal antibody therapeutics. *Nat Rev Drug Discov*, **9**, 767-74.
- NICE. (2003a). Guidance on the use of capecitabine and tegafur with uracil for metastatic colorectal cancer: Technology Appraisal 61. National Institute of Health and Clinical Excellence: London.
- NICE. (2003b). Guidance on the use of paclitaxel in the treatment of ovarian cancer, Vol. January. National Institute of Health and Clinical Excellence: London.
- NICE. (2004). Improving outcomes in colorectal cancers: manual update. *London*, National Institute for Clinical Excellence.
- NICE. (2008). Irinotecan, oxaliplatin and raltitrexed for the treatment of advanced colorectal cancer. In *Review of technology Appraisal*.
- NICE. (2009). Cetuximab for the first line treatment of metastatic colorectal cancer. *National Institute for Health and Clinical Excellence*.
- Nimmerjahn, F. & Ravetch, J.V. (2008). Fcγ receptors as regulators of immune responses. *Nat Rev Immunol*, **8**, 34-47.
- Nitschke, L. (2009). CD22 and Siglec-G: B-cell inhibitory receptors with distinct functions. *Immunol Rev*, **230**, 128-43.
- Nitschke, L. & Tsubata, T. (2004). Molecular interactions regulate BCR signal inhibition by CD22 and CD72. *Trends Immunol*, **25**, 543-50.
- Niwa, R., Natsume, A., Uehara, A., Wakitani, M., Iida, S., Uchida, K., Satoh, M. & Shitara, K. (2005). IgG subclass-independent improvement of antibody-dependent cellular cytotoxicity by fucose removal from Asn297-linked oligosaccharides. *J Immunol Methods*, **306**, 151-60.
- Norman, D.J. (1995). Mechanisms of action and overview of OKT3. *Ther Drug Monit*, **17**, 615-20.
- O'Connell, J., Bennett, M.W., Nally, K., Houston, A., O'Sullivan, G.C. & Shanahan, F. (2000). Altered mechanisms of apoptosis in colon cancer: Fas resistance and counterattack in the tumor-immune conflict. *Ann N Y Acad Sci*, **910**, 178-92; discussion 193-5.
- Ogawa, J., Inoue, H. & Koide, S. (1997). Glucose-transporter-type-I-gene amplification correlates with sialyl-Lewis-X synthesis and proliferation in lung cancer. *Int J Cancer*, **74**, 189-92.
- Okazaki, A., Shoji-Hosaka, E., Nakamura, K., Wakitani, M., Uchida, K., Kakita, S., Tsumoto, K., Kumagai, I. & Shitara, K. (2004). Fucose depletion from human IgG1 oligosaccharide enhances binding enthalpy and association rate between IgG1 and FcγRIIIa. *J Mol Biol*, **336**, 1239-49.
- Olayioye, M.A., Neve, R.M., Lane, H.A. & Hynes, N.E. (2000). The ErbB signaling network: receptor heterodimerization in development and cancer. *Embo J*, **19**, 3159-67.
- Oliva, J.P., Valdes, Z., Casaco, A., Pimentel, G., Gonzalez, J., Alvarez, I., Osorio, M., Velazco, M., Figueroa, M., Ortiz, R., Escobar, X., Orozco, M., Cruz, J., Franco, S., Diaz, M., Roque, L., Carr, A., Vazquez, A.M., Mateos, C., Rubio, M.C., Perez, R. & Fernandez, L.E. (2006). Clinical evidences of GM3 (NeuGc) ganglioside expression in human breast cancer using the 14F7 monoclonal antibody labelled with (99m)Tc. *Breast Cancer Res Treat*, **96**, 115-21.
- Olumi, A.F., Grossfeld, G.D., Hayward, S.W., Carroll, P.R., Tlsty, T.D. & Cunha, G.R. (1999). Carcinoma-associated fibroblasts direct tumor progression of initiated human prostatic epithelium. *Cancer Res*, **59**, 5002-11.
- Ono, M., Handa, K., Withers, D.A. & Hakomori, S. (2000). Glycosylation effect on membrane domain (GEM) involved in cell adhesion and motility: a preliminary note on functional alpha3, alpha5-CD82 glycosylation complex in Id1D 14 cells. *Biochem Biophys Res Commun*, **279**, 744-50.
- Ostermann, E., Garin-Chesa, P., Heider, K.H., Kalat, M., Lamche, H., Puri, C., Kerjaschki, D., Rettig, W.J. & Adolf, G.R. (2008). Effective immunoconjugate therapy in cancer models targeting a serine protease of tumor fibroblasts. *Clin Cancer Res*, **14**, 4584-92.
- Ostman, A. & Augsten, M. (2009). Cancer-associated fibroblasts and tumor growth--bystanders turning into key players. *Curr Opin Genet Dev*, **19**, 67-73.

- Pahlsson, P., Spitalnik, S.L., Spitalnik, P.F., Fantini, J., Rakotonirainy, O., Ghardashkhani, S., Lindberg, J., Konradsson, P. & Larson, G. (2001). Characterization of galactosyl glycerolipids in the HT29 human colon carcinoma cell line. *Arch Biochem Biophys*, **396**, 187-98.
- Parekh, V.V., Wilson, M.T., Olivares-Villagomez, D., Singh, A.K., Wu, L., Wang, C.R., Joyce, S. & Van Kaer, L. (2005). Glycolipid antigen induces long-term natural killer T cell anergy in mice. *J Clin Invest*, **115**, 2572-83.
- Patz, M., Isaeva, P., Forcob, N., Muller, B., Frenzel, L.P., Wendtner, C.M., Klein, C., Umana, P., Hallek, M. & Krause, G. (2011). Comparison of the in vitro effects of the anti-CD20 antibodies rituximab and GA101 on chronic lymphocytic leukaemia cells. *Br J Haematol*, **152**, 295-306.
- Paulick, M.G. & Bertozzi, C.R. (2008). The glycosylphosphatidylinositol anchor: a complex membrane-anchoring structure for proteins. *Biochemistry*, **47**, 6991-7000.
- Pedersen, I.M., Buhl, A.M., Klausen, P., Geisler, C.H. & Jurlander, J. (2002). The chimeric anti-CD20 antibody rituximab induces apoptosis in B-cell chronic lymphocytic leukemia cells through a p38 mitogen activated protein-kinase-dependent mechanism. *Blood*, **99**, 1314-9.
- Peng, D., Fan, Z., Lu, Y., DeBlasio, T., Scher, H. & Mendelsohn, J. (1996). Anti-epidermal growth factor receptor monoclonal antibody 225 up-regulates p27KIP1 and induces G1 arrest in prostatic cancer cell line DU145. *Cancer Res*, **56**, 3666-9.
- Peng, W., Zhang, X., Mohamed, N., Inghirami, G., Takeshita, K., Pecora, A., Nardone, L.L., Pincus, S.E., Casey, L.S. & Spitalny, G.L. (2005). A DeImmunized chimeric anti-C3b/iC3b monoclonal antibody enhances rituximab-mediated killing in NHL and CLL cells via complement activation. *Cancer Immunol Immunother*, **54**, 1172-9.
- Pescovitz, M.D. (2006). Rituximab, an anti-cd20 monoclonal antibody: history and mechanism of action. *Am J Transplant*, **6**, 859-66.
- Peter-Katalinic, J. (2005). Methods in enzymology: O-glycosylation of proteins. *Methods Enzymol*, **405**, 139-71.
- Petersen-Mahrt, S.K., Harris, R.S. & Neuberger, M.S. (2002). AID mutates E. coli suggesting a DNA deamination mechanism for antibody diversification. *Nature*, **418**, 99-103.
- Pollard, J.W. (2004). Tumour-educated macrophages promote tumour progression and metastasis. *Nat Rev Cancer*, **4**, 71-8.
- Ponnusamy, M.P., Lakshmanan, I., Jain, M., Das, S., Chakraborty, S., Dey, P. & Batra, S.K. (2010). MUC4 mucin-induced epithelial to mesenchymal transition: a novel mechanism for metastasis of human ovarian cancer cells. *Oncogene*, **29**, 5741-54.
- Portoukalian, J., Zwingelstein, G. & Dore, J.F. (1979). Lipid composition of human malignant melanoma tumors at various levels of malignant growth. *Eur J Biochem*, **94**, 19-23.
- Preithner, S., Elm, S., Lippold, S., Locher, M., Wolf, A., da Silva, A.J., Baeuerle, P.A. & Prang, N.S. (2006). High concentrations of therapeutic IgG1 antibodies are needed to compensate for inhibition of antibody-dependent cellular cytotoxicity by excess endogenous immunoglobulin G. *Mol Immunol*, **43**, 1183-93.
- Presta, L.G. (2006). Engineering of therapeutic antibodies to minimize immunogenicity and optimize function. *Adv Drug Deliv Rev*, **58**, 640-56.
- Priola, S.A. & McNally, K.L. (2009). The role of the prion protein membrane anchor in prion infection. *Prion*, **3**, 134-8.
- Pryde, J.G., Walker, A., Rossi, A.G., Hannah, S. & Haslett, C. (2000). Temperature-dependent arrest of neutrophil apoptosis. Failure of Bax insertion into mitochondria at 15 degrees C prevents the release of cytochrome c. *J Biol Chem*, **275**, 33574-84.
- Quinn MJ, B.P., Brock A, Kirby EA, Jones J. (2001). Cancer trends in England and Wales, 1950-1999. *London: Stationery Office*, 206-207.
- Ragupathi, G., Damani, P., Srivastava, G., Srivastava, O., Sucheck, S.J., Ichikawa, Y. & Livingston, P.O. (2009). Synthesis of sialyl Lewis(a) (sLe (a), CA19-9) and construction of an immunogenic sLe(a) vaccine. *Cancer Immunol Immunother*, **58**, 1397-405.

- Ramsland, P., Farrugia, W., PBradford, T., Hogarth, P. & Scott, A. (2004). Structural convergence of antibody binding of carbohydrate determinants in Lewis Y tumor antigens. *J Mol Biol*, **340**, 809-818.
- Reichert, J. & Pavolu, A. (2004). Monoclonal antibodies market. *Nat Rev Drug Discov*, **3**, 383-4.
- Reichert, J.M. (2008). Monoclonal antibodies as innovative therapeutics. *Curr Pharm Biotechnol*, **9**, 423-30.
- Reichert, J.M. (2011). Antibody-based therapeutics to watch in 2011. *MAbs*, **3**, 76-99.
- Reichert, J.M., Rosensweig, C.J., Faden, L.B. & Dewitz, M.C. (2005). Monoclonal antibody successes in the clinic. *Nat Biotechnol*, **23**, 1073-8.
- Reis, C.A., Osorio, H., Silva, L., Gomes, C. & David, L. (2010). Alterations in glycosylation as biomarkers for cancer detection. *J Clin Pathol*, **63**, 322-9.
- Reth, M. & Wienands, J. (1997). Initiation and processing of signals from the B cell antigen receptor. *Annu Rev Immunol*, **15**, 453-79.
- Retter, M.W., Johnson, J.C., Peckham, D.W., Bannink, J.E., Bangur, C.S., Dresser, K., Cai, F., Foy, T.M., Fanger, N.A., Fanger, G.R., Woda, B. & Rock, K.L. (2005). Characterization of a proapoptotic antiganglioside GM2 monoclonal antibody and evaluation of its therapeutic effect on melanoma and small cell lung carcinoma xenografts. *Cancer Res*, **65**, 6425-34.
- Ries, L.A., Wingo, P.A., Miller, D.S., Howe, H.L., Weir, H.K., Rosenberg, H.M., Vernon, S.W., Cronin, K. & Edwards, B.K. (2000). The annual report to the nation on the status of cancer, 1973-1997, with a special section on colorectal cancer. *Cancer*, **88**, 2398-424.
- Ritter, G., Cohen, L.S., Williams, C., Jr., Richards, E.C., Old, L.J. & Welt, S. (2001). Serological analysis of human anti-human antibody responses in colon cancer patients treated with repeated doses of humanized monoclonal antibody A33. *Cancer Res*, **61**, 6851-9.
- Roche. (2011). Third phase III study of Avastin-based regimen met primary endpoint in ovarian cancer, Vol. 2011. pp. Media release of results of third phase III trial of bevacizumab for the treatment of ovarian cancer. Hoffmann-La Roche.
- Rossi, J.F., Negrier, S., James, N.D., Kocak, I., Hawkins, R., Davis, H., Prabhakar, U., Qin, X., Mulders, P. & Berns, B. (2010). A phase I/II study of siltuximab (CNTO 328), an anti-interleukin-6 monoclonal antibody, in metastatic renal cell cancer. *Br J Cancer*, **103**, 1154-62.
- Rowan, W., Tite, J., Topley, P. & Brett, S.J. (1998). Cross-linking of the CAMPATH-1 antigen (CD52) mediates growth inhibition in human B- and T-lymphoma cell lines, and subsequent emergence of CD52-deficient cells. *Immunology*, **95**, 427-36.
- Rudd, P.M. & Dwek, R.A. (1997). Glycosylation: heterogeneity and the 3D structure of proteins. *Crit Rev Biochem Mol Biol*, **32**, 1-100.
- Rush, J.S., Fugmann, S.D. & Schatz, D.G. (2004). Staggered AID-dependent DNA double strand breaks are the predominant DNA lesions targeted to S mu in Ig class switch recombination. *Int Immunol*, **16**, 549-57.
- Sa, G., Das, T., Moon, C., Hilston, C.M., Rayman, P.A., Rini, B.I., Tannenbaum, C.S. & Finke, J.H. (2009). GD3, an overexpressed tumor-derived ganglioside, mediates the apoptosis of activated but not resting T cells. *Cancer Res*, **69**, 3095-104.
- Sakamoto, J., Furukawa, K., Cordon-Cardo, C., Yin, B.W., Rettig, W.J., Oettgen, H.F., Old, L.J. & Lloyd, K.O. (1986). Expression of Lewis<sup>a</sup>, Lewis<sup>b</sup>, X, and Y blood group antigens in human colonic tumors and normal tissue and in human tumor-derived cell lines. *Cancer Res*, **46**, 1553-61.
- Sakamoto, J., Watanabe, T., Tokumaru, T., Takagi, H., Nakazato, H. & Lloyd, K. (1989). Expression of Lewis<sup>a</sup>, Lewis<sup>b</sup>, Lewis<sup>x</sup>, Lewis<sup>y</sup>, Sialyl-Lewis<sup>a</sup> and Sialyl-Lewis<sup>x</sup> Blood Group Antigens in Human Gastric Carcinoma and in Normal Gastric Tissue. *Can Res*, **49**, 745-752.
- Sakano, H., Huppi, K., Heinrich, G. & Tonegawa, S. (1979). Sequences at the somatic recombination sites of immunoglobulin light-chain genes. *Nature*, **280**, 288-94.
- Saleh, M.N., Sugarman, S., Murray, J., Ostroff, J.B., Healey, D., Jones, D., LeBherz, D., Brewer, H., Onetto, N. & Lobuglio, A.F. (2000). Phase I trial of the anti-Lewis Y drug immunoconjugate



- BR96-doxorubicin in patients with lewis Y-expressing epithelial tumors. *J Clin Oncol*, **18**, 2282-2292.
- Salfeld, J.G. (2007). Isotype selection in antibody engineering. *Nat Biotechnol*, **25**, 1369-72.
- Salisbury, J.R., Rapson, N.T., Codd, J.D., Rogers, M.V. & Nethersell, A.B. (1994). Immunohistochemical analysis of CDw52 antigen expression in non-Hodgkin's lymphomas. *J Clin Pathol*, **47**, 313-7.
- Sandhoff, K. & Kolter, T. (1996). Topology of glycosphingolipid degradation. *Trends Cell Biol*, **6**, 98-103.
- Sasisekharan, R., Shriver, Z., Venkataraman, G. & Narayanasami, U. (2002). Roles of heparan-sulphate glycosaminoglycans in cancer. *Nat Rev Cancer*, **2**, 521-8.
- Sawada, R., Sun, S.M., Wu, X., Hong, F., Ragupathi, G., Livingston, P.O. & Scholz, W.W. (2011). Human Monoclonal Antibodies to Sialyl-Lewis<sup>x</sup> (CA19.9) with Potent CDC, ADCC, and Antitumor Activity. *Clin Cancer Res*, **17**, 1024-32.
- Scarlett, J.L. & Murphy, M.P. (1997). Release of apoptogenic proteins from the mitochondrial intermembrane space during the mitochondrial permeability transition. *FEBS Lett*, **418**, 282-6.
- Schinzell, A.C., Takeuchi, O., Huang, Z., Fisher, J.K., Zhou, Z., Rubens, J., Hetz, C., Danial, N.N., Moskowitz, M.A. & Korsmeyer, S.J. (2005). Cyclophilin D is a component of mitochondrial permeability transition and mediates neuronal cell death after focal cerebral ischemia, Vol. 102. pp. 12005-12010.
- Schittny, J.C., Djonov, V., Fine, A. & Burri, P.H. (1998). Programmed cell death contributes to postnatal lung development. *Am J Respir Cell Mol Biol*, **18**, 786-93.
- Schroeder, H.W., Jr. & Cavacini, L. (2010). Structure and function of immunoglobulins. *J Allergy Clin Immunol*, **125**, S41-52.
- Scott, A.M., Wiseman, G., Welt, S., Adjei, A., Lee, F.T., Hopkins, W., Divgi, C.R., Hanson, L.H., Mitchell, P., Gansen, D.N., Larson, S.M., Ingle, J.N., Hoffman, E.W., Tanswell, P., Ritter, G., Cohen, L.S., Bette, P., Arvay, L., Amelsberg, A., Vlock, D., Rettig, W.J. & Old, L.J. (2003). A Phase I dose-escalation study of sibrotuzumab in patients with advanced or metastatic fibroblast activation protein-positive cancer. *Clin Cancer Res*, **9**, 1639-47.
- Scott, D.W. & De Groot, A.S. (2010). Can we prevent immunogenicity of human protein drugs? *Ann Rheum Dis*, **69 Suppl 1**, i72-76.
- Seimetz, D., Lindhofer, H. & Bokemeyer, C. (2010). Development and approval of the trifunctional antibody catumaxomab (anti-EpCAM x anti-CD3) as a targeted cancer immunotherapy. *Cancer Treat Rev*, **36**, 458-67.
- Shan, D., Ledbetter, J.A. & Press, O.W. (1998). Apoptosis of malignant human B cells by ligation of CD20 with monoclonal antibodies. *Blood*, **91**, 1644-52.
- Sheikh, M.S. & Fornace, A.J., Jr. (2000). Death and decoy receptors and p53-mediated apoptosis. *Leukemia*, **14**, 1509-13.
- Shen, M., Chou, C., Hsu, K. & Ellory, J. (2002). Osmotic shrinkage of human cervical cancer cells induces an extracellular C1- dependent nonselective cation channel, which requires p38 MAPK. *J Biol Chem*, **277**, 45776-45784.
- Shi, S.R., Key, M.E. & Kalra, K.L. (1991). Antigen retrieval in formalin-fixed, paraffin-embedded tissues: an enhancement method for immunohistochemical staining based on microwave oven heating of tissue sections. *J Histochem Cytochem*, **39**, 741-8.
- Shibata, S., Kyuwa, S., Lee, S.K., Toyoda, Y. & Goto, N. (1994). Apoptosis induced in mouse hepatitis virus-infected cells by a virus-specific CD8+ cytotoxic T-lymphocyte clone, Vol. 68. pp. 7540-7545.
- Shields, R.L., Namenuk, A.K., Hong, K., Meng, Y.G., Rae, J., Briggs, J., Xie, D., Lai, J., Stadlen, A., Li, B., Fox, J.A. & Presta, L.G. (2001). High resolution mapping of the binding site on human IgG1 for Fc gamma RI, Fc gamma RII, Fc gamma RIII, and FcRn and design of IgG1 variants with improved binding to the Fc gamma R. *J Biol Chem*, **276**, 6591-604.

- Shih, T. & Lindley, C. (2006). Bevacizumab: an angiogenesis inhibitor for the treatment of solid malignancies. *Clin Ther*, **28**, 1779-802.
- Shinkura, R., Ito, S., Begum, N.A., Nagaoka, H., Muramatsu, M., Kinoshita, K., Sakakibara, Y., Hijikata, H. & Honjo, T. (2004). Separate domains of AID are required for somatic hypermutation and class-switch recombination. *Nat Immunol*, **5**, 707-12.
- Shrivastav, M., De Haro, L.P. & Nickoloff, J.A. (2008). Regulation of DNA double-strand break repair pathway choice. *Cell Res*, **18**, 134-47.
- Sica, A., Larghi, P., Mancino, A., Rubino, L., Porta, C., Totaro, M.G., Rimoldi, M., Biswas, S.K., Allavena, P. & Mantovani, A. (2008). Macrophage polarization in tumour progression. *Semin Cancer Biol*, **18**, 349-55.
- Sidobre, S., Hammond, K.J., Benazet-Sidobre, L., Maltsev, S.D., Richardson, S.K., Ndonge, R.M., Howell, A.R., Sakai, T., Besra, G.S., Porcelli, S.A. & Kronenberg, M. (2004). The T cell antigen receptor expressed by Valpha14i NKT cells has a unique mode of glycosphingolipid antigen recognition. *Proc Natl Acad Sci U S A*, **101**, 12254-9.
- Sievers, E.L., Appelbaum, F.R., Spielberger, R.T., Forman, S.J., Flowers, D., Smith, F.O., Shannon-Dorcy, K., Berger, M.S. & Bernstein, I.D. (1999). Selective ablation of acute myeloid leukemia using antibody-targeted chemotherapy: a phase I study of an anti-CD33 calicheamicin immunoconjugate. *Blood*, **93**, 3678-84.
- Simpson, J.A., Al-Attar, A., Watson, N.F., Scholefield, J.H., Ilyas, M. & Durrant, L.G. (2010). Intratumoral T cell infiltration, MHC class I and STAT1 as biomarkers of good prognosis in colorectal cancer. *Gut*, **59**, 926-33.
- Slamon, D.J., Clark, G.M., Wong, S.G., Levin, W.J., Ullrich, A. & McGuire, W.L. (1987). Human breast cancer: correlation of relapse and survival with amplification of the HER-2/neu oncogene. *Science*, **235**, 177-82.
- Smith, K.G., Tarlinton, D.M., Doody, G.M., Hibbs, M.L. & Fearon, D.T. (1998). Inhibition of the B cell by CD22: a requirement for Lyn. *J Exp Med*, **187**, 807-11.
- Soung, Y.H., Lee, J.W., Kim, S.Y., Park, W.S., Nam, S.W., Lee, J.Y., Yoo, N.J. & Lee, S.H. (2004). Somatic mutations of CASP3 gene in human cancers. *Hum Genet*, **115**, 112-5.
- Spratlin, J.L., Cohen, R.B., Eadens, M., Gore, L., Camidge, D.R., Diab, S., Leong, S., O'Bryant, C., Chow, L.Q., Serkova, N.J., Meropol, N.J., Lewis, N.L., Chiorean, E.G., Fox, F., Youssoufian, H., Rowinsky, E.K. & Eckhardt, S.G. (2010). Phase I pharmacologic and biologic study of ramucirumab (IMC-1121B), a fully human immunoglobulin G1 monoclonal antibody targeting the vascular endothelial growth factor receptor-2. *J Clin Oncol*, **28**, 780-7.
- Sprong, H., Kruithof, B., Leijendekker, R., Slot, J.W., van Meer, G. & van der Sluijs, P. (1998). UDP-galactose:ceramide galactosyltransferase is a class I integral membrane protein of the endoplasmic reticulum. *J Biol Chem*, **273**, 25880-8.
- St Hill, C.A., Baharo-Hassan, D. & Farooqui, M. (2011). C2-O-sLe Glycoproteins Are E-Selectin Ligands that Regulate Invasion of Human Colon and Hepatic Carcinoma Cells. *PLoS One*, **6**, e16281.
- Stancovski, I., Hurwitz, E., Leitner, O., Ullrich, A., Yarden, Y. & Sela, M. (1991). Mechanistic aspects of the opposing effects of monoclonal antibodies to the ERBB2 receptor on tumor growth. *Proc Natl Acad Sci U S A*, **88**, 8691-5.
- Stanglmaier, M., Reis, S. & Hallek, M. (2004). Rituximab and alemtuzumab induce a nonclassic, caspase-independent apoptotic pathway in B-lymphoid cell lines and in chronic lymphocytic leukemia cells. *Ann Hematol*, **83**, 634-45.
- Stein, K.E. (1992). Thymus-independent and thymus-dependent responses to polysaccharide antigens. *J Infect Dis*, **165 Suppl 1**, S49-52.
- Stennicke, H.R., Jurgensmeier, J.M., Shin, H., Deveraux, Q., Wolf, B.B., Yang, X., Zhou, Q., Ellerby, H.M., Ellerby, L.M., Bredesen, D., Green, D.R., Reed, J.C., Froelich, C.J. & Salvesen, G.S. (1998). Pro-caspase-3 is a major physiologic target of caspase-8. *J Biol Chem*, **273**, 27084-90.
- Stern, M. & Herrmann, R. (2005). Overview of monoclonal antibodies in cancer therapy: present and promise. *Crit Rev Oncol Hematol*, **54**, 11-29.

- Stevenson, R.A., Huang, J.A., Studdert, M.J. & Hartley, C.A. (2004). Sialic acid acts as a receptor for equine rhinitis A virus binding and infection. *J Gen Virol*, **85**, 2535-43.
- Strohl, W.R. (2009). Optimization of Fc-mediated effector functions of monoclonal antibodies. *Curr Opin Biotechnol*, **20**, 685-91.
- Stroud, M.R., Levery, S.B., Nudelman, E.D., Salyan, M.E., Towell, J.A., Roberts, C.E., Watanabe, M. & Hakomori, S. (1991). Extended type 1 chain glycosphingolipids: dimeric Lea (III4V4Fuc2Lc6) as human tumor-associated antigen. *J Biol Chem*, **266**, 8439-46.
- Susin, S., Daugas, E., Ravagnan, L., Samejima, K., Zamzami, N., Loeffler, M., Costantini, P., Ferri, K., Irinopoulou, T., Prevost, M., Brothers, G., Mak, T., Penninger, J., Earnshaw, W. & Kroemer, G. (2000). Two distinct pathways leading to nuclear apoptosis. *J Exp Med*, **192**, 571-580.
- Suzuki, C. & Kojima, N. (2007). A cholesterol-independent membrane microdomain serves as a functional counter-receptor for E-selectin at the Colo201 cell surface and initiates signalling on E-selectin binding. *J Biochem*, **142**, 55-64.
- Szewczyk, A. & Wojtczak, L. (2002). Mitochondria as a pharmacological target. *Pharmacol Rev*, **54**, 101-27.
- Tan, H.L., Fong, W.J., Lee, E.H., Yap, M. & Choo, A. (2009). mAb 84, a cytotoxic antibody that kills undifferentiated human embryonic stem cells via oncosis. *Stem Cells*, **27**, 1792-801.
- Tarhini, A., Lo, E. & Minor, D.R. (2010). Releasing the brake on the immune system: ipilimumab in melanoma and other tumors. *Cancer Biother Radiopharm*, **25**, 601-13.
- Tedder, T.F., Inaoki, M. & Sato, S. (1997). The CD19-CD21 complex regulates signal transduction thresholds governing humoral immunity and autoimmunity. *Immunity*, **6**, 107-18.
- Teeling, J.L., French, R.R., Cragg, M.S., van den Brakel, J., Pluyter, M., Huang, H., Chan, C., Parren, P.W., Hack, C.E., Dechant, M., Valerius, T., van de Winkel, J.G. & Glennie, M.J. (2004). Characterization of new human CD20 monoclonal antibodies with potent cytolytic activity against non-Hodgkin lymphomas. *Blood*, **104**, 1793-800.
- Teeling, J.L., Mackus, W.J., Wiegman, L.J., van den Brakel, J.H., Beers, S.A., French, R.R., van Meerten, T., Ebeling, S., Vink, T., Slootstra, J.W., Parren, P.W., Glennie, M.J. & van de Winkel, J.G. (2006). The biological activity of human CD20 monoclonal antibodies is linked to unique epitopes on CD20. *J Immunol*, **177**, 362-71.
- Tesniere, A., Panaretakis, T., Kepp, O., Apetoh, L., Ghiringhelli, F., Zitvogel, L. & Kroemer, G. (2008). Molecular characteristics of immunogenic cancer cell death. *Cell Death Differ*, **15**, 3-12.
- Thapa, P., Zhang, G., Xia, C., Gelbard, A., Overwijk, W.W., Liu, C., Hwu, P., Chang, D.Z., Courtney, A., Sastry, J.K., Wang, P.G., Li, C. & Zhou, D. (2009). Nanoparticle formulated alpha-galactosylceramide activates NKT cells without inducing anergy. *Vaccine*, **27**, 3484-8.
- Thorne, R.F., Mhaidat, N.M., Ralston, K.J. & Burns, G.F. (2007). Shed gangliosides provide detergent-independent evidence for type-3 glycosynapses. *Biochem Biophys Res Commun*, **356**, 306-11.
- Thorsteinsson, L., O'Dowd, G.M., Harrington, P.M. & Johnson, P.M. (1998). The complement regulatory proteins CD46 and CD59, but not CD55, are highly expressed by glandular epithelium of human breast and colorectal tumour tissues. *Apmis*, **106**, 869-78.
- Tjandra, J.J., Ramadi, L. & McKenzie, I.F. (1990). Development of human anti-murine antibody (HAMA) response in patients. *Immunol Cell Biol*, **68 ( Pt 6)**, 367-76.
- Toellner, K.M., Jenkinson, W.E., Taylor, D.R., Khan, M., Sze, D.M., Sansom, D.M., Vinuesa, C.G. & MacLennan, I.C. (2002). Low-level hypermutation in T cell-independent germinal centers compared with high mutation rates associated with T cell-dependent germinal centers. *J Exp Med*, **195**, 383-9.
- Tolar, P., Hanna, J., Krueger, P.D. & Pierce, S.K. (2009). The constant region of the membrane immunoglobulin mediates B cell-receptor clustering and signaling in response to membrane antigens. *Immunity*, **30**, 44-55.
- Tolcher, A., Sugarman, S., Gelmon, K., Cohen, R., Saleh, M., Isaacs, C., Young, L., Healey, D., Onetto, N. & Slichenmyer, W. (1999). Randomized phase II study of BR96-doxorubicin conjugate in patients with metastatic breast cancer. *J Clin Oncol*, **17**, 478-484.

- Tomioka, R., Minami, N., Kushida, A., Horibe, S., Izumi, I., Kato, A., Fukushima, K., Ideo, H., Yamashita, K., Hirose, S. & Saito, Y. (2009). Neuroblastoma GOTO cells are hypersensitive to disruption of lipid rafts. *Biochem Biophys Res Commun*, **389**, 122-7.
- Tomura, M., Yu, W.G., Ahn, H.J., Yamashita, M., Yang, Y.F., Ono, S., Hamaoka, T., Kawano, T., Taniguchi, M., Koezuka, Y. & Fujiwara, H. (1999). A novel function of Valpha14+CD4+NKT cells: stimulation of IL-12 production by antigen-presenting cells in the innate immune system. *J Immunol*, **163**, 93-101.
- Trump, B.F. & Berezsky, I.K. (1996). The role of altered [Ca<sup>2+</sup>]<sub>i</sub> regulation in apoptosis, oncosis, and necrosis. *Biochim Biophys Acta*, **1313**, 173-8.
- Tsuchida, T., Saxton, R.E., Morton, D.L. & Irie, R.F. (1989). Gangliosides of human melanoma. *Cancer*, **63**, 1166-74.
- Tsujino, T., Seshimo, I., Yamamoto, H., Ngan, C.Y., Ezumi, K., Takemasa, I., Ikeda, M., Sekimoto, M., Matsuura, N. & Monden, M. (2007). Stromal myofibroblasts predict disease recurrence for colorectal cancer. *Clin Cancer Res*, **13**, 2082-90.
- Tyan, S.W., Kuo, W.H., Huang, C.K., Pan, C.C., Shew, J.Y., Chang, K.J., Lee, E.Y. & Lee, W.H. (2011). Breast cancer cells induce cancer-associated fibroblasts to secrete hepatocyte growth factor to enhance breast tumorigenesis. *PLoS One*, **6**, e15313.
- Uldrich, A.P., Crowe, N.Y., Kyparissoudis, K., Pellicci, D.G., Zhan, Y., Lew, A.M., Bouillet, P., Strasser, A., Smyth, M.J. & Godfrey, D.I. (2005). NKT cell stimulation with glycolipid antigen in vivo: costimulation-dependent expansion, Bim-dependent contraction, and hyporesponsiveness to further antigenic challenge. *J Immunol*, **175**, 3092-101.
- Ullenhag, G.J., Mukherjee, A., Watson, N.F., Al-Attar, A.H., Scholefield, J.H. & Durrant, L.G. (2007). Overexpression of FLIPL is an independent marker of poor prognosis in colorectal cancer patients. *Clin Cancer Res*, **13**, 5070-5.
- Urich, K. (1994). *Comparative Animal Biochemistry*. Springer-Verlag.
- Vakkila, J. & Lotze, M.T. (2004). Inflammation and necrosis promote tumour growth. *Nat Rev Immunol*, **4**, 641-8.
- Valabrega, G., Montemurro, F. & Aglietta, M. (2007). Trastuzumab: mechanism of action, resistance and future perspectives in HER2-overexpressing breast cancer. *Ann Oncol*, **18**, 977-84.
- Van Cutsem, E., Kohne, C.H., Hitre, E., Zaluski, J., Chang Chien, C.R., Makhson, A., D'Haens, G., Pinter, T., Lim, R., Bodoky, G., Roh, J.K., Folprecht, G., Ruff, P., Stroh, C., Tejpar, S., Schlichting, M., Nippgen, J. & Rougier, P. (2009). Cetuximab and chemotherapy as initial treatment for metastatic colorectal cancer. *N Engl J Med*, **360**, 1408-17.
- van den Elzen, P., Garg, S., Leon, L., Brigl, M., Leadbetter, E.A., Gumperz, J.E., Dascher, C.C., Cheng, T.Y., Sacks, F.M., Illarionov, P.A., Besra, G.S., Kent, S.C., Moody, D.B. & Brenner, M.B. (2005). Apolipoprotein-mediated pathways of lipid antigen presentation. *Nature*, **437**, 906-10.
- van der Most, R.G., Currie, A.J., Robinson, B.W. & Lake, R.A. (2008). Decoding dangerous death: how cytotoxic chemotherapy invokes inflammation, immunity or nothing at all. *Cell Death Differ*, **15**, 13-20.
- van Meerten, T., van Rijn, R.S., Hol, S., Hagenbeek, A. & Ebeling, S.B. (2006). Complement-induced cell death by rituximab depends on CD20 expression level and acts complementary to antibody-dependent cellular cytotoxicity. *Clin Cancer Res*, **12**, 4027-35.
- Van Poznak, C., Cross, S.S., Saggese, M., Hudis, C., Panageas, K.S., Norton, L., Coleman, R.E. & Holen, I. (2006). Expression of osteoprotegerin (OPG), TNF related apoptosis inducing ligand (TRAIL), and receptor activator of nuclear factor {kappa}B ligand (RANKL) in human breast tumours, Vol. 59. pp. 56-63.
- Vanden Berghe, T., Kalai, M., Denecker, G., Meeus, A., Saelens, X. & Vandenabeele, P. (2006). Necrosis is associated with IL-6 production but apoptosis is not. *Cell Signal*, **18**, 328-35.
- Vander Heiden, M.G. & Thompson, C.B. (1999). Bcl-2 proteins: regulators of apoptosis or of mitochondrial homeostasis? *Nat Cell Biol*, **1**, E209-16.

- Varki, A. (1993). Biological roles of oligosaccharides: all of the theories are correct. *Glycobiology*, **3**, 97-130.
- Varki, A., Cummings, R.D., Esko, J.D. (2009). *Essentials of Glycobiology*. Cold Spring Harbor Laboratory Press: Cold Spring Harbor (NY), USA.
- Vermeulen, K., Van Bockstaele, D.R. & Berneman, Z.N. (2005). Apoptosis: mechanisms and relevance in cancer. *Ann Hematol*, **84**, 627-39.
- Waldhauer, I. & Steinle, A. (2008). NK cells and cancer immunosurveillance. *Oncogene*, **27**, 5932-43.
- Walker, S., Landovitz, R., Ding, W.D., Ellestad, G.A. & Kahne, D. (1992). Cleavage behavior of calicheamicin gamma 1 and calicheamicin T. *Proc Natl Acad Sci U S A*, **89**, 4608-12.
- Walport, M.J. (2001a). Complement. First of two parts. *N Engl J Med*, **344**, 1058-66.
- Walport, M.J. (2001b). Complement. Second of two parts. *N Engl J Med*, **344**, 1140-4.
- Wang, S.Y., Racila, E., Taylor, R.P. & Weiner, G.J. (2008). NK-cell activation and antibody-dependent cellular cytotoxicity induced by rituximab-coated target cells is inhibited by the C3b component of complement. *Blood*, **111**, 1456-63.
- Watson, N.F., Durrant, L.G., Madjd, Z., Ellis, I.O., Scholefield, J.H. & Spendlove, I. (2006a). Expression of the membrane complement regulatory protein CD59 (protectin) is associated with reduced survival in colorectal cancer patients. *Cancer Immunol Immunother*, **55**, 973-80.
- Watson, N.F., Madjd, Z., Scrimgeour, D., Spendlove, I., Ellis, I.O., Scholefield, J.H. & Durrant, L.G. (2005). Evidence that the p53 negative / Bcl-2 positive phenotype is an independent indicator of good prognosis in colorectal cancer: a tissue microarray study of 460 patients. *World J Surg Oncol*, **3**, 47.
- Watson, N.F., Ramage, J.M., Madjd, Z., Spendlove, I., Ellis, I.O., Scholefield, J.H. & Durrant, L.G. (2006b). Immunosurveillance is active in colorectal cancer as downregulation but not complete loss of MHC class I expression correlates with a poor prognosis. *Int J Cancer*, **118**, 6-10.
- Watson, N.F., Spendlove, I., Madjd, Z., McGilvray, R., Green, A.R., Ellis, I.O., Scholefield, J.H. & Durrant, L.G. (2006c). Expression of the stress-related MHC class I chain-related protein MICA is an indicator of good prognosis in colorectal cancer patients. *Int J Cancer*, **118**, 1445-52.
- Wei, J., Cui, L., Liu, F., Fan, Y., Lang, R., Gu, F., Guo, X., Tang, P. & Fu, L. (2010). E-selectin and Sialyl Lewis X expression is associated with lymph node metastasis of invasive micropapillary carcinoma of the breast. *Int J Surg Pathol*, **18**, 193-200.
- Weiner, L.M., Surana, R. & Wang, S. (2010). Monoclonal antibodies: versatile platforms for cancer immunotherapy. *Nat Rev Immunol*, **10**, 317-27.
- Wen, Y., Wang, C.T., Ma, T.T., Li, Z.Y., Zhou, L.N., Mu, B., Leng, F., Shi, H.S., Li, Y.O. & Wei, Y.Q. (2010). Immunotherapy targeting fibroblast activation protein inhibits tumor growth and increases survival in a murine colon cancer model. *Cancer Sci*, **101**, 2325-32.
- Wiley, S.R., Schooley, K., Smolak, P.J., Din, W.S., Huang, C.P., Nicholl, J.K., Sutherland, G.R., Smith, T.D., Rauch, C., Smith, C.A. & et al. (1995). Identification and characterization of a new member of the TNF family that induces apoptosis. *Immunity*, **3**, 673-82.
- Willett, C.G., Boucher, Y., di Tomaso, E., Duda, D.G., Munn, L.L., Tong, R.T., Chung, D.C., Sahani, D.V., Kalva, S.P., Kozin, S.V., Mino, M., Cohen, K.S., Scadden, D.T., Hartford, A.C., Fischman, A.J., Clark, J.W., Ryan, D.P., Zhu, A.X., Blaszkowsky, L.S., Chen, H.X., Shellito, P.C., Lauwers, G.Y. & Jain, R.K. (2004). Direct evidence that the VEGF-specific antibody bevacizumab has antivasular effects in human rectal cancer. *Nat Med*, **10**, 145-7.
- Winter, G. & Milstein, C. (1991). Man-made antibodies. *Nature*, **349**, 293-9.
- Won, J.S., Singh, A.K. & Singh, I. (2007). Lactosylceramide: a lipid second messenger in neuroinflammatory disease. *J Neurochem*, **103 Suppl 1**, 180-91.
- Wu, Y., Xu, J., Shinde, S., Grewal, I., Henderson, T., Flavell, R.A. & Liu, Y. (1995). Rapid induction of a novel costimulatory activity on B cells by CD40 ligand. *Curr Biol*, **5**, 1303-11.

- Wu, Z.L., Schwartz, E., Seeger, R. & Ladisch, S. (1986). Expression of GD2 ganglioside by untreated primary human neuroblastomas. *Cancer Res*, **46**, 440-3.
- Wulff, S., Pries, R. & Wollenberg, B. (2010). Cytokine release of human NK cells solely triggered with Poly I:C. *Cell Immunol*, **263**, 135-7.
- Yamada, N., Chung, Y.S., Takatsuka, S., Arimoto, Y., Sawada, T., Dohi, T. & Sowa, M. (1997). Increased sialyl Lewis A expression and fucosyltransferase activity with acquisition of a high metastatic capacity in a colon cancer cell line. *Br J Cancer*, **76**, 582-7.
- Yamamoto, K., Utsunomiya, A., Tobinai, K., Tsukasaki, K., Uike, N., Uozumi, K., Yamaguchi, K., Yamada, Y., Hanada, S., Tamura, K., Nakamura, S., Inagaki, H., Ohshima, K., Kiyoi, H., Ishida, T., Matsushima, K., Akinaga, S., Ogura, M., Tomonaga, M. & Ueda, R. (2010). Phase I study of KW-0761, a defucosylated humanized anti-CCR4 antibody, in relapsed patients with adult T-cell leukemia-lymphoma and peripheral T-cell lymphoma. *J Clin Oncol*, **28**, 1591-8.
- Yamane-Ohnuki, N., Kinoshita, S., Inoue-Urakubo, M., Kusunoki, M., Iida, S., Nakano, R., Wakitani, M., Niwa, R., Sakurada, M., Uchida, K., Shitara, K. & Satoh, M. (2004). Establishment of FUT8 knockout Chinese hamster ovary cells: an ideal host cell line for producing completely defucosylated antibodies with enhanced antibody-dependent cellular cytotoxicity. *Biotechnol Bioeng*, **87**, 614-22.
- Yamane-Ohnuki, N. & Satoh, M. (2009). Production of therapeutic antibodies with controlled fucosylation. *MAbs*, **1**, 230-6.
- Yang, J. & Reth, M. (2010). Oligomeric organization of the B-cell antigen receptor on resting cells. *Nature*, **467**, 465-9.
- Yang, R.K. & Sondel, P.M. (2010). Anti-GD2 Strategy in the Treatment of Neuroblastoma. *Drugs Future*, **35**, 665.
- Yang, S.Y., Sales, K.M., Fuller, B., Seifalian, A.M. & Winslet, M.C. (2009). Apoptosis and colorectal cancer: implications for therapy. *Trends Mol Med*, **15**, 225-33.
- Yang, X.D., Jia, X.C., Corvalan, J.R., Wang, P. & Davis, C.G. (2001). Development of ABX-EGF, a fully human anti-EGF receptor monoclonal antibody, for cancer therapy. *Crit Rev Oncol Hematol*, **38**, 17-23.
- Yeung, Y.A., Leabman, M.K., Marvin, J.S., Qiu, J., Adams, C.W., Lien, S., Starovasnik, M.A. & Lowman, H.B. (2009). Engineering human IgG1 affinity to human neonatal Fc receptor: impact of affinity improvement on pharmacokinetics in primates. *J Immunol*, **182**, 7663-71.
- Yoshida, S., Kawaguchi, H., Sato, S., Ueda, R. & Furukawa, K. (2002). An anti-GD2 monoclonal antibody enhances apoptotic effects of anti-cancer drugs against small cell lung cancer cells via JNK (c-Jun terminal kinase) activation. *Jpn J Cancer Res*, **93**, 816-24.
- Zein, N., Sinha, A.M., McGahren, W.J. & Ellestad, G.A. (1988). Calicheamicin gamma 1I: an antitumor antibiotic that cleaves double-stranded DNA site specifically. *Science*, **240**, 1198-201.
- Zeissig, S., Dougan, S.K., Barral, D.C., Junker, Y., Chen, Z., Kaser, A., Ho, M., Mandel, H., McIntyre, A., Kennedy, S.M., Painter, G.F., Veerapen, N., Besra, G.S., Cerundolo, V., Yue, S., Beladi, S., Behar, S.M., Chen, X., Gumperz, J.E., Breckpot, K., Raper, A., Baer, A., Exley, M.A., Hegele, R.A., Cuchel, M., Rader, D.J., Davidson, N.O. & Blumberg, R.S. (2010). Primary deficiency of microsomal triglyceride transfer protein in human abetalipoproteinemia is associated with loss of CD1 function. *J Clin Invest*, **120**, 2889-99.
- Zent, C.S., Secreto, C.R., LaPlant, B.R., Bone, N.D., Call, T.G., Shanafelt, T.D., Jelinek, D.F., Tschumper, R.C. & Kay, N.E. (2008). Direct and complement dependent cytotoxicity in CLL cells from patients with high-risk early-intermediate stage chronic lymphocytic leukemia (CLL) treated with alemtuzumab and rituximab. *Leuk Res*, **32**, 1849-56.
- Zhang, C., Xu, Y., Gu, J. & Schlossman, S.F. (1998). A cell surface receptor defined by a mAb mediates a unique type of cell death similar to oncosis. *Proc Natl Acad Sci U S A*, **95**, 6290-5.
- Zhang, G., Zhang, H., Wang, Q., Lal, P., Carroll, A.M., de la Llera-Moya, M., Xu, X. & Greene, M.I. (2010a). Suppression of human prostate tumor growth by a unique prostate-specific monoclonal antibody F77 targeting a glycolipid marker. *Proc Natl Acad Sci U S A*, **107**, 732-7.

- Zhang, Q., Itagaki, K. & Hauser, C.J. (2010b). Mitochondrial DNA is released by shock and activates neutrophils via p38 map kinase. *Shock*, **34**, 55-9.
- Zhao, Y., Lou, D., Burke, J. & Kohler, H. (2002). Enhanced anti-B-cell tumor effects with anti-CD20 superantibody. *J Immunother*, **25**, 57-62.
- Zheng, M., Fang, H. & Hakomori, S. (1994). Functional role of N-glycosylation in alpha 5 beta 1 integrin receptor. De-N-glycosylation induces dissociation or altered association of alpha 5 and beta 1 subunits and concomitant loss of fibronectin binding activity. *J Biol Chem*, **269**, 12325-31.
- Zheng, M., Fang, H., Tsuruoka, T., Tsuji, T., Sasaki, T. & Hakomori, S. (1993). Regulatory role of GM3 ganglioside in alpha 5 beta 1 integrin receptor for fibronectin-mediated adhesion of FUA169 cells. *J Biol Chem*, **268**, 2217-22.
- Zhong, L.T., Manzi, A., Skowronski, E., Notterpek, L., Fluharty, A.L., Faull, K.F., Masada, I., Rabizadeh, S., Varsanyi-Nagy, M., Ruan, Y., Oh, J.D., Butcher, L.L. & Bredesen, D.E. (2001). A monoclonal antibody that induces neuronal apoptosis binds a metastasis marker. *Cancer Res*, **61**, 5741-8.
- Zhou, Q., Hakomori, S., Kitamura, K. & Igarashi, Y. (1994). GM3 directly inhibits tyrosine phosphorylation and de-N-acetyl-GM3 directly enhances serine phosphorylation of epidermal growth factor receptor, independently of receptor-receptor interaction. *J Biol Chem*, **269**, 1959-65.
- Zhu, D., McCarthy, H., Ottensmeier, C.H., Johnson, P., Hamblin, T.J. & Stevenson, F.K. (2002). Acquisition of potential N-glycosylation sites in the immunoglobulin variable region by somatic mutation is a distinctive feature of follicular lymphoma. *Blood*, **99**, 2562-8.